# THE ROLE OF TAU-GUIDANCE DURING DECELERATIVE HELICOPTER APPROACHES

Thesis submitted in accordance with the requirements of the University of Liverpool for the degree of Doctor in Philosophy

by

Heath Alan Lockett

February 2010

# ABSTRACT

The advantages brought by modern computing technology have led to flight safety being improved through the use of guidance tools such as head-up displays. Initially such developments were the preserve of the military, but they have now filtered down into civilian fixed-wing usage, with head-up displays even being found on cars in the early 21st century. However, civilian helicopter pilots are still largely bereft of the advantages that modern guidance technology can bring. The research presented in this thesis aims to provide an insight into the information that pilots find useful in order to guide a manoeuvre, with a specific objective being to develop guidelines for future vision aids. The goals are achieved through flight simulation exercises which examine an Approach to Hover manoeuvre, in both good and poor visual environments and also through a much more clinical test which investigated how useful looming cues are. The main part of the analysis was $\tau$ -theory. The optical variable $\tau$ specifies the time to contact or close to an object or surface and it has been posited that humans and animals use $\tau$ for prospective guidance. The good visual environment Approach to Hover trial suggested that both pilots were using tau guidance, with one pilot demonstrating a more repeatable 2-phase strategy. Recommendations for the design of a $\tau$-based vision aid were also made. The recommendations were based on k, the 'coupling constant', which is the gradient of the linear approximation when $\tau$ is plotted against Time. Recommendations were also made based on $\dot{\tau}$; the instantaneous rate of change of $\tau$. A second test examined a similar Approach to Hover manoeuvre, with changes made to the macrotextural and structural cues to simulate a degraded visual environment. Based on the findings of this test further guidelines were suggested for the design of a $\tau$ -based vision aid, and it was also suggested that the way in which

visual cues interact with the scene is transient. In addition it was found that there is a relationship between the k value and scene content. Finally, the Clinical Deceleration flight trial indicated that there was potential for looming to be considered as the only visual information needed for prospective guidance, although the results were not entirely convincing. As a result of the differences between well-guided and poorly-guided approaches, further guidelines were suggested for the design of a vision aid which would be useful in such a situation.

The primary conclusions of the report are:

- The data for the good visual environment Approach to Hover test shows a strong 'pro-tau' case, especially for one of the two pilots, based on the tau analysis. It was suggested that a two-phase strategy is employed, with an initial general k value of 0.45-0.525 followed by a constant $\dot{\tau}_x$ of approximately 0.45-0.5 when $\tau_x$ is less than 7 seconds.

- The degraded visual environment Approach to Hover test showed that there is a relationship between k value and the visual quality of the scene, indicating that the $\tau$ strategy is sensitive to scene content. The trial also highlighted the way in which the different types of scene content interact to affect task performance, with poorer quality visual scenes not necessarily yielding poorer performance.

- The degraded visual environment trial showed further evidence of a two-phase approach, with an average k value between 0.425-0.525, depending on the quality of the visual cues in the scene. A targeted $R^2$ analysis suggested slightly higher k values of 0.45-0.55 lead to runs which are highly correlated over a long range.

- Based on the Clinical Deceleration results, it is suggested that a $\tau$ - based guidance system would command an initial period of $\dot{\tau}_x = 0$ before the pilot is driven to follow a $\dot{\tau}_x$ =0.4-0.5 approach.

# ACKNOWLEDGMENTS

There are a number of people who I must thank for their help in this research. Firstly, I would like to thank my supervisor Professor Gareth Padfield, for offering me the chance to work on such an interesting project and also for his continued support, advice and enthusiasm towards the research. The financial assistance from the Engineering and Physical Sciences Research Council (EPSRC) is gratefully acknowledged, without their help the research would not have been possible. A huge debt of gratitude is also due to the project's test pilots, Andy Berryman and Steve Cheyne. Their professionalism, insight and ability to make long, repetitive sorties engaging and humorous made the project's flight tests a rewarding experience. I would also like to thank Steve Bode for his help with making my visions for the scene content of the flight tests a reality. To the various members of the FS&T research group who have come and gone over the years, I salute you for your technical help, generosity at the bar, provision of many, many good times and, most importantly of all, for introducing me to snowboarding. I must also thank my friends and family, whose ongoing support throughout the entire project has been invaluable. Also, I feel that I should thank Wolf Blass, the Malbec region of Argentina and 'Steve the Landlord' for fuelling me (in moderation) during the period when the thesis was written. Finally, I'd like to thank Caroline for her support, encouragement and threats, all of which I very much appreciated.

# TABLE OF CONTENTS

**Abstract** ..... i

**Acknowledgments** ..... iv

**Table of Contents** ..... vi

**Nomenclature** ..... xii

**Chapter 1** ..... 1

**Introduction** ..... 1

1.1 Overview ..... 1

1.2 Thesis Structure and Content ..... 2

1.3 Project Objectives ..... 4

1.4 Flight Simulation setup ..... 5

1.4.1 HELIFLIGHT ..... 5

1.4.2 FLIGHTLAB ..... 8

1.4.3 Landscape ..... 9

1.4.4 Multigen Creator ..... 10

**Chapter 2** ..... 12

**Technical Review** ..... 12

2.1 Rotorcraft Safety Review ..... 12

2.1.1 Introduction ..... 12

2.1.2 CAA Safety Review ..... 13

2.1.2.1 UK Public Transport Helicopters ..... 13

2.1.2.2 UK Non Public Transport Helicopters ..... 15

2.1.3 NTSB 'Air Carrier' Statistics 1983-1999 ..... 17

2.1.3.1 Fatalities per Mission Phase ..... 17

2.1.3.2 Accident Review by First Occurrence ..... 18

2.1.3.3 Fatal Accident Review by First Occurrence ..... 20

2.1.3.4 Fatal vs. Non-Fatal Accident Review ..... 22

2.1.4 NTSB Civil Aviation Dataset 1982-03 ..... 24

2.1.4.1 Review by First Occurrence ..... 24

2.1.4.2 Review by Phase of Flight ..... 26

2.1.4.3 Review by Type of Flight (landing phase only) ..... 27

2.1.5 Discussion of Safety Review Documents ..... 29

2.1.6 Conclusions ..... 31

2.2 Literature Review ..... 32

2.3 Visual Perception and Tau ..... 35

2.3.1 Visual Perception Theories ..... 36

2.3.1.1 Constructionist Approach ..... 36

2.3.1.2 Ecological Approach ..... 39

2.3.2 Tau Theory ..... 43

2.3.2.1 $\tau$ and $\dot{\tau}$ ..... 44

2.3.2.2 $\tau$-coupling ..... 47

2.3.2.3 Intrinsic $\tau$-guides ..... 48

2.3.2.4 Is it really $\tau$? ..... 49

**Chapter 3** ..... 52

**Approach To Hover - GVE** ..... 52

3.1 Introduction ..... 52

3.2 Objectives ..... 53

3.3 Appraisal of the NASA tests ..... 53

3.3.1 Methodology ..... 54

3.3.2 Results ..... 55

3.3.3 NASA Findings ..... 56

3.4 Design of UoL flight test ..... 57

3.4.1 Aircraft Type ..... 57

3.4.2 Database ..... 58

3.4.3 Test matrix and variables ..... 59

3.4.4 Remaining faithful to the NASA tests ..... 59

3.4.5 Test Pilots ..... 60

3.5 UoL Simulation Results ..... 61

3.5.1 General Data Analysis ..... 61

3.5.1.1 Pilot AB ..... 61

3.5.1.2 Pilot SC ..... 68

3.5.1.3 Comparison of Piloted data ..... 72

3.5.2 NASA Replication ..... 79

3.5.2.1 Comparison of parametric data ..... 79

3.5.3 Tau Investigation ..... 88

3.5.3.1 Analysis of tau data – AB ..... 89

3.5.3.2 Analysis of tau data – SC ..... 98

3.5.3.3 $\dot{\tau}_x$ Analysis ..... 109

3.6 Conclusions ..... 112

**Chapter 4** ..... 115

**Approach To Hover – DVE** ..... 115

4.1 Introduction ..... 115

4.2 Objectives ..... 116

4.3 Design of the test ..... 116

4.3.1 Defining the test conditions ..... 116

4.3.2 Selecting the scene content ..... 119

4.4 Results ..... 123

4.4.1 General Data Analysis ..... 123

4.4.2 Tau analysis ..... 129

4.4.2.1 $\tau_x$ vs. TTG and associated findings ..... 129

4.4.2.2 $\tau_x$ $R^2$ analysis ..... 137

4.4.2.3 Progressive $R^2$ Analysis ..... 142

4.4.2.4 Targeted $R^2$ Analysis ..... 147

4.4.2.5 k Analysis ..... 152

4.4.2.6 Progressive k Analysis ..... 155

4.4.2.7 Instantaneous $\dot{\tau}_x$ Analysis ..... 158

4.5 Conclusions ..... 163

**Chapter 5** ..... 166

**Clinical Deceleration** ..... 166

5.1 Introduction ..... 166

5.2 Objectives ..... 167

5.3 Design of the test ..... 167

5.3.1 Theory ..... 167

5.3.2 The Task ..... 167

5.3.3 Setting the test conditions ..... 169

5.4 Results ..... 170

5.4.1 General Data Analysis ..... 170

5.4.2 Tau Analysis ..... 177

5.4.2.1 $\tau_x$ vs. TTG ..... 181

5.4.2.2 Instantaneous $\dot{\tau}_x$ Analysis ..... 190

5.4.2.3 Targeted $R^2$ analysis ..... 195

5.5 Conclusions ..... 200

**Chapter 6** ..... 203

**Conclusions** ..... 203

6.1 Conclusions ..... 203

6.2 Suggestions for further work ..... 209

**References** ..... 211

**Appendix A** ..... 217

**Pilot Curriculum Vitae** ..... 217

**Appendix B** ..... 220

**VCR and UCE** ..... 220

# NOMENCLATURE

## General

| | |
|---|---|
| k | Coupling coefficient |
| $k_n$ | NASA constant |
| n | NASA power parameter |
| $R^2$ | Coefficient of determination |
| t | Time [s] |
| $t_0$ | Very small positive time [s] |
| T | Total time [s] |
| vxb | Body x-axis velocity [ft/s] |
| vxbd | Body x-axis deceleration [ft/s$^2$] |
| vxi | Inertial x-axis velocity [ft/s] |
| x | Range [ft] |
| xacc | Inertial x-axis deceleration [ft/s$^2$] |
| $x_d$ | Initial NASA range condition [ft] |
| $\dot{x}_d$ | Initial NASA groundspeed condition [ft/s] |
| $\ddot{x}_d$ | Initial NASA deceleration condition [ft/s$^2$] |
| y | y-axis position [ft] |
| z | Altitude [ft] |
| $\infty$ | Infinity |

## Greek symbols

| | |
|---|---|
| $\alpha$ | Angular hand-mouth gap [degrees] |
| $\theta$ | Pitch Angle [degrees] |

| | |
|---|---|
| $\tau$ | Tau, time to contact [s] |
| $\tau_g$ | Intrinsic tau guide [s] |
| $\dot{\tau}$ | Tau-dot, rate of change of $\tau$ |
| $\gamma$ | Hand-mouth distance [cm] |

**Abbreviations**

| | |
|---|---|
| 3D | Three Dimensional |
| CAA | Civil Aviation Authority |
| DVE | Degraded Visual Environment |
| FAR | Federal Aviation Regulation |
| FGR | FLIGHTLAB Generic Rotorcraft |
| FOV | Field of View |
| FST | Flight Science & Technology |
| GVE | Good Visual Environment |
| HMD | Helmet Mounted Display |
| HUD | Head Up Display |
| IFR | Instrument Flight Rules |
| ILS | Instrument Landing System |
| mtwa | Maximum take-off weight |
| NASA | National Aeronautics and Space Administration |
| NOE | Nap of the Earth |
| NTSB | National Transportation Safety Board |
| OTW | Out the Window |
| PC | Personal Computer |
| TTC | Time to Contact |
| TTG | Time to Go |
| TTP | Time to Passage |
| UCE | Usable Cue Environment |

| | |
|---|---|
| UoL | University of Liverpool |
| VCR | Visual Cue Rating |
| VCS | Visual Cueing Strategy |
| VFR | Visual Flight Rules |

# Chapter 1

# INTRODUCTION

## 1.1 OVERVIEW

This thesis reports an investigation into the way in which helicopter pilots fly manoeuvres based on the visual cues available in the scene. Helicopter pilots make use of nap-of-the-earth (NOE) flight to increase stealth and mission security. This type of flight, which is close to the ground and amongst surrounding obstacles, is characterised by the pilot continuously making corrections in speed, heading and height. This control is guided by the pilot creating a mental model of where his or her aircraft will be in the future. This process, known as prospective control, aims to provide a safe trajectory, or skyway, based on the pilot's perception of the aircraft's continuously changing velocity and heading.

In a good visual environment (GVE) it can be assumed that the pilot can pick up enough information from the visual scene to guarantee flight safety. However in a degraded visual environment (DVE) (for example, in fog or when flying at night), visual cues can be vastly reduced and safety may be compromised. To counteract this degradation the pilot requires either improved aircraft handling qualities, or some form of vision aid. This project will focus entirely on the latter method. One of the central questions that the research will aim to answer is 'how does the pilot use

visual information to guide safe flight?' The key research method used to achieve this will be flight simulation.

In addition to the visual aspect of the testing, the main focus of the research was an optical variable which specifies times to contact or close to a surface at the current closing rate – tau ( $\tau$ ) (Lee, 2005). $\tau$ will feature as the major analysis tool, with the intention being to initially determine whether the experimental data shows that the pilot is using tau to provide prospective guidance. This research aims to show that this appears to be the case, before moving on to consider how the pilot is using $\tau$, and then recommending guidelines for a $\tau$-based vision aid.

In summary, the novel contribution that this thesis presents is initially through the general and $\tau$-based analyses of data from the flight simulations which are conducted in GVE and DVE, with a number of macro and microtextural changes made to the visual database. By then considering the $\tau$ analysis in terms of the visual challenges presented by the scene and providing guidelines for a rotorcraft-specific, $\tau$-based vision aid, the research intends to suggest a unique approach to the way in which $\tau$ is considered and applied in this context.

## 1.2 THESIS STRUCTURE AND CONTENT

In addition to the overview and this examination of the structure and content, Chapter 1 of the thesis also considers the project's objectives before detailing the hardware and software used as part of the flight simulation testing.

Chapter 2 presents a technical review which encompasses a number of subject areas. The first is a safety review which examines data from a

number of sources in order to determine which phases of flight are particularly susceptible to incidents and would therefore benefit most from the development of a vision aid. The Chapter then reviews the available literature, initially examining general literature related to the field of research in section 2.2. Section 2.3 focuses on visual perception, with an initial appraisal of Ecological and Constructionist Theories before moving onto a detailed examination of the ecologically-based Tau Theory.

The experimental work commences in Chapter 3 with an Approach to Hover manoeuvre being investigated in GVE. The reasons for this manoeuvre being selected are explained and extracts from a National Aeronautics and Space Administration (NASA) paper which is part of the initial analysis are briefly summarised. The design of the flight test is discussed and the results are then analysed and discussed in terms of the general data analysis, NASA-based analysis and $\tau$ analysis.

Chapter 4 develops the Approach to Hover manoeuvre from Chapter 3, with the focus turning to flight in DVE. Again, the design of the flight test is discussed, with a particular focus being on the selection of the test variables. The analysis then examines the way in which the different visual variable configurations affected performance. The DVE results are compared to those for the GVE trial, with much of the analysis focussing on $\tau$ and the way in which the differing visual challenges affect $\tau$-guidance.

As suggested by the title of Chapter 5, the Clinical Deceleration trial is a much more basic scientific examination somewhat removed from the 'real-life' manoeuvre presented in Chapters 3 and 4. The Chapter examines whether the Ecological Theory based claim that the pilot does not need to know relative size, velocity or distance information to determine the time it will take to reach an object in the scene is true. The aim of conducting the

test in this clinical way was to examine whether the pilot is using tau to guide flight in a visually deprived scene simply based on the optical looming of a target.

Finally, Chapter 6 presents the conclusions of the research and makes some recommendations for further areas of research which might be useful given the results of this project.

## 1.3 PROJECT OBJECTIVES

The main objective of the project was to determine whether pilots used tau guidance in a variety of decelerative trials. If it was found that the pilots were using some form of tau guidance, a secondary objective was to determine how tau was used and, also, how visual changes affected task performance. Guidelines for a tau-based vision aid would then be suggested.

In order to reach this stage a number of other objectives were identified, the first being to determine if there were any particular flight phases which would benefit from a vision aid. This required a safety review to be conducted, with the data analysis aiming to determine the most pertinent contributing factors and phases of flight. The flight testing programme could then focus on any particularly compelling results.

The design of the flight tests would then be such that a baseline set of results could be obtained for flight in GVE, with an appraisal of the various options for degrading the visual cues in the scene informing the design of the DVE phase of the trial.

Finally, the results of the flight testing would be analysed, initially in terms of the general performance data with the objective being to determine the

physical effects of the scene degradations. The analysis would then turn to proving or disproving the existence of tau as a method of prospective guidance.

## 1.4 FLIGHT SIMULATION SETUP

In order to conduct the flight tests to a level of accuracy where the results can be confidently compared to what might happen in 'the real world' it is necessary to use experimental equipment which provides as realistic a simulation experience as possible.

In addition to the physical facility itself, there are a number of sub-elements which combine to make the simulation as realistic as possible. These fall under two main headings:

- The modelling of the aircraft – the more accurately the forces and moments which govern the dynamics of the vehicle are represented, the more lifelike the flying experience will be.

- The simulation environment – this term encompasses the motion base, visuals, cockpit controls and audio cues. The focus in this section will be on the visual element.

### 1.4.1 HELIFLIGHT

The flight tests which feature in Chapters 3-5 were conducted on the Flight Science & Technology (FST) research group's original flight simulator, otherwise known as HELIFLIGHT, at the University of Liverpool (UoL). The HELIFLIGHT simulator is shown in figure 1.1.

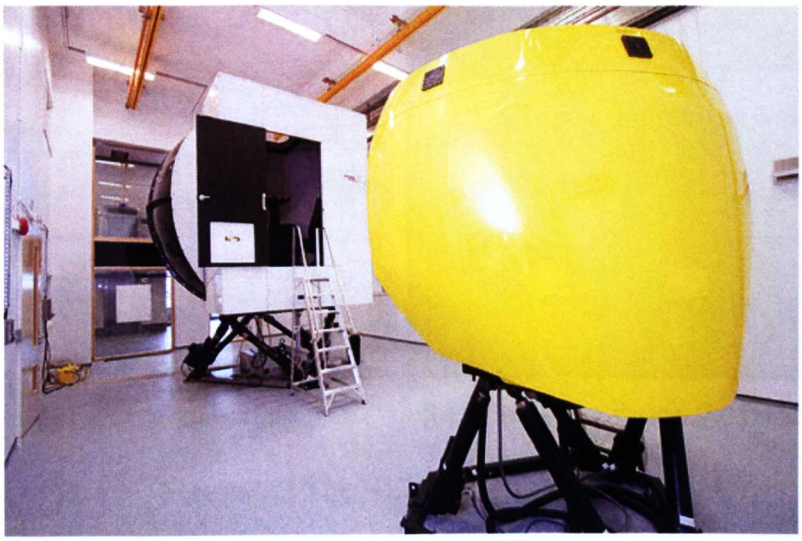

**Figure 1.1** Simulator cockpit room and 'pod' in foreground

The system is personal computer (PC) based, with one PC controlling each of the six visual channels. Three of these constitute the main 'out of the window' (OTW) view, which provides a 135° field of view (FOV), projected onto a collimated display to provide infinity optics for enhanced depth perception (Padfield and White, 2003). Two further channels provide a downwards view, also known as the 'chin' windows. These are primarily used for helicopter simulation although there are other applications for which they can be useful. The final visual channel is a 'soft' instrument panel. Figure 1.2(a) shows a field of view map for the outside view visual channels, with the 3 main OTW channels providing a 135° x 40° horizontal and vertical range. The vertical range is augmented to 60° by the two chin windows. Figure 1.2(b) presents a typical view inside the simulator, with each of the 6 visual channels clearly visible.

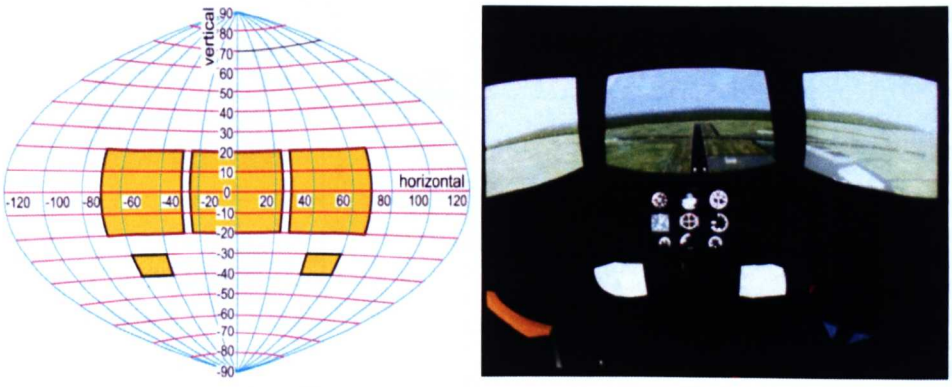


(a) Field of view map (b) Pilots view inside the cockpit

**Figure 1.2** The HELIFLIGHT visual system

The electrically actuated platform provides motion in six axes (heave, surge, sway, pitch, roll and yaw). The motion cueing algorithms can be tuned to correspond to the desired vehicle performance. To maximise the usable motion envelope the drive algorithms feature conventional washout filters that return the simulator to its neutral position at acceleration rates below the pilot's perception thresholds after a period of simulator motion.

The schematic layout of the HELIFLIGHT facility is shown in figure 1.3, with the research group's Eye Tracker also illustrated.

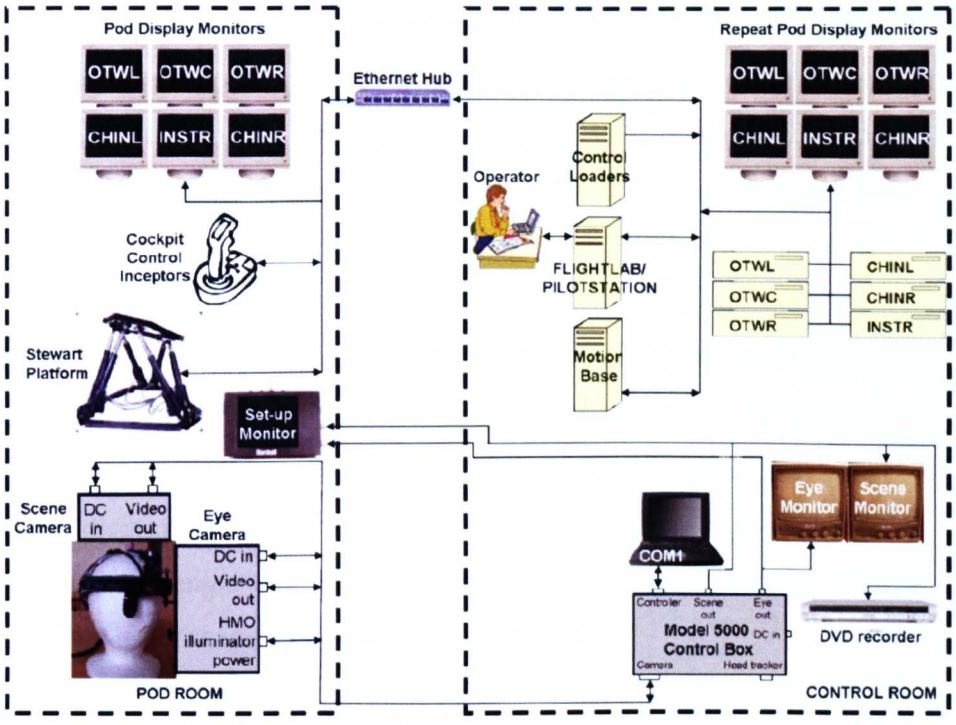


**Figure 1.3** Schematic of the HELIFLIGHT system

## 1.4.2 FLIGHTLAB

The modelling software, which can be thought of as the 'brains' of the facility, is FLIGHTLAB, a proprietary software package by Advanced Rotorcraft Technology Inc (DuVal, 2001). FLIGHTLAB provides a modular approach to developing flight dynamics models, producing a complete vehicle system from a library of predefined components. FLIGHTLAB was originally developed for rotorcraft simulations, but can also be used with fixed-wing aircraft using Blade Element Models. FLIGHTLAB offers advanced and detailed features which allow for a high-fidelity model to be created for use in the flight simulator. The model used throughout the Approach to Hover flight testing is the FLIGHTLAB Generic Rotorcraft (FGR), which is representative of the Sikorsky UH-60 Black Hawk helicopter. Although this is a military aircraft, it was deemed to offer the best option of the models available at the time of testing given

that the model was of a high fidelity with very few operational issues. The FGR also has a control system which would ensure that, within the normal flight envelope and for non-aggressive manoeuvres, controllability would not be an issue, enabling the pilot to completely focus on the visual task.

### 1.4.3 Landscape

Landscape is a piece of software which was developed by BAE Systems (Bickerstaffe, 1998) and enhances the visual capabilities of the flight simulator. The simulator was upgraded to use Landscape as the primary visual display software after the old system had been used for 3 years. As well as providing a generally much more pleasant image than the original software, Landscape also provides the ability to:

- Simulate degraded visual conditions, including night scenes (see figure 1.3).
- Add models of objects to existing databases that are currently not visible e.g. light points, offshore platforms etc.
- Add models to databases that can be animated e.g. a ship model can be driven to move as it would in various sea-states.

The second bullet point above is of particular interest for the project as it allows one common visual database to be used, with a number of 'instances' pre-designed which can virtually 'bolt on' to the main database. The varying helipad heights which form a key part of the DVE Approach to Hover flight testing in Chapter 4 are an excellent example of this. With the previous visual system a number of visual databases would be required to achieve such a range of macrostructural cues, with the time taken to load the assorted scenes being considerable compared to the much more efficient and user-friendly Landscape system.

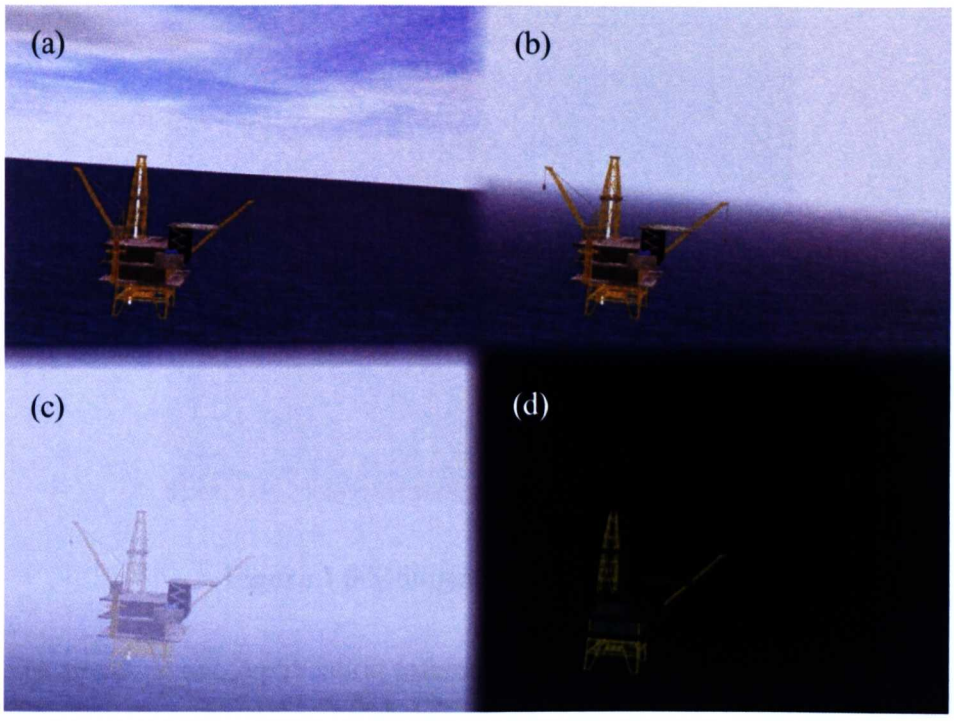


**Figure 1.4** Examples of visual degradation using Landscape; (a) Normal Landscape view, (b) Light fog obscuring natural horizon, (c) Heavy fog, (d) Night scene, with somewhat luminous oil rig.

### 1.4.4 Multigen Creator

Multigen's 'Creator' software offers real-time three dimensional (3D) object, entity and site modelling and is specifically designed for real-time 3D simulation applications. The software allows databases to be developed 'in-house', which can vary in complexity from the very simple (see section 5.3.2) to incredibly detailed cityscapes. A typical screen view of the software is shown in figure 1.5. The lower half of the figure shows the hierarchical tree view which makes complicated database development a much simpler task given the clear way in which the user can easily see the way in which surfaces, faces, objects etc. 'belong' to sub-groups and where those sub-groups fit into larger groups and the rest of the scene.

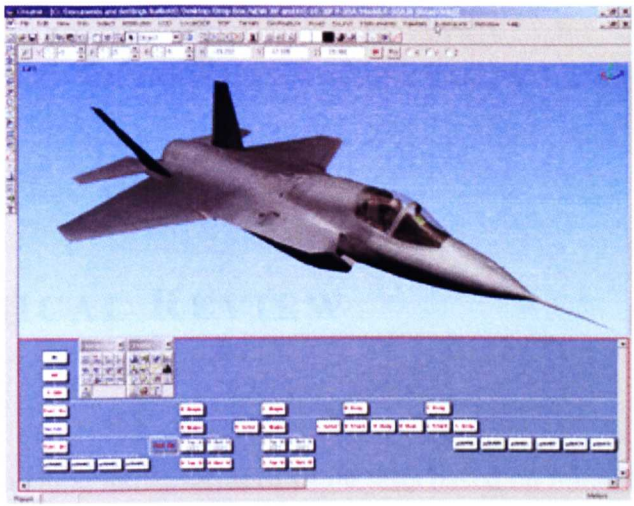

**Figure 1.5** Multigen Creator screenshot.

The sheer range of application offered by the software allows the research to be uninhibited in terms of the visual task requirements, with any visualised flight test concepts able to be developed in Creator. The concepts can also be tested in the flight simulator at any point during the development of the database allowing feedback and changes to be made at a much earlier stage than would be possible it the facility was not available in-house.

# Chapter 2

# TECHNICAL REVIEW

Rather than rushing into a series of flight tests based on initial thoughts and theories surrounding Prospective SkyGuides, NOE and DVE flight it was important to gain an understanding of the current level of knowledge in the field. The review which was conducted covered many areas including safety, the perception of motion and, perhaps most importantly, tau theory.

## 2.1 ROTORCRAFT SAFETY REVIEW

### 2.1.1 Introduction

Based on the findings of the tau investigation, the overriding objective of the research was to develop guidelines to inform the design of future tau-based head-up displays (HUD) in civil helicopter operations. Almost by default this suggests that flight safety issues were at the heart of the project, with the intention being that the suggested guidelines would not only improve flight safety but also afford civilian helicopter pilots some form of head-up guidance information which has been available to their fixed wing colleagues for many years. The aim of the safety review was to determine how accidents, both fatal and non-fatal, occurred, specifically examining the phases of flight and potentially targeting the research around the most vulnerable areas.

Data was taken from two sources, the Civil Aviation Authority (CAA) and the National Transportation Safety Board (NTSB). The CAA (UK) data covered the period 1990-2001 over two overlapping reports, CAP701 (Anonymous, 2000) and CAP735 (Anonymous, 2002). The NTSB (US) data is split into two sections corresponding to two separate datasets. The first concerns 'Air Carrier' accident data between 1983-1999 (Anonymous, 1999), more specifically this concerns flights which fall into Federal Aviation Regulation (FAR) parts 121 and 135 (Domestic, Flag and Supplemental Air Carriers and Commercial Operators of Large Aircraft & Air Taxi Operators and Commercial Operators respectively) (McElroy, 2002). The second NTSB dataset covers 'all civil aviation accidents and selected incidents within the US, its territories and possessions, and in international waters' occurring between 1982-2003, the NTSB dataset analysed includes data up to 27th October 2003 (Anonymous, 2003).

### 2.1.2 CAA Safety Review

As the two Civil Aviation Reports are essentially the same document, but for two separate groups of years, the data was merged so that it could be compared more easily. The reports have separate sections for different classes of aircraft and, for rotorcraft, these were public transport helicopters and non-public transport helicopters (<5700kg maximum take-off weight [mtwa]).

#### *2.1.2.1 UK Public Transport Helicopters*

There were 3 fatal accidents public transport flights over the period represented by the two safety reports (1990-2001), the details for which are shown in table 2.1.

| Date | Aircraft | Location | Operation | Description | Fatal | Serious | Minor |
|---|---|---|---|---|---|---|---|
| 25-07-90 | Sikorsky S61 | Brent Spar Oil Rig | Passenger | Tail Rotor struck rig structure | 6 | 4 | 3 |
| 14-03-92 | SA332 Super Puma | North Sea | Passenger | Crashed into sea and sank, in severe winds | 11 | 1 | 5 |
| 22-10-96 | SA355 Twin Squirrel | Middlewich | Passenger | Crashed following disorientation at night | 5 | | |

**Table 2.1** Details of 3 fatal public transport accidents from CAA data

Reportable accidents are also recorded in the CAA report, the definition for which is as follows:

> *An occurrence associated with the operation of an aircraft which takes place between the time any person boards the aircraft with the intention of flight until such time as all such persons have disembarked, in which -*
>
> *a) A person suffers a fatal or serious injury*
>
> *b) The aircraft sustains damage or structural failure*
>
> *c) The aircraft is missing or completely inaccessible*

Figure 2.1 shows a general trend for the number of reportable accidents to decrease over the 12 years considered, although given the relatively small numbers of accidents per year and the relatively short time period considered the trend could be quite easily disturbed by 2 consecutive years of particularly high or low data.

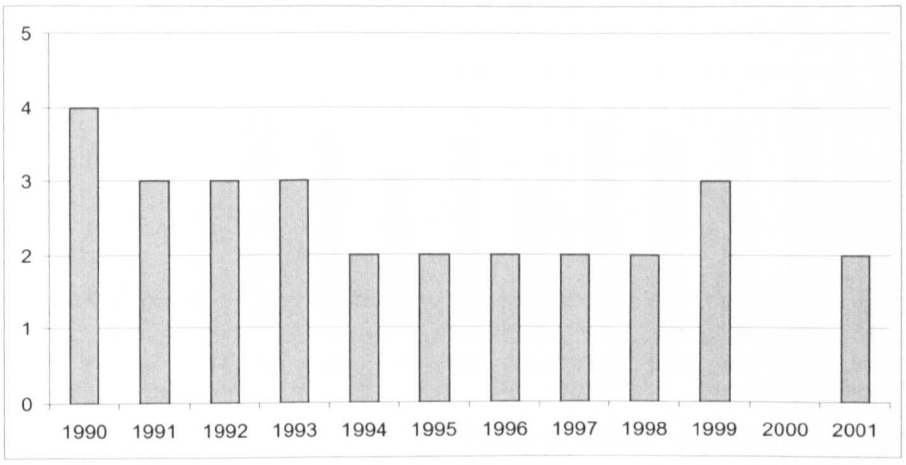


**Figure 2.1** Reportable Accidents for UK Public Transport Helicopters by year

### *2.1.2.2 UK Non Public Transport Helicopters*

Given the inevitably greater number of flights classed as 'Non Public Transport' compared to 'Public Transport', the fatal and reportable accident figures would be expected to rise accordingly. Figure 2.2 shows the number of fatal accidents by year for the given timeframe, the reportable accident data is illustrated in figure 2.3.

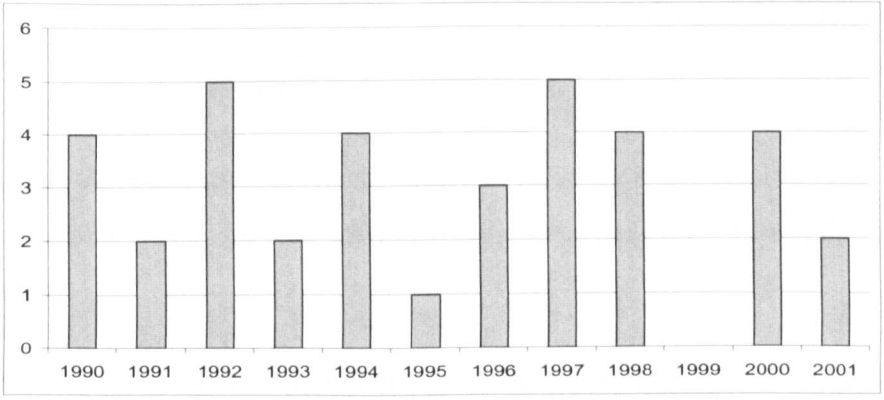


**Figure 2.2** Fatal Accidents for UK Non-Public Transport (<5700kg mtwa) by year

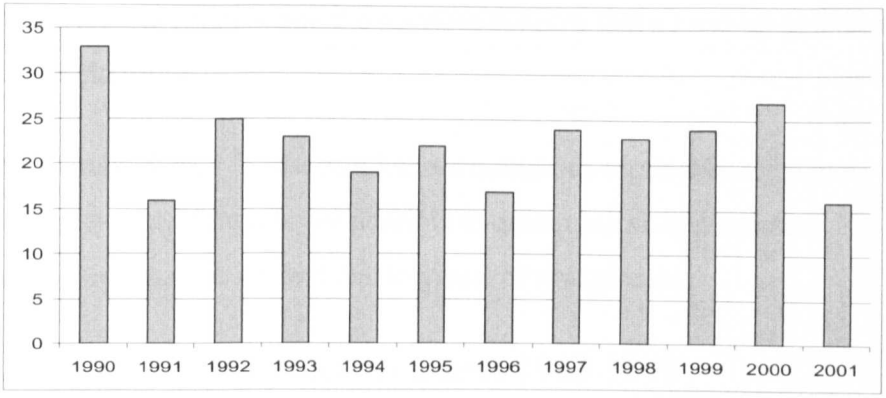


**Figure 2.3** Reportable Accidents for UK Non Public Transport (<5700kg MTWA) by year

Figure 2.2 has no discernable trend, with figures ranging between 0 and 5 for the 12 year period, with figure 2.3 also showing no trend, although there was a sharp fall from 2000 to 2001.

Based on the description of each fatal accident provided by the CAA in their documents it is possible to determine that, of the three fatal UK public transport flights over the 12 year period 1990-2001, 1 could be classed as attributable to problems with visual awareness/spatial disorientation. Specifically this assumption refers to the fatal SA355 Twin Squirrel crash in Middlewich on 22nd October 1996, for which the brief description given was:

*"Crashed following disorientation at night."*

Although the specifics of this accident are not known, it is a possibility that some form of synthetic visual guidance could have helped to prevent the accident.

In terms of the non-public transport flight over the same period, 14 of the 36 fatal accidents could be attributable, in part, to a lack of visual/spatial information. Again, although the particular details of each incident are not known, the data provides a clear indication of the effect of lack of such

visual/spatial information and the possible benefits that a head-up guidance system could bring.

Unfortunately, details for the much more numerous reportable accidents are not given, therefore it is not possible to determine an approximate number which may be attributable to visual or spatial cues.

### 2.1.3 NTSB 'Air Carrier' Statistics 1983-1999

The NTSB Air Carrier Accident Data document contained data for all forms of aircraft, therefore the relevant rotorcraft data was selected and various key areas were analysed, giving some interesting results, which again highlight the possible benefits a novel guidance system could bring to civilian helicopter flight. The data was initially filtered to remove all fixed wing entries. Of 2527 records just 338 correspond to helicopter flight, approximately 13%. All of the rotorcraft entries fall under FAR Part 135 which concerns airtaxi and commuter flights.

#### *2.1.3.1 Fatalities per Mission Phase*

Figure 2.4 gives an indication of the total number of fatalities for each of the defined mission phases, the graph shows that the 'cruise/descent' phase has by far the most fatalities.

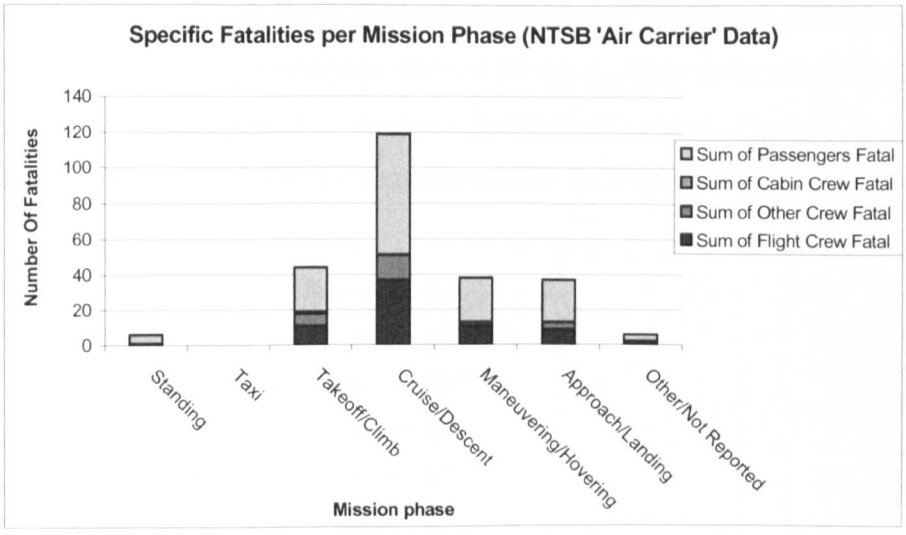


**Figure 2.4** NTSB Air carrier fatalities by phase of flight & status 1983-1999

The three other main areas shown in figure 2.4 in which fatalities were recorded are Takeoff/Climb, Manoeuvring/Hovering and Approach/Landing. The total number of fatalities in these three areas is 119, exactly equal to the number of fatalities in the cruise/descent phase alone. While this seems to provide a compelling case for investigating the cruise/descent phases of flight, the consideration must also turn to how this would be tested in the simulation environment and also, how applicable the cruise/descent data was to the research. Indeed, further investigation of the cruise/descent data showed that a much larger proportion of fatalities occurring in this phase were related to what can be considered as non-project oriented, essentially mechanical, issues. These 'first occurrences' are now considered in the next section.

### *2.1.3.2 Accident Review by First Occurrence*

The second area of analysis of the American accident data concerns what is labelled as 'First Occurrence', essentially the initial cause of the accident. That is, whilst there might be a loss of control in flight leading to an

accident, if the reason for this loss of control was a partial loss of engine power then the first occurrence statistic for the accident is the partial loss of engine power as opposed to the secondary loss of control. Figure 2.5 shows the NTSB Air Carrier first occurrence for 1983-1999.

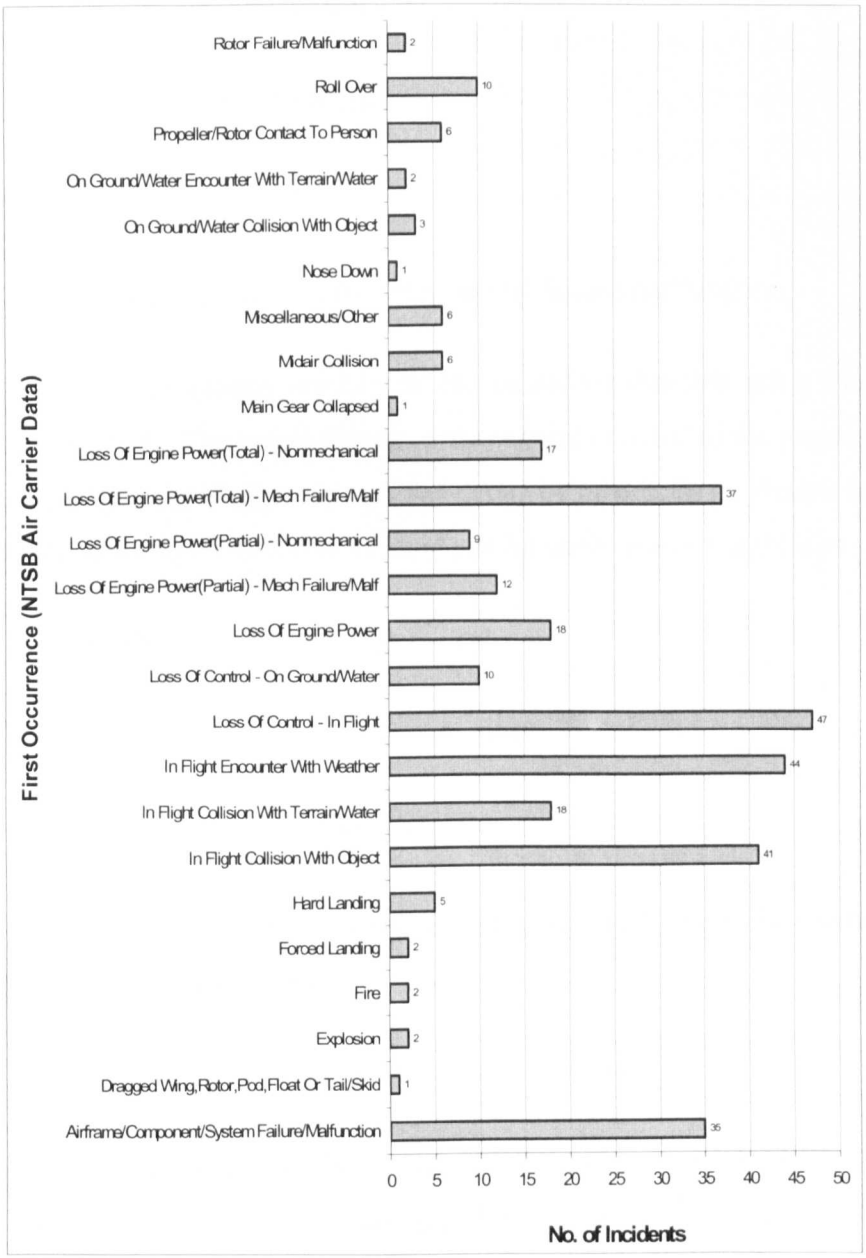


**Figure 2.5** NTSB Air Carrier Accidents by First Occurrence 1983-1999

It is immediately clear to see that that there are 5 main first occurrences which dominate figure 2.5. These are:

- Airframe/component/system failure/malfunction.
- In flight collision with object.
- In flight encounter with weather.
- Loss of control in flight.
- Loss of engine power (total) – mechanical failure/malfunction.

Of these, 2 are essentially mechanical causes and are therefore not a focus for this research. The remaining three are certainly related to the project and, although individual cases may vary, may be inherently applicable to a guidance system. The number of incidents for each case are as follows:

- In flight collision with object – 41.
- In flight encounter with weather – 44.
- Loss of Control In Flight – 47.

Therefore, from a total of 337 cases approximately 132, or 39.1%, can be related to the research project.

### *2.1.3.3 Fatal Accident Review by First Occurrence*

As an additional piece of analysis, data which only corresponded to incidents resulting in fatalities was considered. There were a number of reasons for this, the first being that the unfiltered helicopter incident data which was initially analysed could contain a number of results which could confuse the data. For example, if there were a large number of minor

incidents in a certain phase of flight this could mask the more serious cases if they were to occur in other phases. Secondly, as regrettable as any accident may be, the main focus for this project is to inform the development of technology that is primarily aimed at reducing the number of serious/fatal incidents, therefore it is logical to analyse the corresponding data. Of the 338 helicopter incidents, 92 were fatal.

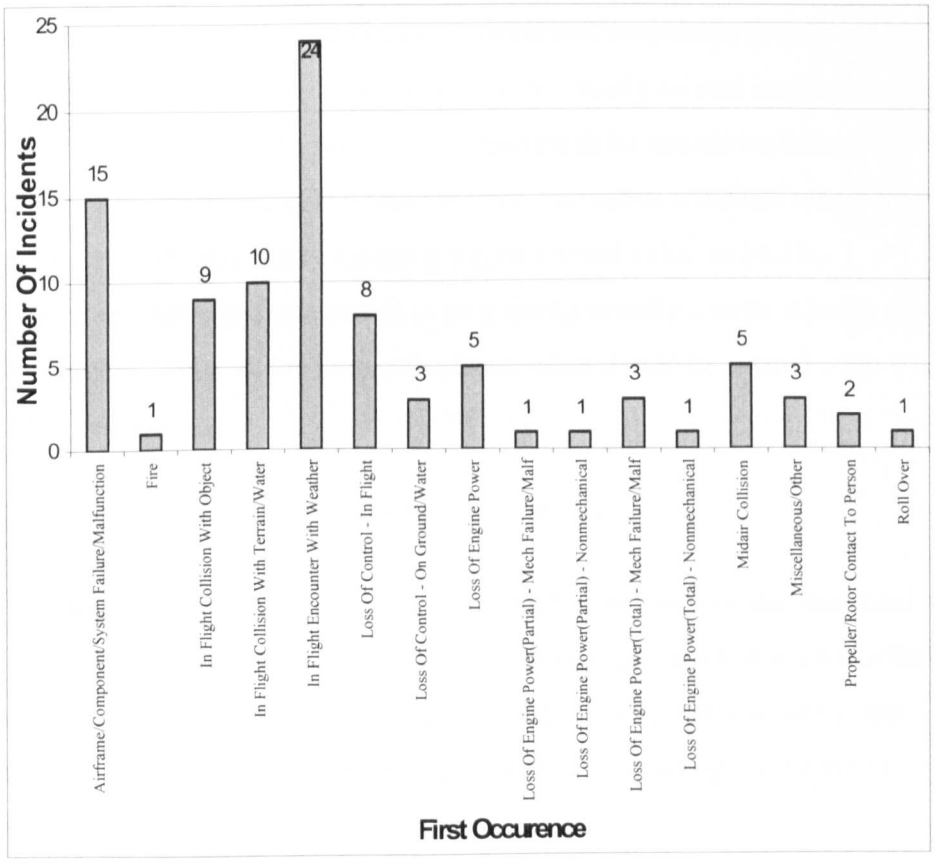


**Figure 2.6** NTSB Fatal Air Carrier Accidents by First Occurrence 1983-1999

Figure 2.6 shows that the most common first occurrence is 'In Flight Encounter With Weather', with 24 cases. 'Airframe/Component/System Failure/Malfunction' is the second most common with 15 incidents. 'In Flight Collision With Terrain/Water', 'In Flight Collision With Object' and 'Loss Of Control – In Flight' were the other results that stood out with 10,

9 and 8 cases respectively. Attempting to categorise the first occurrences into those which are spatial/visual perception related, and those that aren't, can again be used to give an indication as to the percentage of incidents which may have benefited from a guidance system. In this case, 64.1% of the incidents seem to arise from visual/spatial related causes, although it should be noted that this is probably the maximum possible value given the description of the first occurrences in the two categories. I.e. it is unlikely that 'Fire', 'Loss of Engine Power', 'Airframe/Component/System Failure/Malfunction' etc. could include any visually related incidents. Conversely, many of the occurrences deemed to be caused by lack of visual or spatial information could include individual incidents where this is not the case, potentially reducing the calculated value of 64.1%. Therefore, although there seems to be a strong visual element in many of the cases considered, the large calculated value should be treated with some caution.

#### *2.1.3.4 Fatal vs. Non-Fatal Accident Review*

In order to compare the first occurrence profile for the fatal and non-fatal data, figure 2.7 considers the results as a percentage rather than an absolute value. This is because there are approximately three times as many non-fatal incidents as fatal incidents, which lead to misleading results when considered in absolute terms.

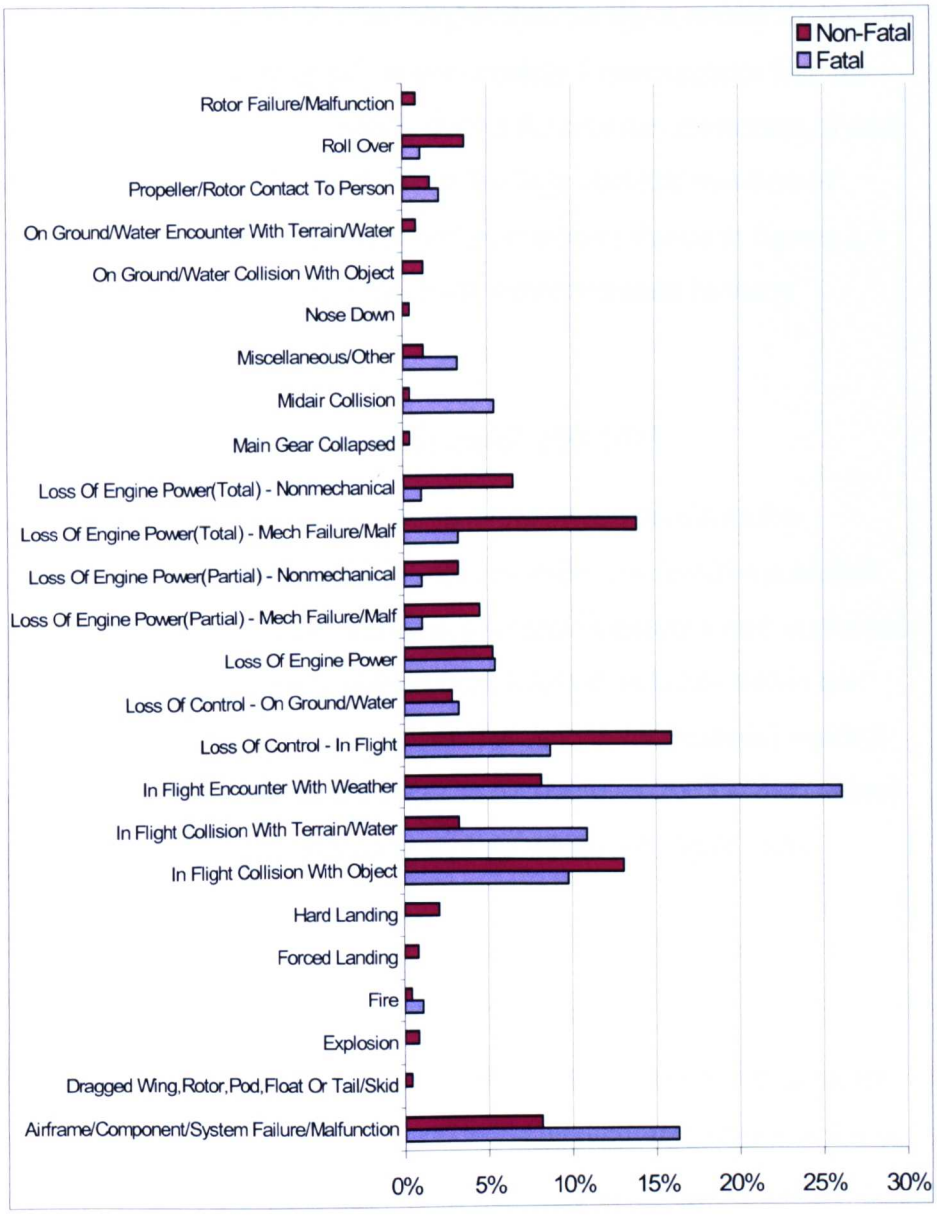


**Figure 2.7** NTSB Fatal & Non Fatal Air Carrier Accidents by First Occurrence 1983-1999

One of the most noticeable features of figure 2.7 is the high percentage of fatal incidents caused by 'In Flight Encounter With Weather', which is over 25%.

The 'In Flight Collision With Terrain/Water' data is similar to the 'In Flight Encounter With Weather' data in that the percentage of occurrences

are considerably larger for the fatal flights than for the non-fatal flights. In both cases the fatal percentage is approximately 3 times greater than the non-fatal percentage. This disparity shows the relative seriousness of each of these occurrences, and coupled with the large absolute numbers of accidents which occur due to these first occurrences shown in figures 2.5 and 2.6, indicates again the strong visual element present in many accidents.

### 2.1.4 NTSB Civil Aviation Dataset 1982-03

In order to perform analysis on a much larger selection of data the American National Transportation Safety Board website was researched. The website made available a Microsoft Access Database which contained details for all civil aviation accidents (and selected incidents within the United States, its territories and possessions, and in international waters). The data covered accidents from 1982 to 27$^{th}$ October 2003 and contained over 55000 records, 4733 of which were related to helicopter flight.

#### *2.1.4.1 Review by First Occurrence*

A detailed analysis proved complicated due to the way in which some of the data was arranged, making cross referencing with the various tables in the database difficult. As a result a manual analysis was performed over 1000 records in order to give a large sample size which it was hoped would yield results similar to those that would have been obtained with a full sample of the data. The results of the manual analysis are shown in figure 2.8.

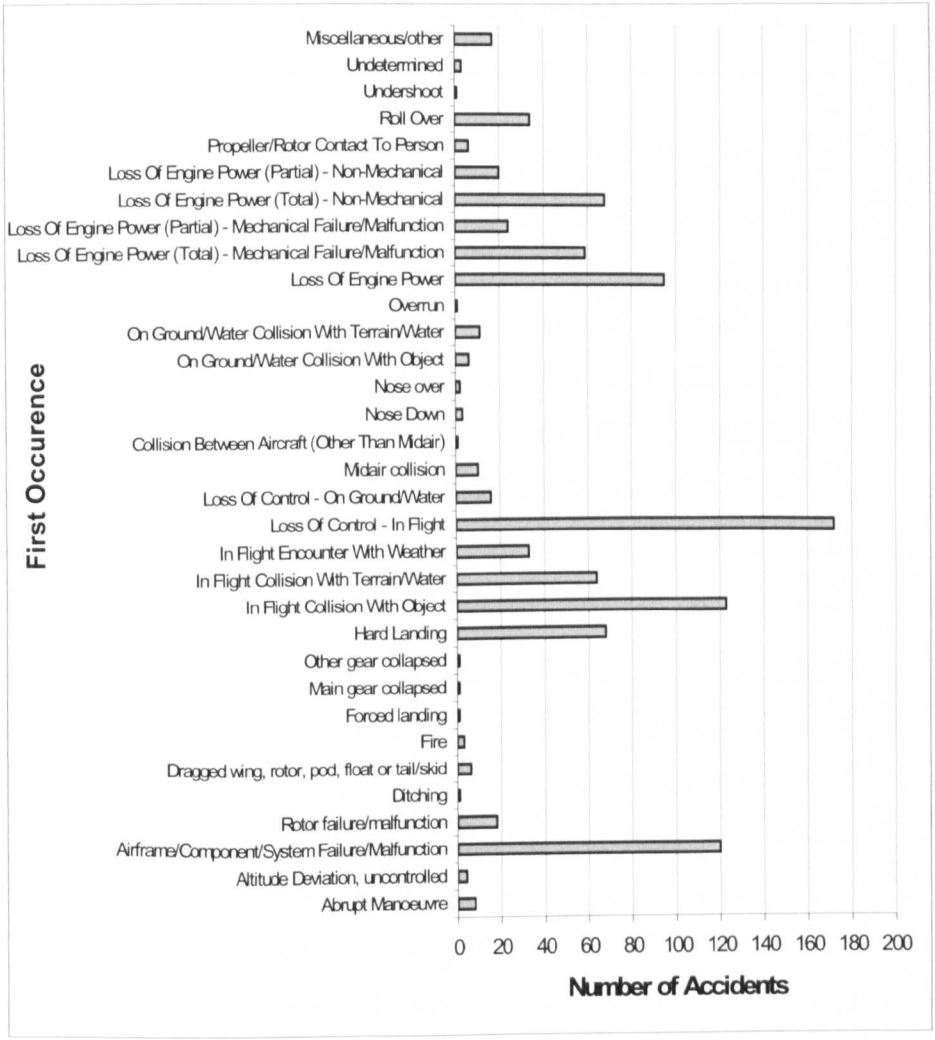


**Figure 2.8** First Occurrence for 1000 samples of all US Civil Aviation Data 1983-2003

Figure 2.8 shows that the most common first occurrence was 'Loss of Control (In Flight)' with 172 cases. The nearest other occurrences were 'In Flight Collision with Object' (123) and 'Airframe/Component/System Failure/malfunction' (120). Loss of engine power is responsible for 95 incidents then there are a number of other cases each with approximately 60 occurrences. Of particular interest are 'Hard Landing' and 'In Flight Collision With Terrain/Water'. These 'main' cases make up over 75% of the total first occurrences and while the other cases may involve scenarios

in which a guidance system could be used, the main focus for any testing will inevitably be in areas where incidents are most common.

In terms of occurrences which may have been caused by a lack of visual information (e.g. loss of control in flight, in flight collision with object/terrain/water etc), the total percent of visual perception related cases was found to be 42.9%. Again this is an approximate figure and should be treated with a degree of caution as some of the cases which are presumed to be visual perception related may not actually be and, similarly, cases which are not considered to have a visual element could well have had.

#### *2.1.4.2 Review by Phase of Flight*

Further analysis was conducted to determine the phase, or phases, of flight in which most incidents occurred, the results of which are shown in figure 2.9. The phase with the largest number of incidents was clearly landing, with 1311 cases (over 25%). The second largest group was manoeuvring with 669 followed by cruise (494). There were then 3 phases with similar values, descent (410), take-off (392) and hover (365). The only other notable category was approach with 181 cases. All other phases registered less than 100 incidents.

While it is somewhat inevitable that the main phases of flight would have the highest values for incidents, the degree to which the landing phase dominates the results is unexpected. An interesting comparison would be with the data for fixed wing aircraft to see if this result is repeated.

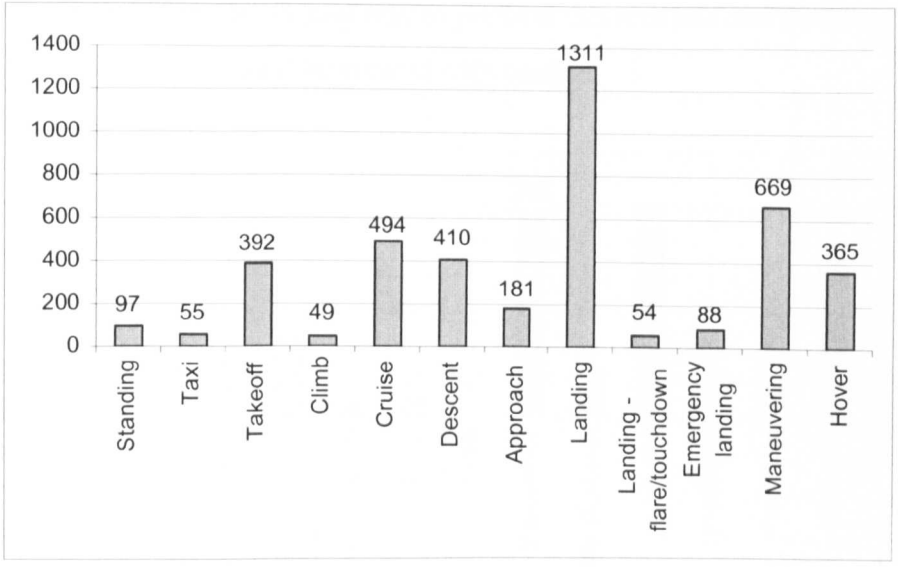


**Figure 2.9** US Civil Aviation Helicopter Accidents by Phase of Flight 1983-2003

*2.1.4.3 Review by Type of Flight (landing phase only)*

Further analysis of the landing phase in relation to 'Type of Flying' is shown in figure 2.10 and indicates that, although there are a large number of unknown flights (255), the majority of incidents occur during instructional (290) or personal (267) flight.

This result can be interpreted in a number of ways. The first is that the landing phase is extremely difficult for novice pilots and therefore this explains why the number of incidents is large for instructional flight. However, as the figure for personal flight is similar this could indicate that, even for qualified pilots, the landing phase is difficult. It should be noted however that due to insufficient data it isn't possible to express these incidents as a percentage of the total flights and therefore the conclusions drawn from the graphical evidence could be inaccurate. For example if there were a total of 1000 instructional landings and 100000 personal landings, both yielding a similar total number of incidents, the likelihood of an incident occurring in instructional flight is 100 times greater.

Unfortunately there is no easy way to perform this analysis and therefore the data presented should be viewed with caution.

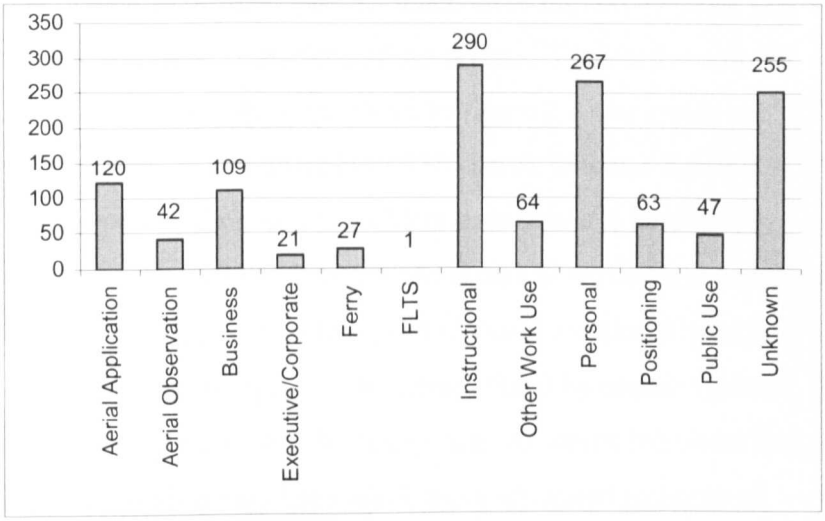


**Figure 2.10** US Civil Aviation Accidents by Type of Flying for landing phase only 1983-2003

Due to the arrangement of the data it was difficult to perform any analysis regarding injuries, fatalities etc. Although this would have been possible in theory, the method used would have been the same as that for the analysis of the first occurrence data i.e. the relevant fields would have been extracted manually from the entire data set. Given the amount of time that this would take it was decided not to repeat the procedure again as the injury/fatality figures were not as useful to the analysis as the occurrence data.

However, a sample of data which recorded the damage to the aircraft was taken. Although this doesn't inform the project in any way, it does give an indication of the seriousness of many helicopter crashes, with 3307 of 4733 cases causing substantial damage and 1300 destroying the aircraft. Thus, over 97% of the incidents caused substantial damage or destroyed the aircraft, a statistic which emphasises the need to improve the safety of helicopter flight in any way possible.

### 2.1.5 Discussion of Safety Review Documents

The CAA and NTSB documents were used to gain an insight into the causes and outcomes of helicopter accidents over the last 20 years (13 years for the CAA data) at the time of the review. Figures 2.4 and 2.9 provide somewhat misleading results as, in figure 2.4, the cruise and descent phases seem to dominate (119/338 cases), whereas figure 2.9 shows that the principal phase for accident occurrence is landing (1311/4733). As the figure 2.4 data is based on US Airtaxi and Commuter flights and the figure 2.9 data refers to all US civil aviation flights this could be indicative of the specific challenges faced by certain types of flight (as defined by the FAR). In theory, aircraft which fall under the 'commuter' description may have much more advanced technology onboard than general civil aviation aircraft, for example instrument landing system (ILS) guidance, which could drastically reduce the number of accident occurrences in the landing phase.

Figures 2.5, 2.6 and 2.7 show first occurrence results for the NTSB 'Airtaxi and Commuter' dataset. Clearly the most common occurrence throughout is 'In Flight Encounter With Weather', which is particularly prevalent when assessing fatal accidents. Figure 2.7 shows that over 25% of all fatal flights are attributable to this event. Other occurrences such as 'In Flight Collision with Object' and 'In Flight Collision with Terrain/Water' also feature prominently in figure 2.7 with values of 9.8% and 10.9% respectively. In terms of the research project this is an interesting result as visual perception related results therefore contribute to approximately 45% of all fatal accidents. This result shows that any successful prospective guidance based system could be useful for a large number of incidents and could, ultimately, save lives.

Continuing to examine the first occurrence of accidents, the graphs produced from the NTSB Civil Aviation data again show slightly differing results to those produced from the NTSB Air Carrier data. While it should be noted that the first occurrence data plotted in figure 2.8 is only a representative sample (1000 pieces of data from 4733), the 'main' occurrences as noted in figure 2.5 also seem to be well represented in figure 2.8. For example, 'Loss Of Control - In Flight' and 'Airframe/Component/System Failure/Malfunction' are prominent in both figures. One of the most noticeable differences between the two figures is the reduced eminence of the 'In Flight Encounter With Weather' occurrence which is responsible for 44/338 accidents (approximately 13%) in the Airtaxi and Commuter data (Reference 3) and just 33/1000 accidents (approx. 3.3%) in the Civil Aviation data. While this difference may be due to the restricted sample size (approx. 21% or the total data), it seems unlikely that this would result in such a large difference between the two values. Although this is not a critical factor in the results of the analysis, it had been assumed that weather would play a major role in many accidents, especially in relation to helicopter flight. This view was reinforced after reading the CAA documents which showed that, of the 36 fatal flights between 1990-2001, 14 were deemed to be project related and of these, 10 were due to weather effects, i.e. approximately 28% of all fatal flights. This percentage is remarkably similar to that shown in figure 2.7 for the 'In Flight Encounter With Weather – Fatal' column (26%). By way of further investigation into these figures, the complete dataset found in the NTSB's Civil Aviation Data could be analysed in order to determine if the 'In Flight Encounter With Weather' figures are accurate, or whether a larger sample size may influence the results.

### 2.1.6 Conclusions

Research has been conducted into causes of rotorcraft accidents over the last 20 years of available data (at the time of the review) using readily available information for both the UK and USA. The data has been analysed, with the focus on results that could inform the future direction of this research project. In particular, areas such as the phase of flight that accidents take place in and the first occurrence have been investigated.

The following conclusions can be drawn from the analysis:

- The most common phases in which accidents occur are cruise/descent (data for the individual phases was not available) and also landing. Data taken from the NTSB Civil Aviation Data also shows that manoeuvring produces a large number of accidents (669/4419).

- The first occurrences 'In Flight Collision With Object' and 'Loss Of Control - In Flight' figure prominently in both sets of US data. Both can be assumed to be related to this research project due to the visual/spatial perception elements of each.

- The most common occurrence for fatal Airtaxi and Commuter flights is 'In Flight Encounter With Weather' which is the first occurrence for over 25% of all accidents. Given the importance of this occurrence it was thought that flight trials could be designed to investigate the effects in more detail. Although the Landscape software was theoretically capable of such meteorological effects, it was thought that such research was not suited to the initial flight testing. Instead, the intention was for weather effects to be considered both when the in-house technology was at a more usable stage of operation and, also, after this project had investigated and gained a

level of understanding of performance in non-weather affected conditions.

- Of 36 fatal flights listed in the CAA documents, 14 were assumed to be related to the SkyGuides project given the description of the incidents (approximately 39%). Of these cases, 10 stated that the weather was a contributing factor (i.e. 71% of all SkyGuides related incidents and 28% of all fatal accidents).

- The general prominence of accidents in the descent, approach and landing phases through the NTSB data suggests that a flight test based around these phases would offer a useful 'real world' aspect to the research, with the investigation targeted around aspects of flight for which a guidance system could make an impact on flight safety.

## 2.2 LITERATURE REVIEW

In addition to the safety review, a more general literature search was conducted in order to discover what research had already been conducted in the field, with a specific focus being on civilian rather than military research. Several examples relate directly to tau theory and these are discussed in the next sub-section, whilst this particular section examines non tau-related research.

When attempting to simulate degraded visual conditions there are a number of ways in which the degradation can be achieved, be it through the introduction of fog (Jump and Padfield, 2005) or reduction of macro textures (e.g. trees within the scene) or micro textures (e.g. the detail of surface texture) within the scene (Padfield et al, 2002). One particular investigation examined the way in which degraded visual cues affect the

pilot's ability to avoid obstructions (Hoh, 1990). One of the conclusions drawn was that a lack of fine detail (i.e. microtextures) can result in a substantial increase in the workload required simply to control a helicopter in hover or low speed NOE flight. This linking of the task to increasing workload, while not a profoundly surprising result, provides a clear indication of the way in which a relatively simple task such as hovering can lead to excessive workload if the visual cues are not sufficient. With workload increasing by large amounts simply because of the requirements of the primary task, this leaves the pilot with very little spare capacity to maintain awareness of the rotorcraft's position and rates with respect to the ground or obstructions within the environment. With any other detrimental effects to compound the problem, such as turbulence, generally poor weather conditions, basic rotorcraft handling qualities etc., this can create a workload which exceeds the pilot's capacity, resulting in flight safety being compromised. Therefore, what can initially be a relatively simple task with a lack of detailed microtextural cues can quickly escalate into a major test of a pilots flying skill, with the pilots control of the aircraft, and therefore flight safety, becoming threatened.

The most critical aspect which a Prospective Skyguide in the form of a HUD would seek to remedy is task performance in degraded visual conditions, although HUDs have other associated advantages in GVE such as a general improvement of situational awareness, reduced workload and a large reduction of 'eyes down' time needed whilst looking at the traditional instrument panel. However, performance in DVE can also be improved by better stabilisation through control system development. One pertinent question is, which is the better option? Previous research (Hoh, 1990) has sought to answer this question. The conclusion drawn was that although the use of attitude command augmentation in low speed flight and hover was found to be effective as a means to make up for visual cue

deficiencies in the scene, there was a corresponding loss of agility with the tested attitude command/attitude hold system which led to negative pilot comments. The specifics of attitude command/attitude hold etc. control systems are beyond the scope of this research, although (Anon, 2000) is a useful place to start should further reading be required. The main conclusion reached with regard to the relative benefits between the control system and synthetic visual aid was that the best solution would be to improve the visual content of the scene, preferably through the improvement of microtexture visibility (Hoh, 1986).

Other researchers have taken a slightly different approach to determining what is important within a scene. For example, (Deighton, 1996) rated a variety of visual cueing strategies (VCS), e.g. streaming, line features, vertical backdrop etc., alongside the specific activity that the VCS was being conducted within, e.g. track, heading, ground position etc. A relative 'importance' rating was given based on the importance of VCS to visual flight activities, visual flight activities to tasks and for the precision needed for a task within a particular mission. The three numerical values for each of the initial importance ratings were multiplied and the cube root of the resulting number was taken, which gave the 'relative importance'. The two highest ranked tasks were found to be nap-of-the-earth, with map position the corresponding activity for the task. In terms of the VCS, 'coincidence of objects' received the highest rating (9.32), whilst 'recognisable features' was the second equal highest rated (9.00). It should be noted that this research was specifically aimed at battlefield operations, although from a civil perspective the visual requirements will be similar, with the pilot aiming to pick up the same information from the scene. The results show the particular difficulties associated with NOE flight, with low level operations requiring reliable, and preferably multiple, sources of visual cues.

Moving away from flight in the aerospace sense, research has suggested that honeybees may hold useful clues as to what visual cue information in the scene may be the most valuable (Fox, 2001). By coaxing honeybees to travel through a perspex tunnel, researchers observed that they travelled through the centre of the tunnel. Clearly there is nothing particularly stunning about this revelation as the bees were simply picking the lateral position which ensured they stayed as far away from the walls of the tunnel as possible. However, the experimental setup was such that along either side of the tunnel was a polka-dot pattern attached to a belt drive. When activated, the pattern moved forwards in the direction of flight on just one side of the tunnel. Because the bees were moving with the polka-dot pattern it would seem as if the visual information on that side was moving slower in relation to the other, unaffected side of the tunnel. Optic flow dictates that the closer that something is to the observer, the faster it seems to move (imagine travelling on a train and looking at trackside hedges compared to hedges in a field a large distance away). Therefore the bees, which depend on optic flow for visual perception, would move towards the side of the tunnel with the moving belt in order to balance the rate of optic flow on both sides of the tunnel.

Clearly optic flow seems to be a powerful perceptive tool which honeybees use to guide motion, but does it apply to humans as well? Optic flow is part of the theory of ecological psychology, which in turn is just one branch of psychology which is postulated to be responsible for visual perception in humans. The review will now examine this subject area.

## 2.3 VISUAL PERCEPTION AND TAU

The key area upon which the project was based was tau theory. Tau has its roots in ecological psychology, one of the most basic elements of which

states that the motion of the observer and the perception of the environment are inextricably linked. Before focusing on tau in detail, it is worth noting where ecological psychology, and therefore tau, sit in the expansive subject of visual perception.

## 2.3.1 Visual Perception Theories

There are two schools of thought which essentially compete with each other in an attempt to explain how we perceive the world around us. As we have already noted, tau falls under the ecological psychology banner, with cognitive psychology, or the constructionist view (also referred to as 'constructivist' amongst many other labels) forming the other viewpoint.

### *2.3.1.1 Constructionist Approach*

The Constructionist viewpoint generally points to the 19th Century German physicist Hermann von Helmholtz as its forefather, although its roots are much older than this. Helmholtz's belief was that we come to see the world around us through experience, interacting and experimenting with it. Essentially perception needs to be learned and, in addition, must go beyond what is available to the senses. A classically referenced term when discussing constructionist theory is 'unconscious inference', that is, vision requires the derivation of a probable interpretation from incomplete data (Helmholtz, 1867; Helmholtz, 1910). The implication of this, based on the inferences made, is that there is some sort of choice to be made between alternative interpretations of a stimulus, or in Helmholtz's words:

> *"The sensations of the senses are tokens for consciousness, it being left to our intelligence to learn how to comprehend their meaning. The only psychic activity required for this purpose is the regularly recurrent association between two ideas which have often been connected before." (Helmholtz 1910).*

More recently Helmholtz's Constructionist work has been furthered by, the perhaps unfortunately named, Boring. In one particular experiment (Holway and Boring, 1941) subjects were required to judge the size of a disk which was presented at varying distances under what was termed as a condition of increasing 'reduction'. Reduction referred to the gradual reduction of distance cues in the scene, and does not seem to be dissimilar to flight testing in DVE. The experiment found that as the cues were reduced, the poorer the size constancy was, that is, more of the judgements were of the proximal size of the disk rather than the distal size. Boring used the results of this experiment to further the work of another eminent Constructionist, Titchener, who had developed the 'core-context theory of meaning' (Titchener, 1914). The theory states that any new mental process (the core) acquires its meaning from the context of other mental processes within which it occurs. Boring suggests that the core is the basic sensory excitation that identifies the perception that connects it most directly with the object of which it is a perception. The other sensory data which modifies or corrects the data of the core as it forms the perception is the context (Boring, 1946). Boring combines the core-context theory with the essence of the Constructionist view when he concludes:

> *"The context also includes certain acquired properties of the brain, properties that are specific to the particular perception and contribute to the modification of its core. In other words, the context includes knowledge about the perceived object as determined by past experience, that is, by all the brain habits which affect perceiving." (Boring 1946).*

The most prolific advocate of the constructionist approach in more recent years has been Irvin Rock (Rock, 1977; Rock, 1983; Rock, 1997). In (Rock, 1983) the entire document is devoted to documenting the evidence in favour of the constructionist view, with the very first sentence in the work being:

> *"The thesis of this book is that perception is intelligent in that it is based on operations similar to those that characterize thought" (Rock, 1983, p. 1).*

Perhaps the clearest indication of the differences between the constructionist and ecological views of visual perception, and a theory which is particularly relevant given the work conducted in Chapter 5, are Rock's thoughts on the question of size perception:

> *I will argue that the process of achieving constancy is one of deductive inference where the relevant 'premises' are immediately known. That is to say, in the case of a specific constancy such as that of size, two aspects of the proximal stimulus are most relevant, one being the visual angle subtended by the object and the other being information about the object's distance. ( Rock, 1983 p. 240)*

In keeping with all proponents of the Constructionist theory, Rock sees size perception as depending, in turn, on two further perceptions, proximal size and distance. Although the emphases of the various advocates of the Constructionist viewpoint vary slightly, the essence of the argument is that in order to achieve size constancy there must be some form of combination of proximal size information and distance information.

The following brief analysis of the Ecological approach and discussion of $\tau$ will show how the two theories oppose each other.

#### *2.3.1.2 Ecological Approach*

In purely historical terms, the ecological approach is much younger than the Constructionist view, having been developed and pioneered by James Gibson in the mid-20$^{th}$ Century (Gibson, 1950). Gibson's approach was based in the natural world and its interaction with the surrounding environment from the outset. Hence, as Gibson moved into more philosophical areas in his later work, he applied the term 'Ecological Psychology' (Gibson, 1977), inextricably relating his work to the environment around us.

Perhaps the most relevant work on ecological psychology is found as Gibson develops his theories further and directly questions the Constructionist Theory, whilst also exploring the concept of affordances which had been introduced earlier (Gibson, 1977) in much more detail (Gibson, 1979).

> *"The affordances of the environment are what it offers the animal, what it provides or furnishes, either for good or for ill." (Gibson, 1979).*

The suggestion is that when we look at objects we perceive their affordances rather than their qualities. In addition, Gibson hypothesised that the basic affordances of an environment are perceivable, usually directly, without a significant amount of learning, a view that was clearly opposed to that of the constructionist view. The affordance of an object depends on the individual's perception of what the object can do for them or, in other words, it is an opportunity of action. Therefore an adult may perceive that an empty cardboard box affords storage, whilst a young child might determine that it affords shelter or, more commonly, 'fun'.

In his earlier work Gibson also investigated size perception during World War II. A number of aviation cadets were required to match the height of a series of stakes planted at various distances in a large field with a set of stakes of varying size nearby. The experiment found that although the subjects' judgement became more variable with distance, they did not become smaller, therefore size constancy did not break down (Gibson, 1979).

> *"No matter how far away the object was, it intercepted or occluded the same number of texture elements of the ground. This is an invariant ratio. For any distance the proportion of the stake extending above the horizon to that extending below the horizon was invariant. These invariants are not cues but information for direct size perception." (Gibson, 1979).*

In making the proposal that these invariant ratios are responsible for direct size perception Gibson also goes on to state that they are picked up 'unawares'. There is therefore, in Gibson's view, no need for perceived distance to be involved in the perceptual process, again a view that wholly opposes the Constructionist Theory.

The final part of Gibson's work to be considered in this brief evaluation is optic flow. Again, this work was initially based around aviation, with Gibson preparing training films for pilots during World War II. The training films showed a picture of a typical scene in which the pilot might be flying, with optic flow information overlaid to give an impression of the motion through the scene. Figure 2.11 shows an example of an optic flow scene (taken from (Gibson, 1979)). From this Gibson went on to develop his theory of optic flow which, in contrast to much of the previous perception work, did not focus on static images. Gibson's viewpoint was that we rarely view a static world, either the environment around us is moving or we ourselves (in psychological terms, the 'actor') are moving. This movement generates patterns of image motion on the retina which follow a very lawful and systematic transformation. The pattern is that the rate at which the image moves across the retina is an inverse function of its distance from the actor.

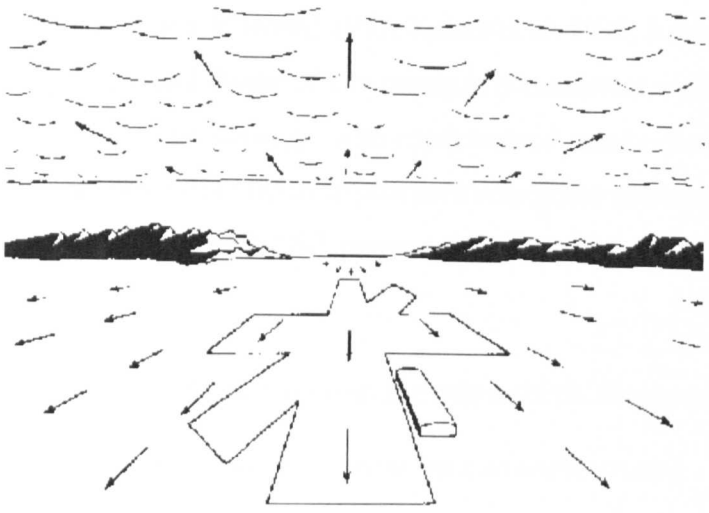

**Figure 2.11** Optic flow fields seen by pilot approaching a runway

As per his environmental roots, Gibson's work on optic flow covered investigations into both aircraft landings (Gibson, 1955) and, more generally, locomotion and orientation in animals (Gibson, 1958). In concluding his work on aircraft landings Gibson says:

> *"Assuming that these variables (of the optic flow pattern) are stimuli for perception, they can determine not only the experience of a stable tridimensional world, but provide a basis for the judgements required for the control of locomotion in that world." (Gibson, 1955).*

These initial musings and theories on optic flow over 50 years ago are still entirely relevant for this project, with the predominantly tau based research being part of Gibson's original ecological theory.

Indeed, more current research, more specifically NASA research, still focuses on the nature of optic flow and its usefulness to pilots as a means of extracting temporal range information without the use of velocity or

distance cues (Kaiser and Mowafy, 1993; Kaiser et al, 1993; Johnson and Awe, 1994). The general theme of this research is consistent with the Gibsonian approach to psychology, with experimental results confirming that test pilots use optic flow fields to prospectively guide passage through the visual environment. The NASA research has also gone on to examine optical tau variables::

> *"We propose that these tau cues provide a useful temporal metric for pilots to employ in planning and orchestrating vehicular control." (Kaiser and Mowafy, 1993)*

There are even some researchers who have attempted to straddle the divide of the constructionist and ecological theories by suggesting that, in a broader theory of perception, both can coexist in harmony (Norman, 2002).

The Constructionist vs. Ecological debate will no doubt continue unabated for many years to come, possibly to be joined by another, as yet, undiscovered and unnamed theory to add to the confusion. However, for the purposes of this research, the intention is not to attempt to prove or disprove the arguments of Ecological or Constructionist Theory. The focus is, merely, on tau and whether it exists as a tool for prospective guidance in the flight tests conducted.

### 2.3.2 Tau Theory

In a metaphorical sense the beacon of ecological psychology theories developed by Gibson were passed on, amongst others, to Lee, probably as a direct result of the discussions between the two at Cornell University during 1969-70. Initially $\tau$ was essentially based in optics, with the focus being on light, with the stimulating effects of other forms of energy such as sound somewhat neglected. However, as $\tau$ developed it also grew and

encompassed a much larger range of stimuli, eventually resulting in General Tau Theory.

*2.3.2.1 $\tau$ and $\dot{\tau}$*

Tau is defined as the time-to-contact or close to an obstacle or surface at the current rate of closure. If the specific closure being considered is one that will result in direct contact with an object or surface the term used is time-to-contact (TTC). In the event that the motion (if indeed we are considering the $\tau$ of a motion) being considered is not heading directly for an object or surface, time-to-passage (TTP) is used.

In this research the focus has been firmly on the tau of the motion gap in the $x$ axis, $\tau_x$. However, there are a wide range of gaps which can be considered, including angular gaps (e.g. turning a thermostat dial to the required temperature marker), pitch gaps (e.g. a singer changing the pitch of their voice when singing a song) and many more. In terms of this project, the simplest representation of $\tau$ is in terms of the $x$ axis motion gap. If $x$ is the distance to the target and $\dot{x}$ is the velocity in the $x$ direction then the $\tau$ of the motion gap is:

$$\tau_x = \frac{x}{\dot{x}} \tag{2-1}$$

One of the critical points to understand about Eq. 2-1 is that the observer is not controlling $\Delta x$ or $\dot{x}$ in an attempt to subsequently control $\tau_x$, but is instead picking up $\tau_x$ directly from the optic flow in the scene and using that to prospectively guide motion.

The first incarnation of $\tau$ examined the visual control of locomotion with drivers being asked to brake to stop at a certain point. In this sense $\tau$ was

simply considered as an optical variable which specifies TTC if the closing velocity is maintained (Lee, 1976). One of the focal points for this investigation, and for many more since, was the question 'how does the observer/organism avoid crashing?' or, in other words, how is deceleration controlled?

The control of the rate of change of $\tau_x$, i.e. $\dot{\tau}_x$, is thought to be one strategy used to avoid collisions. Therefore, differentiating Eq. 2-1:

$$\dot{\tau}_x = 1 - \frac{x\ddot{x}}{\dot{x}^2} \tag{2-2}$$

The normal convention is to use negative distances to indicate that the target has not been reached, therefore with $x<0$, then $\dot{\tau}_x>1$ implies accelerative flight (i.e. $\ddot{x}>0$), $\dot{\tau}_x=1$ corresponds to constant velocity ($\ddot{x}=0$) and $\dot{\tau}_x<1$ implies a deceleration ($\ddot{x}<0$).

If we consider a constant deceleration, $-\ddot{x}$, then the stopping distance from a velocity $\dot{x}$ will be:

$$x = -\frac{\dot{x}^2}{2\ddot{x}} \tag{2-3}$$

Therefore, the object will stop short of the target if:

$$\frac{-\dot{x}^2}{2\ddot{x}} < -x \quad \text{or} \quad \frac{x\ddot{x}}{\dot{x}^2} > 0.5 \tag{2-4}$$

Therefore by combining Eq. 2-4 with Eq. 2-2 we have the required condition in order to stop short of the target and avoid a collision:

$$\dot{\tau}_x < 0.5 \tag{2-5}$$

In the aforementioned experiment which investigated the braking behaviour of test drivers (Lee, 1976), it was found that the test subjects followed Eq. 2-5 with $\dot{\tau}_x$ equal to a mean of 0.425. In this case a $\dot{\tau}_x$ =0.5 would have not been desirable as the motion gap was measured between the front of the moving vehicle and the back of the stationary one, therefore $\dot{\tau}_x$ = 0.5 would have led to a mild bumper-to-bumper contact. A $\dot{\tau}_x$ of less than 0.5 is often referred to as a 'soft stop', whereas a $\dot{\tau}_x$ of greater than 0.5 is a hard stop given the deceleration requirements immediately before contact is made.

The hypothesis which has been developed over the course of many such experiments (Lee, 1981; Lee, 1992; Lee, 1993) is that evolution has provided humans and animals with the ability to rapidly detect and process visual information in terms of the optical variables $\tau$ and $\dot{\tau}$.

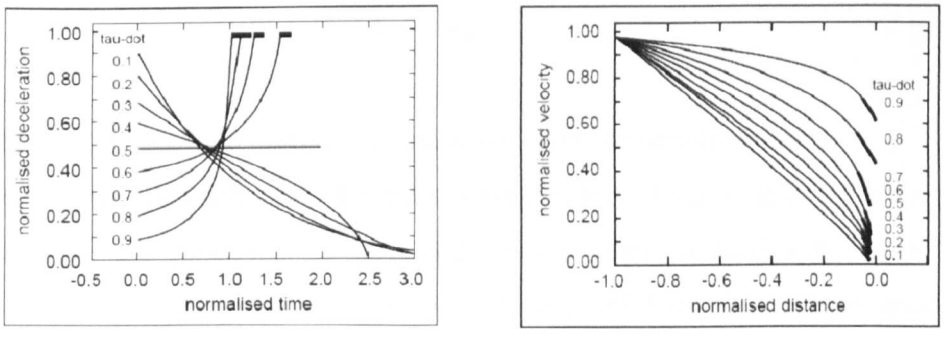


(a) (b)

**Figure 2.12** Kinematics of the Constant $\dot{\tau}$ guide (From Lee, 1992)

Figure 2.12 shows the normalised kinematic profiles when approaching an object or surface and braking so that $\dot{\tau}$ remains constant at the various values shown. As shown in figure 2.12(a), for $0 < \dot{\tau} < 0.5$ this gives a profile where deceleration gradually decreases. When $\dot{\tau}$ =0.5 the

deceleration is constant, with $0.5 < \dot{\tau} < 1$ yielding a gradually increasing level of deceleration. The thicker bars at the top of each of the curves for $\dot{\tau} < 0.5$ represent the deceleration ceiling. Figure 2.12(b) shows the corresponding normalised velocity profiles for the same constant $\dot{\tau}$ values.

### *2.3.2.2 $\tau$-coupling*

As discussed, the concept of a closing a single gap, usually motion based, using tau has been well documented and the experimental evidence provides a powerful argument for the use of $\tau$. However, motion is often active in more than one axis. For example, if a ball is thrown then in order to catch it we have to interpret the flight path of the ball and also move our hand to a position where the ball and hand will meet. In order to achieve this we must quickly and accurately detect and close more than one motion gap. $\tau$ theory hypothesises that $\tau$-coupling is the way in which this is achieved, that is, the $\tau$'s of the gaps are kept in constant ratio during the movement, i.e.:

$$\tau_x = k\tau_z \tag{2-6}$$

Eq. 2-6 shows $\tau$ in terms of $x$ and z, which could be utilised for a helicopter approach where the pilot is decelerating along $x$ and descending along z. The subscripts can be changed to represent any particular $\tau$ gap of interest. Experiments have been conducted with bats using echolocation to land on a perch and also adults passing food to their mouths (Lee, 1995; Lee, 1999), both of which show the use of $\tau$-coupling techniques.

### 2.3.2.3 *Intrinsic $\tau$-guides*

In many cases the $\tau$-coupling is based on an extrinsic guide, in the case of the adults passing food to their mouth there was a coupling between $\tau_r$ (the hand-mouth gap) and $\tau_\alpha$ (the angular gap to be closed). However, there are cases where there is only one gap to be controlled, for example, beating a drum, or putting a golf ball. The kinematics of the controlled closure of motion gaps in these examples is similar whether there are two coupled motion gaps or just one. These findings led to the development of the intrinsically-generated tau-guide hypothesis. That is, the tau of the single motion gap between, say, the face of the putter and the golf ball is coupled onto an intrinsically generated tau guide, $\tau_g$ (Lee, 1998).

$$\tau_x = k\tau_g \tag{2-7}$$

Eq. 2-7 shows the way in which $\tau_x$ and $\tau_g$ are coupled, again with a coupling constant, k. Intrinsic $\tau_g$ theory theorises that, as it is thought that neural processes have evolved to enable us to guide movement using $\tau$-coupling of extrinsic taus, it is possible that the same evolutionary steps might have occurred to guide movement when there are no extrinsic taus to couple onto (Lee, 1998). Therefore, while extrinsic coupling relies on the senses to provide information, intrinsic coupling relies on the nervous system generating the intrinsic $\tau_g$.

Since the $\tau$-guide was initially conceptualised it has evolved into a number of separate $\tau$-guides, each of which can be used in various situations depending on the nature of the task being conducted. For example:

- The constant velocity $\tau$ -guide:

$$\tau_g = (t - T) \tag{2-8}$$

- The constant deceleration $\tau$ -guide:

$$\tau_g = \frac{1}{2}(t - T) \tag{2-9}$$

- The constant acceleration $\tau$ -guide

$$\tau_g = \frac{1}{2}\left(t - \frac{T^2}{t}\right) \tag{2-10}$$

- The general intrinsic $\tau$ -guide

$$\tau_G = \frac{t(T + t)}{T + 2t} \tag{2-11}$$

*2.3.2.4 Is it really $\tau$ ?*

To close this section on $\tau$ it is only fair to consider the views of those who disagree with $\tau$ theory. Just as the Constructionists argue against Ecological theory, there are some researchers who believe that there are other ways to explain the ability to capture motion gaps which do not involve and, indeed, actively dismiss $\tau$ .

In one such example, the misinterpretation of road drivers' TTC with pedestrians was investigated. The suggestion of the investigation was that as TTC increases, its cognitive derivation should transfer from optic flow to separate perceptions of distance and speed (Stewart et al, 1993). Furthermore, the authors propose that when drivers are in a potential

collision with pedestrians perception of distance is primarily based on familiar size, resulting in overestimation of size, and therefore TTC, with child pedestrians. While the authors did not dismiss the validity of $\tau$, they suggest that at large distances observers perceive size, distance and velocity/acceleration separately and then integrate them. At short distances they surmise that TTC information is available directly via $\tau$. Clearly this reliance on size, distance and 'familiar size' is based in the Constructionist view of psychology, further exemplifying the debate between the two viewpoints.

In a separate paper, there is a more damning rebuffal of $\tau$, with the author claiming that "$\tau$ *-hypothesis is false*" (Tresilian, 1999). However, it is again proposed, within the same paper, that despite the above quote, $\tau$ simply can not account for all judgements of TTC and does still has a very definite place in TTC estimation.

Other research has been more dismissive of $\tau$. One particular investigation examined the judgement of TTC between a laterally moving object and a bar (Smeets et al, 1996). The researchers used moving backgrounds to induce changes in perceived velocities without changing the optical variables which specify TTC. This background motion was found to induce large systematic errors in the subjects' estimated TTC. The authors therefore concluded that judgement of TTC is essentially based on the ratio between perceived distance and perceived velocity as opposed to $\tau$.

As a final example, testing with pigeons approaching a perch with an experimental setup similar to (Lee, 1993) was conducted in (Wann, 1996). The simulated results presented took into account the pigeon's natural head-bobbing and the fact that the image of the perch is projected onto a spherical, rather than flat, surface. In this investigation, the $\tau$ of the foot-

perch distance (and, hence, $\dot{\tau}$ ) was shown to be non-linear and discontinuous.

Whether $\tau$ -theory is an adequate explanation for all forms of gaps, with any animal and at any distance is not a matter for this author to prove or disprove. The flight tests conducted were simply analysed with a focus on whether some form of $\tau$ -guidance is present and, if so, whether it could be used to provide guidelines for the design of a prospective guidance system.

# Chapter 3

# APPROACH TO HOVER - GVE

## 3.1 INTRODUCTION

The intention of the Approach to Hover research was to develop a test which would offer a clearer indication of a pilots visual cueing, whilst also retaining a definite real-life aspect. Both of these goals were achieved by selecting a relatively simple manoeuvre which would require a reduced number of simultaneously active axes. An approach is clearly a manoeuvre that occurs towards the end of every single up-and-away flight, whether it is precision, non-precision or visual, thus retaining the real-life characteristic. Although the approach is still conducted in an unrestricted environment allowing for movement in the x, y and z axes, on a straight approach with no wind, the motion in the y axis should be negligible. In addition, motion in the x and z axes are ones of controlled deceleration, therefore the task is largely one of guidance with continuous stabilisation corrections.

Before the flight simulation trial design was considered in much more detail, the results of a NASA investigation into a large number of real-life visual approaches to hover to a helipad at an airfield (Moen et al, 1976) were assessed. The reference contained an equation which was similar to

part of Eq. 2-2, suggesting that the NASA tests could have 'discovered' a $\tau$ -based nature to the guidance strategy, without realising it.

Based on this potential $\tau$ relationship, and given that the descent/approach/landing phases of flight were of particular interest from the safety review, it was decided to investigate the approach to hover manoeuvre. In addition to examining the way in which $\tau$ may have been used during the manoeuvre, an analysis was conducted to determine whether the UoL results matched the NASA results. Aspects of the correlation between the NASA and UoL results will be discussed in more detail in section 3.3.2.

## 3.2 OBJECTIVES

The main objective of the analysis was to determine whether the approach to hover manoeuvre (in GVE) was prospectively aided by some form of $\tau$ -guidance, with the results serving as a baseline for a future DVE trial. A follow-on objective was to translate any $\tau$ -guidance findings into a recommendation for the development of a $\tau$ -based Prospective SkyGuide.

Another objective of the Approach to Hover task was to replicate, as far as possible, the NASA experimental setup and determine whether the UoL trial could replicate their findings.

## 3.3 APPRAISAL OF THE NASA TESTS

The NASA tests were conducted to investigate the characteristic shapes of altitude, ground-speed and deceleration profiles for visual approaches in helicopters, in support of the design of a flight director system.

### 3.3.1 Methodology

The tests were designed to give the pilot a free choice over the approach profile chosen. Previous studies to improve the instrument flight capability of helicopters during the final approach phase had examined a number of approach procedures - from the relatively straight-forward Instrument Landing System (ILS) approach to a curved, decelerating, variable glide slope approach. The common feature of these investigations was that the pilots were constrained to fly defined altitude and velocity profiles. Such constraints, no matter how valid to achieve the task, often led to pilots being reluctant to fully commit to the manoeuvre due to unnatural physiological cues. Giving the pilots freedom to select the approach profile would, in principle, reflect a completely "natural" manoeuvre strategy.

The testing was expansive, with 3 initial heights, 3 initial speeds and, to reflect a cross section of operational aircraft at the time, 4 different helicopters used. In total 236 approaches were flown, all from a range in excess of 10000ft. The 3 initial speeds were 50kts, 80kts and 100kts, with the initial altitudes being 500ft, 1000ft and 1500ft. The pilots (the number used is unspecified in the report) were instructed to fly a visual approach from the given initial conditions, avoiding abrupt manoeuvres and assuming that there were fare-paying passengers aboard the aircraft. Test guidelines such as these were completely in keeping with the civil-based focus of this project, allowing the NASA procedure to be faithfully and purposefully replicated.

### 3.3.2 Results

The NASA tests examined a wide range of parameters including altitude, deceleration and pitch attitude profiles. A complete replication of the analysis for all areas of the NASA test would be difficult because of the lack of data for many aspects of the investigation. One of the most intriguing results in the report is provided with the use of the parametric equation selected by NASA, developed to model a generic profile. A number of different parameters were tested during the NASA analysis (although none of these were detailed and no analysis of them was provided), with an '$\frac{\dot{x}^2}{\ddot{x}}$' parameter being deemed to give the best results when plotted as a function of x on a log-log scale. One important area of interest which would be used to compare the Liverpool test results with the NASA results was the NASA defined 'exponent', n. The equation of a straight line plot on a log-log scale is $y = ax^b$ or, $\frac{\dot{x}^2}{\ddot{x}} = cx^n$, where c is the y-axis intercept for $x = 1$ and n is the geometric slope of the straight line.

A key feature of the NASA analysis was their editing of the full range of the data such that their calculations were based only on the deceleration data. The selected range was 2800ft, as it was found that 80% of the deceleration occurred in this range of the approach. This was indicated by a 'd' subscript for all values taken at 2800ft. Plotting the power coefficient 'n' against the initial ground speed $\dot{x}_d$ (i.e. the instantaneous ground speed at 2800ft), it was observed that the values of n decreased as the initial ground speed increased and, more strikingly, a smooth curve could be drawn through seven of the nine data, as shown in figure 3.1.

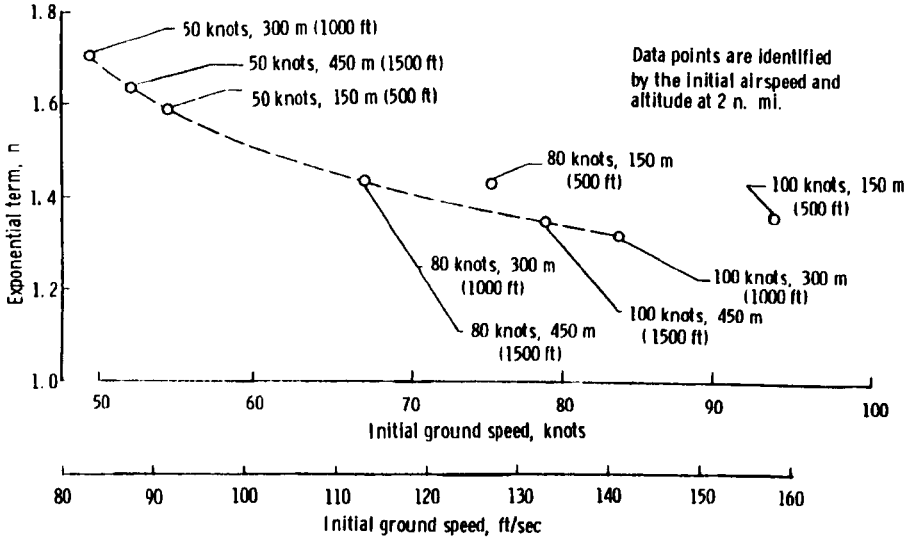


**Figure 3.1** Power parameter, n vs. Groundspeed at 2800ft for decelerating approach to hover (Courtesy, NASA)

One of the more interesting results presented was a slight re-working of the logarithmic straight line equation stated earlier:

$$k_n = \frac{x_d^{\,n}}{\dot{x}_d^{\,2}} \ddot{x}_d \qquad (3\text{-}1)$$

Where $k_n = \frac{1}{c}$. This is very similar to Eq. 2-2, with the implication being that if n=1, $\dot{\tau} = 1 - k_n$. Although the value of n in the NASA results did not fall below 1.3, this still provided an intriguing result, suggesting a $\tau$-based strategy which varied with range. A particular focus for the $\tau$ analysis of the UoL tests would be to determine if the pilots used the variable profile or the simpler $\dot{\tau}$ =constant profile.

the initial test conditions the variations in the characteristic profiles as a function of initial height and speed changes were determined.

All test points showed a concave-up profile over the last 1000ft of the approach. The maximum values for deceleration and pitch attitude occurred during the final 200ft of the manoeuvre.

The equations developed by NASA to represent the ground speed and deceleration profiles were found to closely represent the data obtained during their flight tests.

The results of the NASA trial posed interesting questions which tied in perfectly with the initial objective of the Approach to Hover trial; was there a $\tau$-based relationship being used to guide the manoeuvre? Additionally, could aspects of the NASA results be repeated in the Liverpool flight simulator with an almost identical test setup?

## 3.4 DESIGN OF UOL FLIGHT TEST

### 3.4.1 Aircraft Type

The aircraft used for the trial was a version of the UH-60 Black Hawk, a medium-lift utility helicopter. The aircraft was chosen for a number of reasons. Firstly, both participating test pilots were familiar with this UoL FLIGHTLAB model, therefore they would both be comfortable with the aircraft immediately. Secondly, the Black Hawk was the most computationally stable simulation model available on the UoL flight simulator at the time. Finally, the NASA report gave a brief overview of the four helicopter types used in their trials and the Black Hawk fitted well into this range of types.

### 3.4.2 Database

The first stage to replicating the NASA research involved staging as accurate a reproduction of the trial as possible in good visual conditions. However, it would have been a difficult and time-consuming task to attempt to faithfully replicate the NASA Wallops Flight Centre, circa 1976, in a visual database, so it was assumed that a generic airfield in GVE would offer a similar enough level of detail, and hence visual cues, to be comparable to the NASA test. The selected airfield featured a runway, taxiways, an apron area, some terminal buildings and was surrounded by fields, providing a visually rich scene for the pilot. The hover target point was a helipad, located at the junction of a taxiway exit ramp and the main taxiway. The helipad was visible from the start of the manoeuvre. Figure 3.2 shows the pilot's centre screen view of the database from the start point.

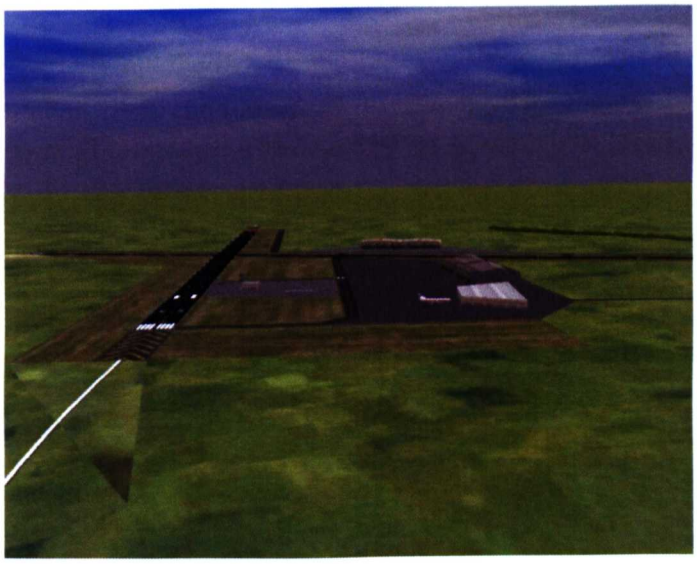

**Figure 3.2** Centre monitor view of scene at start of manoeuvre

### 3.4.3 Test matrix and variables

The test matrix for the approach to hover task replicated the NASA setup with three initial altitudes, 500ft, 1000ft and 1500ft and three initial speeds, 50kts, 80kts and 100kts. When each test run began in the simulator the aircraft was trimmed in straight and level flight. Each pilot flew the 3x3 matrix of test points three times to give a total of 27 runs with 9 unique test matrix points per pilot. The matrix order itself was completely random in order to give the pilot as little indication as possible as to the settings for each test point. In reality however it would be very easy to deduce the initial altitude variable and not especially difficult to do the same with the initial speed variable.

### 3.4.4 Remaining faithful to the NASA tests

In order to conduct as accurate a replication of the NASA tests as possible in a simulation environment it was important to consider all aspects of the test setup, from the physical position of the aircraft at the start of each run to other visual and task conditions surrounding the manoeuvre

One area of uncertainty was the provision of an instrument panel. The NASA report states:

> *"No approach guidance was provided except for the standard aircraft instruments normally used for visual approaches."*

Although the task was intended to be purely visual it was deemed that this statement indicated that the instrument panel was not covered in any way and that, if absolutely necessary, the pilots could still use it for reference. Therefore the experimental setup for this project was such that the pilot had

a full instrument panel, but was briefed to rely solely on visual cues during the approach.

The pilot briefing document which was sent to the test pilots in advance of the trial reiterated the instructions that the NASA report contained, namely that the pilots were free to choose when to commence the descent and deceleration based solely on the visual cues available to them. This information was then restated during the briefing session on the morning of the trials to ensure that the format and aims of the manoeuvre were absolutely clear.

Finally, the pilots were instructed not to mentally prepare for the trial before or during individual manoeuvres. The briefing document stated the values for the three initial heights and speeds that were to be used during the testing, allowing the pilots to calculate an appropriate descent rate for each test point. Previous trial work had shown that at least one of the test pilots used could quite easily calculate and second guess trial settings based upon the briefest of information. While this is an impressive skill it was decided that it might only have an adverse effect on the results if the pilots prepared too much and therefore the briefing guidelines were very clear on this matter.

### 3.4.5 Test Pilots

As previously stated, two test pilots participated in this trial. Both pilots offered considerable experience both in terms of fixed wing and helicopter flight, and also in terms of simulator and real-life experience. In addition, both had flown the Liverpool flight simulator for previous flight trials so were familiar with the visuals, controls etc.

More specific information can be found in their aviation Curriculum Vitae, shown in Appendix A.

## 3.5 UOL SIMULATION RESULTS

The following analysis covers several areas, beginning with a general examination of the data and an appraisal of the individual and comparative strategies of the two pilots to the task. The comparison with the NASA results is then examined, focusing on the power parameter, n. This will be followed by an examination of tau-based data, including $\tau_x$ and $\dot{\tau}_x$ with the results discussed in detail and conclusions are drawn.

Initially the analysis examines the results for the two pilots individually before comparing the results for both.

### 3.5.1 General Data Analysis

#### *3.5.1.1 Pilot AB*

Although most of the analysis has been performed from a range of 2800ft, a number of cases will show results for the full 10000ft range in order to illustrate the piloting strategy in the initial stages of the manoeuvre.

Figures 3.3(a-c) show a series of plots with altitude (z) plotted against range (x). Each figure shows runs for a specific initial test speed. The nine sets of data within each figure correspond to the 3 initial altitudes and the 3 runs within each speed-altitude test matrix setting.

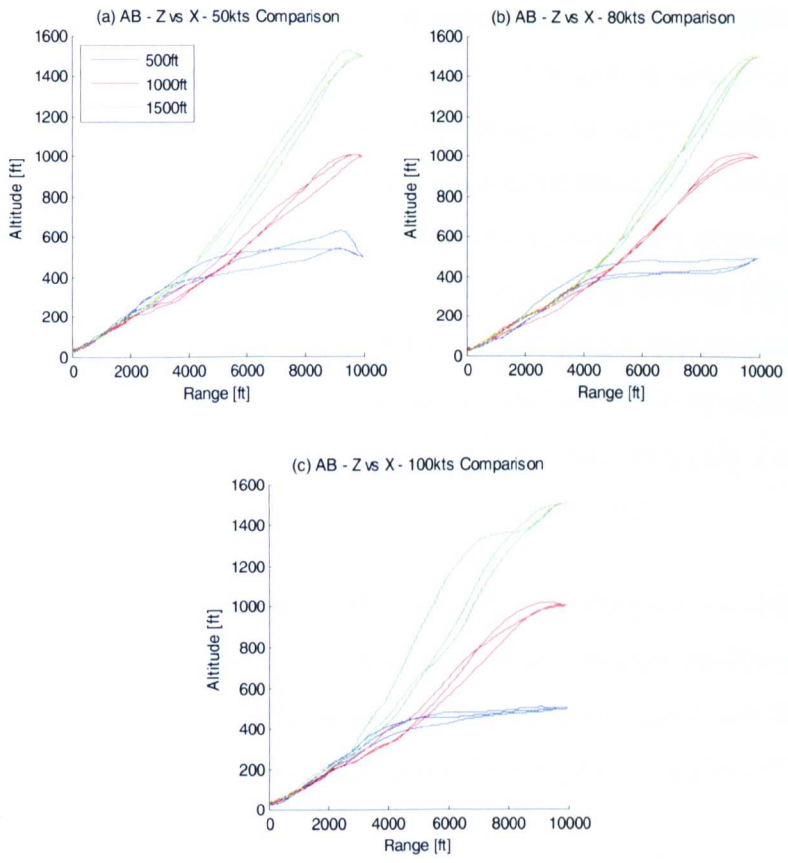


**Figure 3.3** Altitude vs. range for AB (a) 50kts, (b) 80kts and (c) 100kts approaches

Grouping the data together as in figure 3.3 provides a clearer picture of the pilot's overall strategy.

In almost every example shown the pilot appears to split the task into two phases. The first, from the start of the run until approximately 3000ft from the helipad, shows the pilot seemingly adjusting the altitude in order to arrive at a pre-determined condition - an altitude of 300ft at a range of 3000ft. There are some slight 'target-altitude' discrepancies at 3000ft, with 2000ft being the point by which all runs merge on the same glideslope condition (at an altitude of 200ft). However, with no instruments to guide the approach it is inevitable that some scatter will occur, but a general pattern does appear to exist. The second phase of the approach then starts

with each of the 27 runs beginning from approximately the same altitude at the same range, giving a descent angle of 5.7°. For tests starting at an altitude of 500ft the pilot opts to maintain virtually the same altitude for the first 5000ft of the task, only starting any purposeful descent in the final half of the range. In contrast, the 1500ft tasks show a fairly eager descent (giving a flight path angle of 10°) over the first 5-6000ft with the pilot then gradually decreasing the rate of descent to give an overall concave-up profile. Finally, the 1000ft runs are characterised by a much more linear descent (albeit it with a very slight concave-up profile), with only 2 of the 100kts runs showing any great deviation from this profile.

This result indicates a number of things, Firstly, that the pilot is competent and experienced enough to establish himself on an approach profile with a high degree of accuracy and consistency. Secondly it suggests that the scene provides sufficient visual cues to enable the pilot to perform at this level.

Such consistently applied strategies suggest that the pilot could be following an internally generated model which is being used to guide the aircraft, in altitude at least. The immediate question which arises from this conclusion is 'does the groundspeed control follow a similar characteristic?'

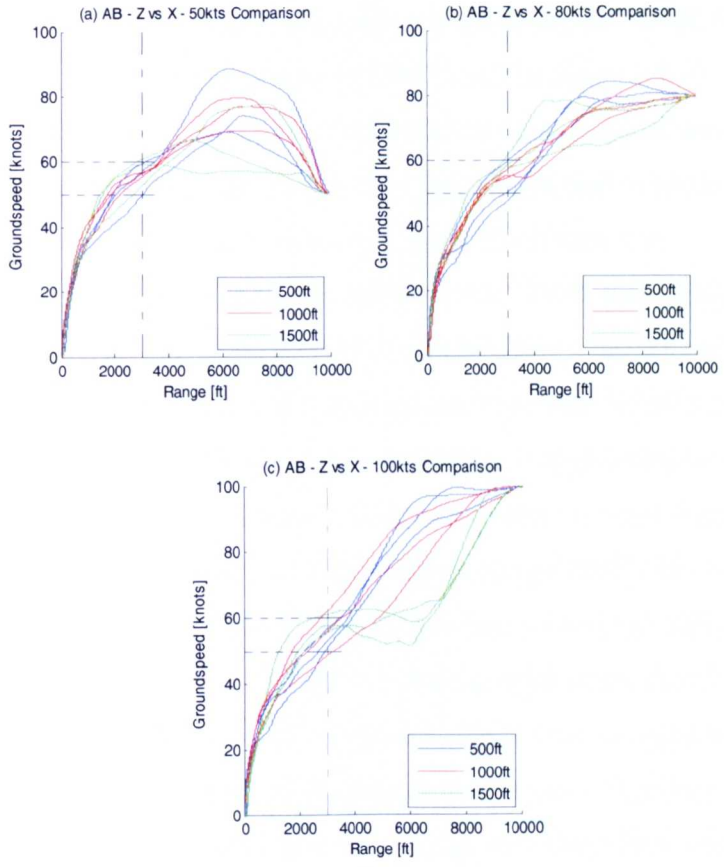


**Figure 3.4** Groundspeed vs. range comparison for AB (a) 50kts, (b) 80kts and (c) 100kts tests

Figure 3.4(a-c) shows groundspeed profiles for all 27 test points, with the three subplots separated again by initial speed. In order to assess the speed more easily, a vertical line at a range of 3000ft and horizontal lines at 50kts and 60kts have been added to the plot.

Despite assorted groundspeed profiles in the 7000ft leading up to the 3000ft point, there is a repeated pattern through the majority of runs, with groundspeed stabilising between 50-60kts at this range. Of the 27 runs, only six have speeds outside the 50-60kts range at 3000ft, with the 'greatest' deviation from the range being just 2kts. As with the altitude vs. range profiles in figure 3.3, it appears that the pilot is purposefully guiding the approach and carefully controlling the speed throughout. Many runs

show the pilot has actively decided upon a specific profile which relates to that test matrix point, for example, the 500ft tests in figure 3.4(c). In these runs the pilot elects to fly for at least 2000ft before any significant deceleration begins (one run does show a slight reduction in speed over this range but there is a much more purposeful deceleration at approximately 7000ft in this test.) Similarly, the 1500ft tests in figure 3.4(c) show a very definite strategy with an immediate, rapid deceleration followed by a period of relatively constant speed around 6-7000ft which continues until the final deceleration commences at approximately 3000ft. The pilot seems to be attempting to attain a consistent height-range profile (i.e. glideslope) throughout the 27 approaches and generally this is an achievable task. However the 1500ft-100kts tests provide an added level of difficulty because there is a need to reduce ground speed significantly whilst descending. Figure 3.4(c) suggests that the pilot recognises that he can only effectively achieve one of these tasks at a time, therefore the ground speed is held constant between a range of 3000-6500ft whilst the pilot attends to the descent task.

With such decisive altitude and groundspeed profiles it is worth examining the deceleration data in order to determine if there are further, precise inputs in keeping with the overall strategy.

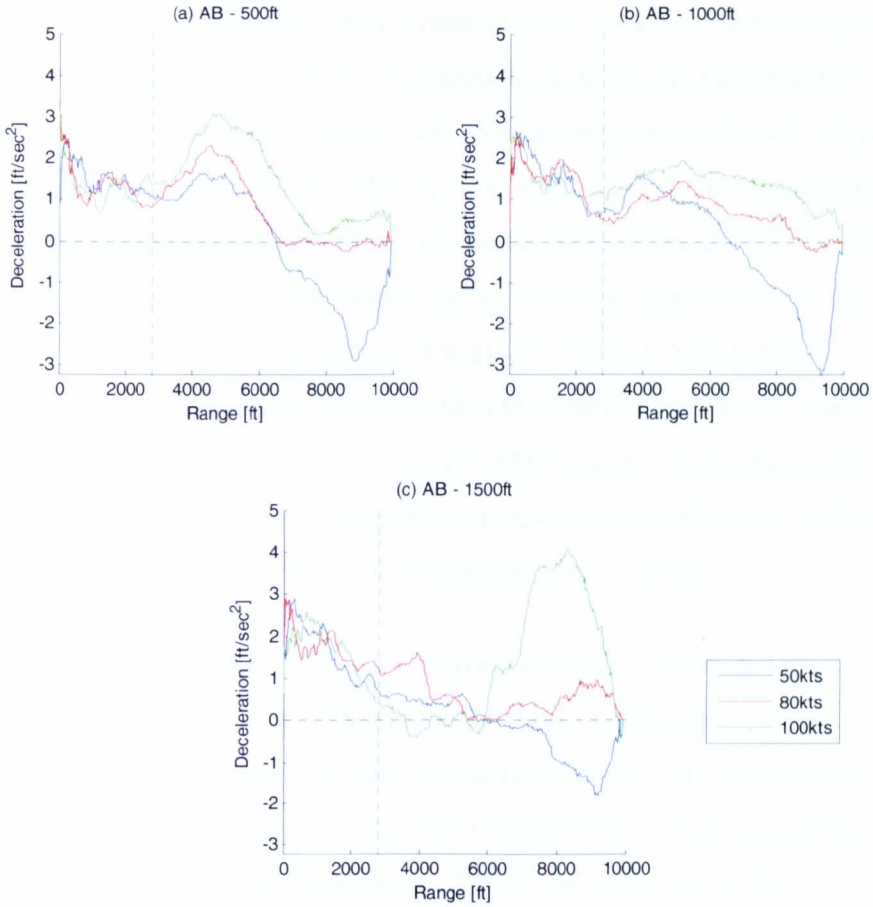


**Figure 3.5** Averaged deceleration profiles for (a) 500ft, (b) 1000ft and (c) 1500ft AB approaches from 10000ft

Given the 'noisier' nature of deceleration plots, the data in figure 3.5 have been averaged in order to make the overall trends easier to observe. The averaging was achieved by taking the three runs for each identical matrix point and then calculating the average deceleration based on the deceleration value for each run. As the range data for each run was unique to that particular run, the method used was to specify a target range value (which, with each iteration, reduced from 10000ft in 5ft steps) and for each 'target' value the deceleration data collected was that which corresponded to the largest range value which was below the target. For example, if the target was 9350ft the range values for each run may have been 9348.8ft, 9349.1ft and 9349.9ft.

The dotted lines on each plot show a deceleration of 0ft/sec$^2$ and a range of 2800ft, respectively. The latter is included because this was the point at which NASA trimmed their data to perform the associated analyses. Based on AB's data it is apparent that picking one point to act as the focus for all deceleration is relatively difficult as, in several cases, there are two phases of deceleration (or, in the 50kts cases, an acceleration phase followed by a deceleration phase). For this data, although 2800ft does not entirely describe all decelerations, it does provide a satisfactory level of accuracy. This is particularly true for the 500ft and 1000ft tests in which the initial, early decelerations (phase one) reaches a momentary pause before the final deceleration resulting in capture of the helipad (phase two).

Strong patterns are more difficult to interpret in the deceleration data, although some do still exist. The first is the point at which 'phase one' ends and 'phase two' begins, as has just been discussed with regard to the NASA trim point. The pilot also reacts to the different initial groundspeed conditions in similar ways throughout. This is shown by the initial accelerations for the 50kts tests and generally strong initial decelerations for the 100kts tests, with the exception of the 500ft 100kts test average in which the deceleration only occurs at a range of 7500ft. This is possibly because the low starting altitude poses less of an issue to the overall task as there is no urgent need to find a balance between descent and deceleration.

Of particular interest after examining the data for the first piloted trial would be how the second pilots' results compared. In theory, as both pilots had thousands of hours of experience it would seem likely that their approach profiles would also follow a similar pattern, which would be a useful result with regard to the original aims of the NASA trial.

### *3.5.1.2 Pilot SC*

The second piloted assessment was conducted in exactly the same manner as the first, with the same aircraft model, database, task conditions and briefing document used. Therefore, although the two trials were conducted several months apart, the procedure was identical, facilitating direct comparison.

Initial examination of the results of the second trial revealed that there were differences in the pilot's technique. This was most evident in the altitude profiles for SC, which showed a more direct approach strategy.

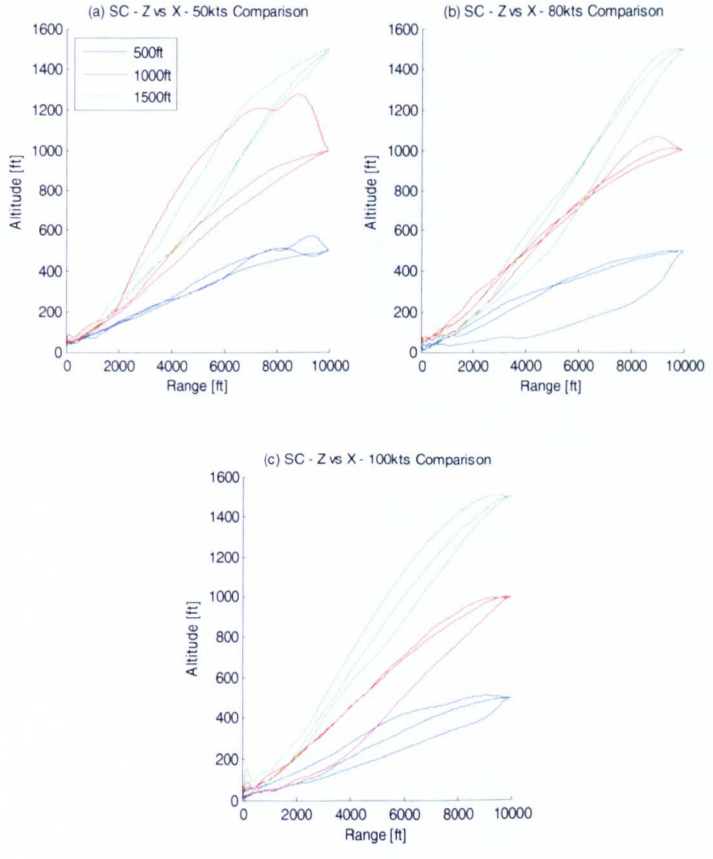


**Figure 3.6** Altitude vs. range for SC approaches

Figure 3.6 shows the altitude vs. range data for pilot SC's approaches, again separated by initial speed as in figure 3.3. Although there are some exceptions to the general trend, two main points can be observed. Firstly, the approaches are much more direct than AB's. In many cases shown in figure 3.6 the data approximate to a straight line drawn between the start and end points of the tests, a point which was only especially true for AB's 1000ft runs. This point is especially clear in figure 3.6(c). Secondly, as a result of the first point, SC does not show a similar strategy to AB in terms of attempting to converge all runs at the same range and altitude to give a consistent approach over the final 3000ft of the tests. Instead, the range of altitudes at 3000ft is very wide, from 74ft to 512ft.

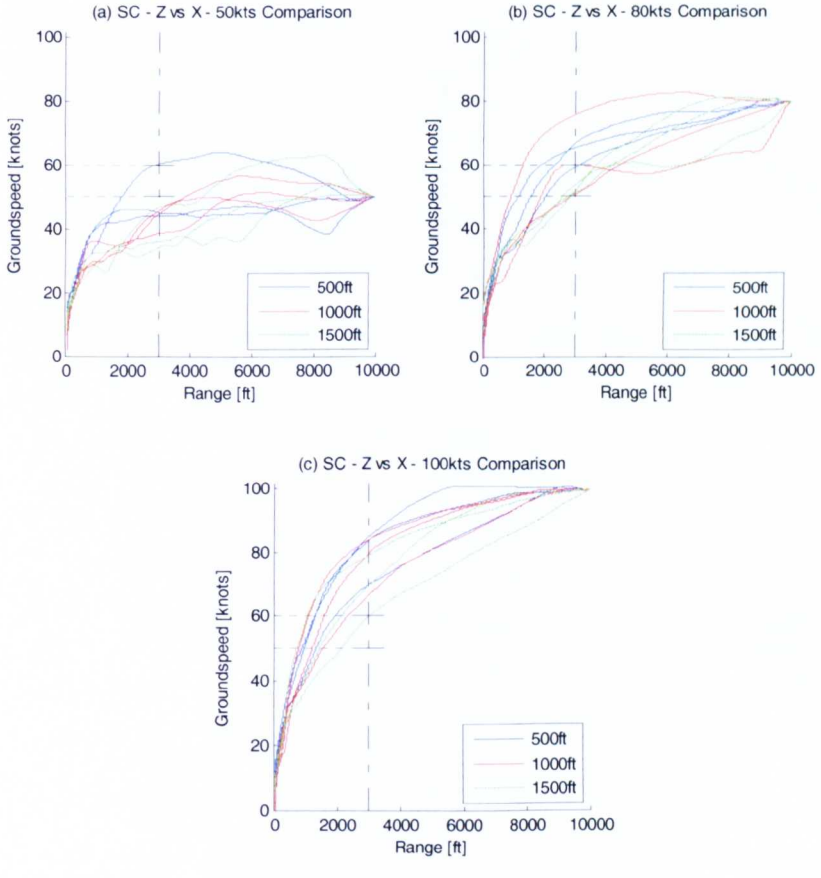


**Figure 3.7** Groundspeed vs. range comparison for (a) 50kts, (b) 80kts and (c) 100kts SC tests

The data in figure 3.7 again provide a contrast to the findings from AB's data when the range of speeds at 2800ft is considered. The same markings at 3000ft, 50 and 60kts have been added to figure 3.7 as they were in figure 3.4. SC's results show a range of speeds at 2800ft which is over 3 times as large as AB's. This is not to suggest that SC is flying the approach incorrectly, but serves to highlight the considerable difference between the two pilots' strategies. Figure 3.7 does indicate some level of consistency, however. The three subplots, each representing a different initial speed condition, show broadly the same profile for the 9 approaches completed at each initial speed.

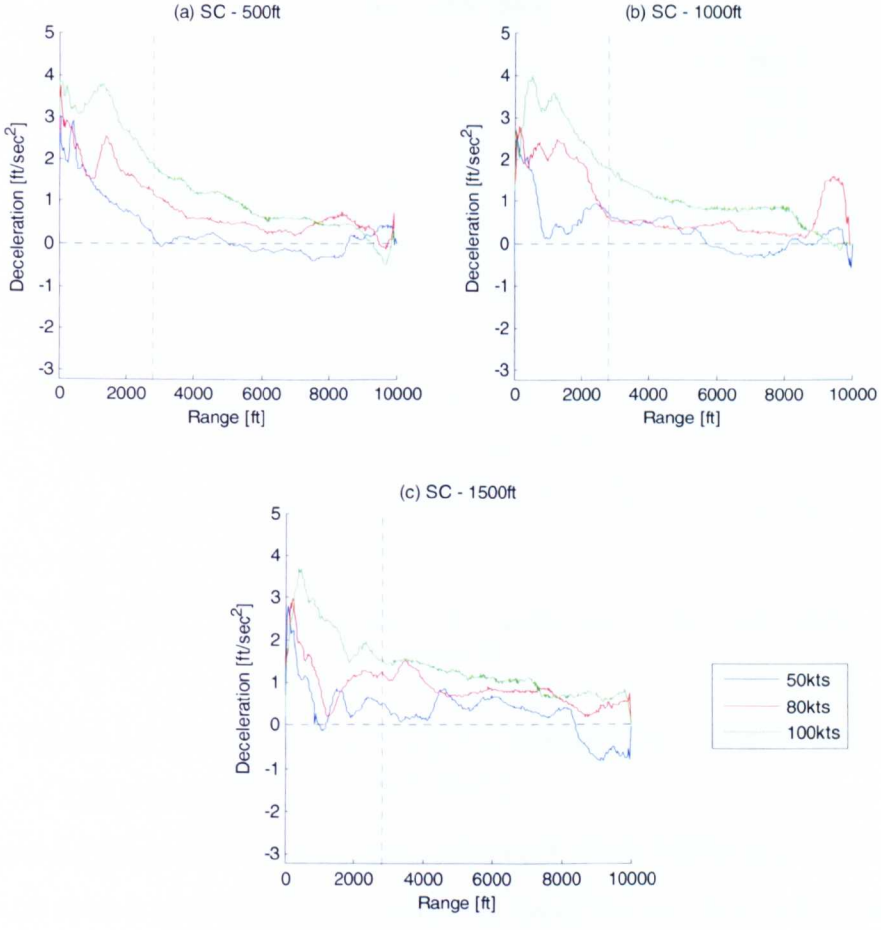


**Figure 3.8** Averaged deceleration profiles for (a) 500ft, (b) 1000ft and (c) 1500ft SC approaches from 10000ft

The deceleration profiles in figure 3.8 show a generally repeated pattern in which the deceleration is gradually increased through the full range of the approach, peaking approximately 500ft from the helipad before a period of final correction is applied. This technique is most noticeable in the 100kts tests, although it is still apparent in the 50kts and 80kts runs.

Although the data in figure 3.8 show a more consistent piloting strategy, with deceleration gradually increasing until it peaks approximately 500ft from the helipad, there are still differences in the original, non-averaged data. An example of this is shown in figure 3.9.

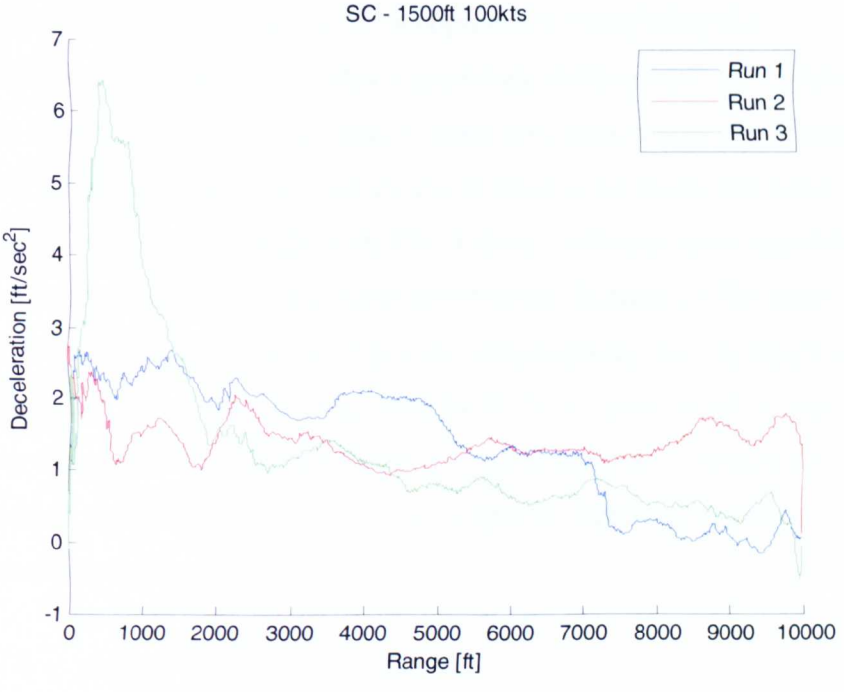


**Figure 3.9** Deceleration vs. Range for individual SC 1500ft 100kts approaches

Figure 3.9 shows data for SC's three individual 1500ft 100kts runs. The matrix point is particularly interesting in terms of the deceleration profiles as the pilot adopts three very different strategies for exactly the same test point. The first run shows a gradually increasing deceleration which

steadily rises through the majority of the approach with no large changes in the deceleration rate until less than 100ft from the pad. In contrast, run 2 shows the pilot applying an almost immediate deceleration of 1.5ft/sec$^2$ which is held approximately constant throughout almost the entire approach, with a small increase applied in the final 500ft. Run 3 is also unique, with deceleration gradually increasing in a similar, but slower manner to run 1. There is then a rapid change in the deceleration rate 2000ft from the helipad and the value increases to a much larger value than is seen in either of the other two runs.

This result suggests that even within nominally the same test setups there are quite distinct differences in SC's approach to completing the manoeuvre. The question is, what causes these differences? Given that the scene content is the same throughout, there is no reason why visual cues should be responsible as they are clear and reliable for every test point. Varying levels of pilot fatigue could be a factor, although close inspection of the results shows quite individual patterns which make up the overall trend for each of the 9 test matrix points. Alternatively, the explanation could be that the piloting strategy used by SC is different to AB's, with SC flying each run as a unique test point with no conscious, or indeed sub-conscious, thought put into trying to fly a specific approach based on previous experience.

#### *3.5.1.3 Comparison of Piloted data*

In addition to considering the data in section 3.5.1 with a focus on understanding and comparing each pilot's strategy, the aims of the original NASA trial also provided an interesting area for comparison. The main aim of the NASA trial was to develop parametric equations which would model a generic approach technique based on the results of several pilots.

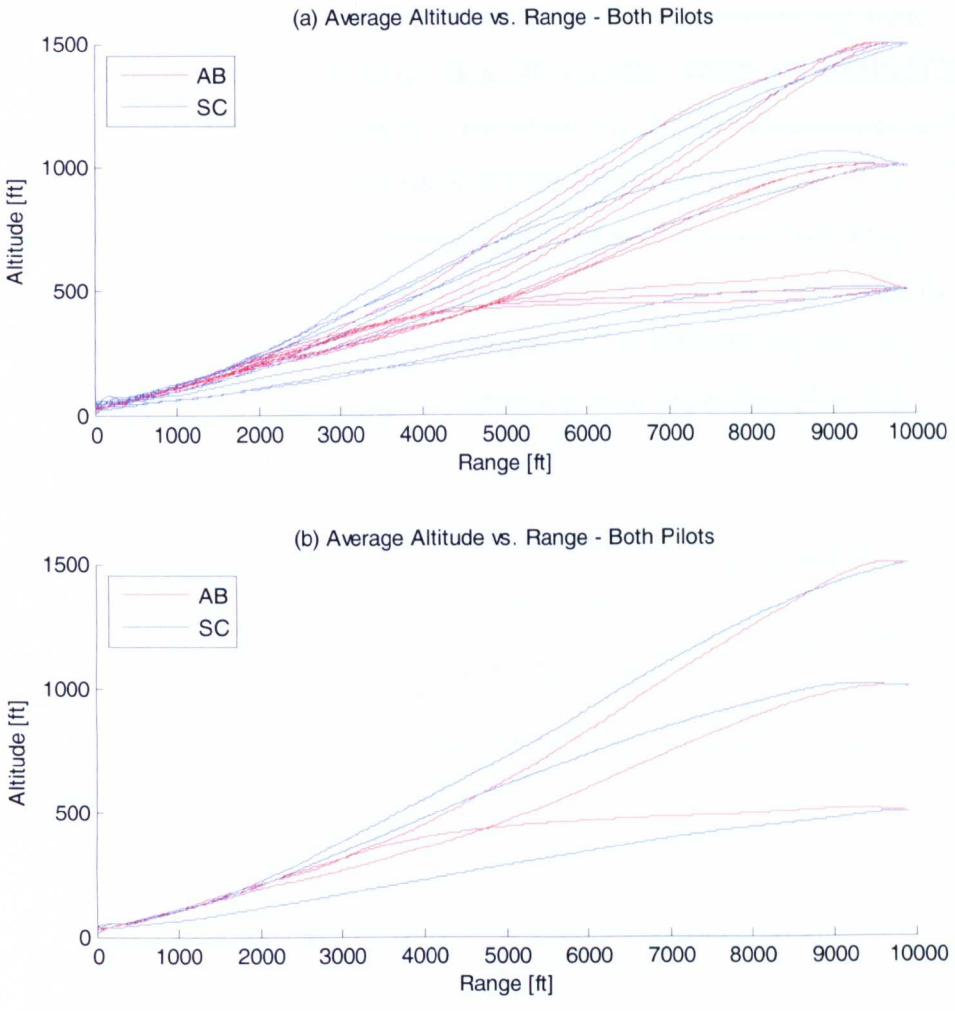


**Figure 3.10** Average Altitude vs. Range comparison for both pilots

Figure 3.10 shows averaged altitude data for both pilots plotted against range to give a clear comparison between the two. Figure 3.10(a) shows 9 data for each pilot, produced by averaging the data for the three runs at each test matrix setting. Figure 3.10(b) shows the data given by averaging the 9 runs at each initial altitude.

One of the first differences that seemed apparent during the individual analysis of the piloted results were the altitude vs. range profile plots for the two pilots. Both subplots of figure 3.10 highlight the differences between AB's consistent two-phase approach and SC's much more

individual technique. SC's 500ft runs in figure 3.10(a) are more apparent in their difference to the rest of the data, although the 1000ft and 1500ft SC approaches are still less precise than the entire AB dataset. Examining the range of altitudes at 3000ft, the spread of the AB data is just 85ft, compared to a spread of 279ft for the SC averaged data, over three times the range of the AB data. Such a disparity again emphasises what seems to be a considerable difference in the strategies of the pilots during the task. These differences are inevitably manifested in the comparative plots for groundspeed and deceleration.

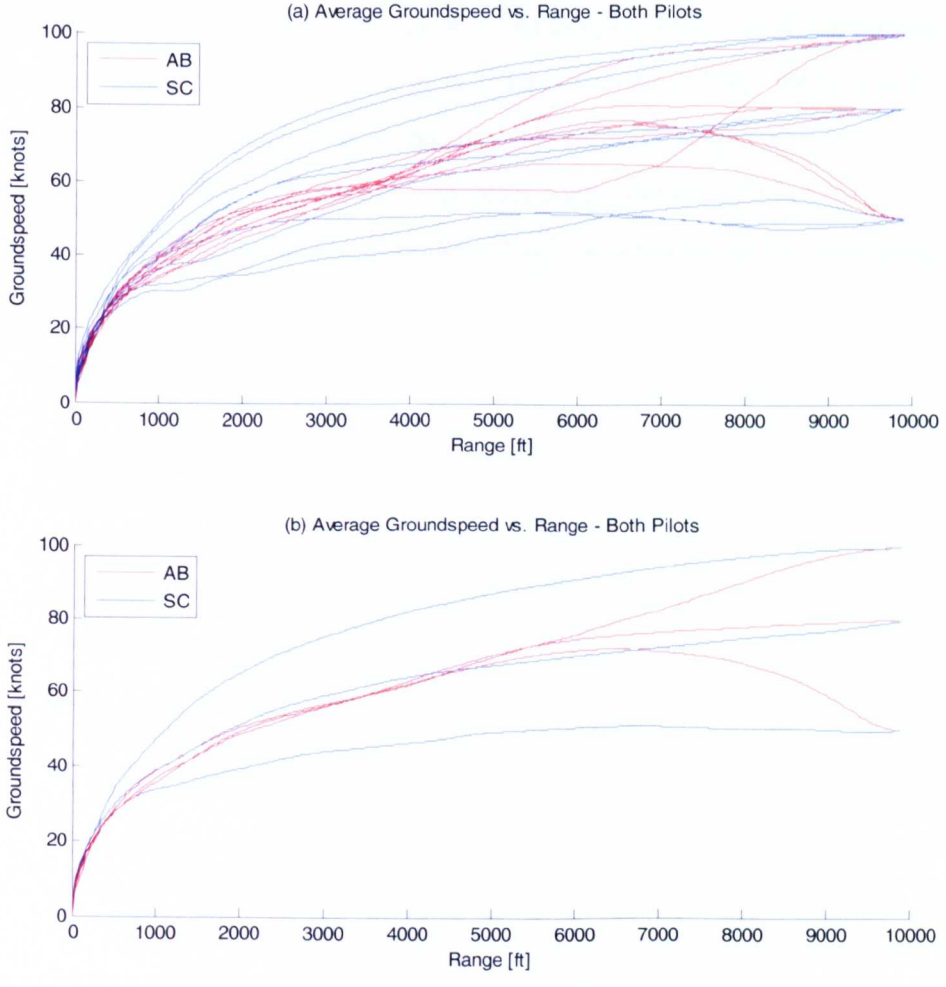


**Figure 3.11** Average Groundspeed vs. Range comparison for both pilots

Figure 3.11 follows the same pattern as figure 3.10, with figure 3.11(a) showing data averaged by test matrix point and figure 3.11(b) averaged by initial groundspeed. Figure 3.11(b), in particular, shows the strategy employed by AB in a very explicit, unmistakable form. The three average initial groundspeeds merge at approximately 5000ft, with the values being incredibly similar even at a range of 6000ft. This result would be impressive on its own but, when compared to the vastly different strategy of SC, is even more striking.

By way of a numerical comparison, the range of groundspeed values at 5000ft is 38kts for SC and 2kts for AB. At the previously used comparison point of 3000ft the SC speed range is 31kts, in contrast AB's range is just 0.69kts. Given the lack of instruments such accuracy seems almost unbelievable. However, the pilot-operator audio recorded during the testing does indicate that the pilot definitively was not using the instrument panel for guidance.

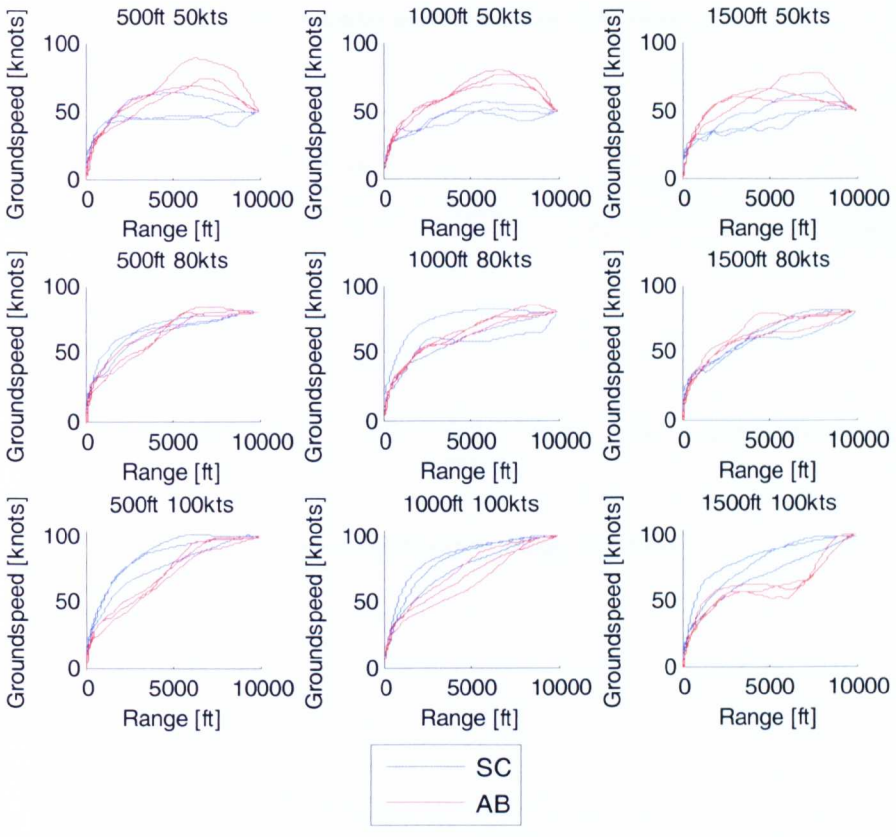


**Figure 3.12** Task separated Groundspeed vs. Range comparison for all approaches of both pilots

Figure 3.12 shows a test matrix separated plot of all of the original (i.e. non-averaged) experimental data for both pilots. The seemingly task-focused approach of AB is equally apparent when considered alongside the data for SC in this manner. Whereas the SC groundspeed data follows a general pattern where speed is slowly reduced over approximately the first 6-7000ft of the approach and is then subject to a much larger deceleration to intercept the helipad, the AB data shows a range of techniques. The 50kts conditions all show an increase in speed whereas the 100kts test points with a 500ft and 1000ft start height show a relatively linear reduction in speed. The 1500ft 100kts tests are different again, with a two stage deceleration. The only tests in which the two pilots show some form of agreement are those with an initial speed of 80kts.

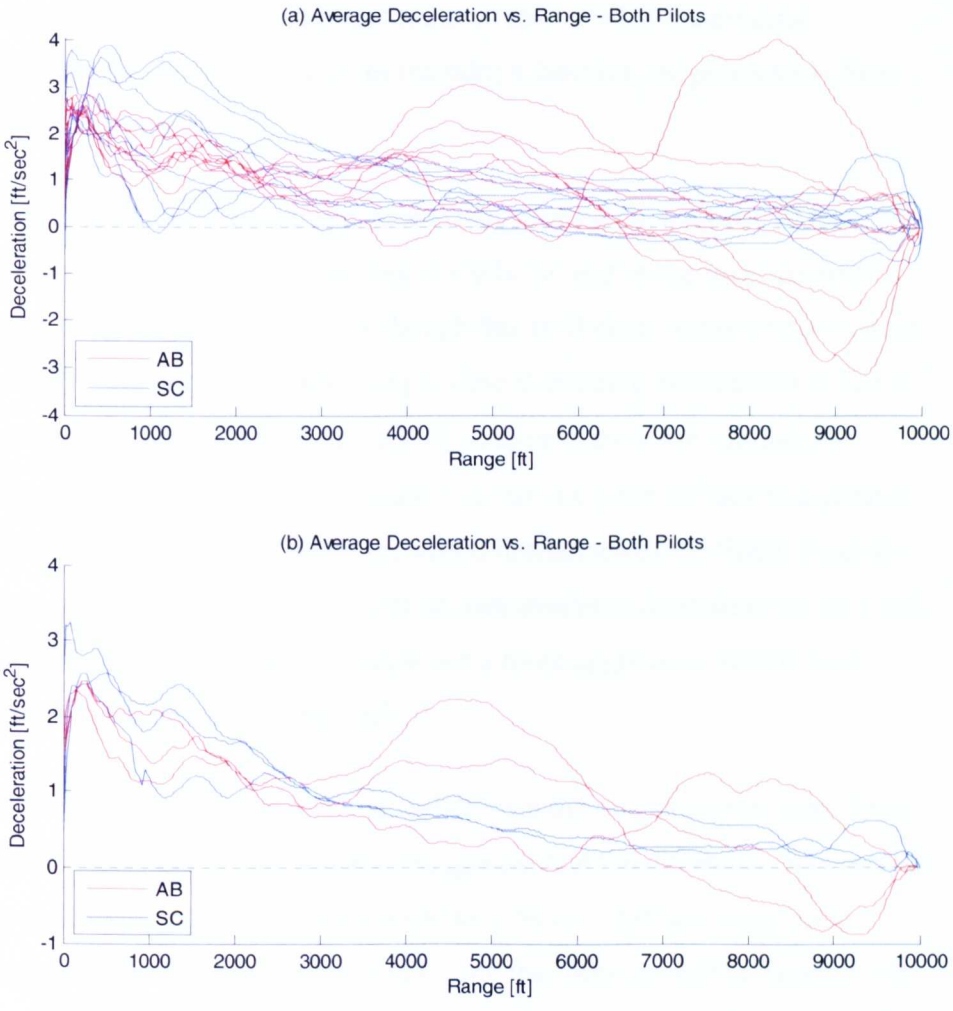


**Figure 3.13** Average Deceleration vs. Range comparison for both pilots

As with previous comparative plots, figure 3.13 again shows a variation with the approach strategy employed by the two pilots. The groundspeed increase for the 50kts test points is represented as an early acceleration with the AB data, whilst the much larger, earlier decelerations for the 100kts test points show how AB was more concerned with reducing groundspeed earlier into the approach than SC.

The AB data also shows the theorised two-phase approach, with the first phase which seems to be aimed at getting the aircraft 'on condition' ending 3000ft from the pad. The second phase can then begin, with very similar

conditions for all second phase tests, no matter what the original conditions. This strategy gives the pilot a familiar and predictable final approach phase.

Given the lack of any strong deceleration during the majority of the approach, the peak decelerations towards the end of the manoeuvre are higher for SC than for AB. Although this is likely to simply be a product of differing pilot strategies, one possible alternative explanation is that SC was more confident with the lack of nose-up cues in the simulation environment and felt that he could increase the pitch attitude to a greater value than AB could. While the visual limitations of the flight simulator would greatly reduce the amount of cues available depending on the pitch angle reached, it would also allow for a more aggressive deceleration towards the end of the approach.

An explanation for the differences between the two strategies came from discussions with SC in which he suggested that the difference between his and AB's flying backgrounds could be a factor. AB has much more experience as an instructor than SC, and therefore he will be familiar with teaching students to recognise the 'picture' in the scene. That is, he will place the target, whether it is a helipad or touchdown point on a runway, at a certain point 'on' the windscreen based on what is deemed to look 'right', thus forming a picture. By approaching the manoeuvre in this way the pilot will consistently be aiming to achieve the same picture by a certain range from the target. SC does not have this same instructional experience and suggested that the two very different methodologies seen during the testing may be because of the pilots' unique backgrounds.

Despite the variation of results seen in the plots considered so far it is still possible that the variations in position, speed, deceleration etc. profiles may not be so significant when considering analyses which are not simply

direct measures of spatial performance. Therefore, of interest now will be to determine whether the differing strategies in the test are noticeable in the $\tau$ and NASA analyses, or if either of the two methods are robust enough to satisfactorily explain both techniques.

## 3.5.2 NASA Replication

A key area of the analysis for the approach to hover trial was the reproduction of parts of the NASA research, in particular the use of a power parameter, which showed a strong correlation when plotted against instantaneous groundspeed from a range of 2800ft.

### *3.5.2.1 Comparison of parametric data*

The first stage of the data reproduction was to produce a plot of the compound variable, $\frac{\dot{x}^2}{\ddot{x}}$, against range. An issue which arose when attempting to relate the UoL simulation data to the NASA data was that the NASA results appeared to have been considerably smoothed. The UoL simulation data were much noisier than the NASA flights. This issue was prominent enough to affect the measured gradient, i.e. the n value, which was a critical component of the comparison with the NASA results. As such, it was decided to smooth the data as NASA had done. This was achieved by averaging the $\frac{\dot{x}^2}{\ddot{x}}$ and $x$ values in 100ft windows. Individual n and c values were calculated using this method; the results were then averaged by test matrix point to give 9 values for n and c, respectively.

Figure 3.14 shows the original NASA data for the 1000ft 100kts test point (the only matrix point for which this particular figure was included), compared with the results from the two Liverpool pilots.

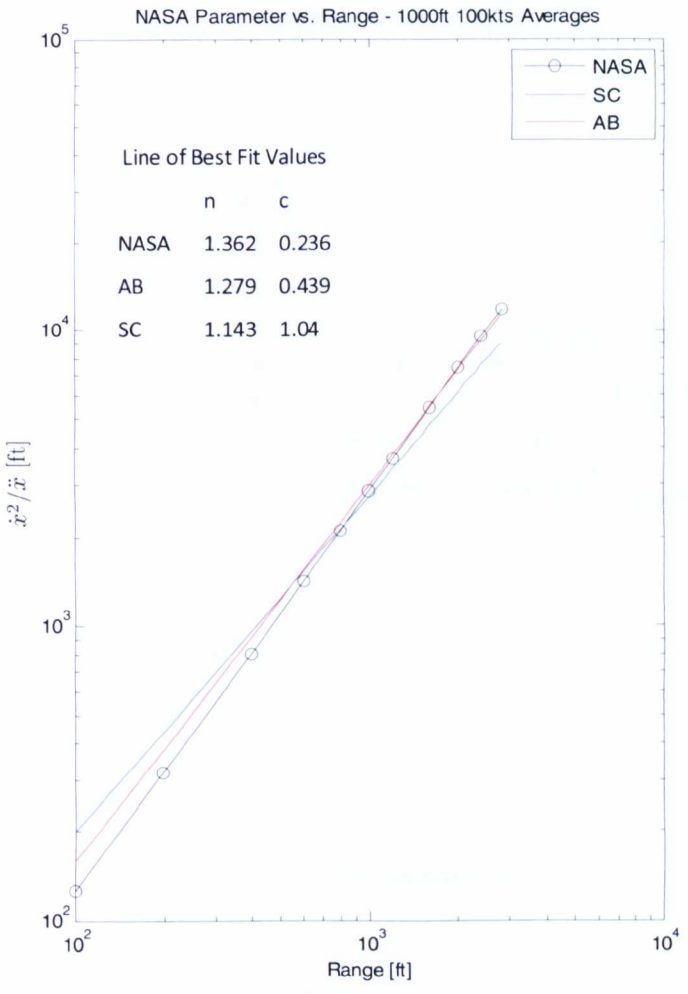


**Figure 3.14** NASA power parameter vs. Range for 1000ft 100kts tests

The values for n and c are also shown on figure 3.14. n is the gradient of the line of best fit and c is determined by extracting the y-axis value of the line of best fit at $10^0$.

Data for the gradient of each test point was extracted and plotted against the instantaneous groundspeed at a range of 2800ft for the corresponding test. The NASA data from the original plot (see figure 3.1) was included alongside the new data to provide a comparison between the results, shown in figure 3.15.

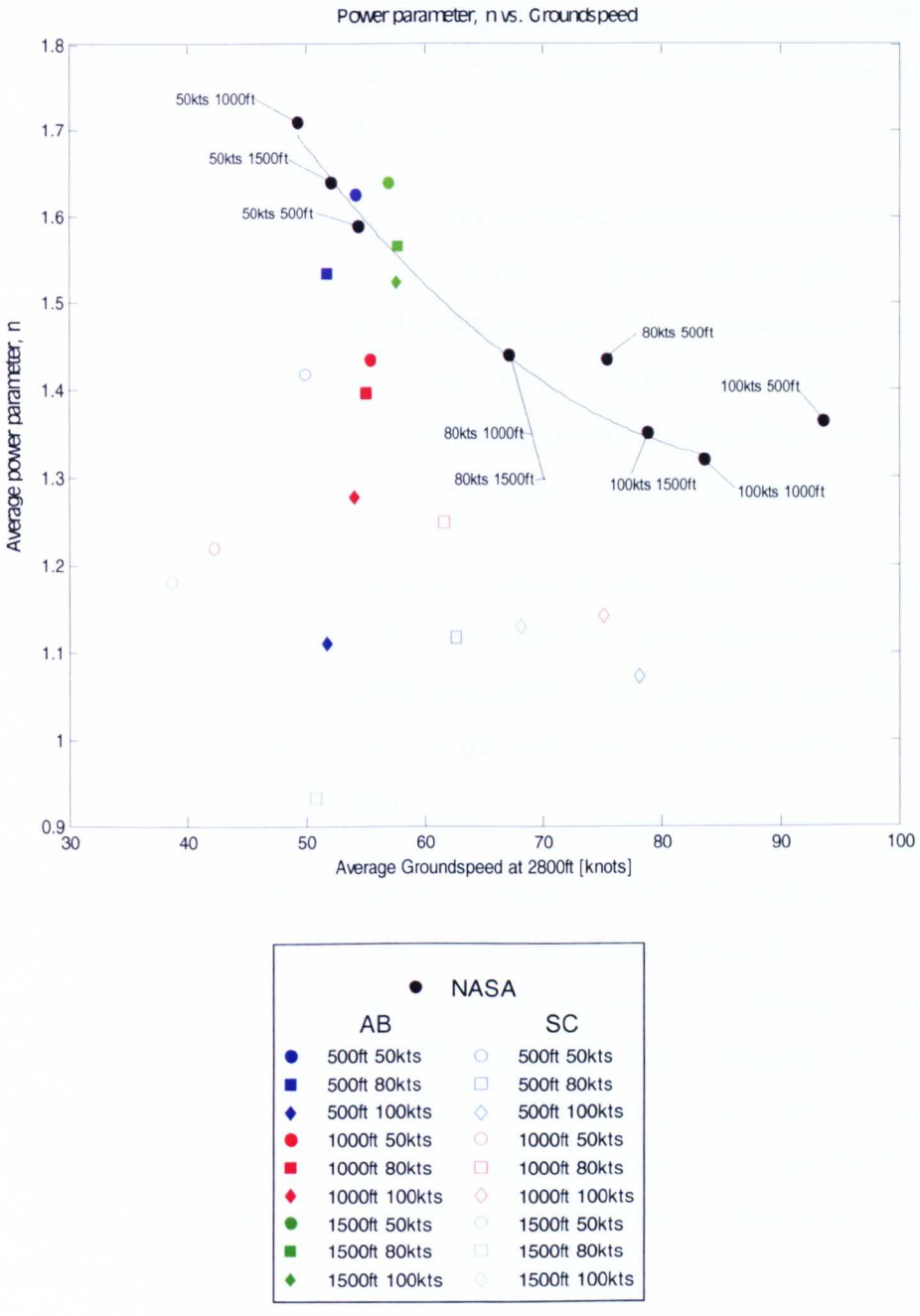


**Figure 3.15** Average power parameter, n vs. average groundspeed at 2800ft for all AB, SC and NASA data

The first point to note from figure 3.15 is that the AB data, whether raw or averaged, shows a completely opposite trend to the NASA data. The

values of n for the AB data become progressively larger with higher 2800ft groundspeed values, whereas the NASA data shows the highest n values to be at the lowest 2800ft groundspeeds.

Another feature of the AB figures is that the range of groundspeed is very small, with a spread of just 6kts in comparison to the NASA spread of approximately 45kts. Although the narrow range of AB's groundspeeds at 2800ft is not unexpected given figures 3.4 and 3.10, the contrast with the NASA data is marked. Such a large discrepancy shows that AB adopted a strategy which was very much different to pilots in the NASA trial.

Looking more closely at the AB data, one area in which they do agree with the NASA findings is the trend for the slower initial groundspeed runs to have a higher value for n. In each of the AB's initial altitude batches, the 50kts runs have a higher n-value than the 80kts runs, which in turn have a higher value than the 100kts runs.

In a result which is in almost complete contrast to the NASA findings, a line of best fit which is most applicable to the AB data would be a near vertical line starting at the 500ft 100kts point and moving up through all of the 1000ft data and two of the 1500ft results. This line would take in 6 of the 9 data, with the 1500ft 50kts result being extremely close to the line. In addition, the final two 500ft results would lie no further away from the AB line of best fit than the two outliers in the NASA results do from their best fit curve.

On its own, this result for AB could be deemed to be useful, however in comparison to the SC and NASA results on the same figure it is immediately obvious that the fit would not be applicable to those results. Despite this, the trend did seem to be quite clear and although there was no

agreement with the SC or NASA data, this did not mean that the result was not valid.

After drawing a test line of best fit it was noted that the two points which did not fit well seemed a little out of place given the way in which, for the other 7 results, n increased with increasing test altitude. Therefore the individual n-values for the 500ft 50kts and 500ft 80kts runs were examined. It was found that for each of the matrix points in question there was one n-value result which was much higher than the other two runs for the same test. When compared with the other individual 21 n-values it became apparent that these two values were the two largest values for n in the entire analysis by a relatively large margin.

Further analysis of each of the three runs in the 500ft 50kts and 500ft 80kts matrix points showed that the two runs of interest had a brief period of acceleration, and therefore speed increase, close to the helipad. It seemed apparent, therefore, that this acceleration was leading to a much higher value for n and possibly skewing the results. By way of an exploratory test, the potentially anomalous data within the 500ft 50kts and 500ft 80kts tests was removed and the respective values for each matrix point were calculated with the data for the two remaining runs. Figure 3.16 shows the results of this analysis, with a line of best fit added to the modified AB data.

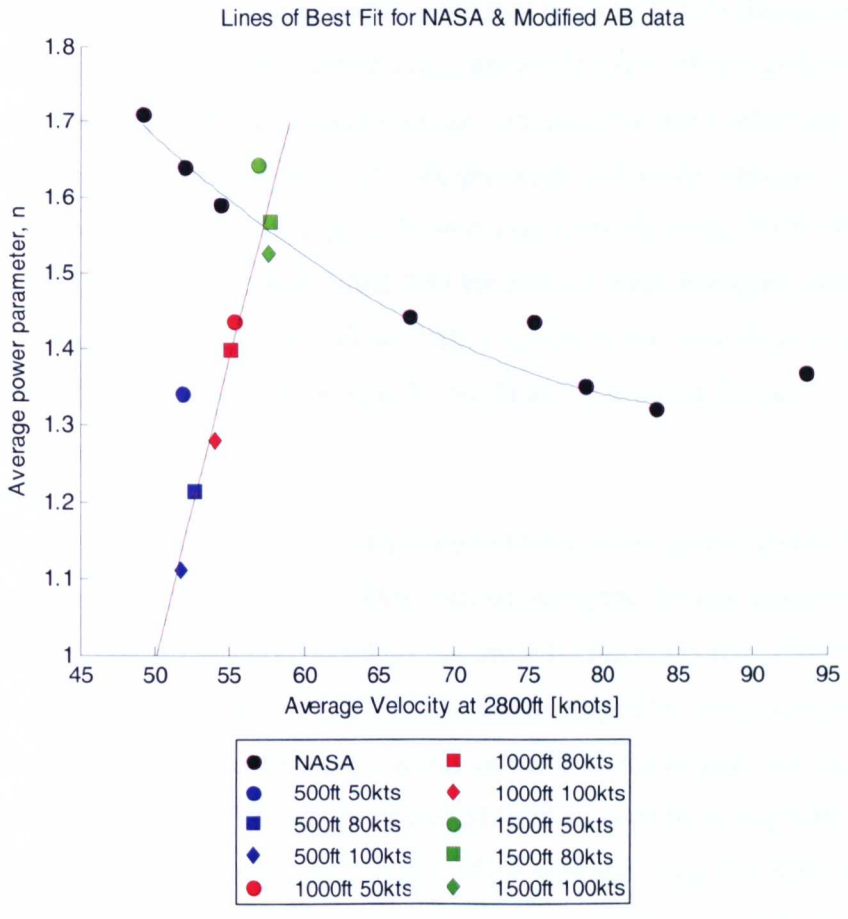


**Figure 3.16** NASA and modified AB power parameter vs. range at 2800ft

Figure 3.16 shows the difference made by removing the two potentially anomalous results to the overall trend. The new trend now shows that n becomes larger with increasing initial altitude, with only the 500ft 50kts value proving an exception to this rule. The line of best fit provides a very good approximation for 7 of the 9 data and the two results which don't fall on or near it are still close enough to agree with the general trend.

Therefore, whether we take into account the original or modified AB parametric result the conclusion is broadly the same; the data does follow a trend but it is almost entirely different to the trend found by NASA.

Moving onto the SC results possibly the first point to note is the general difference in the spread of the results compared to AB. Whereas the AB results were spread over a narrow range on the x-axis and a relatively wide range on the y-axis, the SC results are generally almost the opposite of this. There are two points which provide an exception to this rule, 500ft 50kts and 1500ft 80kts. The individual data for each of these averaged values was examined (as with the AB results), although in this case there were no potentially anomalous values which could have warranted further investigation.

Figure 3.15 does show a clear structure in terms of the groundspeeds for the various SC tests, with the 50kts tests showing the slowest groundspeed at 2800ft (approximately 38-50kts), followed by the 80kts tests (50-63kts) and finally the 100kts tests (68-78kts). The averaged SC results also show that 8 of the 9 data points have lower n values than the lowest recorded NASA value, 1.32. This suggests that SC had an even more aggressive deceleration profile in the final stages of the approach than the NASA pilots, with more of SC's deceleration occurring closer to the helipad.

One final point to note from figure 3.15 is the order in which the groundspeeds rise. As has already been observed, the results are separated by initial groundspeed, but within each of those batches of data there is another theme, with groundspeed for a fixed speed rising as altitude decreases. Although the increases are quite small at times, this does suggest that the pilot was applying a considered strategy to some extent, with an earlier deceleration applied to the 1500ft runs due to the requirement to find a balance between descent and deceleration.

Although some of the SC data does suggest a vague correlation, there is no clear pattern and several points would lie a considerable distance from any curve of best fit. The data, while similar to NASA's in terms of initial

groundspeed, disagrees quite strongly when the power parameter, n is taken into account.

As the NASA data is based on the averaged results for an unspecified number of pilots, the final phase of this project's analysis examined the absolute UoL test results, with the data for AB and SC averaged to produce just one dataset, as shown in figure 3.17.

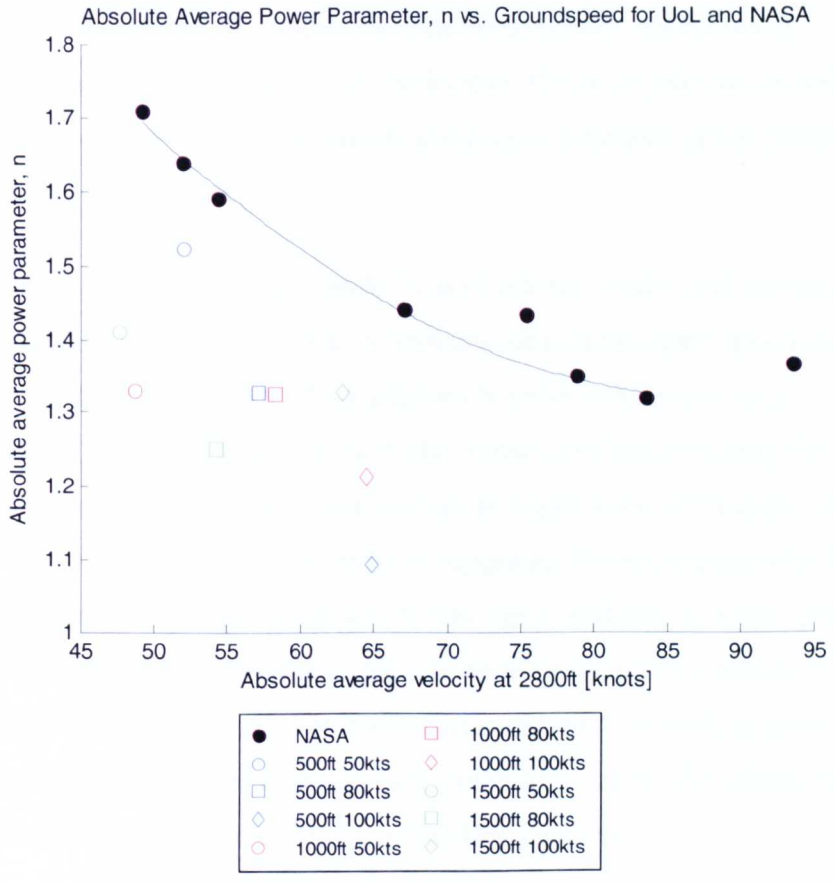


**Figure 3.17** Average power parameter vs. average groundspeed for UoL and NASA results

Figure 3.17 shows the absolute iteration of this project's averaged results to give a replication of figure 3.1. Although it could be argued that the UoL data vaguely follows a similar pattern to NASA (increasing initial task speed giving a greater value for groundspeed at 2800ft and a lower n-

value), there is very little agreement with NASA's results. The process of averaging the results of the two pilots has masked the narrow range of groundspeeds at 2800ft which was a characteristic of the AB tests, but the range is still narrow in comparison to NASA. In addition, the UoL data is still quite widely spread in the y-axis, which results in there being no clear pattern within the data. Therefore it is not possible to draw any line of best fit which can account for more than 4 of the 9 data points.

As shown in figure 3.17, despite the individual piloted results being relatively unique and distinct from each other, the averaged UoL results show the value of a testing approach which uses a number of test pilots to achieve a typical result.

However, we must not forget the individual piloted results and, indeed, the original aims of the experiment. NASA set out to investigate approaches under visual flight rules (VFR) conditions in order to ascertain what constituted a 'natural approach' with the intention of incorporating this information into computer driven instrument flight rules (IFR) approaches. However, as this project's results have suggested, for every pilot who flies an individual set of approaches which may agree with the 'average' profile, there will be another pilot whose natural visual approach is markedly different. For those pilots, their technique could quite possibly present "unnatural physiological cues", a quote taken from the NASA report from a pilot unhappy with the already existing IFR guidance.

The UoL GVE trial has shown that a flight test with just two test pilots can still show up quite considerable differences between pilot strategies for a very simple manoeuvre.

### 3.5.3 Tau Investigation

A tau analysis was conducted on the flight test data in order to determine whether the pilots were using tau guidance during the approach to hover trial. If so, the findings could then serve as baseline information to be compared with the results of a DVE version of the approach to hover trial.

The initial $\tau$ analysis examined the basic $\tau_x$ relationship from the 2800ft trim point. Although this point was selected as part of the NASA comparison, it also provided a sensible starting point for the tau analysis given the same desire to limit the full 10000ft range to a portion which contained the majority of the final deceleration.

After plotting and analysing the $\tau_x$ vs. Time To Go data, a linear approximation was added to the tau plots. In addition to the linear approximation were corresponding $R^2$ and k values, where k is the gradient of the linear approximation over the relevant period and $R^2$ is the coefficient of determination. Finally, $\dot{\tau}$, the instantaneous rate of change of $\tau$ with respect to TTG, through each approach was calculated and analysed.

When considering $\tau_x$ we should remember that the physical size of this test is much larger than many other $\tau$ investigations, some of which considered $\tau$ over very short durations in which the total 'manoeuvre' time was little more than 1 second (Lee, 1992). This analysis will consider $\tau_x$ from 2800ft, little more than a quarter of the total range, but this can still correspond to an approach time of over one minute. Therefore, of particular interest in this analysis and the DVE trial analysis to follow, will be the pilots control of tau both at close and long range and also if there are definite points at which the pilot 'locks on' to a tau guidance strategy.

In order to give the analysis an extra dimension, and one which might offer an alternative insight into tau control at close range, the data are also analysed from the end of the manoeuvre backwards. The intention is to focus the analysis on the vital closing stages of the approaches and to determine over what range the quality of the tau fit is high. This method will be explained in more detail at the appropriate stage of the analysis.

In order to present the data in a more sensible form it is necessary to pre-process the data before computing tau. This is commonly achieved by trimming off a small percentage of the start or end of the test data, as required (Padfield et al, 2001). The trimming was conducted based on the specific nature of each run as there were various factors which could affect the quality of the tau data:

- If the pilot flew past the helipad the x-axis positional data moves through 0 and also changes sign, which in turn causes tau to briefly become zero and then increase to a positive value. In these cases the data was trimmed with the last data point before the aircraft passed the centre of the helipad being the end of the manoeuvre.

- If the pilot stopped short of the helipad, $x$ would still have a positive value, whereas $\dot{x}$ would be 0, causing $\tau_x$ to be infinite. In these cases the x-axis positional data was re-calibrated such that the point that the pilot reached was referred to as $x = 0$.

#### *3.5.3.1 Analysis of tau data – AB*

One of the most significant aspects of the AB $\tau_x$ is the accuracy of the approaches in terms of tau control. Most of the 27 runs show a very strong linear relationship between $\tau_x$ and time (see figure 3.18).

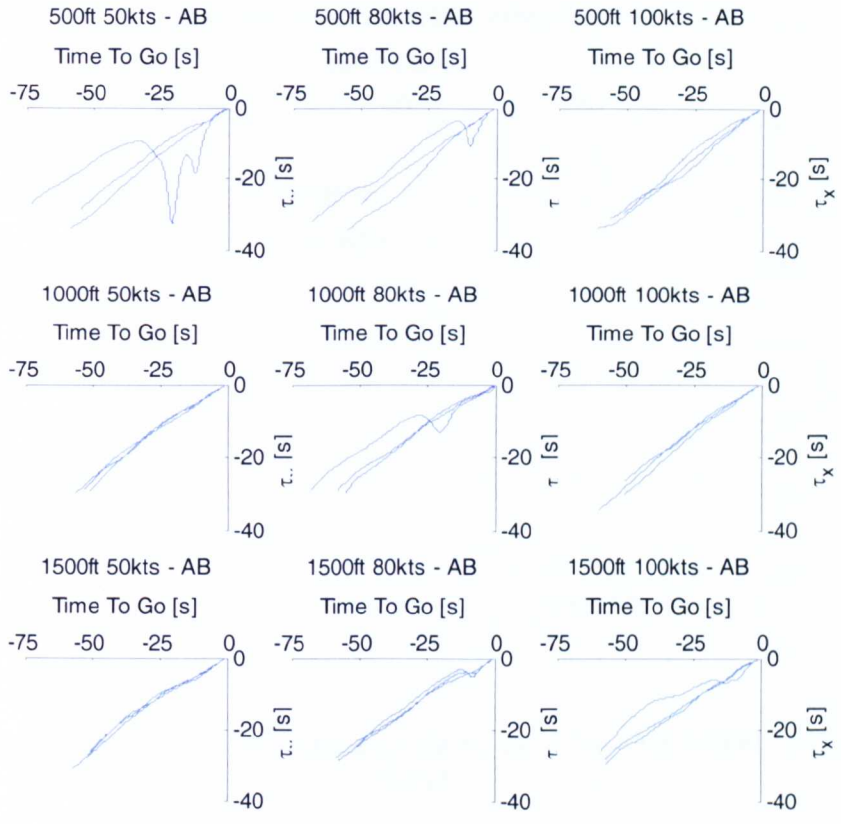


**Figure 3.18** $\tau_x$ vs. Time To Go (TTG) for all AB approaches from 2800ft

The repetitive nature of the approaches is shown by figure 3.18 above, with only 3 of the 27 tests showing a significant amount of deviation from the linear trend.

An example of the linear fit for one of the AB approaches is shown in figure 3.19. The flight test data matches up well with the linear approximation, giving a relatively high $R^2$ value of 0.989 and a k value of 0.548.

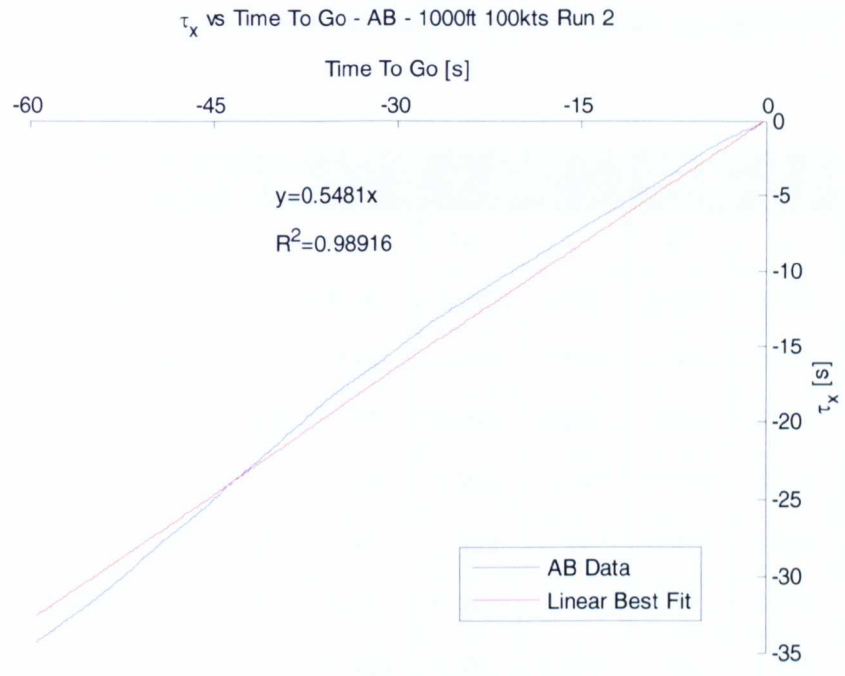


**Figure 3.19** Linear approximation for $\tau_x$ vs. TTG - AB 1000ft 100kts Run2

Although the tau data is relatively linear, especially when examined in figure 3.18, there are two changes in the gradient of the data at $\tau_x$ values of approximately 19 and 14 seconds respectively. If the regression analysis had been conducted over a $\tau_x$ range of 15 seconds it is likely that the $R^2$ value would have been even higher and the k value (i.e. the gradient of the line of best fit) would have been a little lower. The second point is important as the value of $\dot{\tau}_x$ dictates the resultant contact, or lack thereof, at the end of the manoeuvre, as discussed in section 2.3.2.1. A $\dot{\tau}_x$ of greater than 0.5 implies a hard stop, with a value of less than 0.5 being a soft stop. In the context of this test the pilot may well aim for a $\dot{\tau}_x$ of 0.5 (constant deceleration), with groundspeed reaching 0kts at exactly the same time that the aircraft was over the centre of the helipad.

As figure 3.18 shows, the majority of AB's approaches show a similar, strong relationship between $\tau_x$ and TTG , and this is highlighted in the $R^2$

values, which are shown below for each test matrix point alongside the k values.

| | *Run 1* | | *Run 2* | | *Run 3* | |
|---|---|---|---|---|---|---|
| | $R^2$ | k | $R^2$ | k | $R^2$ | k |
| **500ft 50kts** | 0.122 | 0.361 | 0.992 | 0.572 | 0.983 | 0.485 |
| **500ft 80kts** | 0.951 | 0.445 | 0.998 | 0.529 | 0.990 | 0.650 |
| **500ft 100kts** | 0.996 | 0.578 | 0.994 | 0.603 | 0.981 | 0.541 |
| **1000ft 50kts** | 0.987 | 0.489 | 0.996 | 0.507 | 0.978 | 0.518 |
| **1000ft 80kts** | 0.989 | 0.471 | 0.989 | 0.499 | 0.929 | 0.381 |
| **1000ft 100kts** | 0.994 | 0.582 | 0.989 | 0.548 | 0.992 | 0.510 |
| **1500ft 50kts** | 0.978 | 0.469 | 0.986 | 0.470 | 0.982 | 0.504 |
| **1500ft 80kts** | 0.982 | 0.476 | 0.994 | 0.461 | 0.953 | 0.440 |
| **1500ft 100kts** | 0.998 | 0.501 | 0.928 | 0.369 | 0.999 | 0.474 |

**Table 3.1** $R^2$ and k results for all AB approaches

All but three runs show an $R^2$ of over 0.95, with 20 of the values being over 0.98. In the 3 cases where the $R^2$ value is lower than 0.95, the plots show an initially smooth approach phase with the pilot then possibly realising that he is approaching the helipad too quickly, therefore as a larger deceleration is applied, $\tau_x$ increases and the quality of the linear approximation is reduced.

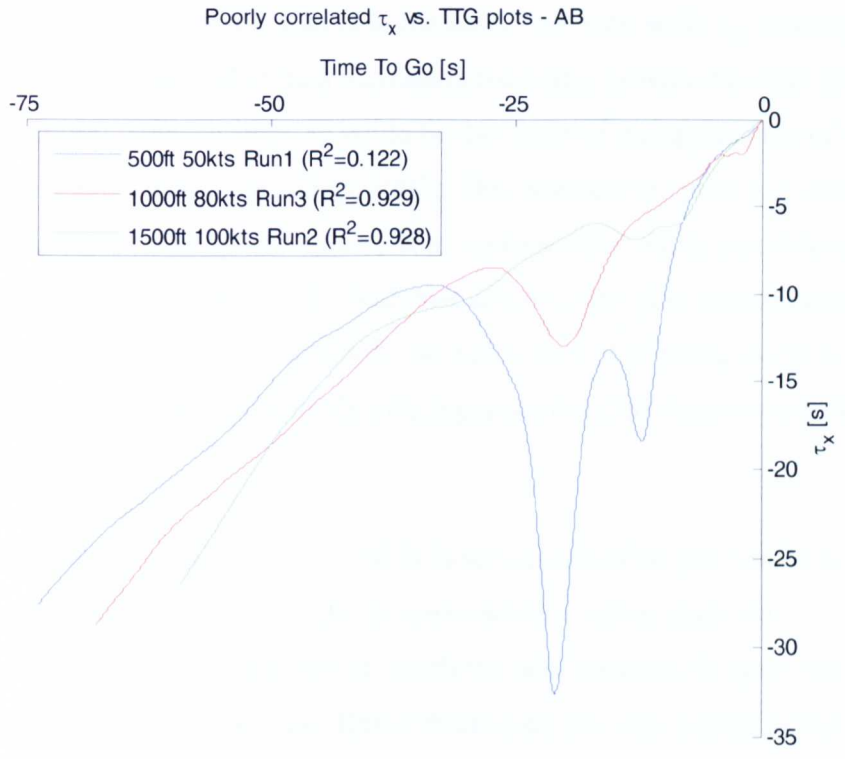


**Figure 3.20** $\tau_x$ vs. TTG for lowest $R^2$ value AB approaches

The blue curve in figure 3.20, representing the 500ft 50kts Run1 test, shows the $\tau_x$ profile which gave the lowest $R^2$ value. There is no apparent reason for any change in strategy and fatigue does not appear to be a factor as this was the 6th run of the session and was not the last run before a break or the first run after a break.

One area of particular interest is the point at which the pilot decides to take positive action to change the approach strategy, shown on the plots by a sudden change in the $\tau$ values. In both the 500ft 50kts and 1000ft 80kts runs the initial change in the gradient of the data occurs at $\tau_x$ values of approximately 10-11 seconds, with $\dot{\tau}_x$ moving through 0 at 9.5 and 8.5 seconds, respectively. The 1500ft 100ks test is an exception (although there are two smaller changes in the gradient at $\tau_x$ = 12 and 10 seconds), with the main change in approach strategy occurring at $\tau_x$ = 6 seconds.

This change is different in nature to the other two tests, with $\tau_x$ seemingly being held constant rather than increasing markedly as with the other runs in the figure. This pause in $\tau_x$ could be the result of the application of a 'cautious pilot' technique (Jump, 2007). This is where the pilot is in control of the approach, but opts to hold $\tau_x$ at a constant value while groundspeed reduces to an acceptable level. With that achieved the pilot can commit to the final phase of the approach with the added benefit of being closer to the target and the ground, potentially offering more detailed cues to guide the manoeuvre.

Previous studies (Padfield et al, 2002) have indicated that pilots need to see a minimum of 9 seconds into the future to achieve robust and safe prospective control. The points at which the pilot changes his approach strategy in the 500ft 50kts and 1000ft 80kts tests are very similar to this theorised threshold of perception. This could point to a $\tau_x$ value of approximately 9 seconds being a vital point within a manoeuvre at which the pilot becomes aware of whether a strategy is likely to be successful or not.

Figure 3.21 shows the average k values for the test matrix points. The figure also shows 3 theoretical values (represented by unfilled, black markers), which were calculated by omitting k values for the 3 tests in which $R^2$ fell below 0.95. These alternative values are included to give an indication as to the potential changes in the data should the runs in question actually be anomalous.

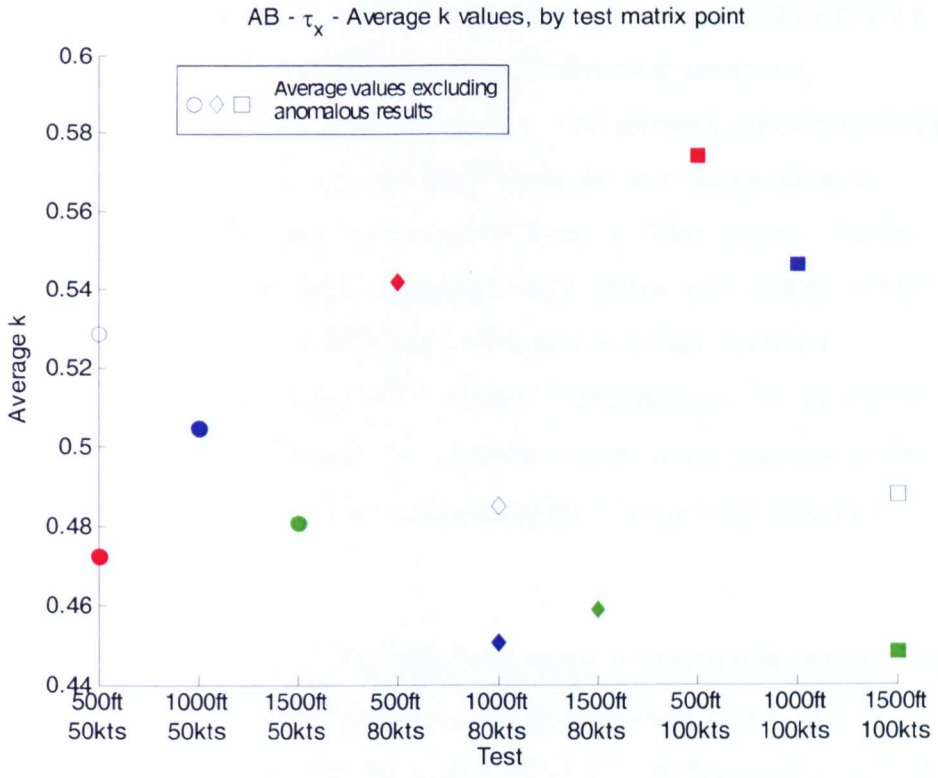


**Figure 3.21** Average k values vs. test point for AB approaches

The three k values for the 50kts tests shown in figure 3.21 are close to k=0.5, with the average k for all 50kts tests being 0.486, very close to the constant deceleration $\dot{\tau}_x$ value of 0.5. With a k of 0.5 and a high $R^2$ correlation (i.e. $R^2 \cong 1$), this would imply a constant deceleration approach. However, although the $R^2$ values are high, it has been shown that AB's deceleration does generally rise in the final 2800ft of the approach.

Despite the close agreement of the 50kts runs, there is no strong evidence of the other matrix points having a k of approximately 0.5, despite AB's apparent two-phase strategy. It might have been expected that, by establishing almost all runs at very similar groundspeed and altitude conditions at 2800ft, the $\tau$ analysis would show a general agreement between the tests. However, in terms of k this does not seem to be the case, with the values being relatively spread out.

There are two changes in the structure of the data in figure 3.21 when we consider the alternative values calculated without the potentially anomalous runs (as discussed previously). The averages which exclude the anomalous runs is shown for the three applicable test matrix points in figure 3.21, with the data represented by black, unfilled shapes. The first change is that the average k values for '1000ft 80kts' and '1500ft 100kts' respectively move up to 0.485 and 0.488, giving a slightly greater emphasis on the $\dot{\tau}_x$=0.5 trend, $R^2$ values notwithstanding. The second is that the data are now arranged such that increasing initial test altitude for the same initial groundspeed condition results in decreasing average k values.

To explore the variation of strategy with range, the regression analysis was computed using 25ft data windows along the trajectory as part of a 'progressive' analysis. Therefore after the initial correlation data had been calculated at 2800ft, the data range was reduced to 2775ft and a new calculation was performed, with the k value for that point being noted. The range was then reduced to 2750ft for the next calculation, and so on. The results for this analysis are shown in figure 3.22.

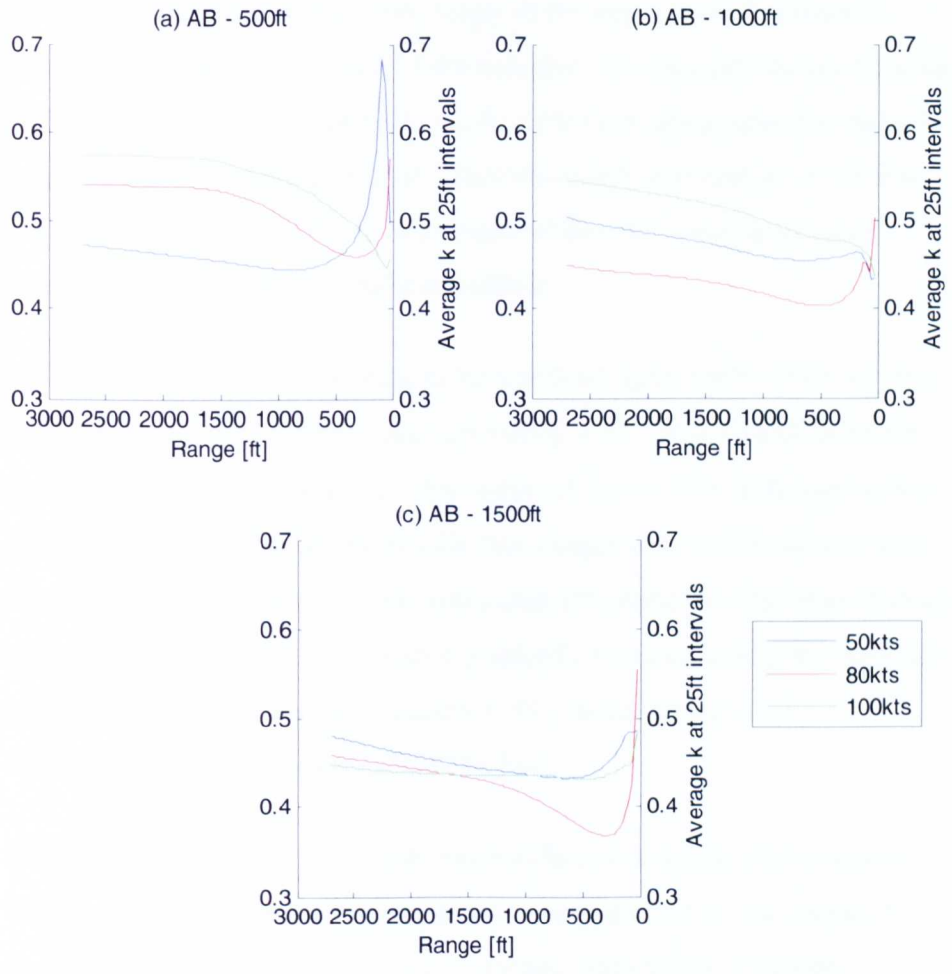


**Figure 3.22** Average k vs. range for progressive AB 25ft analysis

Figure 3.22 shows subplots separated by initial altitude. As with previous plots (e.g. figure 3.8), the data has also been averaged by test matrix point to give just 9 data allowing an easier comparison of results.

In many cases the data show k gradually decreasing as the pilot approaches the helipad, eventually converging on a value of approximately 0.45 at about 100ft from the helipad. This is best shown in figure 3.22(b), with all three data following this pattern. As the pilot gets even closer to the helipad the values do tend to deviate from k=0.45. This is because the main phase of the approach is essentially over by this point. The pilot has

guided the aircraft to within close range of the target, at both a suitable altitude and speed. The nature of the task then changes and the pilot has to pitch the nose of the aircraft up to wash off the remaining speed in order to establish a hover over the helipad. This increased deceleration leads to a different k profile over the closing stages of the task, causing the short range deviations from the nearly constant k.

Up to this point, there does seem to be a general agreement within the data with k approaching a value of approximately 0.45. This is slightly lower than the values noted during the discussion of figure 3.21, although such a difference is inevitable given the different ranges over which the analyses are conducted. It is possible that at the start of 'phase two' the pilot flies an approach with k=0.5-0.55. k is then gradually reduced during the approach to the pad, dropping to approximately 0.45 just before the final deceleration to intercept the helipad begins.

Of interest now are the SC results, especially in relation to the k profiles. With noticeable differences in the general strategies of the two pilots the question is, can a $\tau$-profile be used to explain both pilots' methods?

### *3.5.3.2 Analysis of tau data – SC*

The $\tau_x$ vs. TTG plots in figure 3.23 show that, while there are several smooth traces showing good correlation, there are a number of approaches where the $\tau$ data strays noticeably from a linear closure. A characteristic of the SC plots is that, rather than showing a single large deviation and re-capture of $\tau_x$, as seen with the AB approaches, there are often a number of more gentle deviations, over-corrections and then re-corrections through the approaches.

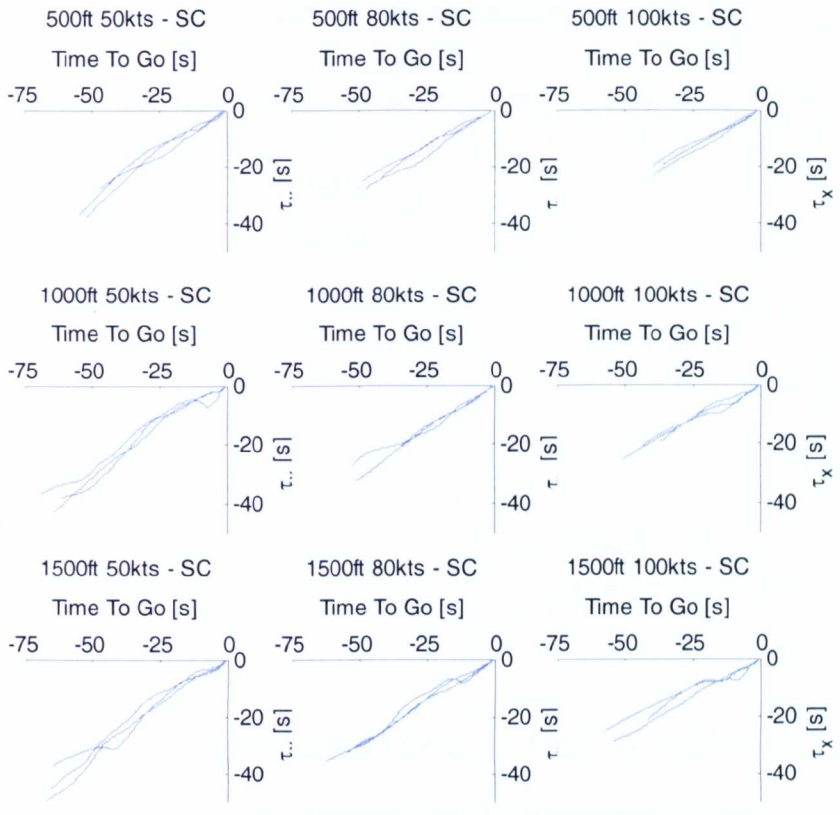


**Figure 3.23** $\tau_x$ vs. TTG for all SC approaches from 2800ft

A typical SC approach is shown in figure 3.24, with a key feature being the number of adjustments in $\tau_x$ throughout the approach. The figure offers further evidence that SC's approaches are characterised by many small adjustments to the flight path (and possibly changes in strategy) as the pilot approached the helipad. Whether the changes were conscious or sub-conscious is not clear given the apparent lack of a decisive strategy.

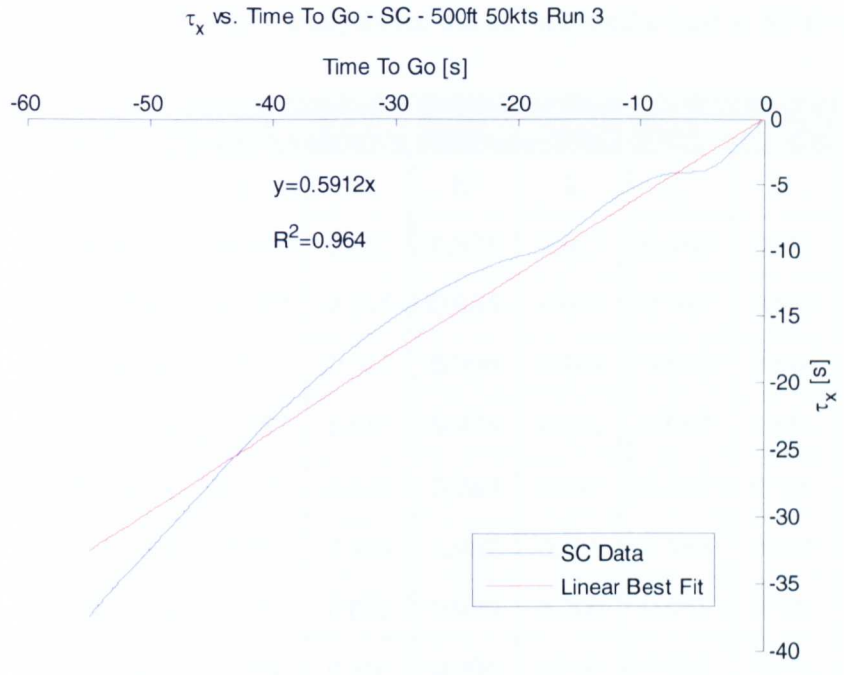


**Figure 3.24** Linear approximation for $\tau_x$ vs. TTG - SC 500ft 50kts Run3

Figure 3.24 shows that, despite a number of adjustments during the approach, the $R^2$ value still remains relatively high. With adjustments at $\tau_x$ values of 4 and 10 seconds the pilot is possibly not happy with his approach profile, even when he is relatively close to the pad. Therefore this test point shows an approach profile which would be undesirable if it were directed by a synthetic display and the pilot was simply following instructions. As such it may be necessary to treat $R^2$ values with caution, especially those which are measured over the full 2800ft range.

The results of the $R^2$ and k analysis for the SC approaches are as follows:

| | *Run 1* | | *Run 2* | | *Run 3* | |
|---|---|---|---|---|---|---|
| | $R^2$ | k | $R^2$ | k | $R^2$ | k |
| **500ft 50kts** | 0.980 | 0.612 | 0.971 | 0.655 | 0.964 | 0.591 |
| **500ft 80kts** | 0.997 | 0.515 | 0.985 | 0.622 | 0.987 | 0.552 |
| **500ft 100kts** | 0.991 | 0.607 | 0.996 | 0.489 | 0.998 | 0.546 |
| **1000ft 50kts** | 0.957 | 0.617 | 0.976 | 0.616 | 0.962 | 0.536 |
| **1000ft 80kts** | 0.949 | 0.547 | 0.989 | 0.597 | 0.997 | 0.626 |
| **1000ft 100kts** | 0.952 | 0.486 | 0.962 | 0.500 | 0.988 | 0.484 |
| **1500ft 50kts** | 0.961 | 0.612 | 0.979 | 0.700 | 0.958 | 0.628 |
| **1500ft 80kts** | 0.996 | 0.610 | 0.991 | 0.595 | 0.973 | 0.576 |
| **1500ft 100kts** | 0.948 | 0.425 | 0.998 | 0.541 | 0.940 | 0.455 |

**Table 3.2** $R^2$ and k results for all SC approaches

Extending the same comparison to the SC data as was given to the AB data, there are 13 values over 0.98 (20 for AB) with 24 over 0.95 (also 24 for AB). Although there are several runs with a high $R^2$ value (more than 0.98), there are much fewer for the SC data than for AB's data. In addition, despite the same number of runs for both pilots having an $R^2$ value of over 0.95, the SC data in figure 3.23 is much more inconsistent than AB's data in figure 3.18. As we have already considered, while the inconsistencies may not be apparent in the $R^2$ values for data evaluated over 2800ft, there can be no question that SC's approaches are not as smooth and direct as AB's. Therefore, if the $R^2$ values are to be used as a guide to indicate the quality of an approach it may be necessary to consider them over a shorter range or more progressively (as with k in figure 3.22).

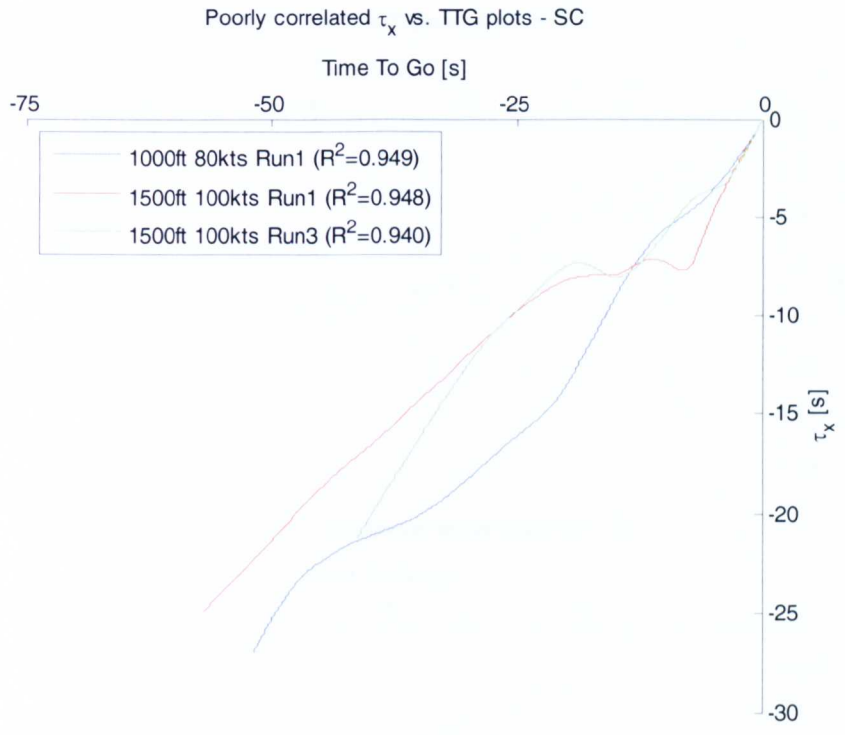


**Figure 3.25** $\tau_x$ vs. TTG for lowest $R^2$ value SC approaches

Figure 3.25 shows the 3 SC runs with the lowest $R^2$ values. Despite these being the worst cases of the 27 tests (in the sense of varying $\dot{\tau}_x$), each of the values falls only marginally below $R^2$=0.95, one of the values at which the SC and AB tests have been compared. In addition, each of the 3 poorest AB runs had $R^2$ values below the poorest SC run (0.122, 0.928 and 0.929). The two SC 1500ft 100kts runs in figure 3.25 feature a similar 'pause' to the AB 1500ft 100kts shown in figure 3.20. Until this point in both runs the approach had been smooth and direct, which was not often the case for SC. An equally common technique was that seen with the 1000ft 80kts test shown in figure 3.25, where the $R^2$ value is dictated by the small but continuous changes in $\tau_x$. Of interest is the point at which $\tau_x$ is held approximately constant in the 1500ft tests. The two examples in figure 3.25 show this pause occurring at approximately $\tau_x$=7 seconds, a similar figure to that seen with the AB data in figure 3.20 when the pause occurred at $\tau_x$=6-6.5 seconds.

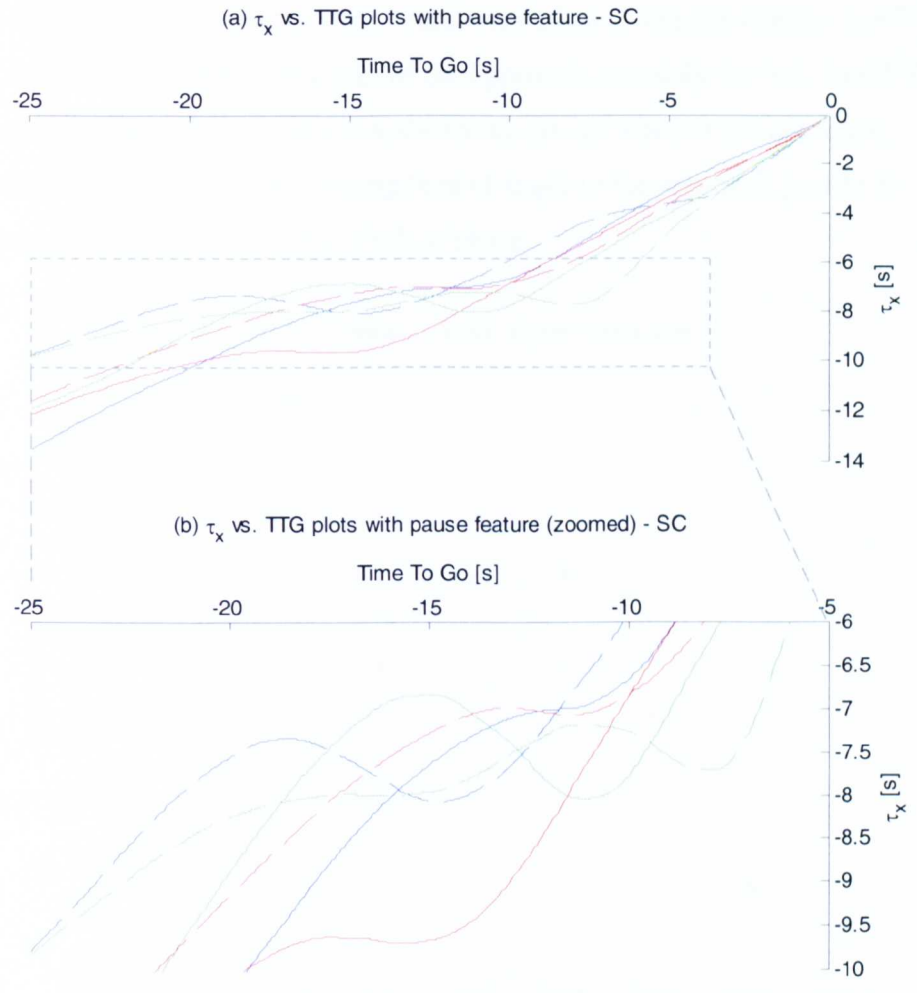


**Figure 3.26** $\tau_x$ vs. TTG for SC approaches with 'pause'

Figure 3.26 shows 6 SC runs, all of which feature a pause, otherwise known as a 'cautious pilot' technique in a previous study. Figure 3.26(b) is simply a zoomed version of figure 3.26(a), affording an easier inspection of the various $\tau_x$ values at which the cautious pilot technique is implemented. Before considering figure 3.26(b), figure 3.26(a) offers a telling result in terms of the point at which the cautious pilot technique begins. With the exception of one data (the solid red line), the technique commences between $\tau_x$=7-8 seconds. In addition, figure 3.26(a) shows that in all of the examined cases (with the exception of the blue dashed line) the cautious pilot pause was followed by a well correlated capture.

It appears that for the majority of runs with a late change in strategy $\tau_x$=7-8 seconds represents a vital part of the approach, certainly for SC. In GVE conditions the pilot appears to realise at this point whether the approach will be successful or not, making final changes to the approach profile as required, allowing for a smooth final phase.

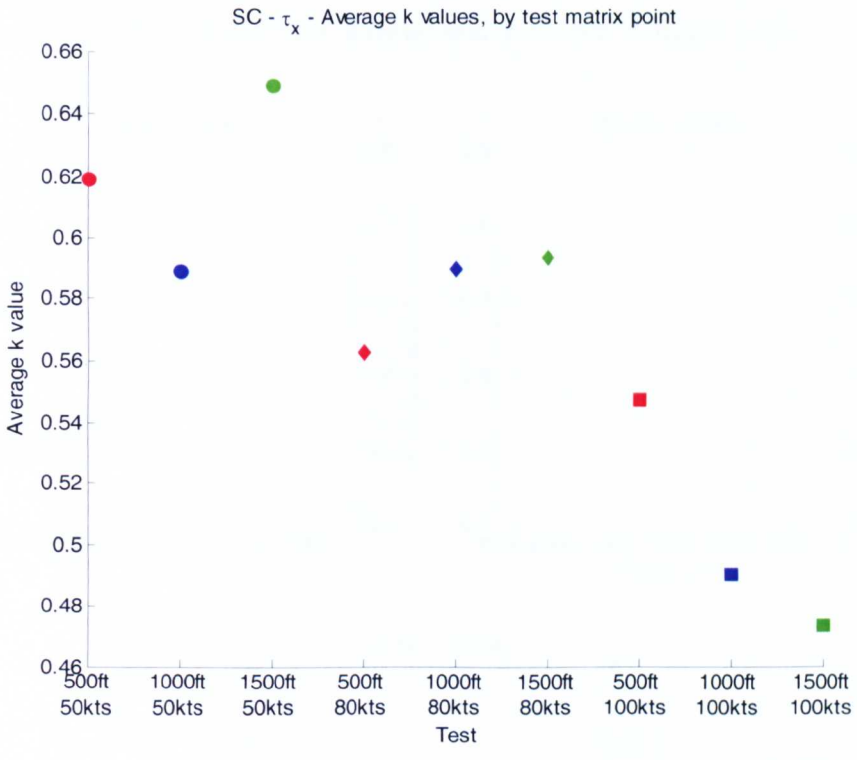


**Figure 3.27** Average k values vs. test point for SC approaches

Figure 3.27 shows the average k values for all SC tests measured over a range of 2800ft.The most noticeable trend is for a general decrease in k with increasing initial groundspeed. This is somewhat in contrast with the AB results (figure 3.21) where there was a lack of any clear pattern and, if anything, k increased with increasing groundspeed, especially when considering the data which did not include the potentially anomalous runs.

The lower k values for higher initial groundspeeds are not unexpected for SC given his approach method. At 2800ft, SC's groundspeeds were still

markedly separated based on initial task groundspeed. Therefore $\tau_x$ for the 100kts tests was smaller than $\tau_x$ for the 80kts tests, which was in turn smaller than the 50kts tests. However, the deceleration for higher initial groundspeed tests would then be required to take place over a longer time period, extending the total task time (and therefore the TTG data plotted in figure 3.23). The outcome of this longer deceleration period was a flatter slope for the high speed runs, a result which is seen in figure 3.27.

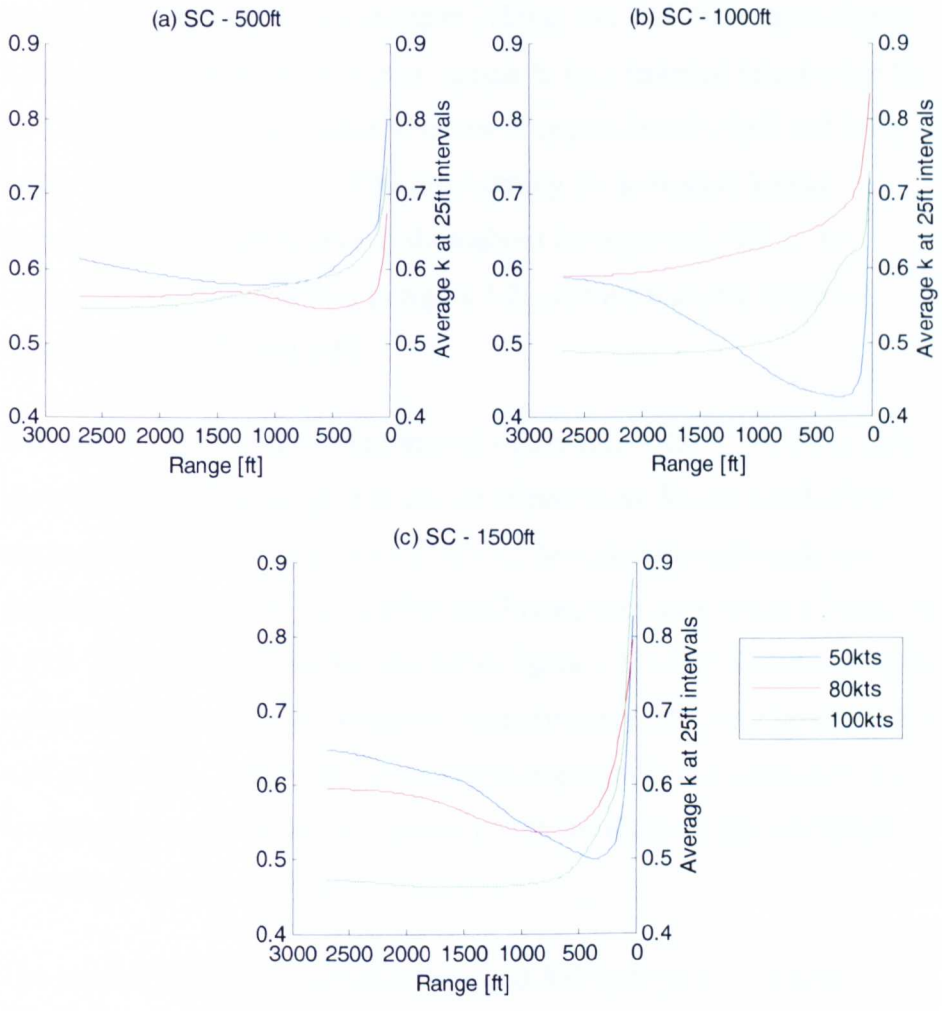


**Figure 3.28** Average k vs. range for progressive SC 25ft analysis

Figure 3.28 shows the averaged progressive k analysis of SC's approaches, evaluated in 25ft steps through the approach with subplots (a)-(c) separated

by initial height. A noticeable trend throughout each of the runs is the increase in k towards the end of each manoeuvre. In most cases k is increased to between 0.7 and 0.9, indicating an increasing level of deceleration at the end of the approaches which results in a 'hard-stop'.

Before this increase in the k values there is, in 4 of the 9 data, a trend for k to be held approximately constant. The clearest example of this is the averaged 100kts data in figure 3.28(c). The other results showing the trend are the 50kts and 80kts runs in figure 3.28(a) and the100kts run in figure 3.28(b). There does not, however, appear to be a repeated target value for k. The two 100kts cases show k values of approximately 0.47 and 0.49, which could be indicative of the pilot aiming for a constant k (and therefore $\dot{\tau}_x$ if $R^2$ approaches 1) throughout the approach of 0.5. In contrast, the k=constant data in figure 3.28(a) have higher k values of approximately 0.56 and 0.59.

It should be added that an examination of the individual $\tau_x$ vs. TTG data showed that the best results for any set of runs were for the 500ft-100kts test matrix point. There was very little $\tau_x$ deviation through each run, yielding a very high $R^2$ fit for all of the 3 runs, with an average $R^2$ value of 0.995. However, the data for this run in figure 3.28(a) shows an average k value which is only held constant at approximately 0.54 very briefly at the start of the data. This is then followed by a gradually increasing k value through the remainder of the approach, with the sharpest rate of change occurring over the final 350ft.

The general differences between SC's and AB's progressive k plots pose a number of questions. One of the more important questions is 'what constitutes an optimum approach?'

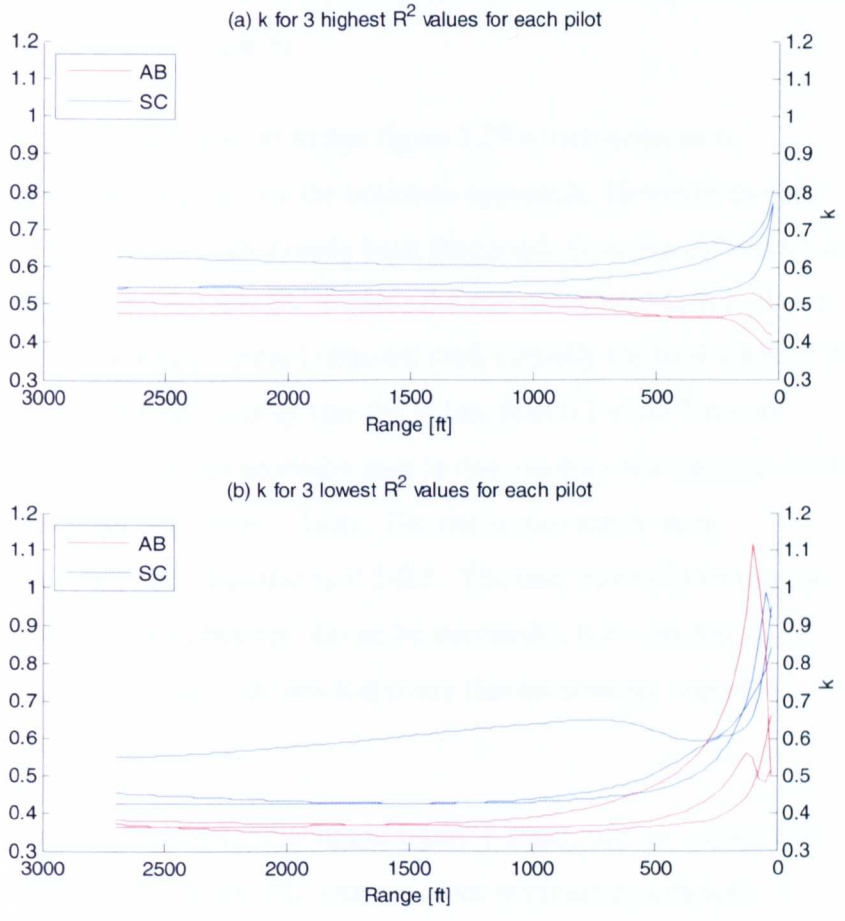


**Figure 3.29** k vs. range for 3 best and worst $R^2$ values for both pilots

Figure 3.29 shows original k vs. range data for both pilots; the data has not been averaged. Figure 3.29(a) highlights the data for each pilot's 3 highest rated runs in terms of $R^2$. Conversely, figure 3.29(b) shows data for the 3 worst runs. Although the potential for the $R^2$ values to be misleading has already been discussed, there is no doubt that figure 3.29 shows progressive k data for both pilots' 'best' and 'worst' tests. The $\tau_x$ vs. TTG plots for the 6 'best' cases are all almost linear, with the lowest $R^2$ value being 0.997. The 'worst' cases are also easily selected, particularly for

AB's tests where there are only 3 test points which differ significantly from the $\tau_x$ vs. TTG line of best fit.

There is various information within figure 3.29 which helps us to understand what might create the optimum approach. However the first point to note is that, as has already been discussed, there is a difference in technique between AB and SC towards the end of the approach in figure 3.29(a). AB's k values remain constant until virtually the final 100ft of the approach and then fall slightly (the fall is less than 0.1 in all 3 cases). Conversely, SC's values generally start to rise much earlier (at least 500ft from the helipad in 2 of the 3 data). The rise is also much more pronounced, with k increasing by 0.2-0.3. The tests have shown that the approach strategies of both pilots can be successful, but with AB's runs generally having greater success it appears that his strategy was more repeatable.

Throughout the 3 good approaches in figure 3.29(a), AB's k value never moves significantly above 0.5. One run does maintain a constant k of approximately 0.52, but the pilot appears to be in control of the approach throughout. In contrast, AB's data in figure 3.29(b) shows that k for the 'bad' cases begins to rise significantly above 0.5. In itself this is an important result when compared to AB's 'good' data, however an equally noteworthy feature of the plot are the k values before the large increases past 0.5. In all cases k is well below 0.4, therefore if the pilot were to maintain constant deceleration from this point the aircraft would stop short of the helipad.

In terms of the 'bad' SC approaches, the two runs with starting k values of less than 0.5 are not dissimilar to the 'good' AB test with the lowest initial k value. However, within 1000ft of the pad the SC data differs markedly from the 'good' AB data, with k increasing to between 0.9 and 1. The

reason for this, ostensibly good, initial phase of the approach deteriorating into a poorly correlated run provides another valuable piece of information as to the qualities required to ensure a good run. On further examination, the two runs in question were found to be runs 1 and 3 of the 1500ft 100ks test point. Therefore, it seems that the pilot's relatively cavalier strategy in which groundspeed and height were not reduced with any urgency in the initial phases of the tests leads to a much more demanding final stage in which the chances of a successful capture are greatly reduced. By way of a strange coincidence, two of AB's three 'good' data in figure 3.29(a) are for runs 1 and 3 of the 1500ft 100kts tests.

In terms of answering the question 'what constitutes an optimum approach?', the answer appears to be two-fold. The first part is for the pilot to be established on an approach with similar groundspeed and altitude conditions by a certain fixed point, thus making each approach highly repeatable, regardless of initial conditions. The second aspect is for the pilot to follow a k=constant approach, with k held constant until the aircraft is no more than 100ft away from the target. Ideally k should remain as close to 0.5 as possible (in a more general sense, between 0.45 and 0.5) for as long as possible throughout the approach.

#### *3.5.3.3 $\dot{\tau}_x$ Analysis*

By way of a final method of analysis of the GVE trial data, figures 3.30 and 3.31 show $\dot{\tau}_x$ and $\tau_x$ data for selected AB and SC runs, respectively.

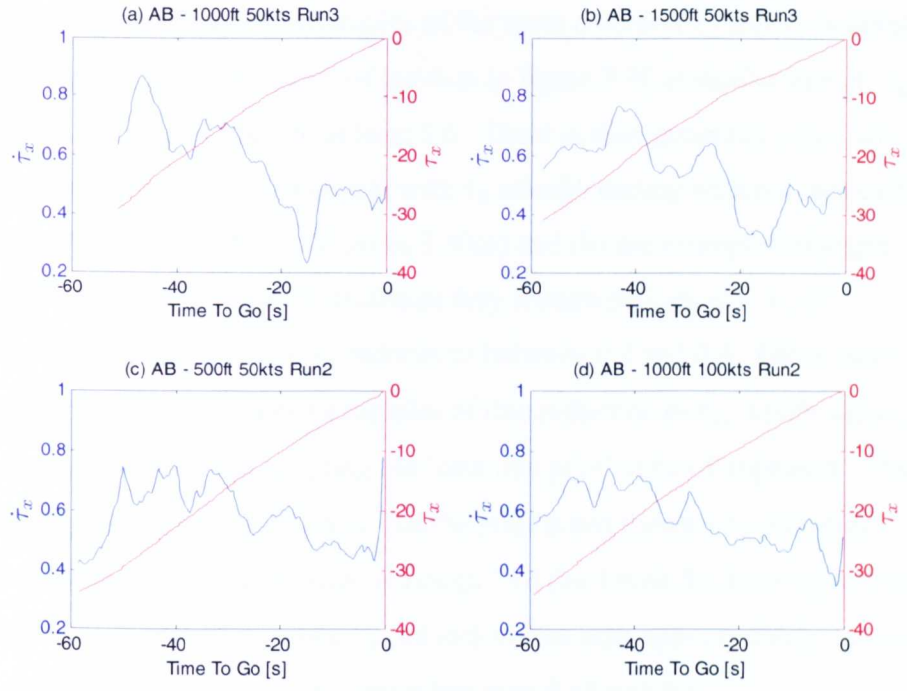


**Figure 3.30** $\dot{\tau}_x$ and $\tau_x$ vs. TTG for selected AB runs

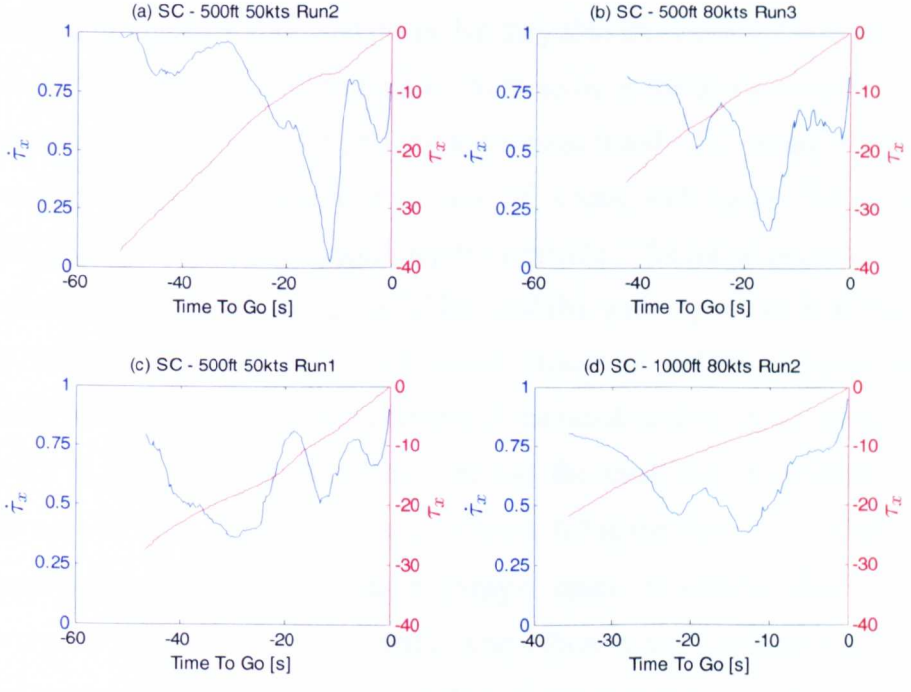


**Figure 3.31** $\dot{\tau}_x$ and $\tau_x$ vs. TTG for selected SC runs

Each figure shows two examples of the most common $\dot{\tau}_x$ and $\tau_x$ profiles during the approach. Each of the data in figure 3.30 is similar in that $\dot{\tau}_x$ starts, or quickly rises, to at least 0.6. There is then generally a gradual decrease through the approach, with $\dot{\tau}_x$ usually ending within a range of approximately 0.45-0.5. Figures 3.30(a) and (b) are examples of slight differences to this typical profile as they feature periods at a $\tau_x$ of approximately 8s where $\dot{\tau}_x$ reduces to between 0.2 and 0.4. Other runs feature more exacerbated examples of this reduction in $\dot{\tau}_x$, which, again, appears to show AB adopting the 'cautious pilot' style of approach. The examples in figure 3.30 show that the pilot is not flying a $\dot{\tau}_x$=constant profile through the approach, although 3 of the 4 runs do show regions of relatively constant $\dot{\tau}_x$ when $\tau_x$ reduces to less than approximately 7s. In each of these examples, $\dot{\tau}_x$ varies between 0.45 and 0.5.

The SC results shown in figures 3.31(a) and (b) are similar to the AB results in figures 3.30(a) and (b) in that they also show examples of SC using the 'cautious pilot' technique. In these cases the pause is more pronounced, resulting in $\dot{\tau}_x$ falling to between 0 and 0.15. Again, these examples are representative of many of SC's runs, with figures 3.31(c) and (d) highlighting another typical approach profile. The initial phase is similar to that shown in figures 3.31(a) and (b), with $\dot{\tau}_x$ values of at least 0.75 which reduce as the run progresses. However, in these examples there does not appear to be a clear example of the usual cautious pilot 'pause', with $\dot{\tau}_x$ then beginning to increase through the remainder of the approach. In each of SC's 27 runs, $\dot{\tau}_x$ increases above 0.5 in the final stages of the approach, exceeding 0.75 in the majority of cases. In addition, there are very few examples in the SC results where there is any significant period of constant $\dot{\tau}_x$. Of the SC runs which do show a constant $\dot{\tau}_x$, the technique is never used to capture the target, unlike several examples in the AB results (e.g. figure 3.30(a)).

As with the previous analyses, the $\dot{\tau}_x$ analysis has shown that AB and SC use very different techniques in order to capture the helipad. However, despite the differences, both techniques are equally successful in the GVE trial. Of particular interest will be the ability of the pilot to fly precise and efficient approaches in a degraded environment and, if so, whether the $\dot{\tau}_x$ used is similar to either of those seen in AB and SC's approaches.

## 3.6 CONCLUSIONS

The main objective of the GVE trial was to determine whether there was any use of $\tau$-guidance in the approach to hover manoeuvre. The analysis has shown that the pilots do indeed appear to use $\tau$-guidance during the approach to the helipad. Although both pilots' results showed high levels of correlation, AB's strategy was much more repeatable and led to a greater number of successful approaches. Any SkyGuide developed to aid an approach to hover manoeuvre should incorporate two phases. The first establishes the pilot on an identical approach pattern, no matter what the preceding task conditions. It is suggested that at a range of 3000ft the altitude should be 300ft and the groundspeed approximately 56.5kts. Once established at this point the second phase of the approach begins, with a k value of approximately 0.5. It is suggested that future research experiments with SkyGuides which command k values ranging from 0.45 to 0.525, with a range of constant and slightly varying profiles tested.

In addition to the recommendation for an approach in which k is controlled within the above tolerances, the $\dot{\tau}_x$ analysis has shown the strategies employed by both pilots during their approaches. Although there does not appear to be a significant period of constant $\dot{\tau}_x$ in the results, a number of AB's data do show some regions of $\dot{\tau}_x$=constant, some of which occur immediately prior to capture of the helipad. In these tests, $\dot{\tau}_x$ is held

constant between values of approximately 0.45-0.5, a range which complements the previous finding in the progressive analysis.

In terms of the NASA analysis it has not been possible to replicate the original results with any significant degree of accuracy. The power parameter results for AB showed a very narrow range of groundspeeds at 2800ft, as expected given the nature of his approach. When discounting two anomalous results, there was a general pattern for AB's power parameter to increase with increasing initial altitude and also decreasing initial speed. SC's range of groundspeeds at 2800ft was much wider than AB's, although the range of power parameters (with 2 exceptions) was much narrower. In addition, there was no general trend within SC's power parameter values.

The hypothesis which suggested there may be a link between the NASA power parameter, n and $\dot{\tau}_x$ has not been proven. Coupled with this lack of agreement, there was also a difference between the results for the two UoL test pilots which called into question the NASA aims of defining a generic approach profile.

The substantial differences between the strategies of the two pilots were noted at an early stage of the basic data analysis and these differences can be seen manifesting themselves in both the NASA analysis and the $\tau$-analysis. Considering the small sample size of just two pilots this presents an important result as it indicates how two highly skilled and experienced test pilots can offer very different results for a standard manoeuvre. When we consider the original goals of the NASA research, this indicates the difficulty of creating IFR procedures which feel natural to all pilots, no matter how organic and unconstrained the research allows the approach to be. $\tau$-based SkyGuides may offer an alternative which may be more

acceptable to all pilots, but extensive research will be required to determine how wide-ranging a solution $\tau$ can provide.

In summary, we have established a good understanding of the differences in piloting strategy through the entire length of the approach and have seen how these differences manifest themselves in the NASA and $\tau$-analyses. A k-based SkyGuide has been suggested, with a specific set of parameters to be investigated further. In addition, we now have an excellent set of baseline results for the approach to hover manoeuvre in GVE and the next stage of the analysis will be to investigate how the deterioration of the visual scene affects the ability of the pilot to complete the task.

# Chapter 4

# APPROACH TO HOVER – DVE

## 4.1 INTRODUCTION

The DVE version of the approach to hover scenario was designed to offer a completely novel approach to the research, with the testing taking place in a number of scenes which gradually became more and more visually deprived, adding to the difficulty of the task while allowing the research to take place in the safety of the simulation environment.

The intention was to keep aspects of the previous NASA test matrix whilst introducing new visual variables which would provide the pilot with an increasingly more difficult task as the visual cues in the scene were reduced. One of the aspects of the trial was designing the new test matrix as there were many ways in which visual variables could be introduced, with each potential option generally tripling the total number of test points. The selection process will be discussed at length in section 4.3.

While the requirements for the test matrix dictated that the DVE trial could not be an exact replica of the Approach to Hover trial, the setup is as similar as possible, to allow the results from the two trials to be compared, with the focus for the DVE analysis being the time to stop, $\tau$.

The test pilot used was AB, who had also flown the GVE Approach to Hover trial, enabling direct comparisons to be made between the GVE and DVE trial data.

## 4.2 OBJECTIVES

The objectives of the DVE trial were to investigate the ways in which the variation of textures and structural elements within the scene affected task performance.

The main focus for the analysis was to investigate how the pilot's use of $\tau$ changed through the various visual conditions. Indeed, the overriding question which the investigation sought to answer was 'Does the pilot use $\tau$ to guide the approach?'

The inevitable follow-up to the main objective was to then determine how each visual change in the database affected the pilot's strategy and ability to complete the approach. This information would then be used to suggest ways in which a Prospective SkyGuide could be designed to provide sufficient information to the pilot to fly an approach safely using tau guidance.

## 4.3 DESIGN OF THE TEST

### 4.3.1 Defining the test conditions

One of the issues with the design of the trial was the need to introduce a series of visual changes to the scene, whilst attempting to retain the original test matrix of the NASA research. Again, time constraints played a role in the variables selected, with the relatively long run time

compounding this problem. The first setup change deemed necessary was shortening the range of the test from 10000 to 5000ft. While there were interesting aspects to the original approaches over the first 5000ft of the 10000ft range, the critical phase of the approach was the final 2-3000ft and it was estimated that this change would save at least 30 minutes of testing time.

Recognising that even with this change, and given the time constraints, it would only be possible to conduct a 27 run trial, the first decision was to remove the repeat runs which had been utilised in the previous trial. While these had been useful for giving more informative averaged plots of the data it was felt that it was impossible to accommodate such a relative luxury given the need for the visual changes to be introduced to the list of variables.

In order to ensure that two of the three test matrix variables were visual elements, there had to be a change to the two previous GVE matrix variables of initial groundspeed and initial altitude. The solution was to combine the height and speed variables, achieved by giving each test point an initial descent rate of 500ft/min, with the three initial speeds of 50, 80 and 100kts retained. Therefore, in order to maintain a descent rate of 500ft/min, the starting altitude was a function of each of the three initial speeds. The reason for choosing 500ft/min was to give a sensible spread of starting altitudes for the three initial speeds. In addition, given the reduced range of the task, this descent rate would lessen the need for the pilot to descend and decelerate aggressively for the high initial altitude and groundspeed conditions. A descent rate of 500ft/min gave glide slopes of 2.8°, 3.5° and 5.6° for the 100kts, 80kts and 50kts cases respectively, values which were much more comparable to real world approaches than the glide slopes of 5.6°, 7° and 11.2° which were calculated for a 1000ft/min descent rate.

The combination of the altitude and groundspeed variables meant that there could be two further test variables with 3 settings for each. A large number of scene adjustments were considered including:

1. Retaining the various airport terminal buildings, providing a wireframe representation of them or simply removing them.

2. Adjusting/removing the runway/taxiway textures.

3. Utilising LANDSCAPE to add fog to the scene. Initially, with a relatively long range visibility which would only obscure the natural horizon, and then with significantly reduced visibility, such that the helipad was only just visible at the start of the manoeuvre, to give the pilot the impression of being in a much more restricted environment.

4. Adjusting the sky detail to give a much more clinical-feeling single-coloured blue sky as opposed to the standard textured sky.

5. Changing/removing the texture of the grass surrounding the airfield to reduce motion cues.

6. Removing runway and taxiway markings.

The various options listed above all offered useful lines of investigation, although it was felt that some were relatively subtle changes which would not affect task performance. Instead the two variables selected were, firstly, various helipad heights (with one ground based helipad) to provide changing levels of macrostructure feedback, and, secondly, a general alteration of the quality of the textures in the scene.

### 4.3.2 Selecting the scene content

With the test variables selected it was then important to design three individual settings for each which would offer a different challenge for the pilot, and also which would combine with the other visual variable to produce 9 unique test points.

The helipad heights were selected so that their structures gave limited (50ft) and somewhat stronger (100ft) looming information to the pilot as he approached. While it is recognised that 100ft may be excessive for a free-standing land based platform, the intention was to investigate how the looming of such an object might affect the results in the critical final phases of the approach.

The most striking change in the scene was the general alteration of the textures presented to the pilot in an attempt to provide a varying amount of visual cues, especially in the crucial final stages of the approach. The changes have been termed 'normal' (or for the purposes of some figures, 'norm'), 'grey' and 'green'. This variable will also be referred to as the 'main' variable in later discussions in order to differentiate it from the helipad height changes in the database.

The visual changes are shown in the figures 4.1(a), (b) and (c).

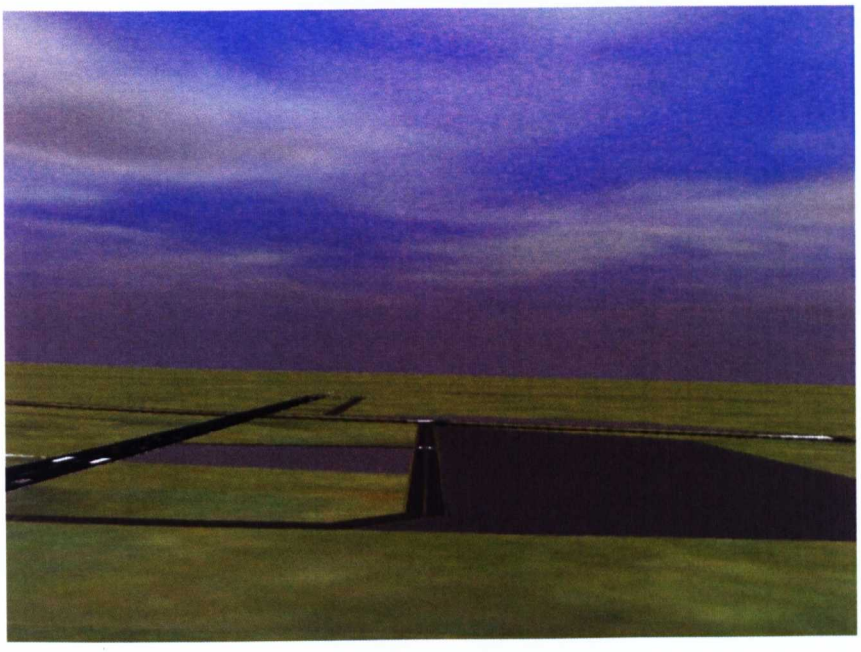

(a)

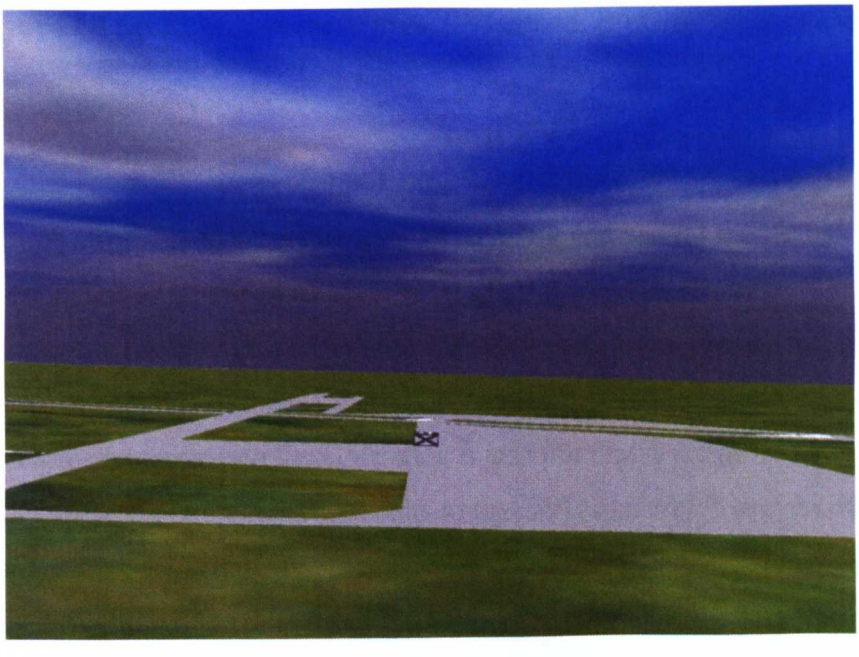

(b)

(c)

**Figure 4.1** (a) Normal scene texture, 0ft helipad; (b) Grey scene texture, 50ft helipad; (c) Green scene texture, 100ft helipad.

It should also be noted that the assorted terminal and hangar buildings present in the original Approach to Hover trial have been removed. This decision was taken to ensure that the best visual condition for this test was not an exact replica of the GVE trial. Although the DVE trial was intended to act as a comparison to the GVE trial, it was felt that if the new test yielded different strategies and results to the GVE trial which prevented comparisons between the two, the normal scene texture condition would act as something of a GVE condition for comparison with the grey and green databases.

The normal, grey and green databases were specifically designed to try to replicate the full range of the Usable Cue Environment (UCE). The UCE

is a representation of the level of the DVE, established through an aggregation of visual cue ratings (VCR) awarded by the pilot. More information about the UCE and the VCR scale can be found in Appendix B.

Figure 4.2 shows the range of UCE ratings awarded during the tests for the 9 visual scenes.

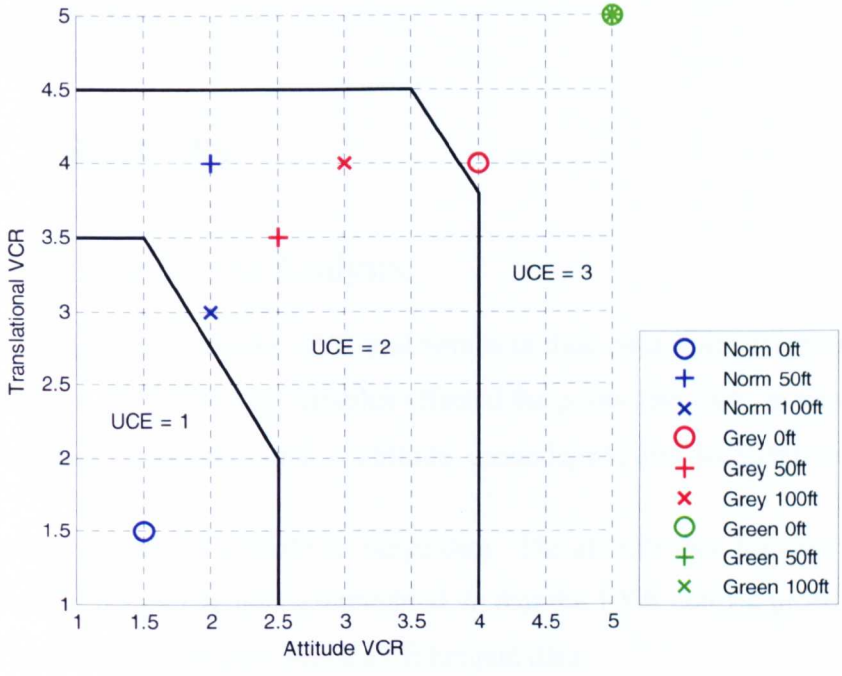


**Figure 4.2** UCE ratings awarded for DVE flight test databases

The figure is very encouraging as it shows a gradual increase in the difficulty of each of the 'main' variable changes (i.e. normal, grey and green), with the normal database offering a UCE of 1 and 2, the grey database providing a UCE of 2 and 3, and the green database providing a very difficult UCE 3 for each helipad height.

Interestingly, the 0ft helipad ratings for the normal and grey databases are very different, with '0ft normal' being the easiest of the three settings,

whereas '0ft grey' is the most difficult helipad height for that particular database. This is an encouraging result as it validates the selection of the helipad height variable because of the way in which the helipad height can be seen to be interacting with the various main database settings. By removing much of the detail of the normal database, the '0ft grey' condition clearly becomes much more challenging than the 50ft or 100ft settings, immediately showing the value of certain structural cues in a degraded environment and providing a useful result for the trial before any data are analysed.

## 4.4 RESULTS

### 4.4.1 General Data Analysis

Initially the focus is on the DVE trial results in their own right, examining the ways in which the test variables affected the pilots approach, in terms of basic task parameters such as altitude, groundspeed and deceleration.

Figure 4.3 shows the altitude vs. range data. The altitude data for each of the various helipad heights are unedited, in that the 100ft helipad profiles start and end 100ft higher than the 0ft helipad data.

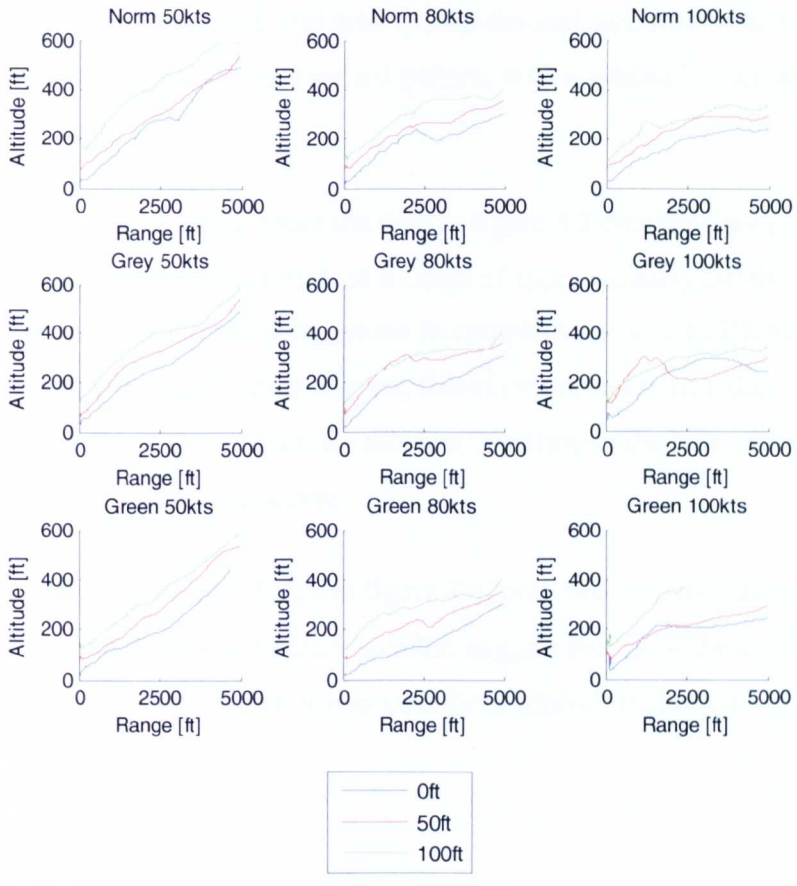


**Figure 4.3** Altitude vs. range for DVE trial

Figure 4.3 shows that the most noticeable differences in the altitude approach profile is caused, not by the changes in the helipad height or the visual database, but by increasing initial groundspeed. Looking more closely at the 50kts runs, there is very little reduction in the accuracy of the approach as the scene degrades from normal to green. However, as initial speed increases the various plots begin to show more altitude adjustment through the approach.

Unlike the GVE trial, there does not seem to be a clear piloting strategy which is repeated through all test points in figure 4.3. The 'grey 100kts' data show three unique approach patterns. The 0ft helipad profile, unusually, features an initial climb, the 50ft profile shows a descent to

2500ft followed by a climb and then a steep descent and, finally, the 100ft data follows a slightly more standard pattern, with a gradually increasing rate of descent.

Another point to be made about the data in figure 4.3 concerns the green 100kts 100ft profile, which starts at a range of approximately 2450ft. This particular run took a much longer time to complete due to the difficulties the pilot had with establishing a hover, therefore the simulation data recording buffer was exceeded for this test, resulting in the loss of data for the first 2550ft of the manoeuvre.

The groundspeed results shown in figure 4.4, presented in this case to compare visual databases on each subplot, suggest that from the earliest stages of the approach the pilot was equally in control of speed for all tests.

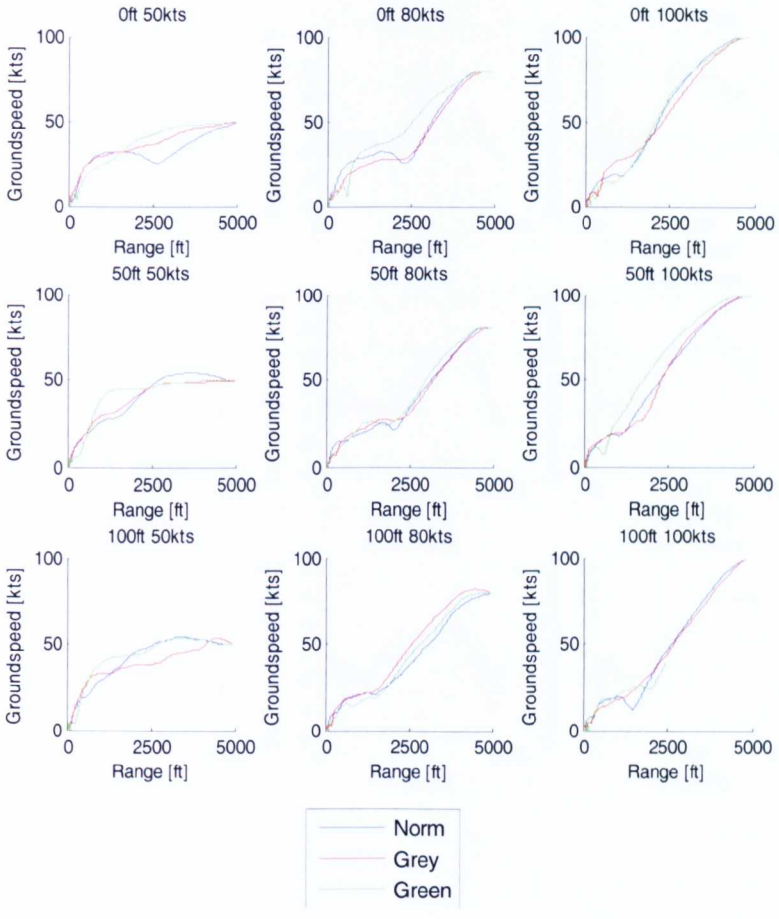


**Figure 4.4** Groundspeed vs. range for DVE trial

The 80kts approaches, with the exception of the green 0ft 80kts run, all feature a characteristic initial deceleration followed by a period of relatively constant speed before the final hover capture. A similar result is apparent in the 100kts data, albeit with a steeper change in groundspeed, rather than a period of constant speed. As might be expected, there is no rapid deceleration for the 50kts runs. In addition it appears as if there is no repeated strategy in the 50kts tests, with some runs showing an increase in groundspeed, some a decrease and others an initially constant groundspeed. The deceleration data, shown in figure 4.5, shows similar patterns to the original AB GVE data.

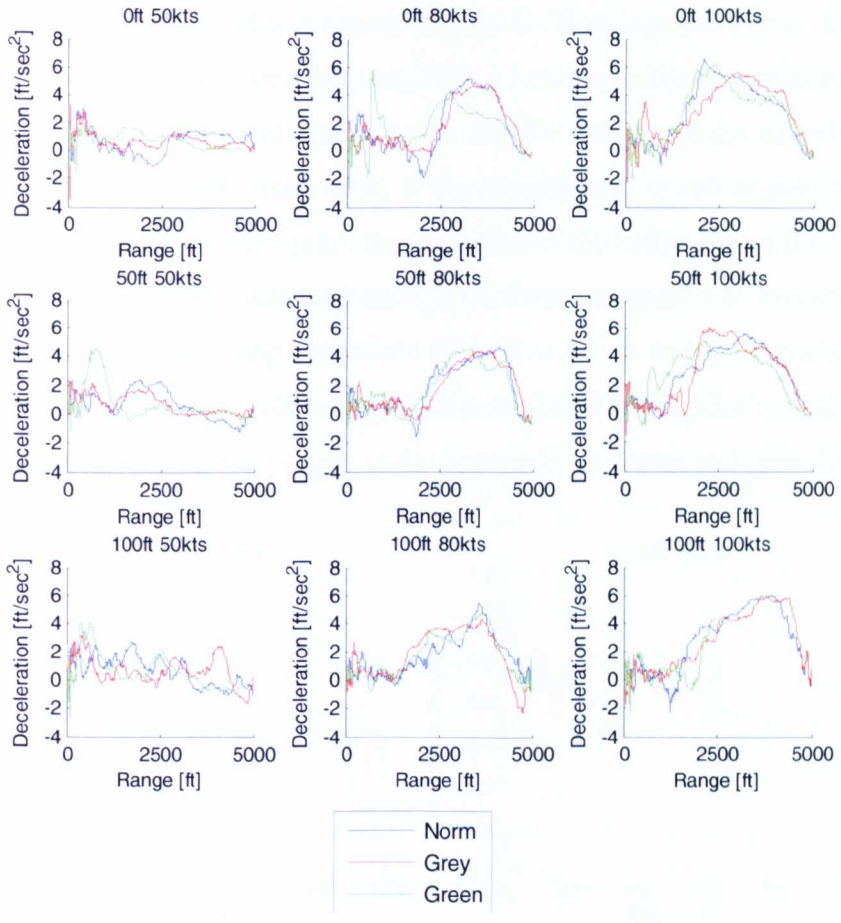


**Figure 4.5** Deceleration vs. Range for DVE trial

The 50kts approaches shown in figure 4.5 exhibit the more classical, gradually increasing deceleration style, seen in much of the SC and NASA data, whereas the higher speed approaches feature a deceleration as soon as the manoeuvre begins.

Despite any initial preparation for the runs, the pilot was still faced with a difficult task over the closing stages of the approach, the most problematic phase of which was the period when the helipad had disappeared out of view on the main simulator OTW displays but had not re-appeared in the chin windows. This issue existed to some extent for the 0ft helipad, but was much more prevalent for the raised helipads. The pilot commented that this was a 'critical phase' of the final hover capture and, for the short

period where the helipad was not visible, the UCE ratings increased. The ability of the pilot to successfully establish a hover quickly depended to a certain extent on the visual database, but also the stability of the aircraft as the helipad disappeared from view. If the groundspeed or roll or yaw rates required attention from the pilot, the transition of the helipad from the OTW to chin windows was long enough for these parameters to become more of an issue, requiring even more corrective action with potentially very few cues. Such a problem was then manifested in the pilot's control inputs through the closing stages of the approach, as shown in figure 4.6.

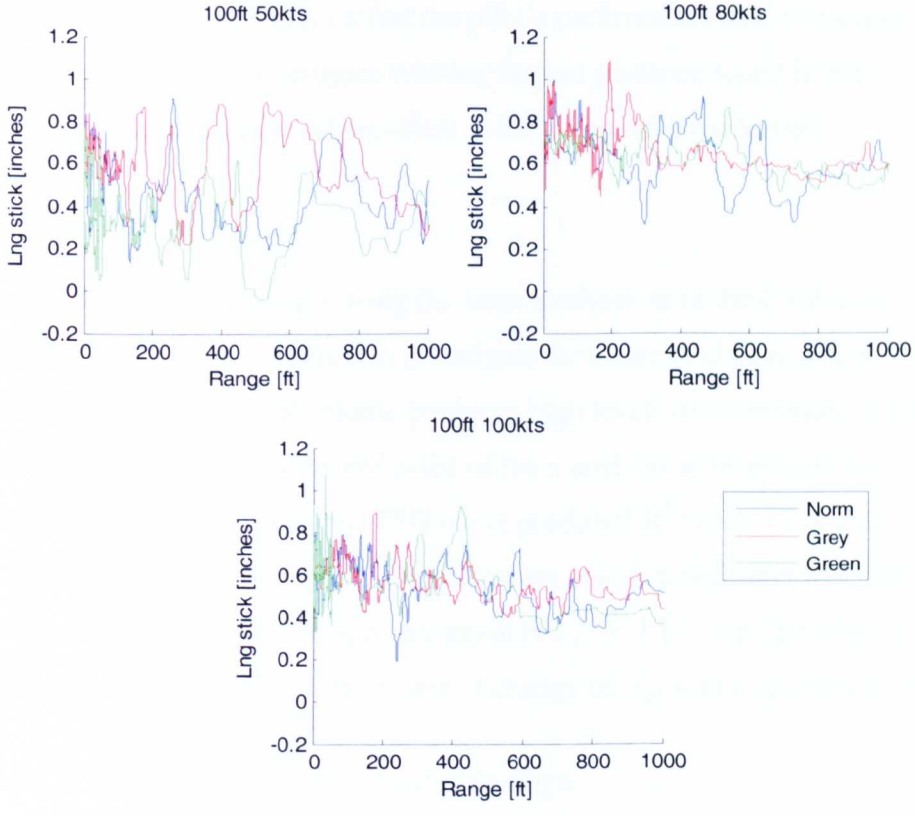


**Figure 4.6** Comparison of Longitudinal stick input vs. range for 100ft helipad approaches

Figure 4.6 shows the pilot's longitudinal cyclic input over the final 1000ft of the approach. The green 50kts and 100kts test points illustrate the result of losing visual cues over the helipad, with relatively large amounts of

longitudinal stick input being required to establish a hover. It should be noted that while the stick inputs are small relative to the total physical range of the cyclic (±5 inches), they are considerable in terms of the range of the control input used through the previous stages of the approaches and also the frequency at which positive and negative maxima are applied over the final 60ft of the approach.

The general data analysis has given some information as to the way in which the pilot flew the various approaches and some of the challenges posed by the varying content of the visual databases. The next step is to consider how these changes affect the pilot's performance in a $\tau$ context and, in particular, to investigate whether the tau guidance found in the GVE AB approaches is still prevalent in the degraded environment.

### 4.4.2 Tau analysis

In addition to considering $\tau$ using the same analyses as in the GVE trial, the DVE analysis is expanded to investigate the range of closure to the helipad over which the $R^2$ metric produces high levels of correlation. That is, measuring back from the end point of the $\tau$ analysis to determine the distance over which the $\tau_x$ vs. TTG curve produced $R^2$ values of at least 0.95 and 0.90. As in Chapter 3, the following analyses will refer to k, the gradient of the straight line approximation to $\tau_x$ vs. TTG over the relevant period, and $\dot{\tau}_x$, the instantaneous rate of change of $\tau_x$ with respect to TTG.

#### *4.4.2.1 $\tau_x$ vs. TTG and associated findings*

The first stage of the $\tau$-analysis is a plot showing $\tau_x$ against TTG. Figure 4.7 shows $\tau_x$ vs. TTG for the DVE trial.

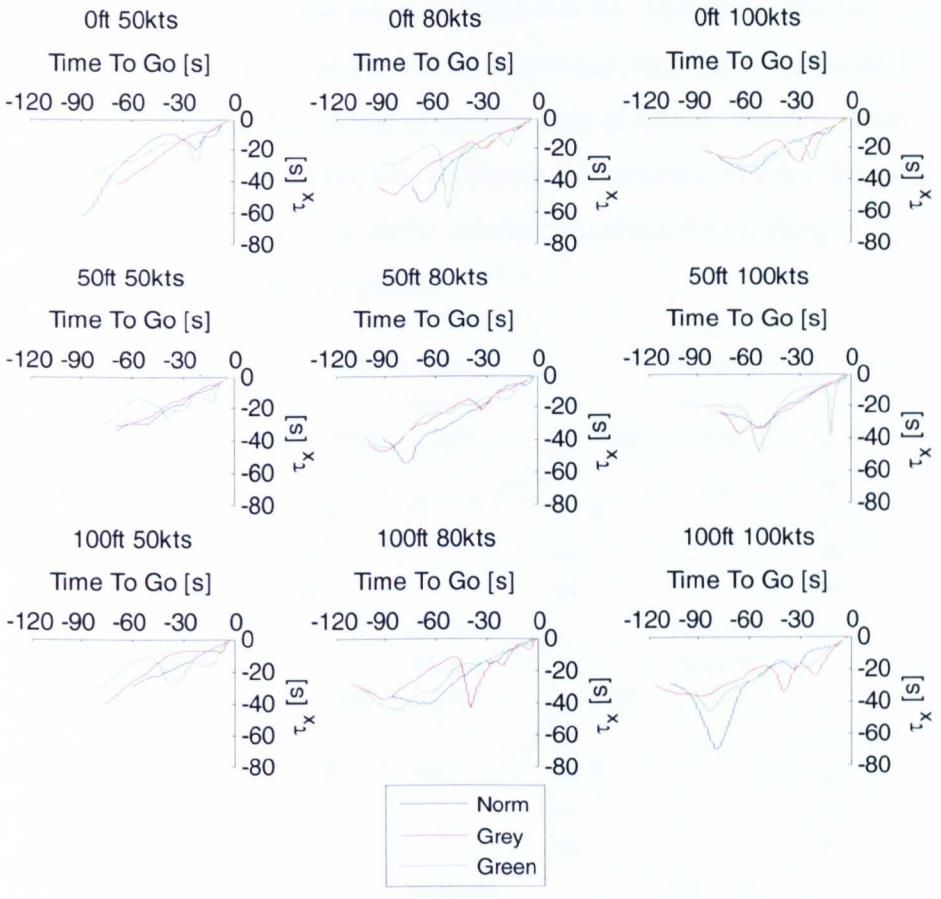


**Figure 4.7** $\tau_x$ vs. TTG for DVE approaches

Figure 4.7 shows $\tau_x$ data calculated from a range of 2800ft. The two-phase AB approach was discussed in Chapter 3 with the initial deceleration phase being, 'task' driven and the final approach being 'target' driven. Unfortunately, given the shorter range of the DVE trial, some of the increases in $\tau_x$ at the start of the data in figure 4.7 were due to the pilot's initial phase one decelerations. By including this section of the approach in the analysis, the $R^2$ and $\dot{\tau}_x$ values for the small number of runs in question will inevitably be affected for the calculations conducted at a range of 2800ft. Although this would have been undesirable if we were conducting a NASA analysis on the data, it is not considered critical to the $\tau$-analysis for two reasons. The first is that few of the runs suffer from this

problem, and it is relatively minor in those that do. Secondly, several different methods of $\tau$-analysis will be conducted, with the other methods not being affected by the choice to trim the data at 2800ft. Finally, when the various text matrix points are compared, the presence of a deceleration within 2800ft can still reveal useful information about the challenges presented by each of the test points.

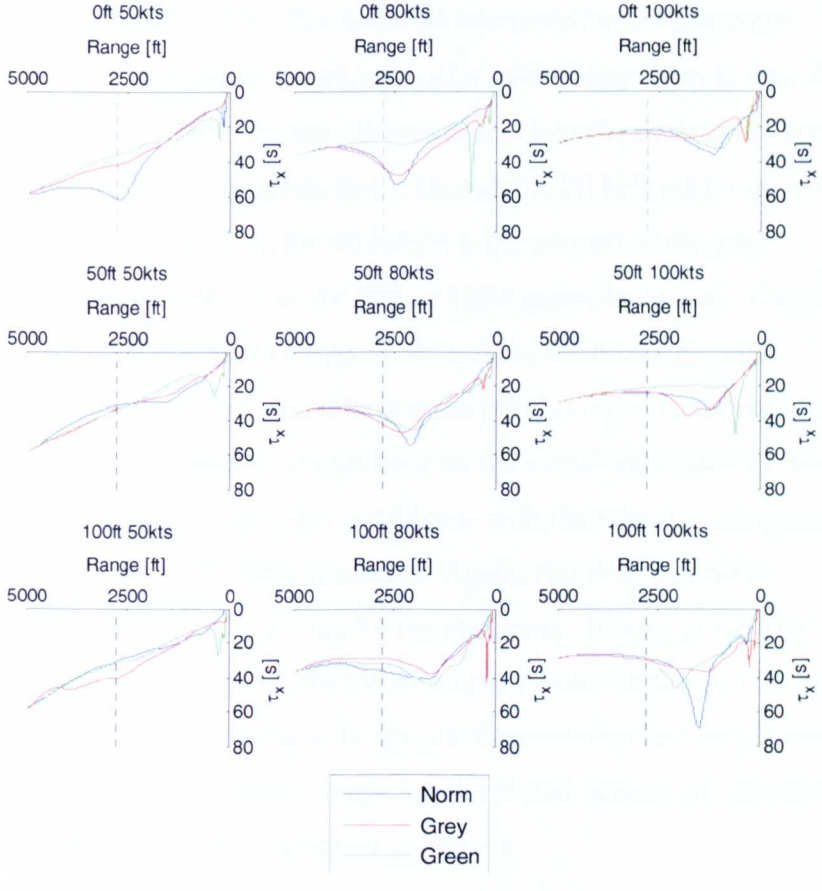


**Figure 4.8** $\tau_x$ vs. range for DVE approaches

Figure 4.8 shows $\tau_x$ plotted against the full 5000ft range of the DVE trial, with a dotted line at 2800ft to show the point at which the data has been trimmed for the first part of the $\tau$-analysis. As might be expected, the 50kts tests show a relatively direct approach, with only the 'Normal 0ft

50kts' test showing any discernable increase in $\tau_x$ over the first half of the approach.

The 80kts tests in figure 4.8 shows that, for each increase in helipad height, $\tau_x$ reaches a maximum value and then begins to close towards zero at slightly later points in the approach. Regardless of the visual database this seems to happen at approximately 2350ft for the 0ft helipad, 2100ft for 50ft and 1600ft for 100ft. This could be interpreted in several ways. The first is that the 0ft helipad height tests offer better visual cues to the pilot than the 50ft and 100ft settings. However this hypothesis does not agree with figure 4.2 which suggests that, although the 0ft helipad for the normal scene offers the best UCE, the 0ft height is the poorest of the grey databases, and no better than the 50ft or 100ft green databases. There is a clear mismatch between this hypothesis and the UCE ratings. An alternative interpretation would be that the pilot's commitment point is later for the larger helipad heights because the visual information is more coherent, allowing greater pilot confidence with the selection of a point at which to commit to the final approach. Again, this theory is not in agreement with the UCE ratings for the databases. Indeed, if we examine the average UCE ratings for the visual scenes (shown in figure 4.9) we can see that, in terms of the helipad height, all three settings are very similar to each other when the average ratings for all helipad heights are considered, casting further doubt over the two hypotheses.

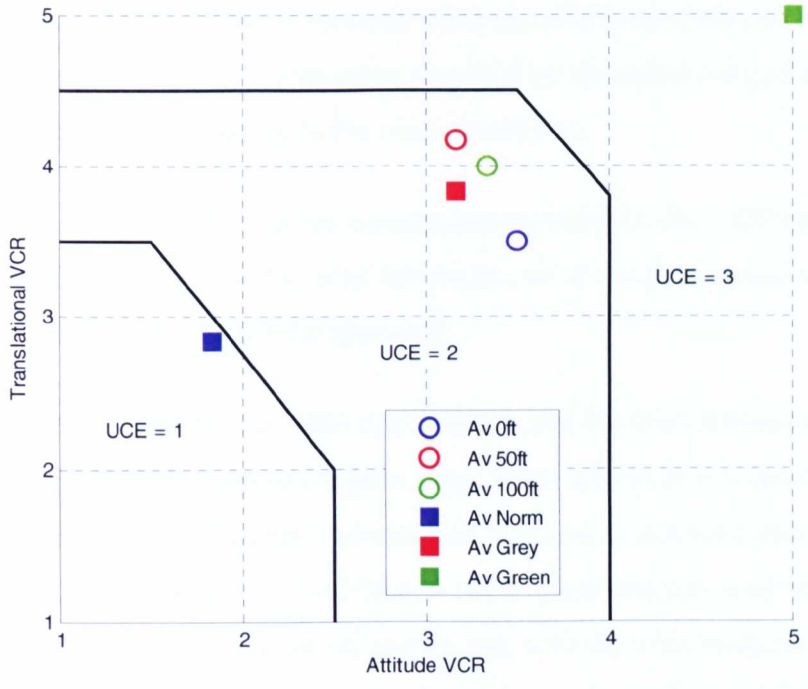


**Figure 4.9** Average UCE ratings for main database content and helipad heights for DVE trial

It seems that the reason for the varying performance through the 80kts tests is due to the changing way in which the helipad heights interact with the main database through the approach. One of the pilot's comments for the green 100ft 80kts test was:

> *"The early approach is slightly less challenging in the green scene with the 100ft deck. When you get there it is harder."*

This effect was also noted in the normal 80kts 50ft run:

> *"The 50ft deck is worse than 0ft when I am over the pad."*

Both pilot quotes tell us that the raised helipads offer useful cues while the superstructure is in view due to the added information in the optical flow

field. However, this effect is reversed when the pilot is over the pad, with the differing optical flow information provided by the raised helipad and the ground beneath it adding to the pilot's workload.

Therefore it would seem that the information provided by the UCE ratings is not an absolute representation of the visual cues for each database setting as they can change through the approach.

Based on the results for the 80kts runs it seems that the macrostructure is initially important in helping the pilot to guide his approach as it provides a looming cue, but then becomes a hindrance with macro and microtextures becoming more important. The 50ft and 100ft raised helipads were the only macrostructures in any of the scenes and, with the pilot being required to aim for the structure, the cues provided by it would inevitably disappear, causing the pilot to rely on other visual information in the scene. One possible future line of investigation could examine the ways in which macrostructures and textures affect performance through a manoeuvre, with the assorted cues introduced and removed at various stages during the run to investigate their impact.

By way of a further example of the powerful cues provided by the macrostructure of the raised helipads, figure 4.10 shows groundspeed plotted against range for the DVE trial. The data in the first subplot, figure 4.10(a), is separated by initial groundspeed, with figure 4.10(b) showing the data separated by helipad height.

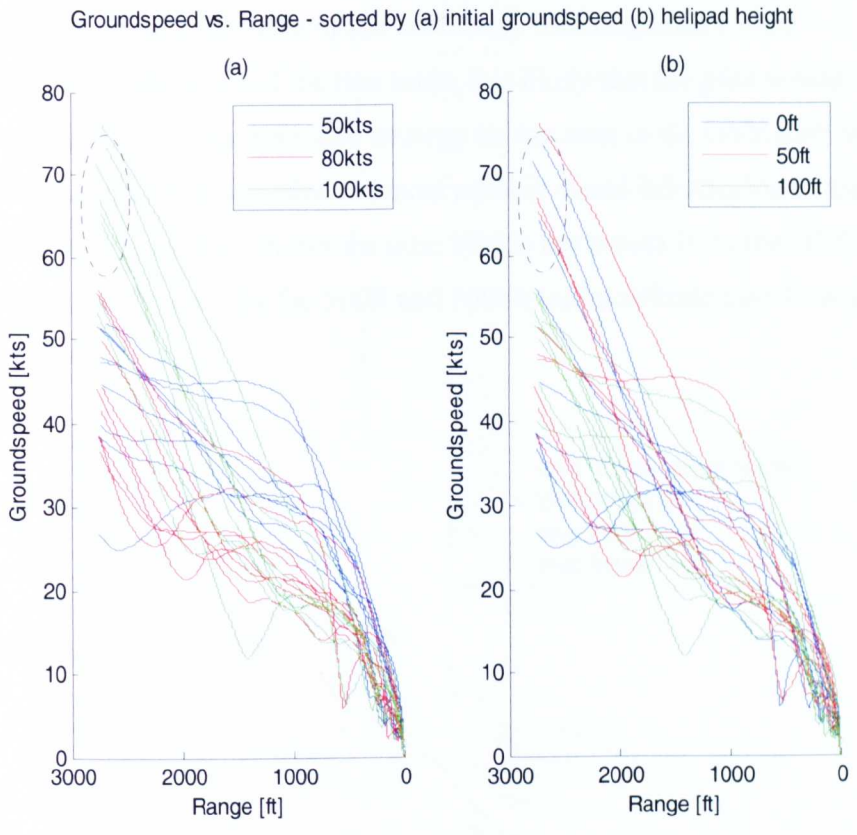


**Figure 4.10** Groundspeed vs. range for DVE approaches

Figure 4.10(a) shows that of the nine 100kts approaches, six runs remained at a noticeably higher speed than the other approaches at 2800ft (highlighted by the dotted ellipse). If we examine the same data in figure 4.10(b), it is shown that the six higher speed approaches correspond only to 0ft and 50ft helipad heights. With all of the 0ft and 50ft helipad runs represented this also means that the six high speed runs represent two normal, grey and green runs respectively.

As with the previous section of the analysis, there are two ways in which this disparity could be interpreted. The higher groundspeeds at 2800ft for the 0ft and 50ft 100kts approaches could be due to confidence with the cues provided by the scene, or they may highlight a lack of visual information with which a deceleration strategy can be formed. In order to discover if either of these two theories is accurate we can compare the

DVE trial results with those of the GVE trial. Although there were differences in the setup of the two trials, it is likely that the pilot would have adopted a similar approach strategy to that seen in the GVE trial with whichever test setup provided the most reliable visual information in the DVE trial. Figure 4.11 shows the nine 100kts test points from the DVE trial and also the data for the 500ft and 1000ft initial altitude runs from the GVE trial.

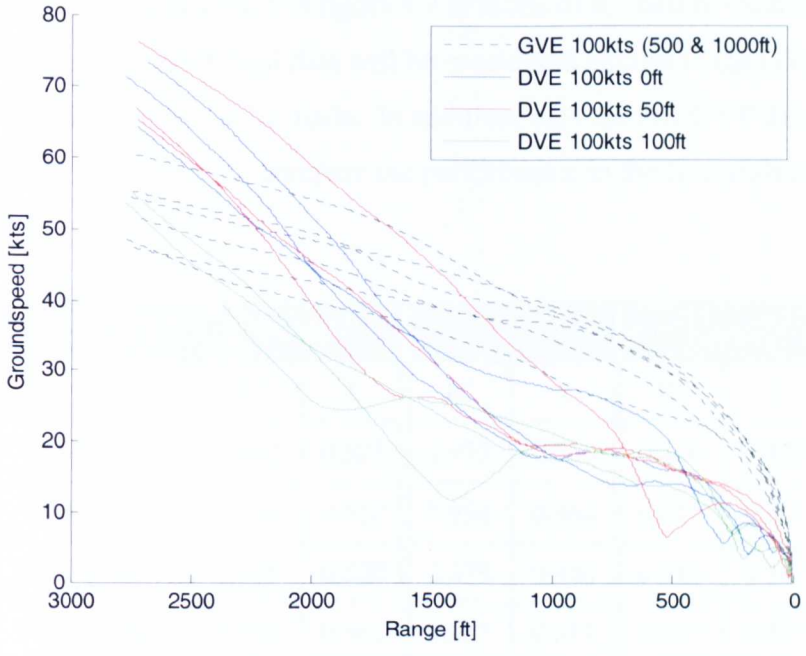


**Figure 4.11** Groundspeed vs. range for selected GVE and DVE 100kts test points

Figure 4.11 shows that in 5 of the 6 100kts GVE runs the pilot had decelerated to speeds similar to those observed in the 100ft 100kts DVE runs. Unfortunately, one of the 100ft DVE profiles does not extend to 2800ft, although it does appear that, if the data were to be extrapolated, the groundspeed in this case would be similar to the other 100ft DVE runs at 2800ft. Therefore it appears that the 100ft helipad gave the pilot better cues during the early stages of the approach, allowing speed to be controlled at a much earlier point. While this does not guarantee a

successful outcome to the manoeuvre it can potentially give the pilot a lower workload over the closing stages of the approach given the reduced requirement to pitch the aircraft up to reduce speed, which would further limit visual cues.

#### *4.4.2.2 $\tau_x$ $R^2$ analysis*

We will now move on to consider the quality of the linear approximation for $\tau_x$ vs. TTG data shown in figure 4.7 in terms of $R^2$, before examining the k value. The DVE trial data will be considered alongside the GVE data so that comparisons can be made. In addition, only the AB GVE data will be considered in order to compare the performance in the two trials more directly.

| | *Norm* | | *Grey* | | *Green* | |
|---|---|---|---|---|---|---|
| | $R^2$ | k | $R^2$ | k | $R^2$ | k |
| **50kts 0ft** | 0.787 | 0.523 | 0.977 | 0.586 | 0.816 | 0.422 |
| **50kts 50ft** | 0.970 | 0.512 | 0.994 | 0.484 | 0.411 | 0.381 |
| **50kts 100ft** | 0.995 | 0.500 | 0.873 | 0.440 | 0.045 | 0.367 |
| **80kts 0ft** | 0.862 | 0.562 | 0.967 | 0.517 | 0.267 | 0.407 |
| **80kts 50ft** | 0.932 | 0.577 | 0.961 | 0.473 | 0.635 | 0.404 |
| **80kts 100ft** | 0.938 | 0.540 | 0.435 | 0.371 | 0.869 | 0.442 |
| **100kts 0ft** | 0.634 | 0.461 | 0.507 | 0.410 | 0.337 | 0.428 |
| **100kts 50ft** | 0.717 | 0.460 | 0.766 | 0.514 | 0.024 | 0.360 |
| **100kts 100ft** | 0.635 | 0.512 | 0.430 | 0.388 | 0.913 | 0.479 |

**Table 4.1** $R^2$ and k results for all DVE approaches

Table 4.1 shows the $R^2$ and k values for the DVE trial measured from 2800ft. The first point to note is the much larger scatter, with relatively few runs having an $R^2$ over 0.95 or 0.98, which were used in Chapter 3 as

benchmarks for performance. As already stated, the analysis considers $R^2$ over alternative ranges later in the chapter; therefore the focus for this section will be $R^2$ over 2800ft. In an attempt to relate task performance to the visual scene, $R^2$ will be considered against the average VCR for each particular run. For example, if we are considering the grey 50ft runs, the 'average VCR' would be 3 as the translational rating was 3.5 and the attitude rating was 2.5. This is not to be confused with UCE, which has distinct levels ranging from 1 to 4. The reason for presenting the data in this way is to give a more detailed method of comparing the scenes which, in terms of UCE, could initially appear to be identical in terms of content. For example, 'Norm 100ft' and 'Grey 100ft' were both UCE2, but 'Norm 100ft' was very close to being UCE1, whereas 'Grey 100ft' was close to being UCE3. It is intended that, by using the average VCR, some of the finer detail with regard to the differences in database quality will be preserved.

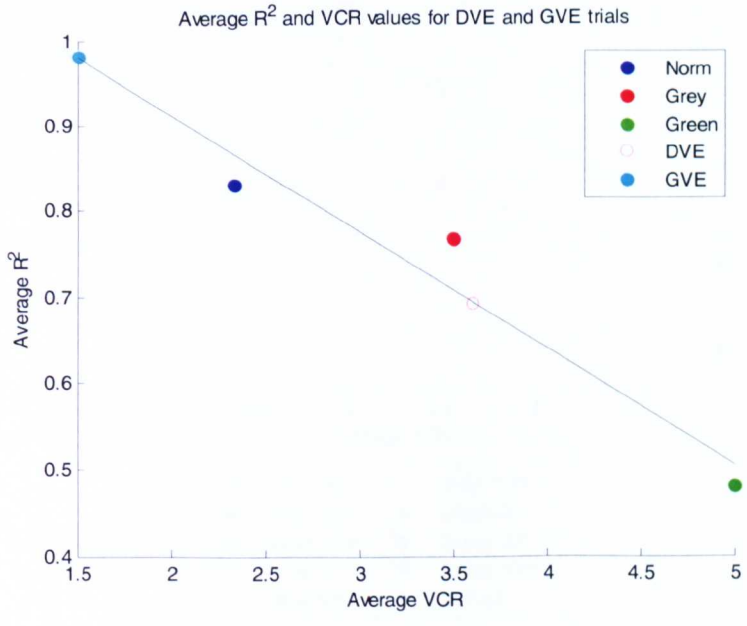


**Figure 4.12** Average $R^2$ values vs. average VCR for various database conditions and overall DVE & GVE trials

The data in figure 4.12 is separated in terms of the main database condition, normal, grey and green. Data is also included based on the overall average VCR and $R^2$ values for the DVE and GVE trials. Unlike the other data, the 'DVE' marker is not filled as it was not included in the calculation to produce the line of best fit which is also shown in the figure. This line shows a relatively strong level of correlation between the average $R^2$ values and average VCR. This is an encouraging result as it is the first time that $R^2$ has been analysed with non-GVE data in this research and shows that it can provide a reliable measure of performance when considered over this range. Figure 4.13 uses the same principle as figure 4.12, with the data now showing each individual visual setting, enabling further analysis of the effects of each visual change.

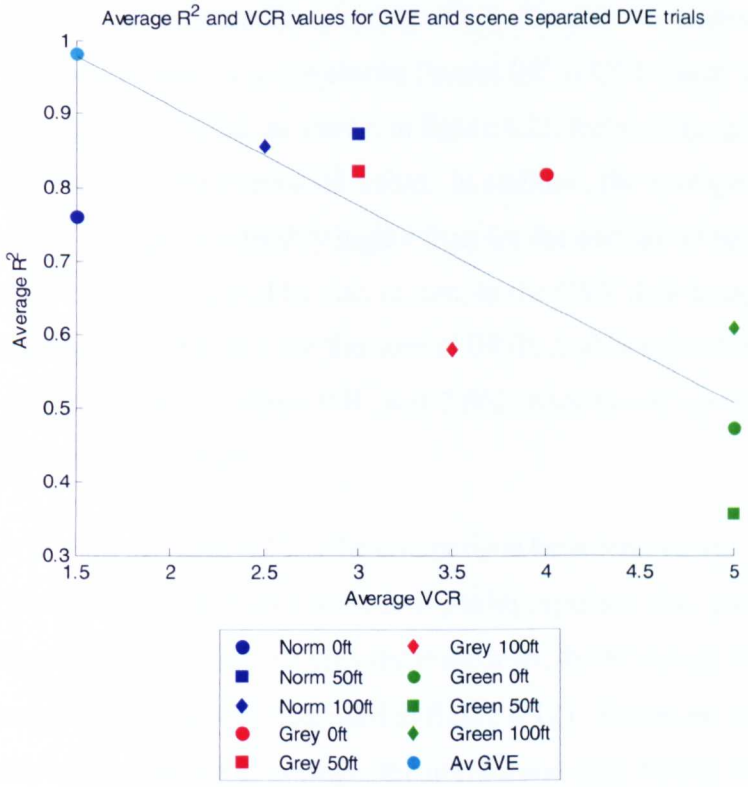


**Figure 4.13** Average $R^2$ values vs. average VCR for GVE and DVE tests, separated by main database conditions

The line of best fit shown in figure 4.13 is the same as was plotted in figure 4.12 in order to offer a continued comparison of the individual visual setting data. Although $R^2$ does still generally degrade with the average VCR, the fit is not as representative of the data in figure 4.13 as it is in figure 4.12.

Considering, initially, the data for the 0ft helipad heights, there is a marked change in the normal and grey data, as shown in figure 4.13. The 0ft helipad data shows a slightly lower $R^2$ value for the normal database and slightly higher $R^2$ value for the grey database when compared to the data for all helipad heights in figure 4.12. This difference is exacerbated by the change in the average VCR rating, with the normal 0ft rating of 1.5 being reduced from the overall normal rating of 2.33, and the grey 0ft rating of 4 being larger than the overall grey rating of 3.5. Despite the ostensibly poorer visual information in the scenes ('norm 0ft' is UCE1 and 'grey 0ft' is, very marginally, UCE3, as shown in figure 4.2), the average grey 0ft $R^2$ value is higher than the normal 0ft value. In addition, the average $R^2$ rating for the GVE trial is considerably higher than for the normal 0ft tests in the DVE trial. This result could be due, in part, to the GVE data being based on 27 results, compared to 3 for the normal 0ft data, although table 4.1 shows that the highest normal 0ft $R^2$ was 0.862, which is still over 0.1 lower than the GVE result.

Another feature of figure 4.13 is the comparison between average $R^2$ values for the normal and grey tests. It might be expected that, given the generally poorer VCRs for the grey database tests, the $R^2$ values would be significantly lower (as was suggested in figure 4.12). However, with the exception of the grey 100ft average, the normal and grey results are very similar. It is possible that the reduction in the microtextural cues available when changing from the normal to grey scenes is partly offset by the introduction of much stronger macrotextural cues. These are the result of

the sharp contrast between the flat grey colour which makes up the runway, taxiway and airfield and the grass which surrounds this area (see figure 4.1(a), (b)). The flat grey colour which runs along the left hand edge of the helipad (originally the edge of the taxiway) provides excellent lateral motion cues to the pilot. Longitudinal cues are provided by the first taxiway which runs normal to the approach path, and also a large grey area leading up to the pad which provides useful translational cues at close range, as shown by figure 4.14.

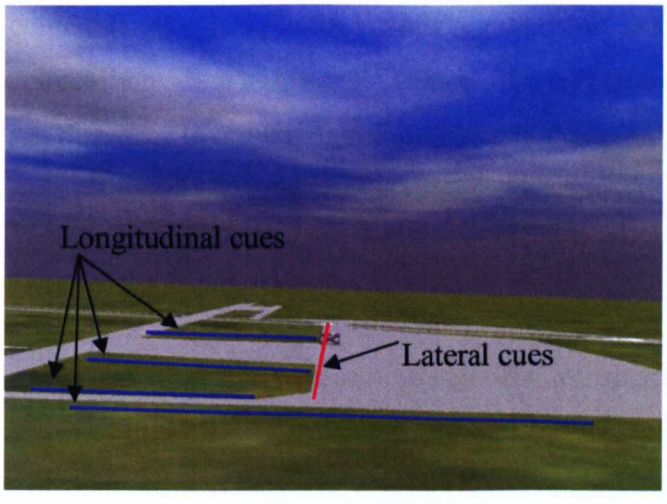


**Figure 4.14** Cues added by flat colour in grey database

The changing correlation of the 50ft helipad in figure 4.13 is a further point of interest, with this setting giving the highest average $R^2$ value for the normal and grey (marginally in this case) databases, but the lowest for the green database runs. This is somewhat unexpected with the normal and grey databases due to the pilot's documented issues with transitioning over the raised helipads. One might imagine the 0ft helipads to provide the best correlation, certainly for the normal scene, but the normal 50ft average is approximately 0.11 higher than the average 0ft value for the normal database. This result suggests that even in a relatively cue rich

environment, the addition of modest macrostructural cues can add to the quality of the visual information in the scene rather than saturate it.

The $R^2$ values have therefore given us valuable information about the ability of the pilot to follow a $\tau$-based approach and have shown how this guidance breaks down depending on the way in which the visual content in the scene is degraded. In particular, it has been shown that, using the average VCR, $R^2$ reduces as scene content is degraded (figure 4.12). However, when the data is considered in terms of both helipad height and main scene content (figure 4.13) further trends are revealed, with higher VCRs not necessarily leading to lower $R^2$ values. We will now examine $R^2$ over shorter distances in order to determine how it changes through the tests.

#### *4.4.2.3 Progressive $R^2$ Analysis*

Although the analysis in the previous section can offer information about the general accuracy of approaches over 2800ft, we need to analyse the data in other ways in order to assess how performance changes throughout each run. The progressive analysis was first introduced in Chapter 3 (an example is shown in figure 3.22), and provides a method to examine the quality of tau-guide following (through $R^2$ changes) as the pilot approaches the helipad. Figure 4.15 shows the progressive $R^2$ data for each of the 27 DVE tests, separated by main database condition.

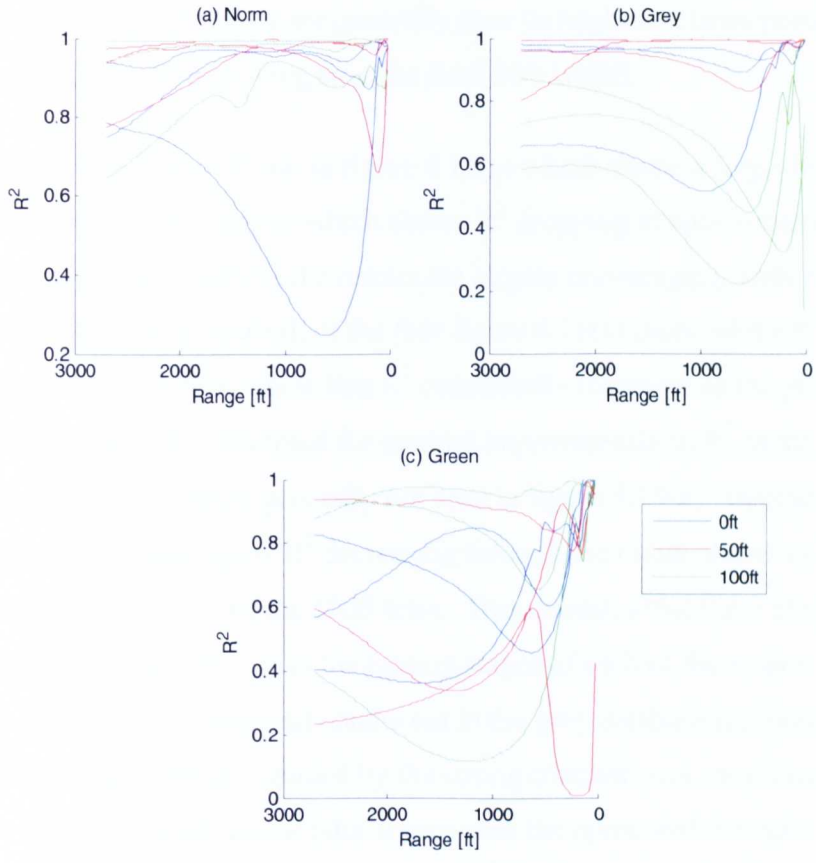


**Figure 4.15** Progressive $R^2$ Analysis for DVE trial, separated by main scene content and helipad height

As with the previous progressive analysis work in Chapter 3, the above result has been achieved by calculating a number of $R^2$ values, starting at the initial 2800ft range and then moving in 25ft steps to take a new value which represents data from 2775ft to capture, then 2750ft etc., continuing to just 25ft from the helipad. The aim of this method is to determine whether there are any trends in the data which show the points at which the $R^2$ correlation suddenly improves or deteriorates.

A general trend which is immediately noticeable is for the $R^2$ values to become poorer as scene quality degrades. It is not surprising that the $R^2$ values are poor at some point during the grey and green approaches, but

figure 4.15 shows that they are generally poor throughout a large portion of the approach, only improving over the final 500-1000ft.

Although there is one 0ft run in figure 4.15(a) which shows a large drop in $R^2$ and another 50ft example which shows $R^2$ dropping to approximately 0.65 shortly before capture, the results are largely encouraging, with high levels of correlation. Indeed, of the four figure 4.15(a) cases where $R^2$ is initially below 0.8, three show that $R^2$ consistently increases as the pilot approaches the pad. This trend for gradual improvements in $R^2$ as the pilot approaches the helipad is generally not seen in figure 4.15(b). Instead, a large number of tests show $R^2$ decreasing through the initial phases of the run, including all three of the 100ft tests. This indicates that there are large adjustments in the $\tau$ profile in the closing stages of each of these runs. Given that these tests were all conducted in the grey database it is possible that the pilot was initially guided by the strong contrast cues, as shown in figure 4.14. However, as the pilot approached the apron and the main focus turned to the raised helipads, he may have then had enough accurate information to suggest that a change in approach strategy was necessary. This is, again, a potential indicator of a two-phase approach.

Another point of interest, especially in comparison to the poorly correlated grey 100ft tests, are the grey 50ft results. Given that the task is, ostensibly, very similar to the 100ft helipad, the results show much better performance in terms of $R^2$, albeit with one result that shows some readjustment. It is thought that this could be a result of the pilot being closer to the ground over the final stages of the 50ft approaches, therefore the ground cues would have been more detailed.

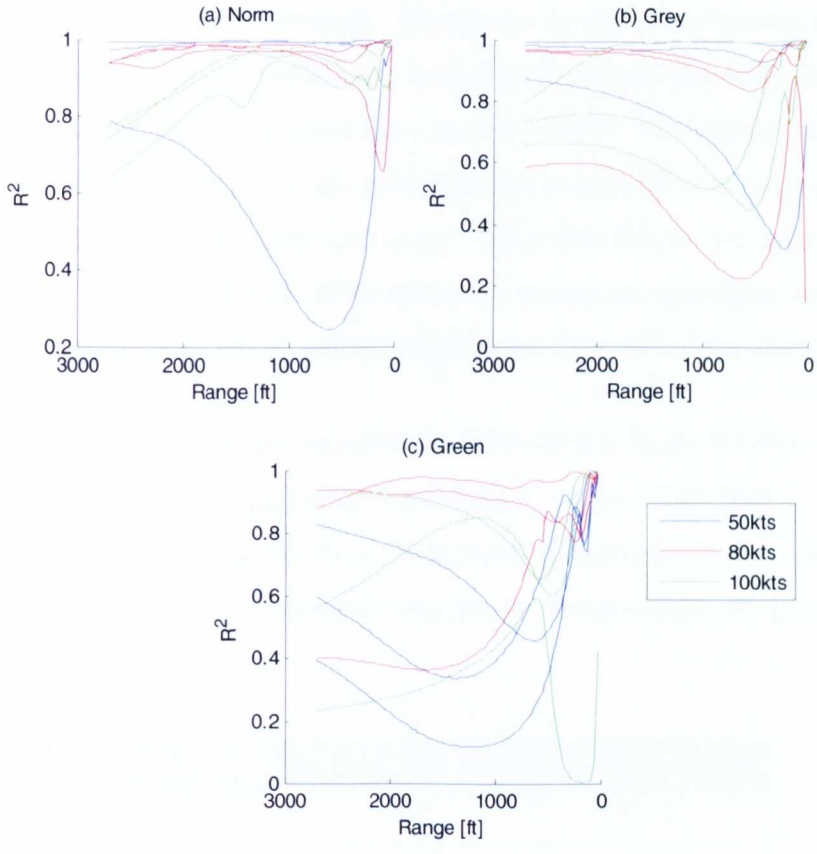


**Figure 4.16** Progressive $R^2$ Analysis for DVE trial, separated by main scene content and initial groundspeed

The data in figures 4.16(a)-(c) is still presented in terms of the main database setting, however the data within each subplot is now shown in terms of initial groundspeed.

There are two points to note when considering figure 4.16, the first of which is shown in figure 4.16(a). With the exception of the poorly correlated 50kts run, the 3 remaining tests for which $R^2$ is not initially well correlated all had an initial groundspeed of 100kts. Although the $R^2$ values do stand out somewhat compared to the 50kts and 80kts data, the pilot does seem to be in control of the approaches, as each of the values rise to 0.9-0.95 by a range of approximately 1000ft. This is another sign of a two-phase approach, with the first phase requiring a lengthy deceleration and

broadly accurate guidance strategy. The reason for the two phases in these examples can be seen in figure 4.4, where the 100kts tests generally feature an abrupt change in groundspeed between 500-1000ft. This change signals the end of the first phase, and the start of the more difficult second phase. This trend is not entirely replicated in the 100kts data for the grey and green runs, although the lack of visual cues in those tests introduce other problems for the pilot which will affect guidance throughout the tasks.

The second point of interest concerns the 50kts data in figure 4.16(c). Each of the tests show a gradually decreasing $R^2$ value, which then improves at various distances from the helipad. Of interest was the value of $\tau$ at the range where $R^2$ reached a minimum. These values are shown in table 4.2.

| *Helipad Height* | *Range [ft]* | *$\tau$ [s]* |
|---|---|---|
| **0ft** | 625 | 17.45 |
| **50ft** | 1375 | 18.12 |
| **100ft** | 1225 | 17.37 |

**Table 4.2** Range and $\tau$ data for minimum progressive $R^2$ values during Green 50kts tests

As shown in table 4.2, despite the $R^2$ minima occurring at a variety of ranges (particularly for the 0ft run), the $\tau$ values are very similar and covered by less than 0.8s. Although there are further adjustments during the approach which lead to slightly reduced $R^2$ values closer to the helipad, it appears that the point at which the pilot is able to affect a more accurate guidance strategy is one that is not driven by distance from the target, but by time to contact it. This is another important result because it suggests that, for a group of very similar tests (only helipad height changes), the pilot is potentially using a $\tau$-based guidance strategy.

#### *4.4.2.4 Targeted $R^2$ Analysis*

By way of a final method of investigating the quality of fit of the tau data, $R^2$ was measured on a data point by data point basis, with the $R^2$ value initially calculated for just the final two data points (a test time of 0.05s). If $R^2$ was greater than the selected target value, the evaluation was performed again with one extra data point considered (i.e. a test time of 0.1s). This iteration was repeated until $R^2$ fell below the target value, at which point the range from the pad and the k value were stored. Two target values were assessed, 0.95 and 0.9. In addition to this, the analysis was also performed on the GVE data. Given the similarity between the individual GVE runs, the results have been averaged to give a single GVE value for range and k.

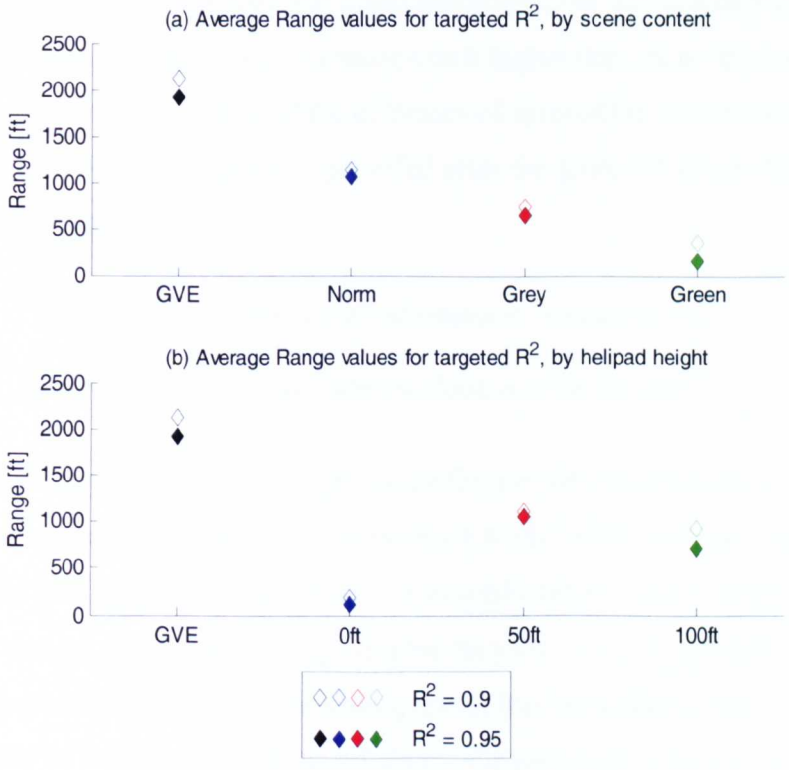


**Figure 4.17** Average Targeted $R^2$ range values for various trial variables

Before considering the k values given by the targeted $R^2$ analysis, figure 4.17 shows the average range values given for various test variables. As we might expect, figure 4.17(a) emphasises the usefulness of a scene with many visual cues in it given the reducing values for range with reduced UCE, regardless of whether the $R^2$ target was 0.9 or 0.95. Although the normal DVE scene was rated as UCE1, it appears that the differences between these tests and those conducted in the GVE trial were significant as the difference in range values between the two tests are approximately 500ft. While some of this difference may be attributable to the introduction of raised helipads in the DVE trial rather than the removal of a number of buildings around the apron, figure 4.17(b) shows that this is not the case. The average normal 0ft range value is just 91.7ft, compared to 1518ft for normal 50ft and 1814ft for normal 100ft pads. The raised pads are useful in the poorer grey and green databases also, as indicated by the average values in figure 4.17(b) being much higher than those for the 0ft helipads. Further evidence of the difficulty of approaches in the poorer scenes with the 0ft helipad was provided after the green 0ft 80kts run when the pilot commented:

> *"I can't interpret the visual information. I can see that things are moving, but I have no idea in what fashion."*

Of interest are the higher average values for the 50ft helipad tests in comparison with the 100ft runs, particularly the $R^2$=0.95 average. This possibly indicates that the addition of a structure which makes up (or is very close to) the target is enough to give the pilot valuable additional cues, whereas the100ft pad whilst providing useful feedback adds to the difficulty of the task. As was noted during the progressive $R^2$ analysis, this added difficulty is a result of the aircraft approaching the helipad at a higher altitude, thus reducing the effectiveness of any ground textures. In

the green tests this would have been a particularly noticeable effect given that, other than the helipad itself, the only texture in the database was the grass.

Targeted $R^2$ data which includes the k values is presented in figure 4.18, with the data arranged by scene content in figure 4.18(a) and by helipad height in figure 4.18(b). Also shown on each plot are selected data for the GVE tests. Given the generally higher levels of correlation in the GVE tests, only the data for $R^2$=0.95 is shown. There is also 'good' $R^2$=0.95 data for the GVE tests. This represents the average GVE values for range and k when only the approaches which were highly correlated over more than 2500ft were considered. The intention of this is to discover what constitutes a good approach in terms of k.

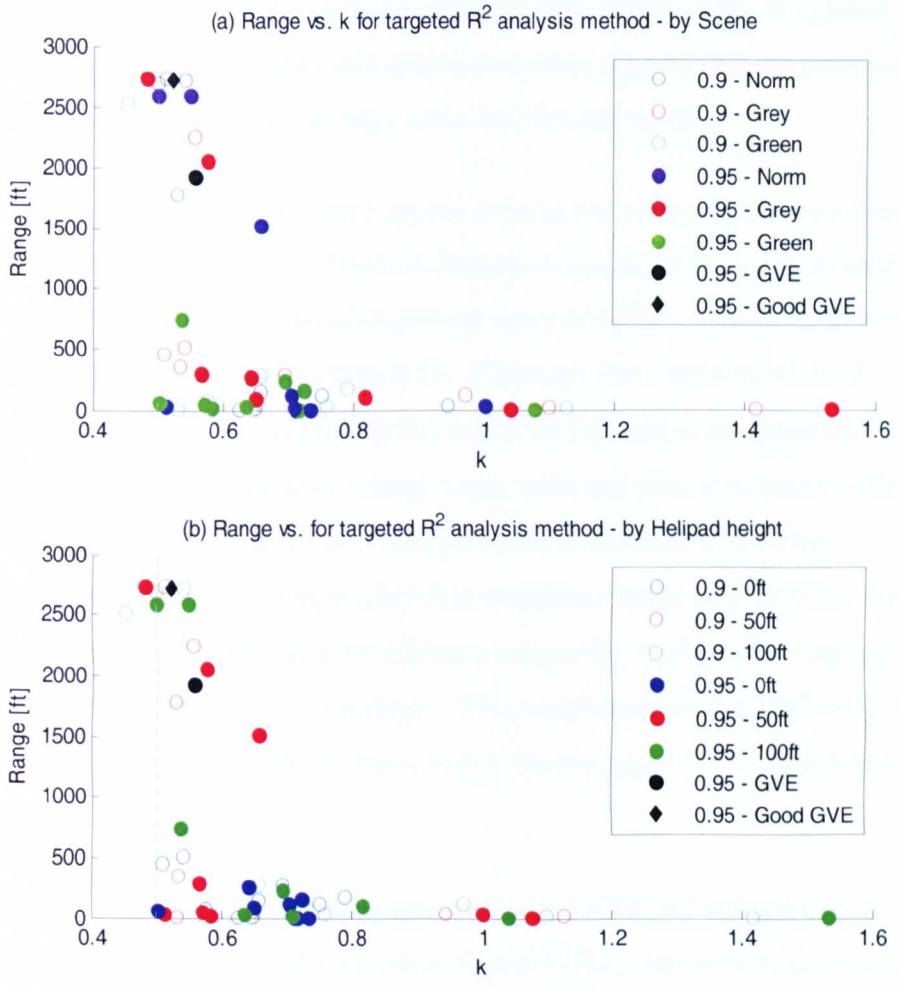


**Figure 4.18** Range vs. k for Targeted $R^2$ analysis by (a) scene, (b) helipad height

The raw data shown in figure 4.18 (a) and (b) are the same, with the highlighted task variables being the only difference. There is also a vertical line added at k=0.5 to indicate the value at which a theoretically perfect $\dot{\tau}_x$=constant deceleration approach would be (if $R^2$ was also approaching 1). The most striking feature of the plots is the general trend for range to increase rapidly as k reduces to approximately 0.5.

The key region of the figure concerns the data for which the range is over 2500ft. In these tests the targeted $R^2$ analysis has extended a large distance

from the target before the value has fallen below 0.90 or 0.95. It is these data which are of particular interest because they suggest that the pilot was locked on to a successful strategy early into the approach.

Examining figure 4.18(a), there appear to be two distinct regions in terms of range from the helipad. The first features a variety of k values, from 0.5 to 1.53; the second has a much narrower array of values, from 0.45 to 0.66, with most values being less than 0.55. Although there are a number of results with a k of approximately 0.5 which do not lead to an approach which is well correlated over a long range, there are almost as many within a range of 0.45-0.55 which do. Despite some of the results showing correlation over a short range when k is within the range of 0.45-0.55, the results show that when the pilot effects a successful, well guided strategy, k almost always falls within this range. This conclusion for the DVE trial is also backed up by the GVE results, with k for the 'good GVE' runs being 0.52.

Considering only the data with a range of over 1500ft, all but one of the eleven 0.90 and 0.95 results shown in figure 4.18(a) are for tests conducted in normal and grey databases. The lack of any long range correlation for the green database is not unexpected given the starkness of the green scenes, which were all rated as UCE3. However, a result that is somewhat unexpected is shown when we consider the same data in figure 4.18(b). All of the results with a range greater than 1500ft are given by tests in which the helipad height was 50ft or 100ft. As almost all land-based helipads are not raised this suggests that the workload a pilot faces when landing is potentially greater than it would be if there were other cues in the environment. In reality, most landings will take place in cue-rich environments, so this result may not be entirely transferable to the real world. However the result does show that, in scenes where there is not a wealth of visual information, the introduction of a modest macrostructure

can give the pilot incredibly powerful cues which can lead to a much more successful, and possibly safer, approach.

Figure 4.18 shows the value of selecting a k of approximately 0.5. If the theoretical time to complete a manoeuvre given a certain starting point was known, this information could potentially be transferred into a Prospective SkyGuide which guided the pilot onto, for example, a k=0.5 τ-approach. In addition, the targeted $R^2$ analysis has again shown the value of the raised helipads for guiding the approach.

#### *4.4.2.5 k Analysis*

Before examining the k values, it is important to consider how the $R^2$ results might affect k. With progressively poorer performance in the grey and green databases, it becomes much more difficult to fit a representative linear approximation to the data. Therefore, in order to maximise $R^2$, k may be compromised. Thus, the analysis will examine k in a number of ways. The first method will consider k over a range of 2800ft, as with the $R^2$ analysis. We will then examine the way in which $\tau$ changes through the approach, with one method featuring a progressive analysis of k and another investigating the instantaneous $\dot{\tau}_x$, as opposed to k. By examining $\dot{\tau}_x$, we will be able to understand how the pilot controls $\tau$ throughout the trial, as opposed to the analysis of k, the coupling constant, which provides an overview which considers a much larger range of data. The aim of these analyses will be to determine the role of $\tau$ through the approaches. Critically, the analysis will also establish whether there are certain $\tau$ profiles which lead to well-correlated, quickly-captured approaches.

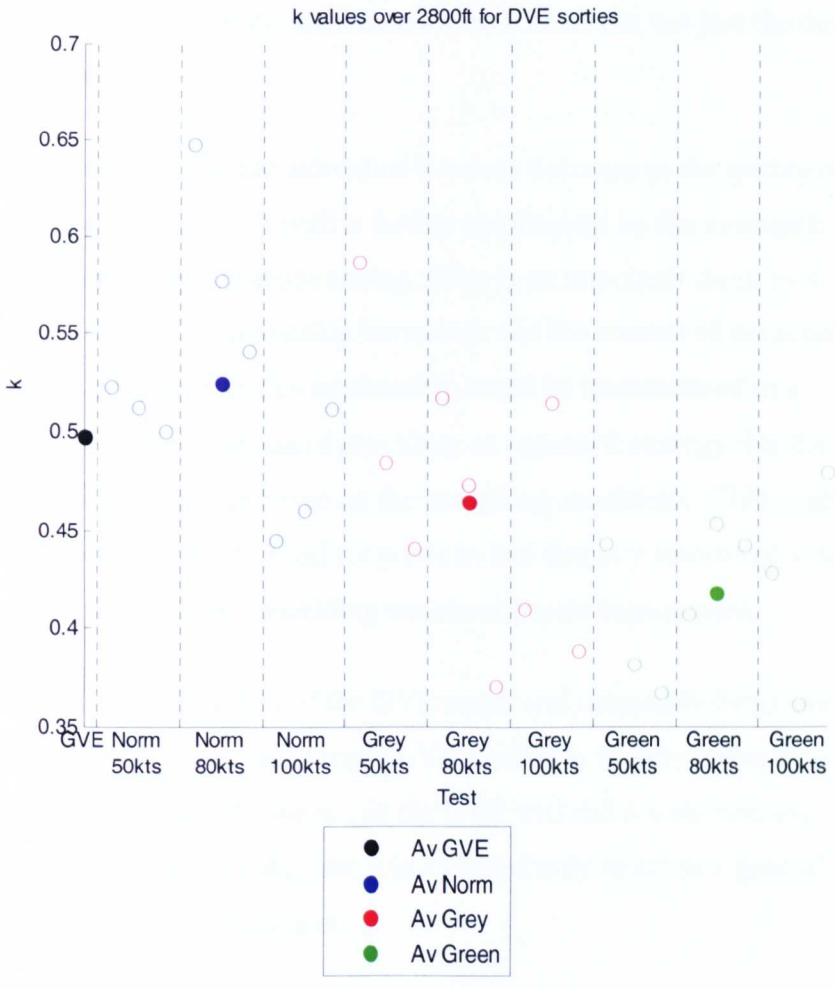


**Figure 4.19** Individual k values for all DVE runs, including average normal, grey, green and GVE values

Figure 4.19 shows the k values for each run, separated by the main database variable and initial groundspeed. Within each batch of three results, the helipad height data running from left to right is 0ft, 50ft and 100ft, respectively. Also included on the figure are filled circles representing the average values for the GVE trial and also the overall average for each main database setting of the DVE trial. It should be noted that the average DVE data is positioned in the centre of each array for that particular database setting purely for aesthetic terms. The average data is

calculated using the 9 individual data for each database, not just the three 80kts results.

Figure 4.19 shows that the individual k values decrease as the quality of the scene is degraded, a result with is further emphasised by the average k values for each main database setting. This is an important result as it shows that there is a relationship between k and the content of the scene. It is therefore possible that this relationship could be implemented in a SkyGuide with the intention of providing an approach strategy that the pilot is comfortable with based on the prevailing conditions. This is an important point given the need for pilots to feel that any automated system they are following is not providing unnatural psychological cues.

Although the visual quality of the GVE scene was ostensibly better than the normal DVE scene, the average GVE k value is slightly lower than the normal DVE average. However, as the GVE trial did not include any raised helipad runs, the data from it is included only to act as a general, rather than a direct, comparison.

Although the issues regarding a tau analysis over 2800ft have already been discussed, figure 4.19 shows that the pilot is using some form of a tau control strategy from a large range, and that this strategy is affected by the visual quality of the scene. As the aircraft moves closer to the target, the extra visual information available to the pilot can then be used to inform a more precise strategy. This, again, shows that the pilot is using a multi-phase approach, with a general guidance phase which takes the aircraft to an acceptable altitude/groundspeed/range, before the pilot commits to a final approach when the visual cues are deemed to be sufficient.

#### *4.4.2.6 Progressive k Analysis*

As with the $R^2$ analysis, it is vital to consider the way in which k changes as the pilot approaches the helipad. Figure 4.20 shows a progressive k value analysis for all runs, with subplots separated by main database content. Given the results of the targeted $R^2$ analysis, dashed lines are included at k=0.45 and 0.55 to give a clearer indication of the values relative to k=0.5.

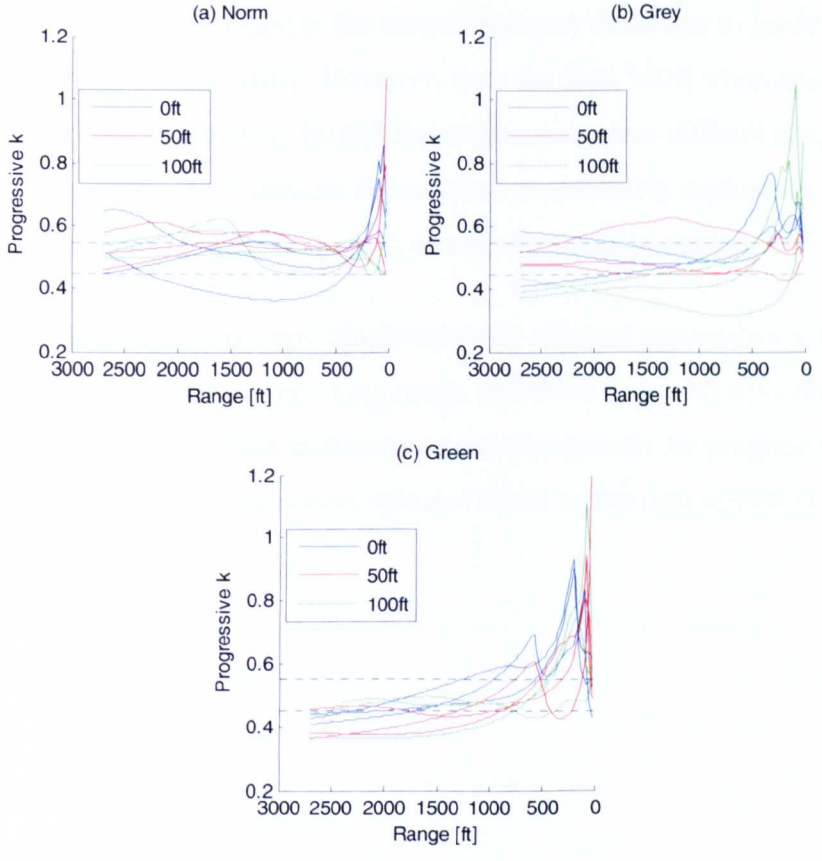


**Figure 4.20** Progressive k value analysis for DVE trial

The dashed lines in figure 4.20 highlight the way in which the k value varies throughout each run. Figure 4.20(a) shows that the normal database

tests remain largely within this $0.45 \leq k \leq 0.55$ range until approximately 300ft from the helipad. Indeed, from a range of approximately 1500ft it appears that many of the data begin to move from a k of 0.55-0.6 towards 0.5. Although there is not a significant trend within figure 4.20(b), a number of the profiles also move towards a k value of approximately 0.45-0.55, before rising to much larger values over the final 500ft of the approach. Finally, despite low starting values for k in figure 4.20(c), there is a slow, but constant, increase, with most of the values over the final 500ft being greater than 0.55. The results suggest that the pilot is able to use the extra cues provided in the normal and grey databases to guide the approach to a certain extent. However, over the final 500ft when much more precision is required, the task becomes much more difficult and, in many cases, large decelerations are required to accurately capture the helipad, or in some cases to 'pause', as was discussed in section 3.5.3.1.

Figure 4.21 shows three runs which represent efficient approaches with a well correlated capture over a long range, and three runs with a poorly correlated capture in order to discover the differences in the progressive k analysis for each. The runs were selected based on the data shown in figure 4.18.

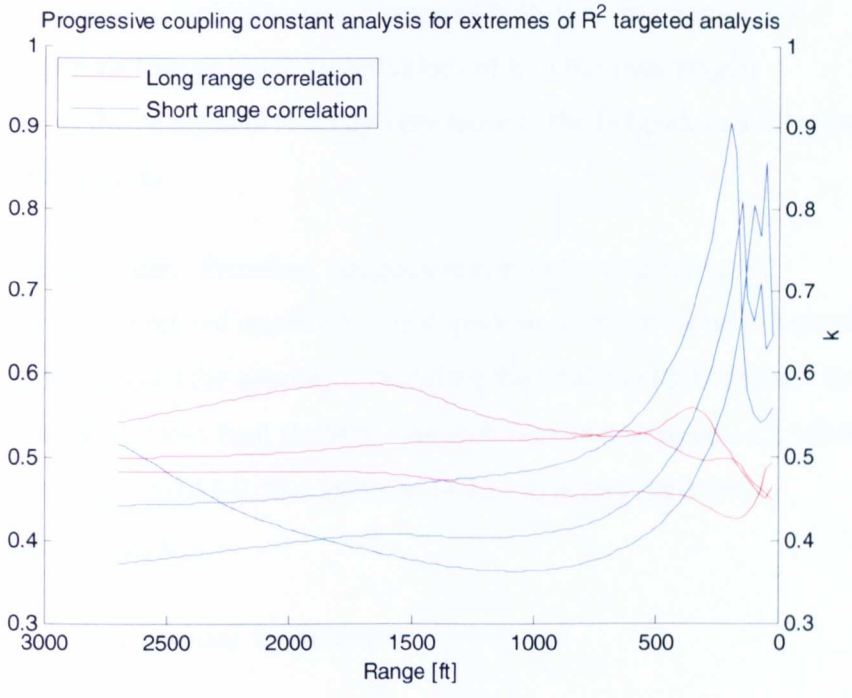


**Figure 4.21** Progressive k value analysis for runs giving long and short correlation ranges in targeted $R^2$ analysis

The differences shown in figure 4.21 give further information as to the need for a well controlled k value throughout the approach. Although one of the short range runs in figure 4.21 (the example with the highest initial range value for k of 0.51) does not show an approximately constant period of k at any stage of the approach, the other two runs are not entirely dissimilar in parts to the 'long range' runs. While the long range runs themselves do not show a lengthy region over which k is constant, there is a general consistency with the individual values for each run over the first 2000ft of the approach. As with many of the runs in figure 4.20, the long range runs in figure 4.21 also show some adjustments of k over the final 500ft of the approach, although these are slight and very well controlled in comparison with the remainder of the data in figure 4.20. As with previous findings, it appears that a k value with an approximate range of 0.45-0.55 is the key to an efficient capture of the helipad, with the final 200ft of all

three long range runs moving into a range of 0.45-0.5. In contrast, the short range runs feature much larger values of k in the final stages, indicative of the changes in strategy very close to the helipad, and therefore inefficient captures.

The progressive data, therefore, suggests that in order to achieve an efficient, well correlated approach, it is important for the k value to be well managed throughout the approach, including the vital final 500ft where the pilot must commit to a final strategy. As with previous analyses, a k value within the range of 0.45-0.55 appears to be key to achieving a well correlated approach.

#### *4.4.2.7 Instantaneous $\dot{\tau}_x$ Analysis*

As a final way of investigating $\tau$ we will use an instantaneous $\dot{\tau}_x$ analysis to compare runs in which the targeted $R^2$ analysis gave long and short range results. The $\dot{\tau}_x$ data in figures 4.22 and 4.23 is obtained by calculating the rate of change of $\tau_x$ over periods of just 0.5s throughout the full dataset.

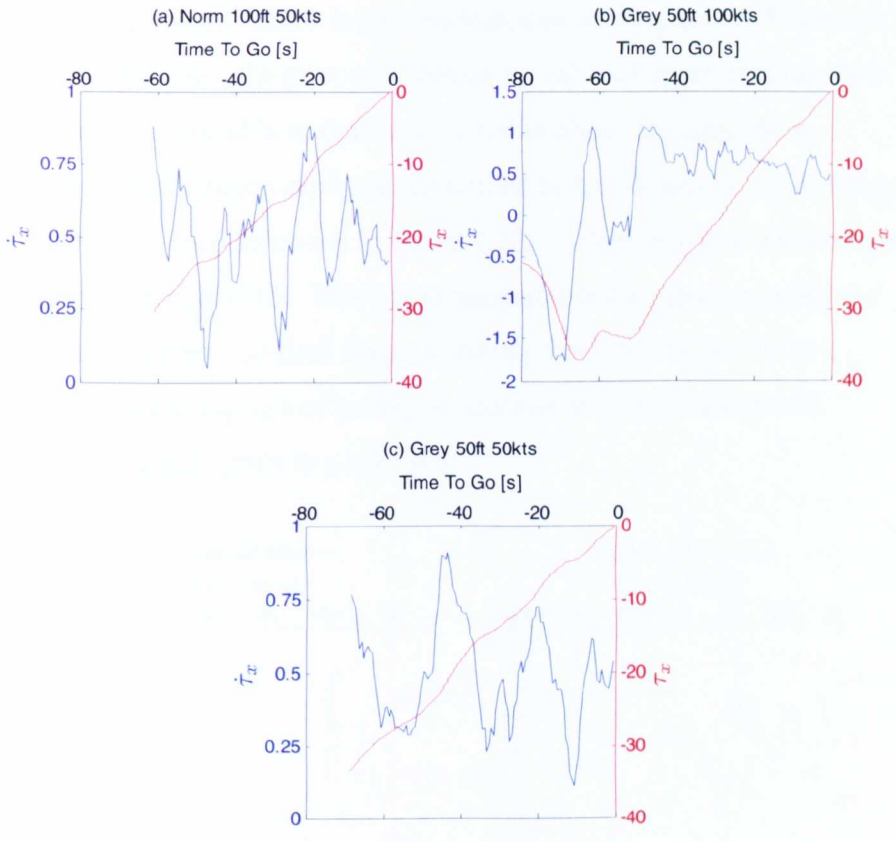


**Figure 4.22** $\dot{\tau}_x$ and $\tau_x$ vs. TTG for 'long range' targeted $R^2$ runs

Figure 4.22 shows three runs for which the targeted $R^2$ analysis showed correlation over a large range. The $\dot{\tau}_x$ vs. TTG profile is shown in blue, alongside the $\tau_x$ vs. TTG profile, in red. Despite the $\tau_x$ profiles for the three runs being among the most linear of the entire trial, the $\dot{\tau}_x$ profiles for each run do not show any significant period during which $\dot{\tau}_x$ is constant. Figure 4.22(b) features a period in which $\dot{\tau}_x$ has a relatively constant value of 0.63 between a TTG of 12 and 40s, although this period still has a number of fluctuations (between 0.42 and 0.9), despite the $\tau_x$ profile appearing to be almost linear. Figure 4.22(a) and (c) are similar, with the $\tau_x$ profiles having correlation coefficients of over 0.99 for the 2800ft range. However, the $\dot{\tau}_x$ data shows large fluctuations between approximately 0.1 and 0.9. In addition, there are no regions where $\dot{\tau}_x$

maintains a constant value. It appears that, discounting some of the peak values in both cases, the pilot maintains a $\dot{\tau}_x$ value of approximately 0.4-0.5, but it is not possible to draw a conclusion about any specific $\dot{\tau}_x$ strategy given the relatively large deviations in $\dot{\tau}_x$. However, in the final few seconds of each approach in figure 4.22, $\dot{\tau}_x$ does move within a range of approximately 0.4-0.5. This could suggest that the pilot is aiming for such values in a precise final stage of the approach which results in a relatively smooth capture of hover, as opposed to a large amount of deceleration which leads to a hard stop.

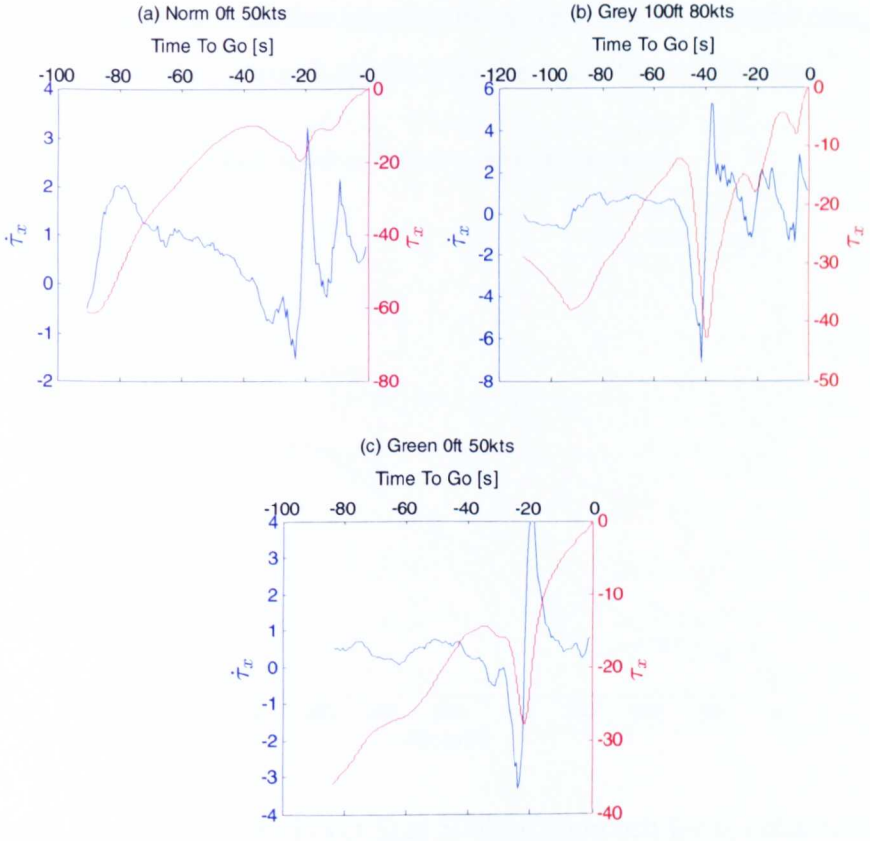


**Figure 4.23** $\dot{\tau}_x$ and $\tau_x$ vs. TTG for 'short range' targeted $R^2$ runs

Figure 4.23 shows a selection of short range runs, based on the targeted $R^2$ analysis. The reasons for the short ranges given by this form of analysis are evident in the $\tau_x$ profiles, with at least one large adjustment made in the

closing stages of each approach. Figure 4.23(a) shows no region of constant $\dot{\tau}_x$, although there is a brief period where it is somewhat constant (approximately 0.67) in figure 4.23(c) between a TTG of -60s and -40s. Another constant period of approximately $\dot{\tau}_x$=0.65 is seen in figure 4.23(b) between -80s and -50s TTG. However, in both of these cases the period of constant $\dot{\tau}_x$ is followed by a large change in the $\tau_x$ profile, indicating that the pilot was not satisfied with the approach.

It appears, therefore, that a steady period of constant $\dot{\tau}_x$ does not guarantee a successful approach, nor does a lack of a precise constant $\dot{\tau}_x$ profile preclude it. In order to further examine the differences between the runs, we will examine the approach speeds over the final 500ft of each run.

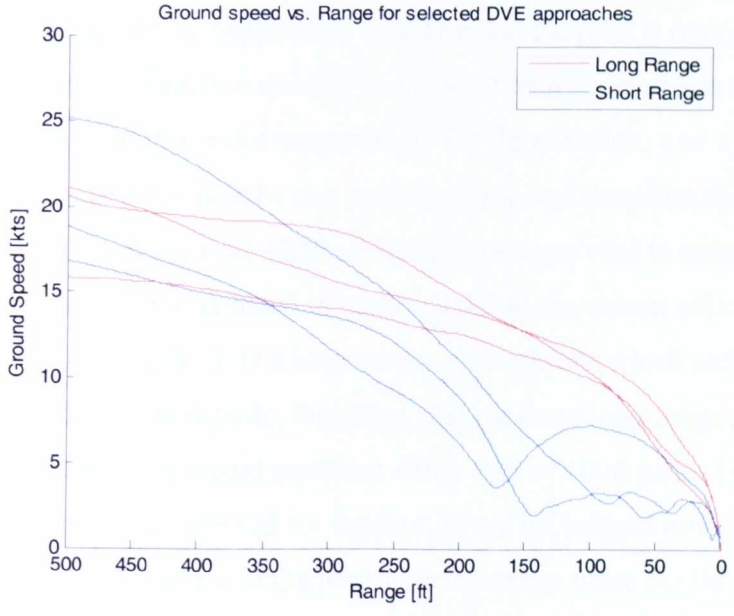


**Figure 4.24** Groundspeed over final 500ft of approach for selected runs

The six ground speed profiles shown in figure 4.24 represent the same six long and short range runs shown in figures 4.22 and 4.23. At a range of 500ft the groundspeeds are largely similar, possibly with the exception of the short range run with a groundspeed of 25kts. However, there are then

significant differences between the groundspeed profiles of the long and short range runs which, in turn, are responsible for the quality of the final stages of the approach. In all of the short range cases shown in figure 4.24, the groundspeed falls below 5kts at least 120ft from the helipad. In contrast, the groundspeeds for the long range runs at the same point are more than double this figure. The premature deceleration requires that the pilot then maintains an approximately constant groundspeed of between 2 and 4kts over the final stages, almost drifting to the helipad. In one case there is a short period of acceleration, with the final 50ft of the approach then resembling the long range runs.

In contrast, the long range runs seem to suggest a confident approach, in which speed is carefully controlled and an efficient capture of the helipad is made. An alternative explanation could be that the pilot is out of control, approaching the helipad too quickly and a large final deceleration is needed. However, this is not supported by the deceleration, $\tau$ or $\dot{\tau}_x$ data. Hence, the conclusion must be that speed control, and therefore the quality of visual cues, over the final 500ft of the approach are vital to ensure an efficient capture. As was stated in section 4.4.2.4, the runs in which the $\tau_x$ correlation was good over a large range were all runs which included a raised helipad. It is inevitable, therefore, that the three long range runs selected in figure 4.22 would represent either 50ft of 100ft pads. However, two of the three cases selected for figure 4.23 are 0ft helipad runs, again highlighting the difference in the pilot's performance when the 0ft helipads were used (see figure 4.17).

Therefore, it has been demonstrated that close $\dot{\tau}_x$ control can be of use to the pilot in order to facilitate an efficient capture of the helipad. However, there is no evidence within the DVE test results which suggests that a constant $\dot{\tau}_x$ approach is a required element of such a capture. More important is effective control of ground speed through the final 500ft of the

approach, which relies on the pilot's confidence in the visual cues provided. Also, a target $\dot{\tau}_x$ value of between 0.4 and 0.5 appears to be useful.

## 4.5 CONCLUSIONS

The objective of the DVE Approach to Hover trial was to investigate the pilot's ability to use tau guidance when presented with degrading scene content, and to answer the question 'Does the pilot use $\tau$ to guide the approach?'

The various methods of tau analysis have provided several useful findings, both in terms of how the visual cues affect performance, and also the way in which tau is used to control the approach. The results presented below support the main conclusion that the pilot does use $\tau$ to guide the approach.

With regard to the changes in scene content, it has been shown that the introduction of raised helipads results in both positive and negative effects. The addition of the structures to the scene gives the pilot valuable visual information which helps to guide the approach, resulting in a targeted $R^2$ correlation over a larger range than for the 0ft helipad. However, as the aircraft moves over the raised helipads, the additional cues cause by their movement relative to the ground adds difficulty to the task, increasing the pilot's workload. It is suggested that further work be conducted with regard to the potential beneficial effects of raised helipads, particularly in cue-deprived environments.

In terms of the main database scenery changes, there was a degradation in task performance as cues in the scene were removed, although it has been noted that a simple removal of texture does not necessarily lead to reduced performance. This has been shown by the general $R^2$ analysis over 2800ft

in which the average grey 0ft $R^2$ value was higher than the average normal 0ft value, and also by the similar overall average values for the normal and grey $R^2$ analyses. It is suggested that the strong contrast in the grey scene provided additional lateral and longitudinal motion cues which aided the pilot's performance.

Although the $R^2$ values showed similar results for the normal and grey tests, the k analysis over 2800ft showed that as the visual quality of the scene degrades, k reduces. This trend was observable in the individual results, but was much clearer when the average k values for each main database setting were considered. The result shows that there is a relationship between k and scene content. In addition, it is also suggested that the pilot employs a two-phase approach, with the initial general guidance phase being responsible for the relationship between k and scene content. This relationship could possibly be used to inform the design of a synthetic SkyGuide, with the commanded k value depending on the quality of the visual cues on any particular day.

In terms of $\tau$ itself, there have also been important findings. The targeted $R^2$ method of analysis showed that a k value of approximately 0.45-0.55 was useful in order to achieve a long range correlation, with larger values resulting in much smaller correlation ranges. This result was also confirmed by a targeted analysis of the GVE data, suggesting a possible avenue for further research. The importance of the raised helipads was also revealed with this method of analysis, highlighting their effectiveness at providing the pilot with useful visual cues over the majority of the approach.

Using the progressive method of analysis to examine the differences between runs with long and short range correlation it was found that k is held within a narrow range of values for the duration of the approach for

long range runs. The reduction of k to approximately 0.45-0.5 over the final 200ft of the approach further emphasises the importance of controlling the value, especially over the critical final stages of the approach.

Finally, the instantaneous $\dot{\tau}_x$ analysis showed that it is important for the pilot to maintain some control over $\dot{\tau}_x$ in order to ensure an efficient capture of the helipad. Key $\dot{\tau}_x$ values over the closing stages of the approach were found to be approximately 0.4-0.5 for 'good' runs. However, the results did not suggest that the pilot used a $\dot{\tau}_x$=constant strategy throughout the approach.

# Chapter 5

# CLINICAL DECELERATION

## 5.1 INTRODUCTION

The third and final flight trial was the most simple and, in essence, was not even a test of piloting skills. As the Chapter title suggests, the trial involved a deceleration manoeuvre, although the aircraft used, the modifications made to it, and the scene content ensured that the trial was very different in design to the previous two Approach to Hover trials, hence its clinical nature. The major difference between this experiment and the two previous flight tests was that the aircraft, a Bo105, had its pitch, roll and yaw axes locked, along with the y and z translational axes. This meant that the pilot could only control the aircraft along the x axis, making the task a single-axis deceleration manoeuvre. This essentially converted the experiment from a flying task into a very basic exercise in visual perception and effective control.

The task itself would place the pilot in a very sparse visual scene, with the intention being that, even though the pilot knew what the task variables were, the cue information was so degraded that he did not know the specific value of the variables. The test pilot used was AB (referred to henceforth as 'the pilot'), who had also flown the GVE and DVE Approach to Hover trials.

## 5.2 OBJECTIVES

The objective of the Clinical Deceleration trial was to investigate the pilot's performance when capturing a target in a scene which was deprived of almost all visual cue information, with a basic aircraft model. Central to the research was the pilot's use of a tau during the capture of the target. The hypothesis being tested was 'can the pilot use only the looming information in the scene to affect an accurate deceleration strategy?'

## 5.3 DESIGN OF THE TEST

### 5.3.1 Theory

The inspiration for this trial are Lee's investigations with temporal optical variables in nature. He concludes that an animal's ability to determine the time to contact an object or surface does not require explicit knowledge of its relative velocity, distance away or size. Instead, Lee hypothesised that the looming of an object provides sufficient information to ensure that accurate approach control can be effected (Lee, 1980).

### 5.3.2 The Task

The initial concept for the task was to create a scene which was almost entirely deprived of visual cues other than a target which the pilot would have to intercept. In order to make the test as much of a visual task as possible it was decided that it should be a single-axis manoeuvre.

When the simulation for each run commenced, the aircraft would be moving with an initial velocity directly towards a target. The initial plan for the target was a hoop, which would be placed as a physical object in the scene which the aircraft would approach. In order to capture this target

there would be another differently coloured hoop which was fixed on the screen as a HUD would be. The pilot would then be required to decelerate as and when he decided to in order to overlay the fixed HUD style hoop exactly on the target hoop, ideally in one smooth manoeuvre. The manoeuvre would be complete when the aircraft was close enough to the target hoop such that it appeared to be the same size as the fixed hoop. Figure 5.1 shows an initial conceptualisation of the clinical deceleration trial, with the start position shown in figure 5.1(a), a mid-flight condition in figure 5.1(b) and the successful capture of the target in figure 5.1(c).

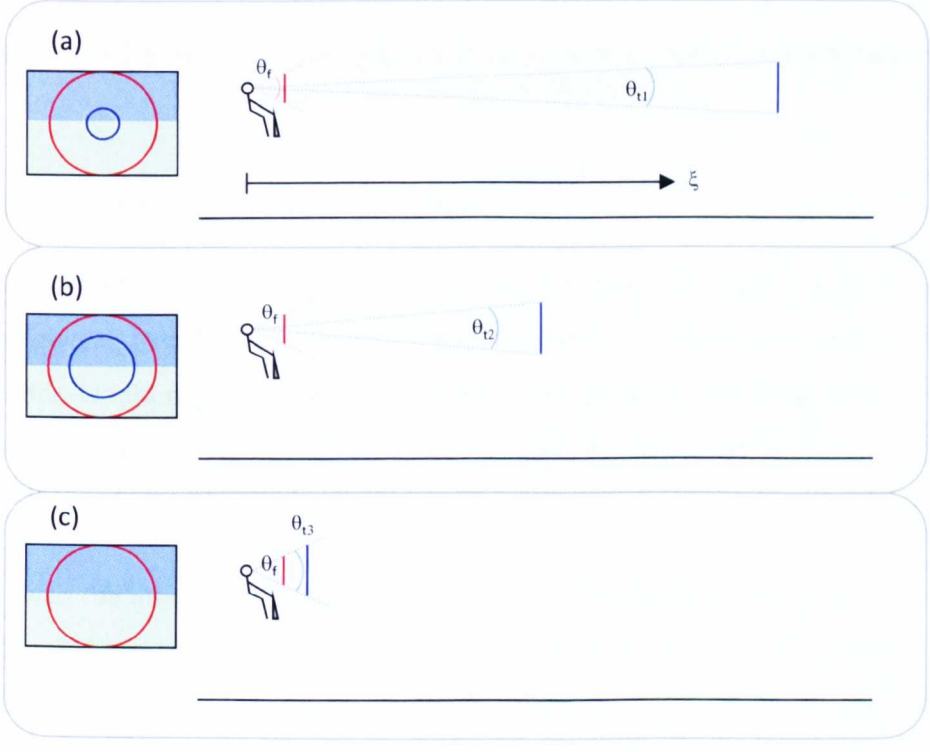


**Figure 5.1** Original concept for clinical deceleration trial

Figure 5.2 shows a screenshot from the trial. A number of changes were made from the concept shown in figure 5.1. In order to make the scene as basic as possible, the horizon and background colours were removed. The target hoop was also filled with colour in order to make the target clearer throughout the approach.

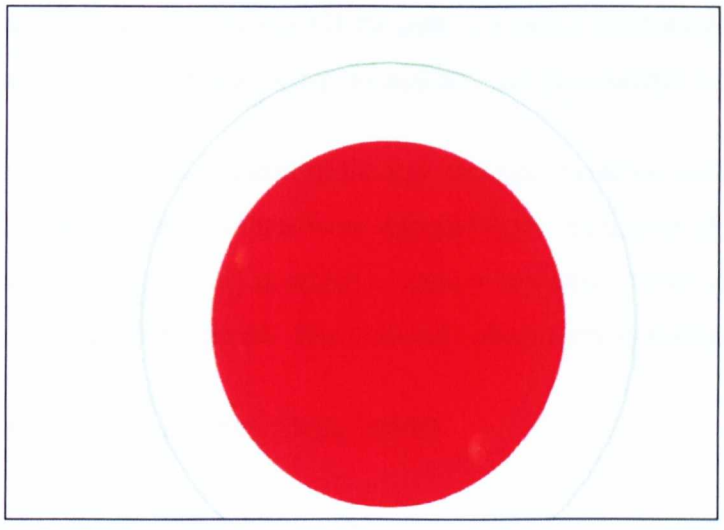

**Figure 5.2** Screenshot during Clinical Deceleration trial showing filled, red target circle and fixed, green hoop

### 5.3.3 Setting the test conditions

The plan for the clinical deceleration trial variables was clear at an early stage and, based on the trial hypothesis which was derived from Lee's work, would require some of the physical properties of the scene to be varied. The selected variables were the physical size of, and starting distance from, the target circle.

Given the time constraints during the Clinical Deceleration trial it was decided that there would be one more test variable, with three values for the variable. It was also decided that, in addition to the target size and distance to target variables, the third variable should be a 'true' variable as opposed to two repeat runs of the initial nine runs. Based on Lee's hypothesis, the obvious choice was to vary the initial approach velocity of the aircraft.

With the variables selected the next task was to decide on their specific values. It was essential to use a range of values which were sufficiently

different to be obvious to the pilot if the task was being conducted in a cue rich environment, whilst also being controllable within realistic boundaries.

Given the influence of the initial speed and distance variables on overall task time, their individual values were selected first. A number of calculations were performed in which a range of potential initial speeds and distances were considered. The selected values were as follows:

- Target distance: 500ft, 750ft, 1000ft
- Initial speed: 25ft/s, 50ft/s, 75ft/s

These values gave a task time range of 6.66s to 40s, assuming the pilot did not decelerate at any point. This range was deemed acceptable after pre-trial testing confirmed that it was physically possible to decelerate quickly enough to complete the 500ft 75ft/s test which corresponded to the 6.66s task time. To give some form of comparable scaling to the task, the target circle sizes were selected as 25ft, 50ft and 75ft.

## 5.4 RESULTS

### 5.4.1 General Data Analysis

We will first begin by assessing the basic performance of the pilot through the runs in terms of control of speed, deceleration and longitudinal cyclic input.

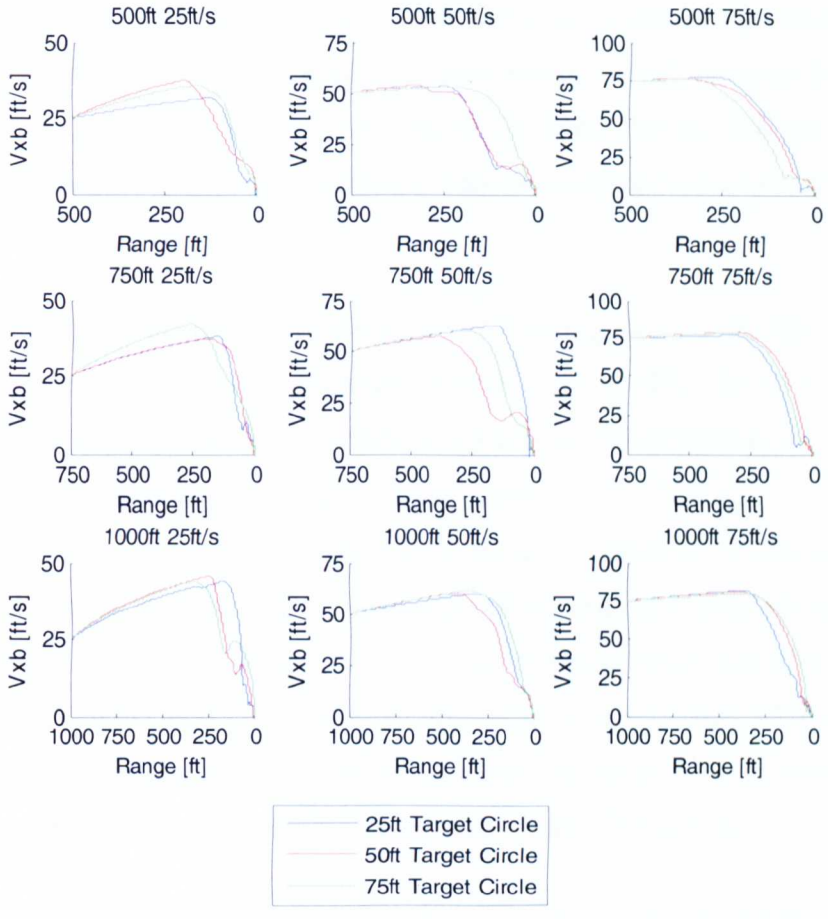


**Figure 5.3** Body X Velocity vs. Range for clinical deceleration trial

Before considering the specifics of the results shown in figure 5.3 it is worth noting that the increases in initial speed shown through the figures are not the result of an intentional acceleration. The pilot's strategy was to literally keep his hand off the cyclic until he felt that a deceleration was necessary, at which point he applied a control input. This brings us on to the first point to note from figure 5.3, the increase in the trimmed speed of all of the trial runs. The increase is much less prevalent in the 75ft/s tests, but occurs to some extent in all runs. The cause for the slow increase is unknown, although the most likely explanation would be a FLIGHTLAB trimming error. As we have already discussed, the pilot did not apply any cyclic input until the very noticeable reductions in speed towards the end of

each manoeuvre. While this is an undesirable issue, it does not adversely affect the results. Also, at the point of deceleration in each of the tests, the maximum speeds are approximately 40, 60 and 80ft/s (for the 25ft/sec, 50ft/sec and 75ft/sec tests respectively), thus preserving some element of relativity through the test points.

With the individual profiles on each subplot showing target circle diameter, we can see that there is no discernable pattern to the results. The 75ft targets cause the earliest deceleration in some cases, but not others, and the 25ft targets marginally produce the latest decelerations. This is a theoretically sensible result given that, for the same speed and distance from the target, the 25ft target circle would be expanding at a slower rate than the 50ft and 75ft targets. This would mean that the pilot would pick up and act on the motion later into the approach. However, this is by no means a clear result, with the three target circle diameters showing very similar results throughout each of the speed and distance settings.

The figure also shows that the pilot was able to decelerate quickly enough to intercept the target in all cases, with the 75ft/s runs potentially posing the greatest problem if the pilot had applied the deceleration too late into the approach. However, despite the relatively late decelerations in the high speed runs, this was not an issue.

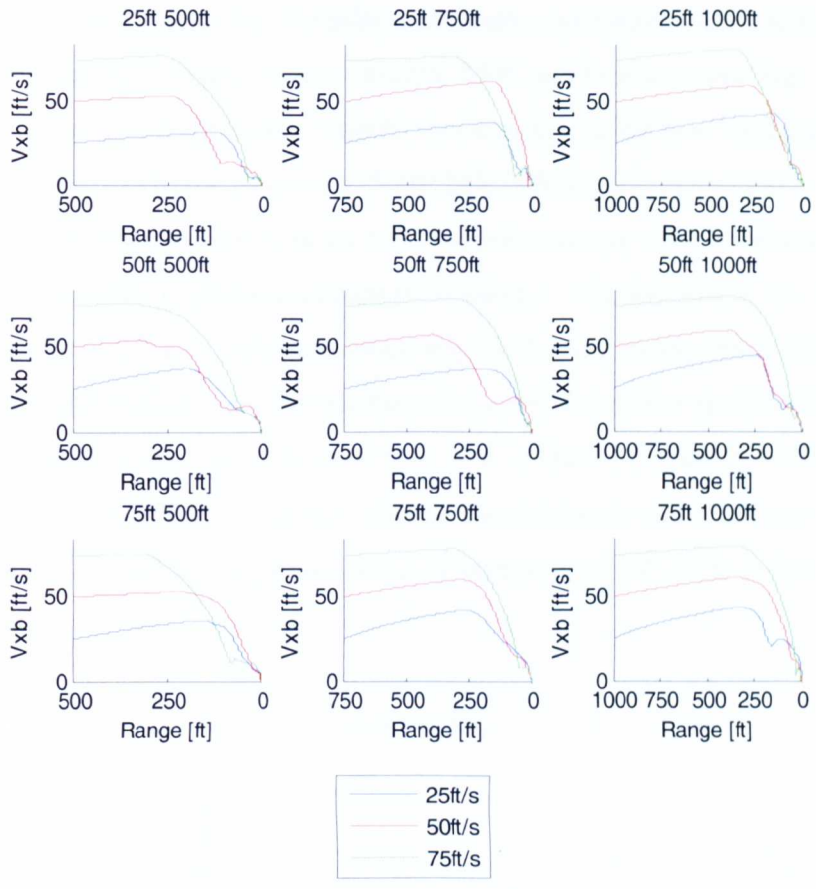


**Figure 5.4** Body X Velocity vs. Range for clinical deceleration trial

Figure 5.4 presents the data with the x-axis body velocity variables (vxb) shown on the sub-plots and allows a clearer examination of the individual runs. The figure shows that a large number of the tests feature a deceleration approximately 250ft from the target, regardless of initial speed, target size or initial target distance. Any exceptions to this rule are generally the 50ft/s and, particularly, 25ft/s tests, in which the deceleration is often closer to the target.

Figure 5.4 shows that several of the approaches do not feature a direct capture of the target. In addition to fine tuning over the closing 50ft of the runs there are also larger adjustments in the approach profile, most notably for the 750ft 50ft 50ft/s test (the red profile on the middle sub-plot). In this

example it can be seen that the pilot decelerates too aggressively, before realising this at a range of approximately 200ft and then accelerating briefly. This run featured the 'middle' settings for each of the variables, and with more extreme cases (e.g. 500ft 25ft 75ft/s) showing much smoother approaches, the reasons for this correction are somewhat unclear, with one possible explanation being pilot fatigue. This particular run was the 25th out of 27 and, with the particularly testing and tiring effect of the visuals in the trial, it could be that the pilot's performance was affected. This theory is borne out by the two final runs of the trial, 500ft 25ft 50ft/s and 1000ft 75ft 25ft/s, which both feature decelerations which are too aggressive, requiring a slight acceleration before the final 100ft of the approach.

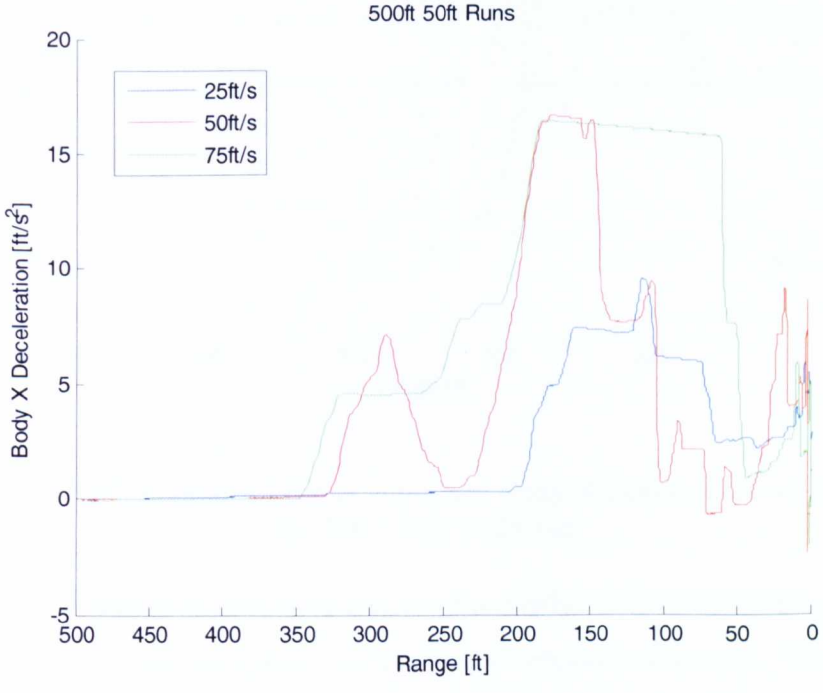


**Figure 5.5** Body X axis deceleration for 500ft 50ft runs

Figure 5.5 shows a recurring theme within the data, with the 75ft/s tests reaching the model's deceleration limit. All of the 75ft/s runs hit this limit during the deceleration phase, with some of the 50ft/s runs also reaching the peak deceleration level. While this is not a problem in itself given that the pilot was able to decelerate before passing the target in every run, it does reveal an interesting result when we consider the deceleration for the 75ft/s run alongside the longitudinal cyclic input.

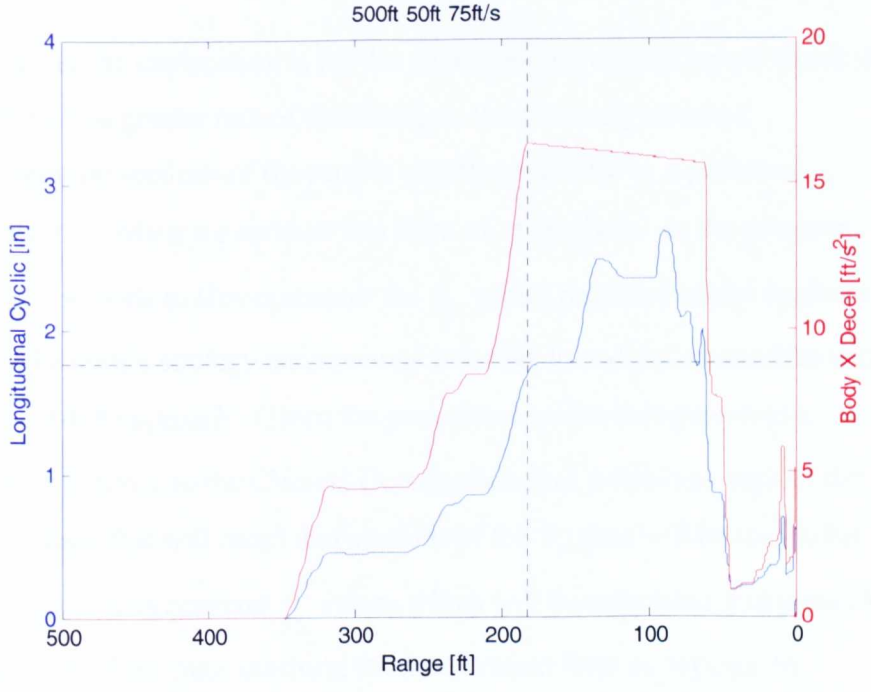


**Figure 5.6** Longitudinal Cyclic input and Body X Deceleration vs. range for 500ft 50ft 75ft/s run

Figure 5.6 shows an important feature of a number of the 75ft/s runs when the rate of deceleration peaks, shown by the vertical dashed line. The horizontal dashed line indicates the amount of longitudinal cyclic required to achieve this peak deceleration. There is clearly additional cyclic input after the deceleration peaks, with the pilot attempting to command an increased rate of deceleration by pulling the stick backwards by almost a

further inch, an additional 20% of the total aft range. This indicates that the pilot is unaware that the additional inputs were not having an effect on the deceleration of the aircraft, which in turn suggests that he is not picking up on the visual cues in the scene with a great deal of accuracy. An alternative explanation for the superfluous cyclic input would be that the pilot was unsure whether he could decelerate quickly enough given the approaching target circle, and applied the extra input as more of panic measure than a calm strategy based on the perceived cues.

Whatever the explanation is for the pilot applying control inputs which did not lead to a greater rate of deceleration, the relatively constant deceleration sections of the runs in question will lead to a period of constant $\dot{\tau}_x$ when we conduct this form of $\tau$ analysis. In the previous DVE Approach to Hover chapter the $\dot{\tau}_x$ values provided useful feedback as to the pilot's strategy and apparent attempts to end the approaches with a $\dot{\tau}_x = 0.4\text{-}0.5$ approach. Given the peak deceleration being reached a number of times in the Clinical Deceleration trial, notably in each of the 75ft/s tests, this will mean that sections of the $\dot{\tau}_x$ data will be somewhat redundant. The constant $\dot{\tau}_x$ values which will be calculated will purely be a function of the pilot reaching the deceleration limit as opposed to purposefully applying such a strategy. This issue is a result of the selected x-force limit for the simulation model, although the limit was chosen to be representative of typical deceleration levels in a civil helicopter. A larger peak x-force value may have avoided this problem as it would have enabled the pilot to make larger decelerations. However it was felt that basing the x-force limit on realistic deceleration rates offered a much more sensible test setup than allowing the pilot to decelerate at physically impossible rates.

Considering this issue with deceleration peaking with approximately 1.76" of aft stick, if future testing were to be conducted it is recommended that the cyclic scaling be adjusted. The aim of the adjustment would be to require that the full aft range of 5", rather than 1.76", be necessary to apply the full x-force deceleration. This would ensure that the pilot was aware of the stick input required to exert the maximum deceleration rate, and would also eradicate the issue shown in figure 5.6. The only negative associated with the change would be that, in one sense, the superfluous attempted deceleration could be considered as a useful visual cue indicator.

### 5.4.2 Tau Analysis

In order to conduct the various tau analyses it was necessary to decide which sections of the tests were the most appropriate for analysis. As has already been noted, the pilot did not make any control input for large sections of the approaches, therefore the tau analysis must start when the pilot initiates the deceleration. This still leaves an issue over where to end the analysis, with most runs showing a deceleration strategy which takes the aircraft very close to the target circle before the main deceleration phase ends. This is then followed by a gradual capture of the target circle which involves somewhat unsteady control of speed. Given the relatively stop-start nature of this final capture from close range, it was decided that the $\tau_x$ data would be misleading if it was considered over the full range of the approach. Therefore each set of data was examined and the data was trimmed to represent the initial main deceleration phase of the runs.

Figure 5.7 shows the velocity profile for the '750ft 50ft/s 25ft' test, with the red section of the profile representing the data which was selected for the $\tau$ analysis. The blue section of the data was discarded because of the velocity increase which occurs after the aircraft had slowed to 0kts at the end of the selected $\tau$ section. The same method was used with the other

runs, with the aim being to use the pilot's initial attempted capture of the target circle as the selected data.

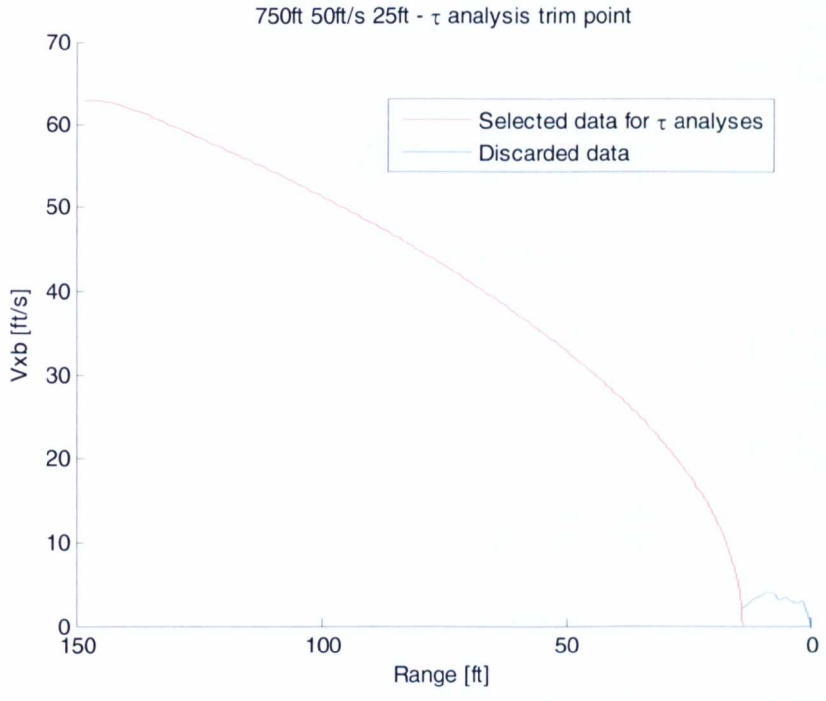


**Figure 5.7** Body velocity vs. range showing selected data for $\tau$ analyses for 750ft 50ft/s 25ft run

Before examining the various $\tau$ analyses it is worth examining one aspect of the data which was revealed by the trimming process, namely the range to the target circle at the endpoint of the trimmed data. This will give some insight into the relative effects of the task variables on the success of the initial closure.

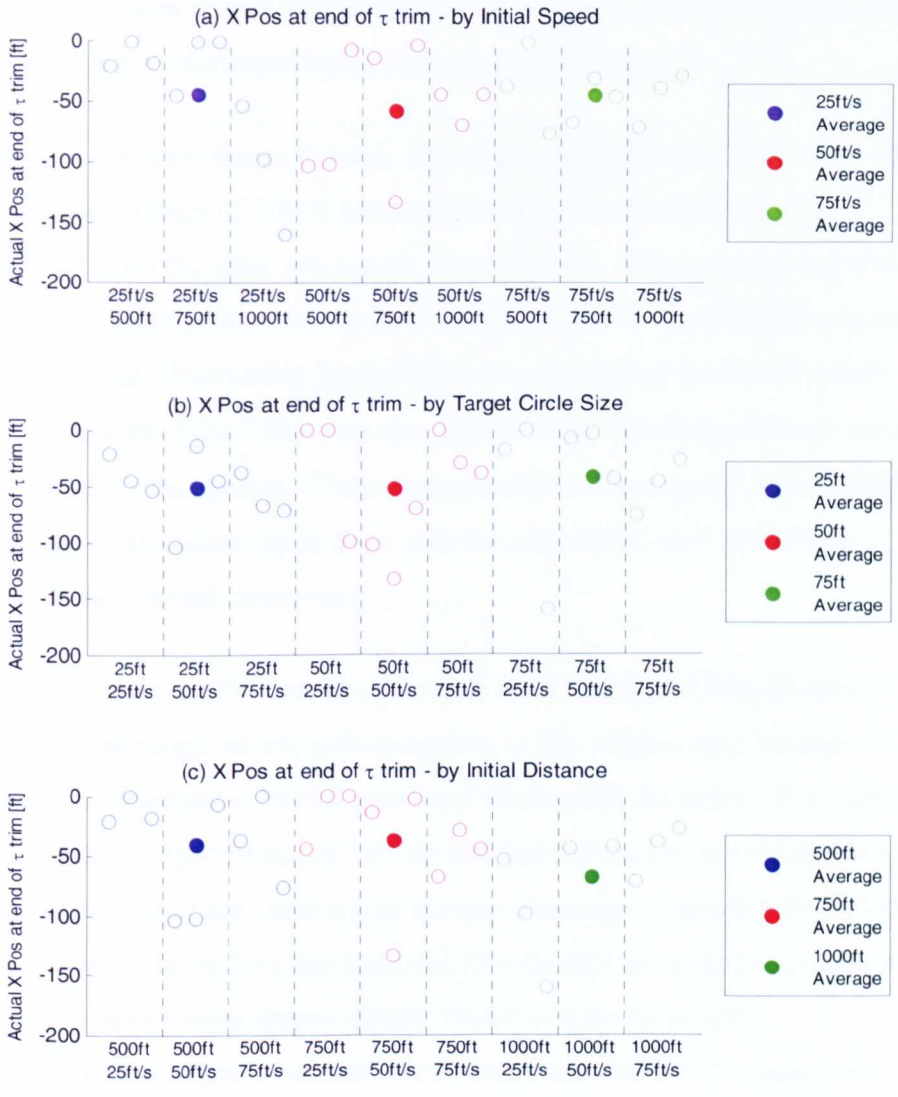


**Figure 5.8** X Range at end of $\tau$ trim in terms of (a) Initial speed, (b) Target Circle Size and (c) Initial Distance

Within the various subplots of figure 5.8 there seem to be some variable settings which yield more success than others. For example, figure 5.8(b) shows three 50ft and three 75ft runs which result in a very small range at the end of the $\tau$ trim. In contrast, the 25ft data shows fewer runs with the initial capture ending very close to the target circle. However, when we consider the average data for the target circle diameter settings, the

differences seen in the individual cases are negated, with the averages for all target circle diameters being almost exactly the same.

This is a common theme through almost all of the averaged data, with only the initial distance of 1000ft producing an average which is notably different from the other two results in the subplot. This average seems to be mainly affected by two sub-points of the 1000ft data, which correspond to 25ft/s runs. Examining figure 5.8(a) we can see that the final 3 results shown as part of the 25ft/s data also represent the three largest range values for the 25ft/s data points. These three points also correspond to the 1000ft runs, possibly indicating an issue with the long range, slow speed tests, regardless of target circle size.

Aside from the 1000ft average, the other sets of averaged data all show very similar range values, indicating that, in this respect, performance is largely independent of initial speed and target circle diameter. The average range value is approximately 50ft for most of the values considered above and, with most of the deceleration starting at a range of roughly 200-250ft (as shown in figure 5.4), this indicates that the first attempt at target circle capture encompasses approximately 75-80% of the range after deceleration. Despite a number of successful runs where the range was less than 20ft at the $\tau$ trim point, this is quite a large figure and suggests that the pilot may not have been able to affect a precise, well guided $\tau$ strategy throughout the tests. The result could also indicate a multi-phase $\tau$ approach, with the initial capture that will be examined in detail being part of a 'low gain' strategy which is designed to take the pilot closer to a target object, before a 'high gain' strategy takes over in the final stages of the manoeuvre. Given the objectives of the task, the low gain strategy will be the focus of the $\tau$ analysis, with the aforementioned '$\tau$ trim' being used extensively. However, the final hypothesised high gain phase will also be considered in section 5.4.2.3.

As with the analyses in the Approach to Hover research, k and $\dot{\tau}_x$ will be used throughout this Chapter. k is the gradient of the linear approximation of $\tau_x$ vs. TTG over the relevant period, and $\dot{\tau}_x$ is the instantaneous rate of change of $\tau_x$ with respect to TTG.

### *5.4.2.1 $\tau_x$ vs. TTG*

The $\tau$ analysis will now examine the results in terms of $\tau_x$, examining the $R^2$ and k values for the TTG method of analysis in order to determine whether performance remains independent of test variables in a $\tau$ context.

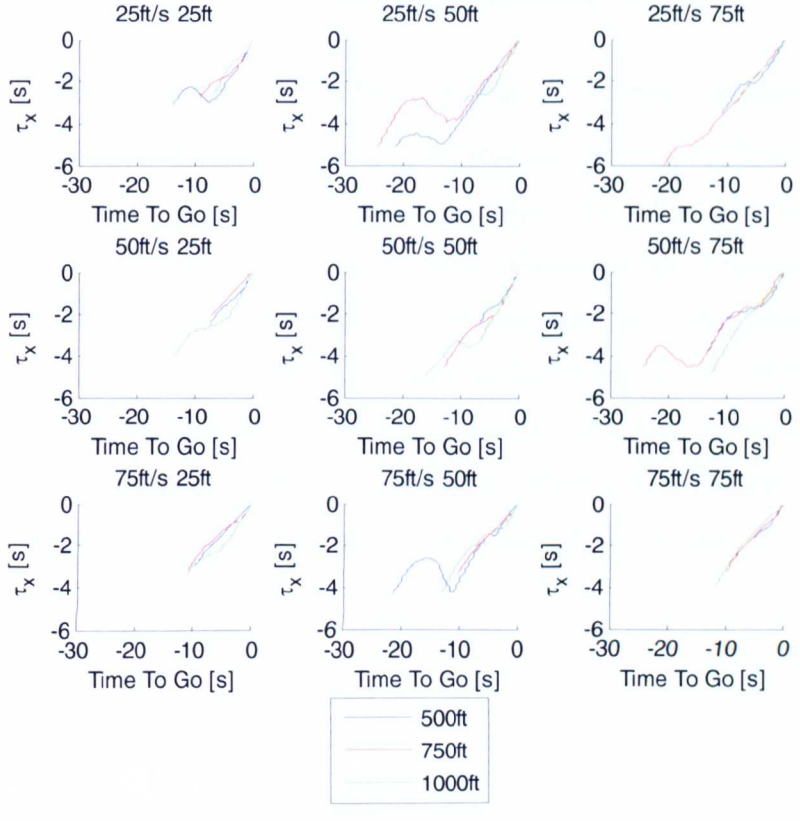


**Figure 5.9** $\tau_x$ vs. TTG for Clinical Deceleration

Figure 5.9 shows that, even when we consider the relatively smooth and adjustment free initial capture of the target circle, there are still a number

of velocity corrections which then impact the $\tau_x$ profile. These adjustments are more prevalent in the 25ft/s and 50ft/s tests, although this could be indicative of the issue already noted with the peak deceleration being reached in each of the 75ft/s tests. With the more aggressive deceleration required for the 75ft/s runs it is possible that the initial trim which is being considered is simply a product of the large initial deceleration. However, examining the 75ft/s data closely does reveal that the $\tau_x$ profiles are not perfectly smooth, with some minor adjustments over the final 5 seconds of the manoeuvre. This indicates that the 75ft/s approaches may provide useful information as opposed to simply representing an unintentional constant deceleration approach.

Many of the $\tau_x$ profiles for the 25ft/s and 50ft/s runs feature an adjustment which leads to the profile becoming somewhat shallower in the final 5-10s of the manoeuvre (the adjustment leads to a negative gradient in a number of cases). This is then followed by a further adjustment which restores a steeper gradient. This is similar to the 'cautious pilot' technique discussed in the previous Chapter, and first hypothesised in (Jump, 2007). Although in several of these cases we are not considering an approach which successfully captures the helipad, it does seem that the pilot could be attempting to affect such a strategy, shown more clearly in figure 5.10.

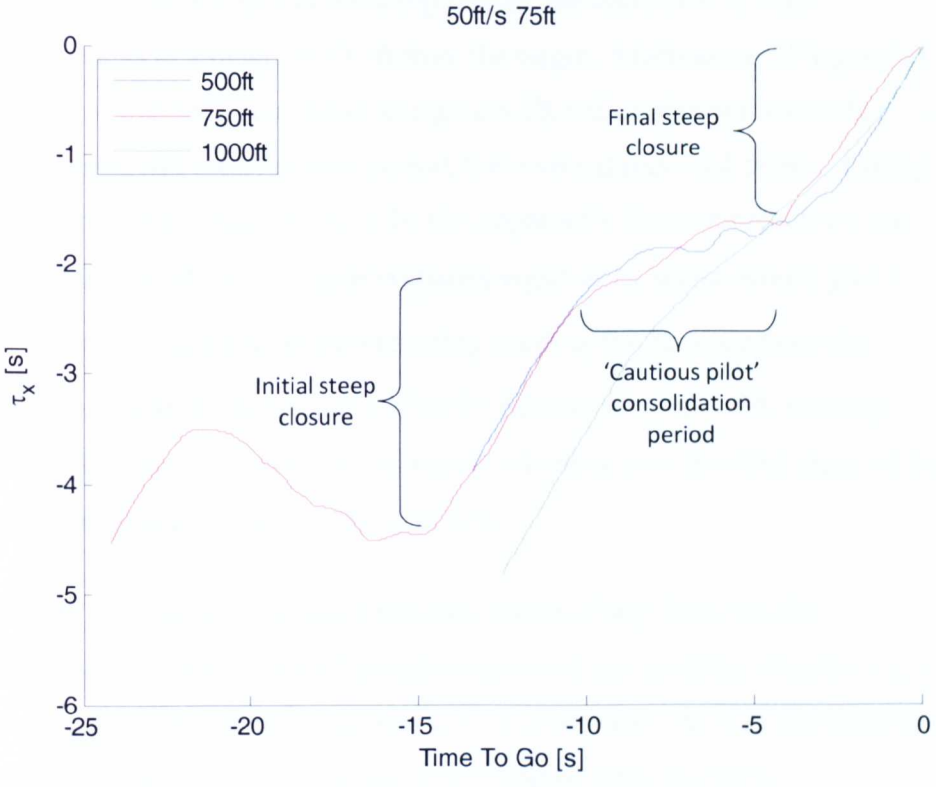


**Figure 5.10** $\tau_x$ vs. TTG multi-phase approaches for 50ft/s 75ft runs

The 1000ft profile in figure 5.10 shows a somewhat different style of approach to the 500ft and 750ft runs, although there is still a characteristic reduction of gradient, followed by a steeper final phase. The 500ft and 750ft runs feature a more distinctive shape, with the steep areas after and, particularly, before the consolidation period showing very similar gradients. The 750ft test also shows a brief period around 5s TTG where $\dot{\tau}_x$ is approximately equal to zero. This is then followed by a step change in gradient, with the pilot seemingly deciding that he wishes to attempt to capture the target. There is, however, a small change in gradient over the final second of the approach, and perhaps this is indicative of the pilot realising that his deceleration strategy is not accurate enough to capture the target circle in one smooth attempt. In this case, despite the seemingly

well controlled steep-shallow-steep phases, the end of the $\tau$ trim corresponds to a range of 30.1ft from the target. Much more telling in this respect is the 500ft run shown in figure 5.10, which shows a somewhat more uncertain consolidation period, but a very direct final phase. Taking an approximate gradient value for this apparently linear approach we see that at a TTG of 2s $\tau_x$ is approximately equal to 1s, which would give a $\dot{\tau}_x$ of 0.5. This could be an interesting result as the distance from the target circle at the end of the $\tau$ trim for this run was just 7.4ft, possibly indicating further correlation between the k value over the final stage of the manoeuvre and success of the approach.

Before moving on to evaluate the differences, if any, between the successful and unsuccessful initial captures we are currently considering, a more general appraisal of the data will be conducted. As with the approach to hover trial, the $R^2$ and k values are extracted from the linear approximation to the $\tau_x$ vs. TTG data and are represented in the following figures alongside the averaged values for the various test variables.


**Figure 5.11** $R^2$ values for TTG analysis in terms of original task variables

If we examine the average values for the 9 variables in figure 5.11 above it is evident that the values are not so large so as to be entirely compelling for the range of approach which the analysis considers. Previous research, including the GVE approach to hover trial, has shown $R^2$ values of well over 0.9, in some cases approaching 1 (Padfield et al, 2001), whereas the $R^2$ values in figure 5.11 range from 0.768 to 0.927. While this shows that there is still good correlation for certain aspects of the trial, it also indicates that there are performance differences between the test variables.

Considering the original objective of the trial, to investigate the pilot's ability to determine time to contact in an environment where relative velocity, distance and size are unknown, it is important to determine the reasons for these performance differences.

| *Test Variable* | | *Average $R^2$ Value* | *Average k value* |
|---|---|---|---|
| **Initial Speed** | 25ft/s | 0.768 | 0.314 |
| | 50ft/s | 0.879 | 0.317 |
| | 75ft/s | 0.913 | 0.294 |
| **Target size** | 25ft | 0.843 | 0.311 |
| | 50ft | 0.789 | 0.307 |
| | 75ft | 0.927 | 0.307 |
| **Target distance** | 500ft | 0.780 | 0.299 |
| | 750ft | 0.873 | 0.290 |
| | 1000ft | 0.905 | 0.337 |

**Table 5.1** Average $R^2$ and k values for TTG analysis of $\tau_x$

Table 5.1 supports figure 5.11, with average values for $R^2$ and k shown. The three average values which are over 0.9 correspond to the 75ft/s, 75ft and 1000ft variables. Earlier in the discussion it was noted that, as the 75ft/s tests all featured the pilot reaching the peak deceleration rate, this might impact the results. It would seem that this is the case, with a number of the 75ft/s $\tau_x$ vs. TTG figures showing extremely linear sections of the approach, which correspond to the periods of peak deceleration. It therefore appears that the larger $R^2$ values noted for the 75ft/s tests are merely the product of the accidentally obtained good correlation which arises as a result of the peak deceleration of the aircraft.

In terms of the average $R^2$ value for the 75ft target circle diameter being considerably higher than the 25ft or 50ft target circles, this could be due to the extra distance between the aircraft and the target circle for the 75ft configuration at the capture position. As the aircraft is further away from the target for the 75ft setting this means that for the same forward speed, the rate of change of angle subtended by the 75ft target circle is smaller than for the 25ft and 50ft targets, possibly allowing for finer control of the approach. The same issue would mean that, if the pilot decided he was not in control of the approach in the final 100ft, any actions with the 25ft target would feel more amplified than the same actions with a 75ft target. This could potentially cause further control issues, with more fore and aft control activity. In this sense the final phase of the approaches with the smaller size target circles could be likened to an aircraft with a higher gain control system than the lower gain nature of the 75ft targets. However, this theory does not explain why the $R^2$ performance with the 25ft target circles is marginally higher than that with the 50ft targets.

In summary, the $R^2$ values for the task variables are relatively well correlated throughout, with the values for each set of the individual variables being broadly similar. Whilst this section of the analysis is not so conclusive as to suggest that the pilot is able to determine time to contact without knowledge of the relative velocity, distance or size of the target, there is some suggestion that the pilot is using a $\tau$ -based strategy to guide the manoeuvre.

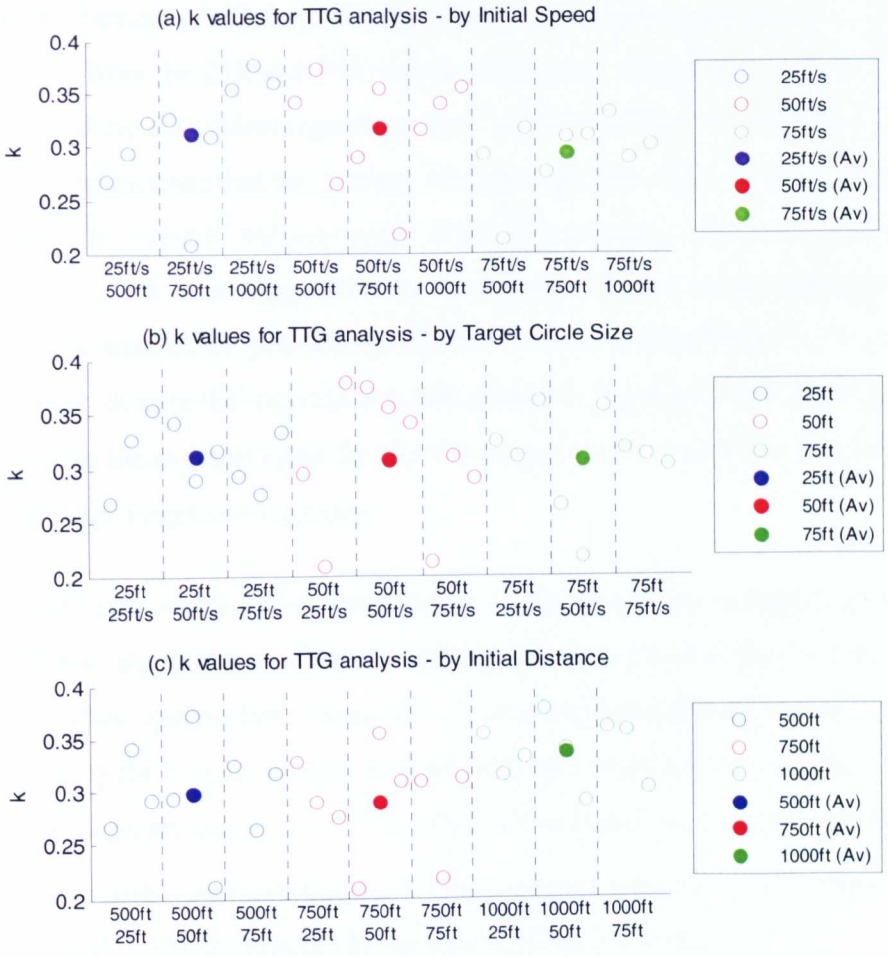


**Figure 5.12** k values for TTG analysis in terms of original task variables

Figure 5.12 shows the k value data for the $\tau_x$ analysis, with each subplot showing data separated by task variable. Although the individual is spread over a range of approximately 0.2-0.4, the averaged data shows a large degree of consistency. Indeed, the average target circle size values are 0.311, 0.307 and 0.307, showing that, for the average data, the k values are essentially identical. The individual 25ft and 75ft results show a number of data points close to the average value with the majority of data for each lying within ±0.05. This is not quite the case with the 50ft data, with four of the nine data representing the two highest and lowest values of k measured in the entire trial. There does not seem to be any specific reason

why performance with the 50ft target circles would be significantly different from the 25ft and 75ft targets. Returning to table 5.1, which prompted the discussion regarding the $R^2$ values for the various target circle sizes, we see that the average value for the 50ft target is 0.789 which is the third lowest $R^2$ value overall. While this is not a significant result in its own right, it does suggest that the individual k values for the 50ft tests are the product of the poor correlation coefficients seen in figure 5.11. However, despite the individual variations within the data, it is interesting to see that the average value for the 50ft targets is still essentially the same as the other target size averages.

The similarity of the initial speed results is intriguing, as one might expect the 75ft/s tests to show different results given the somewhat more artificial nature of the approaches. However, it seems that any differences are masked by the way in which k is calculated as it takes into account the relationship between $\tau_x$ and TTG. This is potentially an important result as, in this particular example, the k value seems to present a result which is unaffected by the differences in the approach speeds and peak decelerations of the various runs.

The analysis of the correlation coefficient and k value for the initial attempted capture of the target has shown extremely interesting results. The consistency of k value used potentially indicates a native value for a $\tau$ -based Prospective SkyGuide. However, this result should be treated with a certain degree of caution as, with many correlation coefficient values below 0.9, k cannot be considered to be a good indicator of runs with poor $R^2$ correlation.

However, with the particular interest in k, the examination will now assess the rate of change of $\tau$, i.e. $\dot{\tau}_x$.

### 5.4.2.2 *Instantaneous $\dot{\tau}_x$ Analysis*

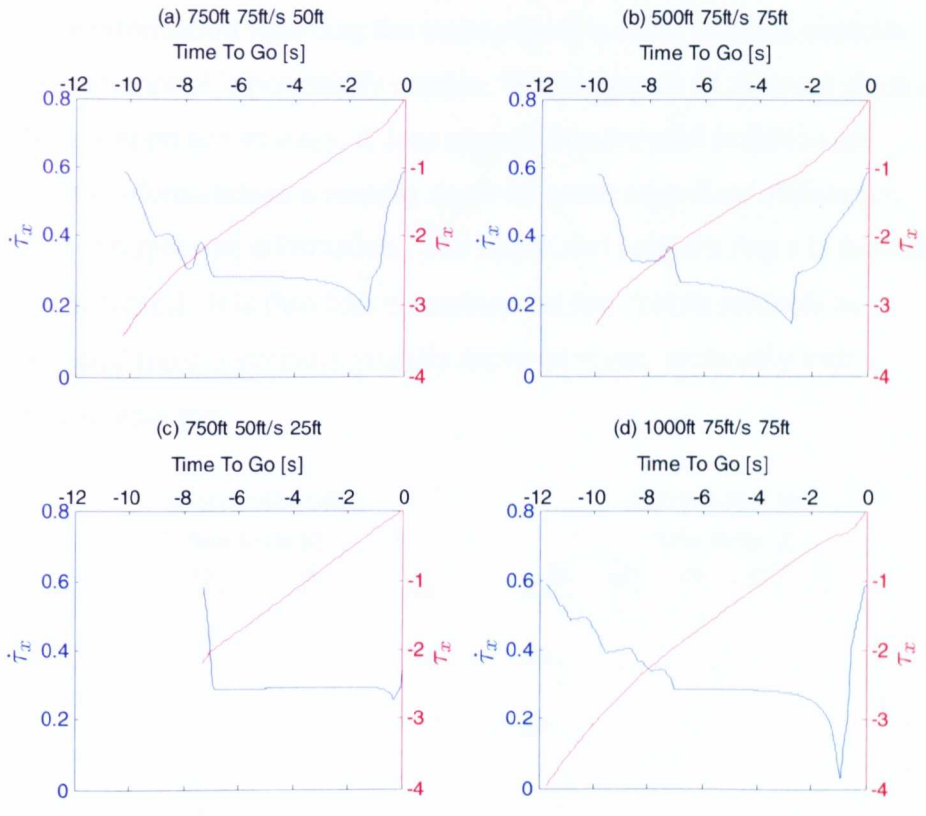


**Figure 5.13** $\dot{\tau}_x$ and $\tau_x$ vs. TTG for selected $\dot{\tau}_x$ = constant runs

Figure 5.13 shows a selection of runs which feature the characteristic constant $\dot{\tau}_x$ profile which represents the periods of constant deceleration. An interesting aspect of each of these tests, and several other runs, is the point at which the peak deceleration is initiated. In each case $\tau_x$ at the point of the artificial $\dot{\tau}_x$=constant initiation is approximately 2s. The TTG at each initiation is also generally the same, approximately 7s. Although the initial speed for many of the results which show this feature is 75ft/s, figure 5.13(c) shows a 50ft/s run. This consistency suggests that, despite the identical initial speed in many cases, the pilot is able to use the looming information to inform a new deceleration strategy at approximately the

same point in each of the cases shown above. This result suggests that the hypothesis which posits that the pilot does not need relative distance, speed or size information regarding the target object in order to affect accurate approach control is potentially correct. While figure 5.13 does not show an effective approach strategy, it does suggest that the pilot is able to use looming information in a visually deprived scene regardless of distance, speed or target size information. The figure also suggests that $\tau$ is the basis for this control. It is therefore recommended that further research be conducted using a similarly visually deprived scene, preferably with a larger sample size.

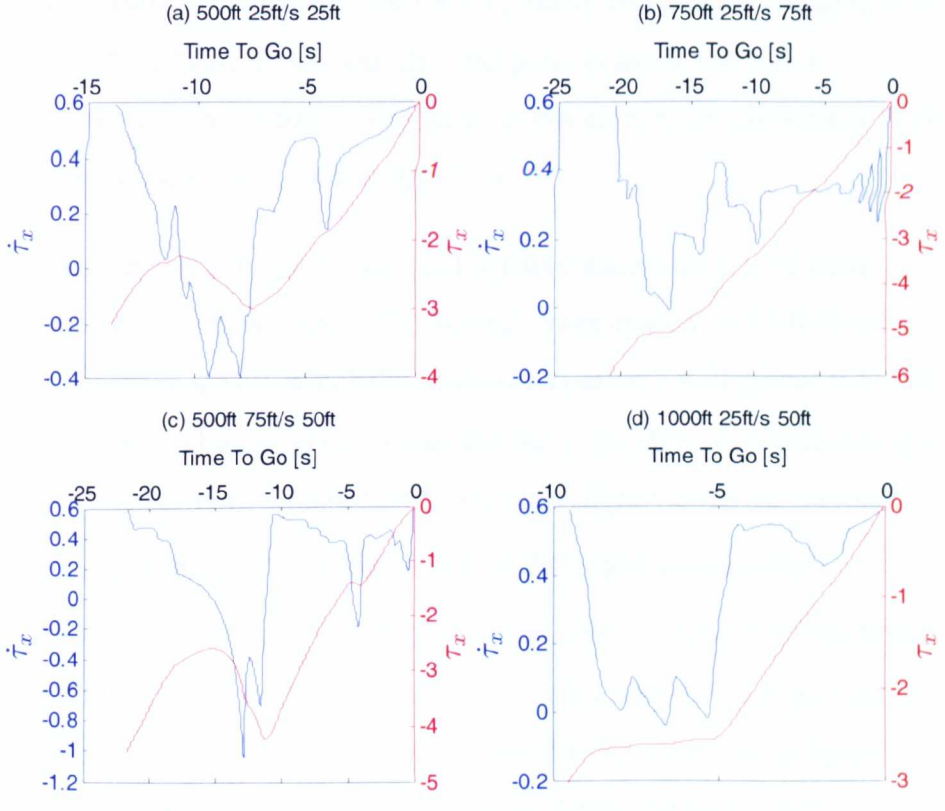


**Figure 5.14** $\dot{\tau}_x$ and $\tau_x$ vs. TTG for selected runs

Figure 5.14 shows a number of different styles of approach, mainly from 25ft/s tests, although figure 5.14(c) shows a 75ft/s run, which features a very brief period where the peak deceleration is reached around TTG= 18s. After a period where $\tau_x$ starts to increase, the pilot commits to an approach and $\dot{\tau}_x$ rises to a relatively constant value between 0.45-0.5, with one further minor adjustment.

A similar strategy is seen in figure 5.14(a), with a well guided $\dot{\tau}_x$ of approximately 0.5 after the pilot commits, and another small adjustment during that phase. Interestingly, with this 25ft/s example the point at which the pilot commits to the approach and $\tau_x$ starts to decrease is roughly at a TTG of 7s, a figure which was often the point at which the 75ft/s decelerations were initiated. However, in this case, $\tau_x$ at this point is 3s as opposed to 2s, as was found in figure 5.13.

The runs shown in figure 5.14(b) and (d) both feature aspects of what could be the 'cautious pilot'. This is much more evident in 5.14(d) with a $\dot{\tau}_x$ of approximately 0, which then rises to a relatively well guided 0.5 with, again, a small adjustment just before the end of the data. In addition to the brief $\dot{\tau}_x = 0$ section of figure 5.14(b) we see a slightly different approach, with $\dot{\tau}_x$ increasing to approximately 0.35-0.4 before a somewhat oscillatory phase towards the end of the run. This $\dot{\tau}_x$ value over the final stage of the manoeuvre is much more in keeping with the average k values shown in figure 5.12. However, as the data for the other tests in figure 5.14 show, the average k value of 0.3 arises simply because it is the average for the entire manoeuvre and not due to it being a specific instantaneous target that the pilot aims for. Instead, the task generally starts and ends with $\dot{\tau}_x$ = 0.5-0.6, with an initial phase where the value drops to 0 or becomes negative, followed by a period of $\dot{\tau}_x$ = 0.4-0.6 over

the closing stages of the manoeuvre. Considering the information revealed by the instantaneous $\dot{\tau}_x$ data, the design of a $\tau$ -based SkyGuide could be better suited to a multi-phased approach. Such a system would force an initial reduction of $\dot{\tau}_x$ such that $\tau_x$ is constant for a period, bringing the pilot closer to the target in a safe manner, $\dot{\tau}_x$ would then rise quickly to 0.4-0.5 as the target was captured.

By way of a final assessment of $\dot{\tau}_x$ we will now examine a series of plots which represent the 5 maximum and 5 minimum x-ranges as shown in figure 5.8.

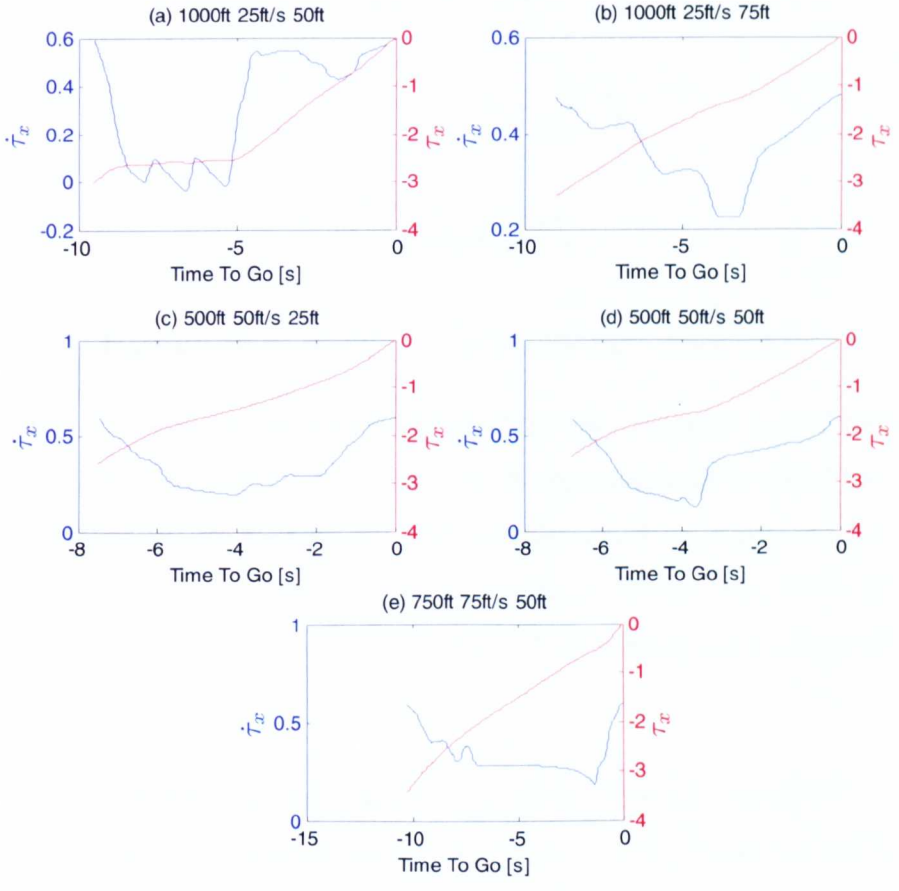


**Figure 5.15** $\dot{\tau}_x$ and $\tau_x$ vs. TTG for 5 worst x-range runs

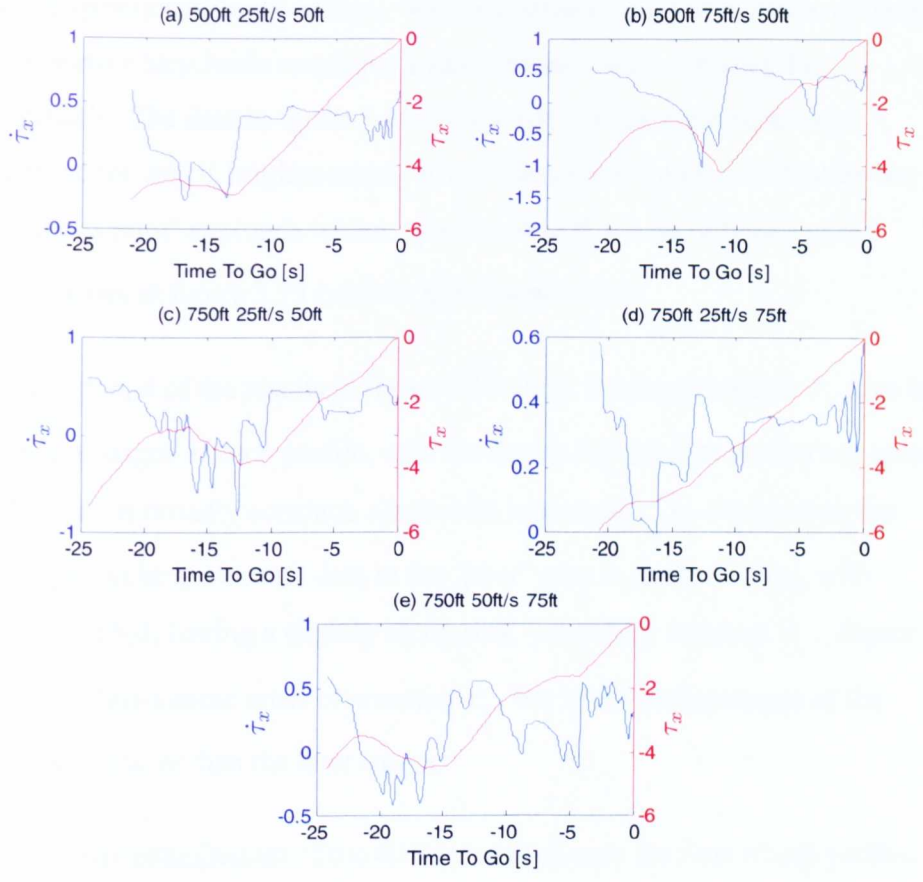


**Figure 5.16** $\dot{\tau}_x$ and $\tau_x$ vs. TTG for 5 best x-range runs

Figure 5.15 represents the 5 runs with the worst x-range, that is the 5 tests for which the end point of the $\tau$ trim (which has been used for all of the analysis thus far) are the furthest away from the target circle as shown in figure 5.8. The 5 worst runs all have range values of more than 100ft. In comparison the 5 best runs, shown in figure 5.16, feature range values of less than 3.04ft.

A point of interest is the comparison of k values for the two batches of tests, with the 'poor' runs represented by figure 5.15 having an average k of 0.352, whereas the 'good' runs average 0.248. This lower value is a result of the more expansive TTG range which generally includes a 'cautious pilot' phase in the approach data, causing the gradient of the

linear approximation to reduce. We have already suggested that a $\tau$ -based prospective SkyGuide may have a multi-phase k value driving the approach. The data in figure 5.16 shows that, for the most successful approaches, this is implemented. All of the runs in figure 5.16 feature the 'cautious pilot' approach where $\dot{\tau}_x$ reduces to 0, where only one of the approaches in figure 5.15 exhibits this characteristic.

In addition, 4 of the results in figure 5.16 show a strong constant $\dot{\tau}_x$ area in the final stages of each profile, with the figure 5.16(e) data containing areas where $\dot{\tau}_x$ is broadly constant, albeit with more noise. In comparison the only particularly constant data in the 'poor' runs is figure 5.15(a), with figure 5.15(d) having a slightly increasing, yet mildly constant $\dot{\tau}_x$. Figure 5.15(c) shows some areas of constant $\dot{\tau}_x$, but in the earlier stages of the approach rather than the later stages.

This closer examination of the differences between the runs which yielded the long and short x-ranges has therefore confirmed the earlier theory regarding the way in which $\dot{\tau}_x$ is controlled through the manoeuvre in order to guide a successful approach. As a result, the suggestions made in relation to the design of a future SkyGuide seem to be valid.

#### *5.4.2.3 Targeted $R^2$ analysis*

The final stage of the $\tau$ investigation was to conduct a targeted $R^2$ analysis over a different range than the '$\tau$ -trim' used previously. In order to investigate performance over the whole capture, the targeted analysis was conducted from the point that the pilot initiated the deceleration to the point at which he captured the target. The method used was the same as with that introduced in the DVE Approach to Hover analysis, with the target $R^2$ values selected as 0.9 and 0.95. However, despite the relatively

low target correlation coefficient values, the analysis, shown in figure 5.17, produced a result which highlighted the extent to which fine positional adjustment made up the majority of the final 20ft of the approach.

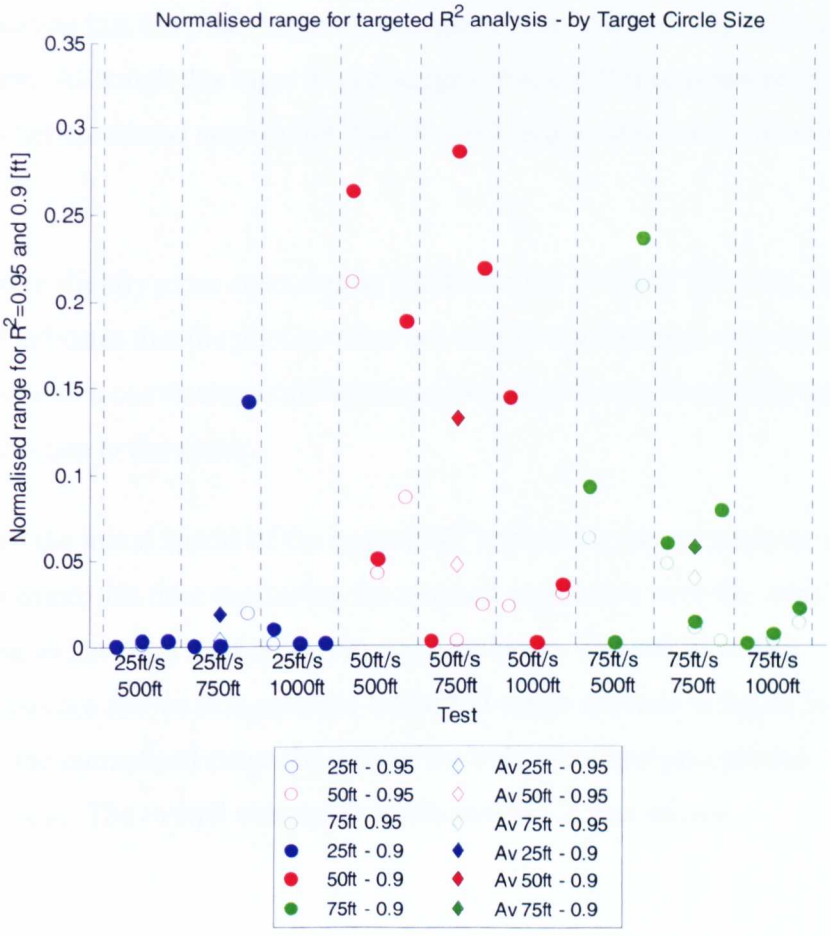


**Figure 5.17** Normalised range values for $R^2 = 0.95$ and 0.9 targeted analysis, by target circle size

Figure 5.17 shows the normalised range values for both $R^2$ target values of 0.95 and 0.9, alongside the average data for both target values presented in terms of target circle diameter. The normalised range was calculated by taking the range represented by each individual targeted $R^2$ analysis and dividing by that run's total deceleration range. A number of points are immediately clear, the first being the extremely low normalised range

values for much of the data, with the 25ft tests essentially showing normalised values of 0 throughout. This seems to confirm the point made earlier in the discussion regarding the much more testing control requirements for the 25ft targets at close range, with the very short ranges indicating that the final stages of the capture had an incredibly 'stop-start' nature. Although this logic would suggest that the 75ft targets would lead to better correlated approaches than the 50ft targets, this is not quite the case.

Despite slightly more encouraging results for the 50ft and 75ft tests, figure 5.19 indicates that the pilot is either not using a tau strategy, or is unable to do so with a convincing correlation coefficient given the extremely sparse visual cues in the scene.

Given the initial results of the targeted $R^2$ analysis, a second analysis was performed, this time examining the targeted correlation over the 'trim' range, as has been used in the previous analyses. The results of this analysis are shown alongside the initial full-range analysis in figure 5.18, with the normalised range for each of the individual analyses plotted against k. The overall average for each analysis is also shown.

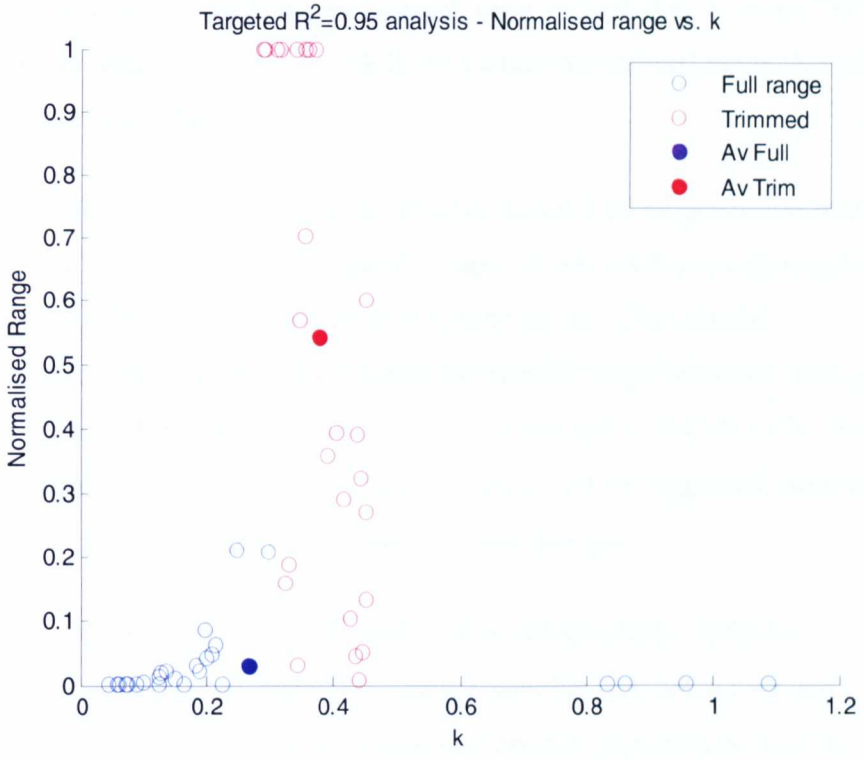


**Figure 5.18** Normalised range vs. k value for both Targeted $R^2$=0.95 analyses

Figure 5.18 immediately shows the large difference in the normalised ranges given by the two methods. Normalised range values for the 50ft/s tests which appeared to be large in figure 5.17 are shown to be small compared to the trimmed data values. Perhaps more importantly, there is *again some* semblance of a pattern between k and range for the targeted analysis.

Considering the full range data, there is a gradual rise in normalised range as the k value increases from approximately 0.05 to 0.3, with the greatest normalised range values from figure 5.17 being shown to have the largest k values of the targeted analysis. A similar pattern also occurs within the trimmed data, although the variation in normalised range happens over a short range of k values. The 10 points which have a normalised range of 1 have a k of between 0.29 and 0.37. 11 of the remaining trimmed results

with smaller normalised ranges have a k value of over 0.4. It should be noted that many of these data still have a larger normalised range than all of the full range data.

As with the DVE Approach to Hover trial, figure 5.18 suggests that there is an ideal k value (or a small range of values) which leads to an approach to a target which is well correlated over a large range. The Clinical Deceleration trial has also shown that the 'useful' range of values changes, with a range of 0.29-0.37 for this trial in comparison to 0.45-0.55 for the DVE Approach to Hover trial. Again, further work is suggested, especially given the need for some experimental improvements.

The targeted $R^2$ analysis therefore provides mixed results, with the trimmed data analysis suggesting, again a possible link between k and well-correlated, long-range approaches. However, the analysis over the full data range did not show any clear use of $\tau$, although there were some similarities with the trimmed data in terms of normalised range peaking for certain k values. In addition, the lack of repeated success in terms of well-correlated approaches over a large normalised range for the full range analysis is not helpful in terms of proving the hypothesis. However, this is not to suggest that the theory is incorrect as there are a number of potential contributing factors to the poor results:

- The limited cues and looming information in the scene may have been so severely degraded that the pilot was not given enough visual information to accurately fly the manoeuvre at close range.

- The physical height of the pilot meant that a percentage of the top of the OTW monitors were obstructed by the structure of the simulator. The pilot raised this issue during the practice runs but also indicated that it was not a serious enough problem to warrant

fixing, although the issue will have mildly limited the looming cues available.

- The fine control needed at close range may have been hampered by the small range over which the cyclic was operative. An input of 1.76" produced the maximum deceleration, with the stick input over the final stages of the approach being generally no more than 0.5". This would have added to the difficulty of the task.

## 5.5 CONCLUSIONS

The clinical deceleration trial has provided a range of results which have contributed to the understanding of how the pilot uses $\tau$ in a scene which is almost entirely deprived of visual cues. The hypothesis that the pilot does not need to know relative distance, velocity or size of the target object has been tested, although the results are inconclusive.

While it is not possible to say with any authority that the pilot was able to use $\tau$ to guide the manoeuvre simply by picking up on the looming cues provided by the target circle, it seems that part of the reason for the poor performance in some of the runs was due to experimental issues. In the case of the 25ft target circle tests the pilot was closer to the target circle in the final stages of the approach, thus requiring finer control to capture the target. The task was therefore made much more difficult because of the limited cyclic range of 1.76", as opposed to 5". Additionally, the problem with the simulator structure blocking part of the upper section of the OTW windows and therefore restricting the looming cues may have had a more general affect on performance.

However, despite some issues with the testing, there were positive results to be taken from the trial. The average values of k for the various variable subsets were remarkably similar, whilst the individual values were relatively consistent, with a spread of approximately ±0.05 from the average value. This suggested that Lee's theory was accurate. The average k value for the 1000ft tests was somewhat higher than for the 500ft and 750ft tests for unknown reasons, therefore further work may be required to test whether the theory extends to relative distance. However, there does seem to be a degree of consistency between the 500ft,750ft and 1000ft tests, with the results showing that the pilot initiated the deceleration at a range of approximately 250ft for the majority of runs, regardless of starting distance or target size.

The $\dot{\tau}_x$ analysis, specifically the comparison between the 'good' and 'poor' runs, has provided extremely useful information with regard to the way in which the pilot controls $\dot{\tau}_x$ instantaneously through the approach. More importantly, the comparison between the successful and unsuccessful approaches has shown a definite and repeated strategy which generally leads to an accurate capture of the target at the first attempt. This variation of $\dot{\tau}_x$, with an initial 'cautious pilot' period where $\tau_x$ is held roughly constant before the pilot commits to an approach with $\dot{\tau}_x$ = 0.4-0.5, is suggested as a design guideline for an initial development of a $\tau$-based prospective SkyGuide. A potential line of flight test investigation could be to evaluate a SkyGuide based on a range of commanded k values, with the aim of the experiment being to determine whether the most successful tests were those with $\dot{\tau}_x$ strategies similar to the $\dot{\tau}_x$ method suggested in this Clinical Deceleration trial.

Finally, the targeted $R^2$ analysis gave mixed results. Evaluating the full range of the approach showed that the majority of runs were well

correlated over less than 10% of the deceleration range. However, the evaluation of trimmed data showed that, again, there is a strong link between k and range, with the most successful k values in this case being between 0.29 and 0.37. Again, it is suggested that more research be conducted.

# Chapter 6

# CONCLUSIONS

## 6.1 CONCLUSIONS

To conclude this thesis we will review each Chapter in turn, before making some recommendations for future work which might follow on from this research project based on the findings presented.

Prior to the experimental work, Chapter 2 considered two of the major psychological theories of visual perception, with particular attention paid to Ecological Theory and one of the key parts of the research, $\tau$. The differences between the ecological and constructionist viewpoints were discussed, with the key points being:

- As suggested by the name, constructivism sees perception as a construction, not a direct, mechanistic process.
- Constructivism assumes that perception is learned, and must also go beyond what is available to the senses. Perception is seen as unconscious inference.
- Ecological theory states that perception is sensed and does not require prior knowledge or learning to function.

- Optic flow and affordances are important aspects of ecological theory and explain how the surrounding environment is a vital part of visual perception.

$\tau$ theory was also introduced at the end of Chapter 2, with the various aspects such as $\tau$-coupling and $\tau$-guides discussed.

Chapter 3 introduced the Approach to Hover trial, with testing taking place in GVE. The NASA flight trial which examined purely visual approaches to hover and contained a $\tau$-based equation was evaluated and the setup of the UoL trial was explained. The analysis covered the general data, a replication of some of the NASA work and also a detailed $\tau$ analysis, the main conclusions of which were:

- The general data analysis of the two pilots showed that the approach strategies they adopted were very different. AB's approach was such that, by a range of approximately 3000ft, he was 'on condition' with an altitude of approximately 300ft, no matter what the original start conditions. The SC approaches were very different, with his altitudes and groundspeeds at the same point showing much more distribution. The SC deceleration traces were also very similar to the NASA results, with deceleration gradually increasing through the duration of the approach, peaking 100-200ft from the target. In this sense the SC results were much more akin to the NASA results given the large spread of groundspeed data at 2800ft. This allowed the SC data to be compared much more favourably to the NASA power parameter, n.

- The attempted replication of the NASA n-parameter vs. groundspeed and deceleration vs. groundspeed plots was not entirely successful, in that the NASA results were not repeated in

the UoL investigation. Part of the reason for this was AB's technique being vastly different to that of the NASA test pilots. However, while SC's approach strategy did bear a resemblance to the NASA pilots, this data did not replicate their results either. An explanation for this could be that NASA used multiple test pilots. Despite the uniqueness of AB's data, the figures produced which considered the averaged data of AB and SC did start to resemble the NASA results somewhat. This suggests that further investigations with a larger number of test pilots could provide more useful data.

- In terms of the power parameters themselves, AB's results showed a general pattern for n, when considered without two anomalous results, to increase with either increasing initial altitude or decreasing initial speed. AB's range of groundspeeds at 2800ft was also very narrow compared to both SC and the NASA result. There was no clear trend within SC's power parameter values, with the range of values (for 7 of the 9 data) being narrow compared to NASA and AB.

- The $\tau$ analysis of the approach data showed, specifically for the AB data, excellent levels of correlation for most of the 27 runs. Further analysis of the data suggested a 2-phase strategy in order to give the optimum approach strategy. The first phase establishes the pilot at an altitude of 300ft at a range of 3000ft, giving a flight path angle of 5.7°. The second phase is then driven by $\tau$, with AB aiming for an approximate k of 0.45-0.5 for most of the remainder of the approach. In the final stages of the approach AB aimed for a constant $\dot{\tau}_x$ of 0.45-0.5 when $\tau_x$ was less than 7s. In contrast, SC's $\dot{\tau}_x$ over the closing stages of the approach gradually increased to values of 0.75 and above.

Chapter 4 took the convincing AB $\tau$ result from the GVE Approach to Hover trial and aimed to discover how a DVE would affect the pilot's ability to use $\tau$ for prospective guidance. The testing was conducted in 'normal', 'grey' and 'green' databases, with helipad heights of 0ft, 50ft and 100ft. The gradual degradation between the normal, grey and green databases yielded UCE ratings of 1, 2 and 3 respectively, with the UCE1 for the normal scene having slightly poorer translational and attitude VCRs than the original GVE trial, as per the aims of the scene design.

The main conclusions of the DVE trial were as follows:

- The relative effects and usefulness of micro and macrotextural and structural cues are transient. While there is evidence in previous research to suggest that microtextural cues are the most useful to the pilot, the author accepts this but also proposes that it is essential to offer the pilot a range of cues as different types of cue are more important at certain times. This has been shown by the way in which the pilot generally made use of the macrostructural cues provided by the 50ft helipads through each database. However, raised helipads can also have undesirable effects, generally when the pilot transitions over the pad itself. The movement of the pad relative to the ground adds to the pilot's workload and this may affect the capture.

- The issue of contrast in the scene could be an important visual cue, as was noted with the possible visual information provided by the strong, flat grey colour in the grey scene. Despite the grey database being an ostensibly UCE2 scene, this powerful contrast could have aided the pilot during certain phases of the approach to the helipad. This, again, raises the issue of the relative usefulness of

micro/macro texture and could offer an interesting line of further investigation.

- The targeted $R^2$ method of analysis has shown that the runs which had a high correlation coefficient over the largest ranges all had a k value of between 0.45 and 0.55. Larger values than this resulted in a much smaller range over which the runs were highly correlated. A similar run was also noted for the GVE analysis. In addition the targeted $R^2$ method also highlighted the usefulness of the raised helipads in providing the pilot with useful visual cues over a long range.

- The progressive analysis examined the change in k through a selection of runs which had yielded both long and short range targeted $R^2$ correlation. It was found that generally the k value was held between 0.45-0.55 for the duration of the approach, with the value over the final 200ft moving within a range of 0.45-0.5. Accurate control of k over the final 500ft of the approach was shown to be crucial to the efficient capture of hover given the large values shown by the short range correlation examples.

- The instantaneous $\dot{\tau}_x$ analysis examined the rate of change of tau at very short intervals throughout the approach. Again the intention of this method of analysis was to determine the differences between a 'good' and a 'bad' run. The analysis showed that it was important for the pilot to maintain $\dot{\tau}_x$ within a certain range of values, although the boundaries were quite large, approximately 0.1-0.9. The results showed that the pilot did not maintain a $\dot{\tau}_x$=constant profile for any convincing length of time, although values for the 'good' runs did converge within a range of 0.4-0.5, as would be expected given the progressive result.

Finally, Chapter 5 took a step back from the 'real life' trials conducted in Chapters 3 and 4 by examining whether the pilot was able to use a tau guidance strategy in a test which attempted to remove all relative distance, velocity and size cues. The conclusions of the clinical trial are highlighted below:

- In terms of testing the hypothesis that a pilot does not need to know relative speed, distance or size information, relying instead on the looming of the target, the clinical deceleration trial was inconclusive. However, closer analysis of the results and the areas in which the hypothesis was shown to break down suggested that this inconclusive result could be due to slight deficiencies in the experimental setup. The main areas of concern were the limited cyclic range and the physical size of the pilot reducing the effective area of the simulator's OTW monitors.

- When the results of the test were examined specifically in relation to the various target sizes there seemed to be a strong suggestion that the pilot's performance was unaffected by this variable. This was shown by the remarkably similar average k values for the TTG analysis. It is difficult to draw a conclusion based on the initial test speeds because of the maximum deceleration issues with the 75ft/s data.

- The $\dot{\tau}_x$ analysis which examined the difference between runs with successful target capture and those with poor target capture suggested a definite strategy for the control of $\dot{\tau}_x$ through the manoeuvre which would lead to accurate target capture at the first attempt. The strategy, which could be implemented as part of the design of a $\tau$-based visual aid, would allow the pilot to approach

the target with a $\tau_x$ = constant strategy. This strategy would allow $\dot{\tau}_x$ to rise from an initially constant value of 0 to approximately 0.4-0.5 at a TTG of between 10-15 seconds. The TTG could be approximately calculated based on distance to the target, current velocity and projected deceleration.

- Finally, the targeted analysis was used to determine whether there was a link between the range over which runs were highly correlated and the k value. The results of this analysis were mixed, with the evaluation over the full range of the approach to capture of the target showing that the majority of runs were correlated over less than 10% of the deceleration range. However, the k values for the full range data and also the values given by the analysis of the trimmed data did show a similar pattern to the targeted DVE analysis. That is, there appeared to be a link between range and k, with the most successful long-range runs having k values of between 0.29 and 0.37.

## 6.2 SUGGESTIONS FOR FURTHER WORK

The suggestions for further work essentially fall into two categories. The first is to repeat the tests conducted as part of this research on a larger scale. In terms of the DVE Approach to Hover and Clinical Deceleration trials, only one test pilot was used to obtain the results and while the author does not wish to suggest that this data is flawed in any way, the results of the GVE Approach to Hover trial highlight the differences between two vastly experienced test pilots. There are also experimental changes which could be made for both trials. The DVE Approach to Hover trial could not be directly related to the GVE Approach to Hover trial given the necessary

changes in test setup. A future trial could test all 4 visual scenes in the same experiment to allow comparison between all conditions, in addition to using as many pilots as possible for the work.

In terms of the Clinical Deceleration trial, the issues with the effective cyclic range could be fixed and a range of visual options designed to ensure that the physical stature of test pilots does not affect the amount of visual information they see on the screen.

The second area of suggestions for future work covers the recommendations that this project has made in terms of guidelines for future prospective SkyGuide. The Approach to Hover and Clinical Deceleration trials have both yielded suggestions as to the ways in which the pilot uses a TTG based instantaneous $\dot{\tau}_x$ to achieve successful capture. These guidelines should be investigated as part of a $\tau$ -based vision aid.

# REFERENCES

Anonymous, (2000) ADS-33E PRF, *Aeronautical Design Standard-33E-PRF, Performance Specification, Handling Qualities Requirements for Military Rotorcraft*, US Army Aviation and Missile Command Engineering Directorate, Redstone Arsenal, Alabama.

Anonymous, (2000) *CAP 701, Aviation Safety Review 1990-1999*, Civil Aviation Authority.

Anonymous, (2002) *CAP 735, Aviation Safety Review 1992-2001*, Civil Aviation Authority.

Anonymous, (1999) *Air Carrier Accident Data 1983-1999*, National Transportation Safety Board.

Anonymous, (2003) *Civil Aviation Accident Data 1982-2003*, National Transportation Safety Board.

Bickerstaffe, I.H., (1998) *Portrait of Landscape* in Proceedings of IMAGE Conference, Scottsdale Arizona.

Boring, E. G., (1946) *Perception of objects*. American Journal of Physics **14**:99–107.

Deighton, C. D. B. and Woodfield, A. A., (1996) *Visual Scenes for Battlefield Helicopter Operations: Evaluation of Requirements and How to Specify Them*, AGARD FCP Symposium, Braunschweig, Germany.

DuVal, R. W., (2001) *A Real-Time Multi-Body Dynamics Architecture for Rotorcraft Simulation, The Challenge of Realistic Rotorcraft Simulation*, RAeS Conference, November 2001, London.

Fox, D., (2001) *Electric eye*, New Scientist Magazine (p. 38), August 2001.

Gibson, J.J., (1950) *The Perception of the Visual World,* ed. L. Carmichael. Boston: Houghton Mifflin Company.

Gibson, J.J., Olum, P. and Rosenblatt, F., (1955) *Parallax and Perspective During Aircraft Landings*, American Journal of Psychology, Vol. **68**, 1955, pp. 372-385

Gibson, J.J., (1958) *Visually Controlled Locomotion and Visual Orientation in Animals*, British Journal of Psychology, Vol. **49**, 1958, pp. 182-194

Gibson, J.J., (1977) *The Theory of Affordances. In Perceiving, Acting, and Knowing,* Eds. Robert Shaw and John Bransford. ISBN 0-470-99014-7.

Gibson, J.J., (1979) *Ecological Approach to Visual Perception.* Houghton Mifflin, Boston.

Helmholtz, H.L., (1867) *Handbuch der physiologischen Optik.* Leipzig: L. Voss. Reprinted, with extensive commentary, in A. Gullstrand, J. von Kries & W. Nagel (Eds.)

Helmholtz, H.L., (1910) *Handbuch der physiologischen Optik* (3rd edn.). Hamburg and Leipzig: L. Voss.

Holway, A. H. and Boring, E. G., (1941) *Determinants of apparent visual size with distance variant.* American Journal of Psychology **54**:21–37.

Hoh, R. H., (1986) Handling Qualities Criterion for Very Low Visibility Rotorcraft NOE Operations. AGARD CP 423, Amsterdam.

Hoh, R. H., (1990) *The Effects of Degraded Visual Cueing and Divided Attention on Obstruction Avoidance in Rotorcraft*, prepared for Starmark Corp., Arlington VA and Systems Control Technology Inc., Arlington VA, under contract to the FAA.

Johnson, W.W. and Awe, C.A., (1994) *The selective use of functional optical variables in the control of forward speed.* NASA TM 108849.

Jump, M., (2007) *Prospective Sky Guides: Developing guidelines for pilot vision aids.*

Jump, M. and Padfield, G.D., (2005) *Tau flare or not tau flare - that is the question? Developing guidelines for an approach and landing skyguide.* In: ed(s) AIAA Guidance, Control and Navigation Conference, San Francisco.

Kaiser, M. K. and Mowafy, L., (1993) *Visual information for judging temporal range.* Proceedings of Piloting Vertical Flight Aircraft: A Conference on Flying Qualities and Human Factors, 4-23. San Francisco, California.

Kaiser, M. K., Perrone, J. A., Stone, L., Banks, M. S., and Crowell, J. A. (1993) *Extracting heading and temporal range from optic flow: Human performance issues.* In M. K. Kaiser & B. T. Sweet (Eds.), Proceedings of the Augmented Visual Display (AVID) Research Workshop. NASA Conference Proceedings #10128.

Lee, D. N., (1976) *A theory of visual control of braking based on information about time to collision* Perception, **5** p. 437-459.

Lee, D. N., (1980) *The Optic Flow-field: The Foundation of Vision*, Phil. Trans. R Soc. London, B **290**, 169-179.

Lee, D. N. and Reddish, P. E., (1981) *Plummeting gannets: a paradigm of ecological optics*. Nature, **293**:, 293-294.

Lee, D. N., Young, D. S., and Rewt, D., (1992) *How do somersaulters land on their feet?* Journal of Experimental Psychology: Human Perception and Performance, **18**, 1195-1202.

Lee, D. N., Davies, M. N. O., Green, P. R., and van der Weel, F. R., (1993) *Visual control of velocity of approach by pigeons when landing.* Journal of Experimental Biology, **180**, 85-104.

Lee, D. N., Simmons, J. A., Saillant, P. A., and Bouffard, F., (1995) *Steering by echolocation: a paradigm of ecological acoustics*. Journal of Comparative Physiology A, **176**, 347-354.

Lee, D. N., (1998) *Guiding movement by coupling taus*. Ecological Psychology, **10**, 221-250.

Lee, D. N., Craig, C. M. and Grealy, M. A., (1999) *Sensory and intrinsic coordination of movement.* Proceedings of the Royal Society of London B, **266**, 2029-2035.

Lee, D. N., (2005) *Tau in Action in Development.* In Rieser, J.J., Lockman, J. J., and Nelson, C.A. Eds. Action as an Organiser of Learning. Hillsdale, N.J.: Erlbaum.

McElroy, R. D., (2002) *Volume III: Federal Aviation Regulations (FAR) Part 119, 121, 135 (Professional Aviation series),* Aviation Supplies & Academics, Inc.

Moen, G. C., Dicarlo, D. J. and Yenni, K. R., (1976) *A parametric analysis of visual approaches for helicopters.* NASA TN D-8275.

Norman, J., (2002) *Constructionist and Ecological Can Go Together: Two visual systems and two theories of perception: An attempt to reconcile the constructivist and ecological approaches.* Behavioural and Brain Sciences (2002) **25**, 73–144.

Padfield, G.D., Charlton, M. T., Lee, D. N. and Bradley, R., (2002) *Prospective Control and Tau-Guides in Helicopter Flight & Implications for the Design of Vision Aids,* FS&C Technical Report TR-02-01.

Padfield, G.D., Clark, G. and Taghizard, A., (2007) *How long do pilots look forward? Prospective Visual Guidance in Terrain-Hugging Flight.* Journal of the American Helicopter Society vol. **52** issue 2 pp 134-145.

Padfield, G.D., Lee, D.N., and Bradley, R., (2003) *How Do Helicopter Pilots Know When to Stop, Turn or Pull Up?* Journal of the American Helicopter Society, Vol **48**, No 2, April 2003.

Padfield, G. D. and White, M. D., (2003) *Flight simulation in academia - HELIFLIGHT in its first year of operation at the University of Liverpool.* The Aeronautical Journal, September 2003, **107**(1075), pp. 529-538.

Rock, I., (1977) *In defense of unconscious inference.* In: Stability and constancy in visual perception: Mechanisms and processes, ed. W. Epstein. Wiley.

Rock, I., (1983) *The logic of perception.* Cambridge, MA: MIT Press.

Rock, I., (1997) *Indirect perception.* Cambridge, MA: MIT Press.

Smeets, J. B. J., Brenner, E., Trébuchet, S. and Mestre, D. R., (1996) *Is judging time-to-contact based on 'tau'?* Perception **25**(5) 583 – 590

Stewart, D., Cudworth, C. J., and Lishman, J. R., (1993) *Misperception of time-to-collision by drivers in pedestrian accidents.* Perception, **22**, 1227-1244.

Tims, J., (2002) *Visual Perception In Flight Control: Liverpool Simulation Programme 2001-2002.* Flight Science & Technology Library, University of Liverpool.

Titchener, E. B., (1914) A textbook of psychology. Macmillan.

Tresilian, J. R., (1999) *Visually timed action: time-out for 'tau'?* Trends Cogn. Sci. **3**, 301–310.

Wann, J. P., (1996) *Anticipating arrival: is the tau margin a specious theory?* J. Exp. Psychol. Hum. Percept. Perform. **22**, 1031–1048.

# Appendix A

## PILOT CURRICULUM VITAE

The flight testing research contained within this thesis was conducted by two test pilots, AB and SC. Their specific flying experience is shown below

**Pilot AB**

AB joined the Royal Navy in 1979 and served on 845 and 846 Squadrons as a Commando Helicopter pilot. He attended Central Flying School in 1985 and served on 705 Squadron as a Qualified Helicopter Instructor gaining an A1(H) QHI qualification. He then trained at the Empire Test Pilots' School in1989 before serving with Rotary Wing Test Squadron, Boscombe Down as test pilot. His responsibilities as test pilot included the introduction of the Lynx HAS Mk8 into Royal Naval Service; Sea King, Wessex and Gazelle project duties: icing project pilot, NVG project pilot and SHOL project pilot.

AB returned to operational service in 1992 with 846 Squadron including duties as Senior Pilot before returning to the Empire Test Pilots' School as a tutor. In 1995 he became Staff Aviation Officer to the Commodore Amphibious Warfare responsible for all aspects of amphibious aviation for the Royal Navy and Marines. He also saw operational service in Northern Ireland, the South Atlantic, Lebanon and Bosnia. AB completed three seasons as display pilot on Gazelle, both solo and as team leader in formation team, and competed in both the World and British Helicopter Championships winning eleven national and international trophies, including the British Helicopter Championship on two occasions. He was awarded the Air Force Cross in 1989.

AB left the Royal Navy in 1996 to become an airline pilot and is currently flying Boeing 747-400 on long haul routes with British Airways. In addition, he carries out instructional flying on light turbine helicopters and corporate helicopter operations on Agusta 109 and Gazelle. AB has conducted Crew Resource Management training for both fixed and rotary wing operators.

In total, AB has amassed 4750 rotary wing flying hours (4000 military, 750 civil) and 8500 fixed wing flying hours (500 military, 8000 civil).

AB also commissioned the James Bibby simulator at Liverpool University in 2000 and continues with both student studies and R&D as a consultant.

**PILOT SC**

SC joined the Royal Navy (RN) on a Medium Career Commission, after first completing an honours degree in Mechanical Engineering. Following flying training he joined 845 Commando Squadron for the first of three consecutive tours, initially on the Wessex then on the Seaking. During this time he served as the principle NVG Instructor, Helicopter Warfare Instructor and finally as a Flight Commander with responsibility for Special Forces Operations. In 1991 he was appointed to Boscombe Down where he completed No 29 Rotary Wing course at The Empire Test Pilots' School. On graduation he was appointed to the Royal Aircraft Establishment at Bedford as the rotary wing experimental test pilot. Whilst serving on the Aerospace Research Squadron he completed a fast jet and also a multi-engine fixed wing conversion and carried out experimental research on both fixed and rotary wing aircraft.

When RAE Bedford closed down in 1994, he moved back to Boscombe Down for a year, serving on the Experimental Flying Squadron. In 1995 he was appointed to the US Naval Aviation Test and Evaluation Centre at Patuxent River Maryland, to instruct on the US Naval Test Pilots' School (USNTPS). SC spent three years at USNTPS, instructing on both helicopters and fixed wing aircraft, eventually becoming the Senior Instructor. Whilst at USNTPS he also carried out classified work for the US Department of Defence. On his return from the States in 1998, he was appointed as the commander, of a tri-service specialist flying unit.

Joining the RNR Air Branch on leaving the RN, he holds the rank of Commander and serves as the CO (Reserves) Commando Helicopter Force. He currently flies the Boeing 747-400 for British Airways.

SC has amassed a total of 8000 flying hours, of which 3500 are civil fixed-wing, 3500 military rotary-wing and 1000 on military fixed-wing aircraft.

# Appendix B

## VCR AND UCE

In order to obtain a UCE rating for a scene the pilot must give a VCR for a number of specific areas. The pilot gives 3 separate attitude ratings, for pitch, roll and yaw, in addition to 3 translational ratings. The scales, and rating guidelines are shown in figure B.1 below.

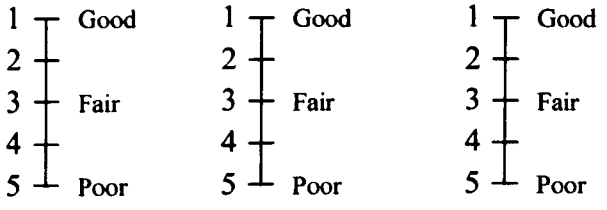


| Attitude | Horizontal Translational Rate | Vertical Translational Rate |
|---|---|---|

Pitch, roll and yaw attitudes, and lateral-longitudinal, and vertical translational rates shall be evaluated for stabilisation effectiveness according to the following definitions:

Good: Can make aggressive and precise corrections with confidence and precision is good.

Fair: Can make limited corrections with confidence and precision is only fair.

Poor: Only small and gentle corrections are possible, and consistent precision is not attainable.

**Figure B.1** Visual cue rating scale

The worst rating of the three attitude and three translational ratings is taken and these are then plotted on the UCE scale, shown in figure B2, to give an overall UCE rating.

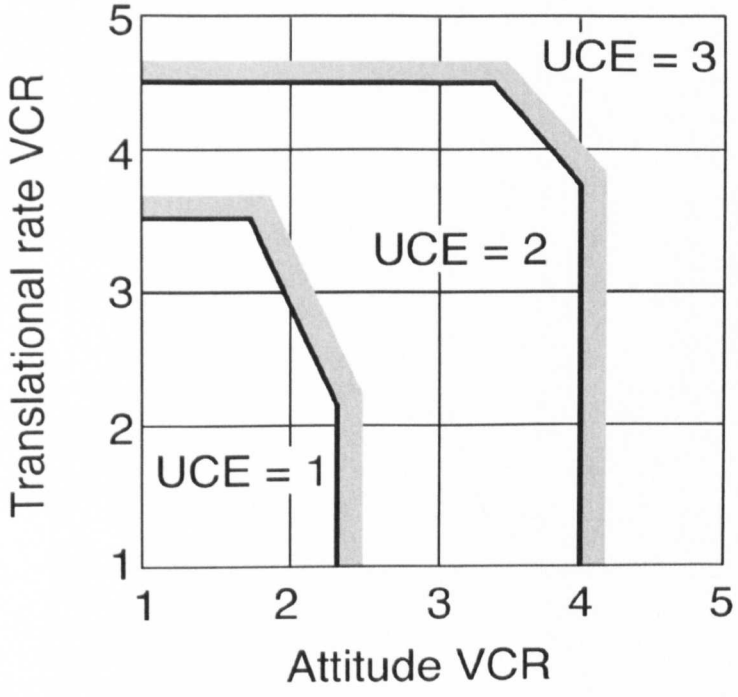


**Figure B.2** UCE rating scale